# TIME DEVELOPMENT OF LOCAL SCOUR AT A BRIDGE PIER FITTED WITH A COLLAR

A THESIS SUBMITTED TO THE

COLLEGE OF GRADUATE STUDIES AND RESEARCH

IN PARTIAL FULFILMENT OF THE REQUIREMENTS FOR THE

DEGREE OF MASTER OF SCIENCE IN THE

DEPARTMENT OF CIVIL AND GEOLOGICAL ENGINEERING

University of Saskatchewan

Saskatoon, Saskatchewan, Canada

**PATRICK DARE ALABI**

## PERMISSION TO USE

In presenting this thesis in partial fulfilment of the requirements for a Postgraduate degree from the University of Saskatchewan, I agree that the Libraries of this University may make it freely available for inspection. I further agree that permission for copying of this thesis in any manner, in whole or in part, for scholarly purposes may be granted by the professor or professors who supervised my thesis work or, in their absence, by the Head of the Department or the Dean of the College in which my thesis work was done. It is understood that any copying or publication or use of this thesis or parts thereof for financial gain shall not be allowed without my written permission. It is also understood that due recognition shall be given to me and to the University of Saskatchewan in any scholarly use which may be made of any material in my thesis.

Requests for permission to copy or to make other use of material in this thesis in whole or part should be addressed to:

Head of the Department of Civil and Geological Engineering
University of Saskatchewan
57 Campus Drive
Saskatoon, Saskatchewan
Canada, S7N 5A9

## ABSTRACT

A series of relatively recent bridge failures due to pier scour, as reported in literature, has rekindled interest in furthering our understanding of the scour process and for developing improved ways of protecting bridges against scour. Moreover, increased attention is being given to the state of Canada's infrastructure, a major aspect of which is the transportation network. In part, there is concern about both the impact of a failure on the handling of traffic flow while the failure is being remedied and on the cost of replacing the failed system component. As such, attention is being given to the scour design of new bridges and to the inspection, maintenance and management of existing bridge structures. The two major countermeasure techniques employed for preventing or minimising local scour at bridge piers are increased scour resistance and flow alteration. In the former case, the objective is to combat the erosive action of the scour-inducing mechanisms using hard engineering materials or physical barriers such as rock riprap. In the latter case, the objective is to either inhibit the formation of the scour-inducing mechanisms or to cause the scour to be shifted away from the immediate vicinity of the pier. This research focuses on a particular application of the latter technique.

In this study, the use of collars for reducing the effects of local scour at a bridge pier is presented together with the time aspect of the scour development. The adoption of a collar is based on the concept that its existence will sufficiently inhibit and/or deflect the local scour mechanisms so as to reduce the local scour immediately adjacent to the pier. The overall objective of the research is to study the temporal development of the scour for a pier fitted with a collar and a pier without a collar. More specifically, the objectives are: i) to evaluate the effectiveness of a pier collar for mitigating the depth of scour that would otherwise occur at a bridge pier; and ii) to assess the occurrence of an equilibrium scour condition, if achieved, or of the implications of not achieving such a condition in respect of interpreting the results obtained from a physical hydraulic model study.

The study was conducted using a physical hydraulic model operated under clear-water conditions in cohesionless bed material. Tests were conducted using two different pier diameters so as to determine the effect of pier diameter on the temporal development of scour for a plain pier. Also investigated was the effect of collar size on the time development of scour and its efficacy at preventing scour at a bridge pier. The time development of the scour hole around the model pier with and without a collar installed was compared with similar studies on bridge piers. Several equations for the temporal development of scour depth and those for the prediction of the equilibrium scour depth were tested as part of this study.

The results of the model study indicated that the maximum depth of scour is highly dependent on the experimental duration. The depth of the scour hole increases as the duration of the increased flow that initiates the scour increases. The extent of scour observed at the pier also increases as the duration of the tests increases. It was found that the temporal development of the scour hole at the pier was dependent on whether or not the pier was fitted with a collar placed at the bed level. The pathway to an equilibrium scour depth is different depending on whether the pier is fitted with a collar or not. With a collar in place, the development of the scour hole is considerably delayed. A truly equilibrium scour condition is not readily attainable and was not achieved in the work reported herein. It was demonstrated that wrong conclusions may be reached if a test is stopped short of an equilibrium state. As regards the temporal development of scour depth and for the tests in which no collar was fitted to the pier, it was noted that the form of equation that fits the experimental data well was the one given by Franzetti et al. (1982). Furthermore, it is possible to reach a variety of conclusions about the efficacy of using collars as a pier scour countermeasure technique, depending on which definition of time to equilibrium scour is adopted.

## ACKNOWLEDGEMENTS

First and foremost, I would like to give grace to the Almighty God for sparing my life and for seeing me through the completion of this research work. I wish to also express my sincere appreciation and deep sense of gratitude to my supervisor Dr. Jim Kells for his guidance, encouragement and personal concern throughout the course of this research work. His wealth of knowledge and enthusiasm to share them with me is most appreciated. I am really humbled! My sincere acknowledgement also goes to my Advisory Committee members, Dr. Gord Putz, Dr. Ian Fleming and Dr. Kerry Mazurek for their invaluable and helpful suggestions and guidance in this work.

Special thanks to Mr. Dale Pavier and Mr. Alex Kozlow for their assistance and help throughout the laboratory program of my research. My special gratitude goes to Mr. Hossein Azinfar, a colleague at the Hydrotechnical Lab and Mr. Dave Cote for their assistance in no small amount in the course of the research work.

I thankfully acknowledge the financial support provided by the Natural Sciences and Engineering Research Council of Canada through my supervisor's NSERC grant.

It is also my great pleasure to give a due recognition to my family members for their "all the time" love, understanding and support in the course of this program and also for their prayers and words of encouragement whenever my enthusiasm waned. Specifically, I want to use this opportunity to express my sincere thankfulness to my father, brothers, cousins, friends and deceased sister and mother for their constant support for my education over the years.

My profound gratitude goes to Engineer Wendell Peterson and Engineer Doug Hansen of the Department of Highways and Transportation (Saskatchewan Government) for their understanding and constant moral support as I completed the revisions to the thesis document.

Lastly, I will also use this opportunity to express my sincere appreciation to Dr. and Mrs. Adelugba for their moral support and word of encouragement all the time.

## DEDICATION

This thesis is dedicated to my late mother, Mrs. Mary Aina Alabi. She passed on in the winter of 2003, just before the start of my program at the University of Saskatchewan.

## TABLE OF CONTENTS

## LIST OF TABLES

## LIST OF FIGURES

## NOMENCLATURE

| | | Units |
|---|---|---|
| A | Area | $m^2$ |
| B | Pier width for non circular pier | mm |
| B | Constant in Franzetti et al. (1982) equation | - |
| C | Constant in Franzetti et al. (1982) equation | - |
| D | Diameter of pier | mm |
| $d_{16}$ | Grain size for which 16% by weight of the sediment is finer | mm |
| $d_{50}$ | Median size of the sediment particle | mm |
| $d_{84}$ | Grain size for which 84% by weight of the sediment is finer | mm |
| $d_s$ | Depth of scour below the original bed level at abutments | mm |
| F | Coefficient in the adjusted Sumer et al. (1993) equation | - |
| Fr | Froude number | - |
| $F_d$ | Densimetric Froude number | - |
| g | Acceleration due to gravity | $m/s^2$ |
| g` | Relative gravitational acceleration | $m/s^2$ |
| G | Coefficient in the adjusted Sumer et al. (1993) equation | - |
| h | Height below the channel bed | mm |
| K | Constant | - |
| $k_s$ | Grain roughness | mm |
| n | Manning's n | - |
| $\rho_s$ | Sediment density | $kg/m^3$ |
| $\rho$ | Water density | $kg/m^3$ |
| R | Hydraulic radius | m |
| $R_b$ | Reynolds number | - |
| t | Time | hrs |
| $S_o$ | Total energy slope | m/m |
| T. | Water temperature | $^oC$ |
| T, $T_1$ | Dimensionless time scale | - |
| $t_e$ | Time to equilibrium scour depth | hrs |

| | | |
|---|---|---|
| $\tau_*$ | Dimensionless stress | - |
| $\tau_c$ | Critical shear stress | $N/m^2$ |
| $\tau_a$ | Actual shear stress | $N/m^2$ |
| $u_*$ | Shear velocity | m/s |
| $u_{*c}$ | Critical shear velocity | m/s |
| u | Mean approach flow velocity | m/s |
| $u_c$ | Critical velocity | m/s |
| $\nu$ | Kinematic viscosity | $m^2/s$ |
| W | Width of collar | mm |
| Y | Vertical position | mm |
| $y_c$ | Collar position above the initial channel bed | mm |
| $y_o$ | Flow depth | mm |
| $y_s$ | Depth of scour below the original bed level at bridge pier | mm |
| $y_{se}$ | Equilibrium scour depth | mm |
| $\gamma$ | Specific weight of water | $kN/m^3$ |
| $\gamma_s$ | Specific weight of the sediment material | $kN/m^3$ |
| $Z_c$ | The elevation of the collar with respect to the channel bed at abutments | mm |
| $\sigma_g$ | Geometric standard deviation of the sand size | - |
| $\hat{w}$ | Fall velocity of sediment particle | m/s |

# CHAPTER 1

# INTRODUCTION

## 1.1 Background

Scour is defined as the erosion of streambed sediment around an obstruction in a flow field (Chang 1988). The mechanism has the potential to threaten the structural integrity of bridges and hydraulic structures, ultimately causing failure when the foundation of the structures is undermined. A series of relatively recent bridge failures due to pier scour, as reported in the literature (e.g., Wardhana and Hadipriono (2003)), has rekindled interest in furthering the understanding of the pier scour process and for developing improved ways of protecting bridges against the ravages of scour. In this regard, it is interesting to note the statement by Lagasse and Richardson (2001) that, in the United States, "hydraulic factors such as stream instability, long-term streambed aggradation or degradation, general scour, local scour, and lateral migration are blamed for 60% of all U.S. highway bridge failures." Hoffmans and Verheij (1997) have also noted that local scour around bridge piers and foundations, as a result of flood flows, is considered to be the major cause of bridge failure.

Scour was found to be the main cause of the 1987 Scholarie Creek Bridge failure in New York in which 10 people were killed (Ting et al. 2001; Wardhana and Hadipriono 2003). The 1989 catastrophic collapse of a U.S. 51 bridge over the Hatchie River in Tennessee resulted in the death of eight people (Lagasse and Richardson 2001). In another example by Lagasse and Richardson (2001), "the southbound and northbound bridges on Interstate 5 over Arroyo Pasajero (Los Gatos Creek) in California collapsed during a large flood; four vehicles plunged into the creek, resulting in seven deaths." Chiew and Lim (2003) and Chiew (2004) reported the case of the August 2000 failure of Kaoping Bridge in Southern Taiwan. Dey and Barbhuiya (2004) made reference to the collapse of Bulls Bridge over the Rangitikei River, New Zealand.

Besides their human toll, bridge failures cost millions of dollars each year in direct expenditure for replacement and restoration in addition to the indirect expenditure related to the disruption of transportation facilities (Lagasse and Richardson 2001). In an intensive study of bridge failure in the United States, Cheremisinoff et al. (1987) reported that the Federal Highways Administration in 1978 claimed that damage to bridges and highways from major regional floods in 1964 and 1972 amounted to about $100 million per event. Citing a survey by Macky (1990), Melville and Coleman (2000) stated that, in New Zealand, scour caused by rivers results in the expenditure of NZ$36 million per year. Indeed, the failure of bridges due to scour is a common occurrence and large sums of money are spent each year on the repair or reconstruction of bridges whose piers have been destroyed by scour (Dey 1997).

The potential losses accruable from bridge failures and the need to guard against same have prompted for better understanding of the scour process and for better scour prediction methods and equations. Under-prediction of pier scour depth can lead to bridge failure while over-prediction leads to excess expenditure of resources in terms of construction costs (Ting et al. 2001). Numerous experimental and numerical studies have been carried out by researchers in an attempt to quantify the equilibrium depth of scour in various types of soil material. Moreover, while a lot of work has been done to develop equations for predicting the depth of scour, researchers have also worked extensively to understand the mechanism of scour. Raudkivi and Ettema (1983), Ahmed and Rajaratnam (1998), Chiew and Melville (1987) and Breusers et al. (1977), among others, are some of the researchers that have worked on pier scour. Local scour around bridge piers was studied by Shen and Schneider (1969) while Breusers et al. (1977) gave a "state of the art" review on local scour around circular piers. Posey (1974) provided guidance on how bridge piers in erodible material can be protected from under-scour by means of an inverted filter extending out a distance of 1.5 to 2.5 pier diameters in all directions from the face of the pier.

Current research areas include understanding the scour processes, temporal development of scour, predicting scour in cohesive soils, parametric studies of local scour, and prediction of scour depth at various types of hydraulic structures. For example, Ansari

et al. (2002) studied the influence of cohesion on scour around bridge piers. Ahmed and Rajaratnam (1998) investigated the flow around bridge piers in their laboratory study on flow past cylindrical piers placed on smooth, rough and mobile beds. Jia et al. (2002) reported the findings of a numerical modeling study for simulating the time-dependent scour hole development around a cylindrical pier founded on a loose bed in an open channel. Lim and Chiew (2001) presented a parametric study on riprap protection and failure around a cylindrical bridge pier with uniform bed sediments. Link and Zanke (2004) studied the time-dependent scour-hole volume evolution at a circular pier in uniform coarse sand and developed a mathematical correlation between the scour volume and the maximum scour depth for water depth to pier diameter ratios between one and two.

In spite of the significant amount of research into scour processes, some aspects of scour are yet to be resolved as shown by the various contradictions reported in the literature. Raudkivi and Ettema (1983) stressed that the scientific basis for the structural design of bridges is well established whereas, in contrast, there is no unifying theory at present which would enable the designer to estimate, with confidence, the depth of scour at bridge piers. Cheremisinoff et al. (1987) and Hoffmans and Verheij (1997) supported the claims of Raudkivi and Ettema. According to the various authors, this is not only due to the extreme complexity of the problem but also due to the fact that stream characteristics, bridge constriction geometry and soil and water interaction are different for each bridge as well as for each flood. Although it has been the subject of theoretical and experimental studies for many years, Federico et al. (2003) have also indicated that a reliable assessment of the general and local erosion of pier foundation soil cannot be safely calculated by means of the empirical correlations available in the technical literature.

Hoffmans and Verheij (1997) indicated that scour analysis should form an integral part of the design of a new bridge substructure in order to ensure that the bridge can withstand the effects of high flows during flood events. The authors were of the opinion that the currently available formulas for calculating the expected depth of scour have limited usage and cannot be relied on. Therefore, it was concluded that considerable

engineering judgment must be used when estimating the depth of scour in order to achieve a satisfactory and also a cost-effective design. With all of these comments about the "state of the art" on pier scour, coupled with the spate of bridge failures recorded within the last few decades, a means of protecting new and existing bridges against local scour is therefore necessary.

Local scour at a bridge pier principally results from the downflow along the upstream face of the pier and the resulting horseshoe vortex which forms at the base of the pier aids the phenomenon (Kumar et al. 1999). One way of reducing pier scour is to combat the erosive action of the horseshoe vortex by armouring the riverbed using hard engineering materials such as stone riprap. Another approach is to weaken and possibly inhibit the formation of the downflow and thus the formation of the horseshoe vortex using a flow-altering device (Chiew and Lim 2003; Melville and Coleman 2000). Flow-altering devices that have been used to protect piers against local scour include sacrificial piles placed upstream of the pier, Iowa vanes, a slot through the pier, and a flow deflector attached to the pier, such as a collar. The use of collars has been studied by several researchers, including Chabert and Engeldinger (1956), Laursen and Toch (1956), Thomas (1967), Tanaka and Yano (1967), Kumar et al. (1999), Chiew (1992), Zarrati et al. (2006) and Fotherby and Jones (1993). In general, the results from collar studies have shown that they can be very effective in reducing the scour depth at a bridge pier.

Since a collar acts to reduce the scour depth at a bridge pier, the parameter of interest, therefore, is the scour depth. However, just as the scour depth is important in scour studies, the time taken to reach a particular scour depth is also very significant as scour holes take some time to form. For this reason, it becomes necessary to understand the development of the local scour hole with time. Also, in clear-water scour conditions, the depth of a scour hole approaches an equilibrium condition asymptotically with time (Breusser 1977). Consequently, time is an important factor in undertaking scour studies. The temporal development of scour has been studied by many researchers (e.g. Melville and Chiew 1999; Yanmaz and Altinbilek 1991). Moreover, the rate of local scour around a bridge pier is a significant factor in scheduling scour mitigation measures and

is also essential in understanding scour under time-varying flows (Gosselin and Sheppard 1995). For adequate representation of the temporal development of scour and also the efficacy of using a collar as a countermeasure in a bridge pier in model studies, the definition of time to equilibrium adopted is very vital as this determines the test duration.

Many different definitions of equilibrium scour depth are given in the literature. Nevertheless, most equations for local scour yield the equilibrium depth and are, therefore, conservative regarding temporal effects (Melville and Coleman 2000). Peak flood flows may last for only a few hours or days in the field. For short duration floods, the peak flow duration may be insufficient for achieving an equilibrium scour depth. In such instances, the actual scour depth may only be a small percentage of the equilibrium scour depth, which could take weeks to fully develop.

As pointed out above, the use of a shield or collar is one strategy that has been studied as a potential mitigation strategy for pier scour. When a collar is installed on a pier, the direct impact of the downflow to the riverbed is prevented (Mashair et al. 2004), which serves to reduce the depth of scour that can take place. In addition to reducing the depth of maximum scour, the rate of scouring is also reduced considerably. In this regard, Mashair et al. (2004) observed that reducing the rate of scouring limits the risk of pier failure when short duration floods occur. On the matter of time development of maximum scour depth, Zarrati et al. (2004) observed that the time to reach an equilibrium condition depends on whether the pier is protected with a collar or not. This difference in the time development of local scour has significant implications for those researchers choosing to stop their tests after a fixed length of time. While the ultimate or equilibrium scour for two situations may be the same, the temporal development of the scour hole may vary. There is, therefore, the need for a critical review of some results in literature relating to excessively short testing times.

## 1.2 Objectives

The principal objective of this study is to carry out a much longer duration test than is currently reported in the literature with a view to evaluating the time development of the

local scour at a bridge pier that has been fitted with a protective collar for the purpose of mitigating the scour. Also to be assessed are some of the common equations in the literature that describe the temporal development of pier scour. A modification is to be made to any of the equations where necessary and possible. Subsidiary objectives also include:

- Evaluation of the effectiveness of a pier collar for mitigating the depth of scour that would otherwise occur at a bridge pier; and

- Assessment of the occurrence of an equilibrium scour condition, if achieved, or of the implications of not achieving such a condition in respect of interpreting the results obtained from a physical hydraulic model study related to pier-collar experiments. Also to be assessed as part of this study are some of the equilibrium scour depth prediction equations as well as some definitions of equilibrium scour depth found in the literature.

## 1.3 Scope

The study reported herein is based on experiments carried out in the Hydrotechnical Laboratory at the University of Saskatchewan using a physical hydraulic model. The study was confined to uniform cohesionless material and clear-water flow conditions.

## 1.4 Synopsis of thesis

In Chapter 2, the background and current state of knowledge of scour, temporal development of scour and literature related to the use of a collar for pier scour mitigation are covered. Chapter 3 gives a description of the experimental apparatus, models and procedures. Results and discussion of results are presented in Chapter 4. Finally, the principal conclusions drawn from the results of the study and recommendations for future studies are presented in Chapter 5.

# CHAPTER 2

# LITERATURE REVIEW

## 2.1 Introduction

A large amount of literature has been published on the local scour of cohesionless bed sediment around a bridge pier. This chapter attempts to summarise the present state of understanding of local scour in cohesionless soil, the temporal development of scour as well as mitigation strategies for minimising the local scour at a bridge pier. The chapter is included to familiarise the reader with terminologies germane to local scour at a bridge pier as well as to facilitate the understanding of scour. The use of collars as a countermeasure for local scour is also reviewed.

### 2.1.1 What is scour?

Breusers et al. (1977) defined scour as a natural phenomenon caused by the flow of water in rivers and streams. It is the consequence of the erosive action of flowing water, which removes and erodes material from the bed and banks of streams and also from the vicinity of bridge piers and abutments. Cheremisinoff et al. (1987) defined scour as the lowering of the level of the river bed by water erosion such that there is a tendency to expose the foundations of riverine structures such as bridges. As noted by the authors, scour can either be caused by the normal flow or flood events. Normal flow can lower the channel bed but scouring is most assisted during a peak flow in which the flow velocity is higher. In other words, scour can occur under any flow condition that makes the bed mobile within the vicinity of the obstruction but the rate of scouring is much higher with larger flow events. The amount of the reduction below an assumed natural level (generally the level of the river bed prior to the commencement of the scour) is termed the scour depth. A scour hole is defined as the void or depression left behind when sediment is washed away from a stream or river bed.

### 2.1.2 Types of scour

Scouring has long been acknowledged as a severe hazard to the performance of bridge piers. The total scour at a river crossing consists of three components that, in general, can be added together (Richardson and Davies 1995). They include *general scour*, *contraction scour,* and *local scour*. Cheremisinoff et al. (1987) on the other hand divided scour into two major types, namely *general scour* and *localised scour*. Some other sub-divisions of scour are as shown in Figure 2.1.

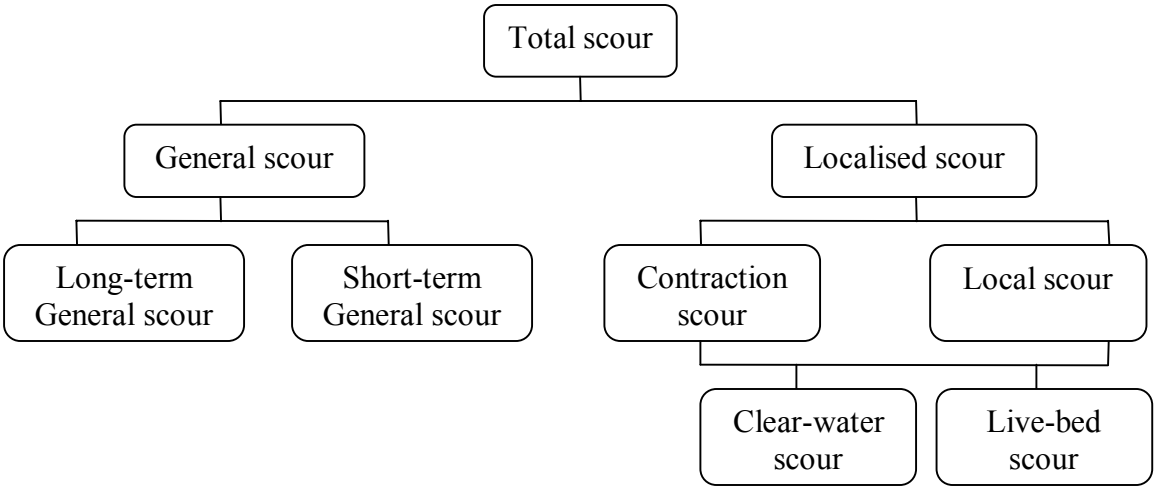


Figure 2.1. An organogram showing various types of scour
(Modified from Cheremisinoff et al. 1987)

*General scour* – This type of scour deals with the changes in river bed elevation due to natural/human-induced causes with the effect of causing an overall lowering of the longitudinal profile of the river channel. It occurs through a change in the river regime resulting in general degradation of the bed level. General scour develops irrespective of the existence of a bridge. General scour can further be divided into long-term and short-term scour, with the two types being differentiated by the temporal development of the scour (Cheremisinoff et al. 1987). Short-term general scour occurs in response to a single or several closely spaced floods whereas long-term general scour develops over a significantly longer time period, usually of the order of several years, and includes progressive degradation and lateral bank erosion.

*Localised scour* – In contrast to general scour, localised scour is directly attributable to the existence of a bridge or other riverine structures. Localised scour can further be divided into *contraction* and *local scour*.

*Contraction scour* – This type of scour occurs as a result of the constriction of a channel or waterway, either due to a natural means or human alteration of the floodplain. The effect of such a constriction is a decrease in the flow area and an increase in the average flow velocity, which consequently causes an increase in the erosive forces exerted on the channel bed. The overall effect of this phenomenon is the lowering of the channel bed. A bridge with approaches or abutments encroaching onto the floodplain of a river is a common example of contraction scour.

*Local scour* – This type of scour refers to the removal of sediment from the immediate vicinity of bridge piers or abutments. It occurs as a result of the interference with the flow by piers or abutments, which result in an acceleration of the flow, creating vortices that remove the sediment material in the surroundings of the bridge piers or abutments. Scour occurring as a result of spur dykes and other river training works is also an example of local scour. Figure 2.2 shows the typical appearance of local scour around bridge piers. As it is related to the main thrust of this study, local scour is discussed in much more detail in the following sections.


Figure 2.2. Photograph of local scour at rectangular piers
(With permission from: www.pepevasquez.com)

## 2.2 Local scour mechanisms

It has long been established that the basic mechanism causing local scour at piers is the down-flow at the upstream face of the pier and formation of vortices at the base (Heidarpour et al. 2003; Muzzammil et al. 2004). The flow decelerates as it approaches the pier coming to rest at the face of the pier. The approach flow velocity, therefore, at the stagnation point on the upstream side of the pier is reduced to zero, which results in a pressure increase at the pier face. The associated stagnation pressures are highest near the surface, where the deceleration is greatest, and decrease downwards (Melville and Raudkivi 1977). In other words, as the velocity is decreasing from the surface to the bed, the stagnation pressure on the face of the pier also decreases accordingly i.e. a downward pressure gradient. The pressure gradient arising from the decreased pressure forces the flow down the face of the pier, resembling that of a vertical jet. The resulting down-flow impinges on the streambed and creates a hole in the vicinity of the pier base. The strength of the down-flow reaches a maximum just below the bed level. The down-flow impinging on the bed is the main scouring agent (Melville and Raudkivi 1977).

Figure 2.3 shows the flow and scour pattern at a circular pier. As illustrated in the figure, the strong vortex motion caused by the existence of the pier entrains bed sediments within the vicinity of the pier base (Lauchlan and Melville 2001). The down-flow rolls up as it continues to create a hole and, through interaction with the oncoming flow, develops into a complex vortex system. The vortex then extends downstream along the sides of the pier. This vortex is often referred to as horseshoe vortex because of its great similarity to a horseshoe (Breusers et al. 1977). Thus the horseshoe vortex developed as a result of separation of flow at the upstream face of the scour hole excavated by the down-flow. "The horseshoe vortex itself is a lee eddy similar to the eddy or ground roller downstream of a dune crest" (Breusers and Raudkivi 1991). The horseshow vortex is very effective at transporting the dislodged particles away past the pier. The horseshoe vortex is as a result of scour but is not the cause of scour (Breusers and Raudkivi 1991). As the scour depth increases, the horseshoe vortex strength diminishes, which automatically leads to a reduction in the sediment transport rate from the base of the pier (Lagasse et al. 2001).

As shown in Figure 2.3, besides the horseshoe vortex in the vicinity of the pier base, there are also the vertical vortices downstream of the pier referred to as wake vortices (Dargahi 1990). The separation of the flow at the sides of the pier produces the so-called wake vortices. These wake vortices are not stable and shed alternately from one side of the pier and then the other. It should be noted, however, that both the horseshoe and wake vortices erode material from the base region of the pier. The intensity of the wake vortices is drastically reduced with distance downstream, such that sediment deposition is common immediately downstream of the pier (Richardson and Davies 1995).

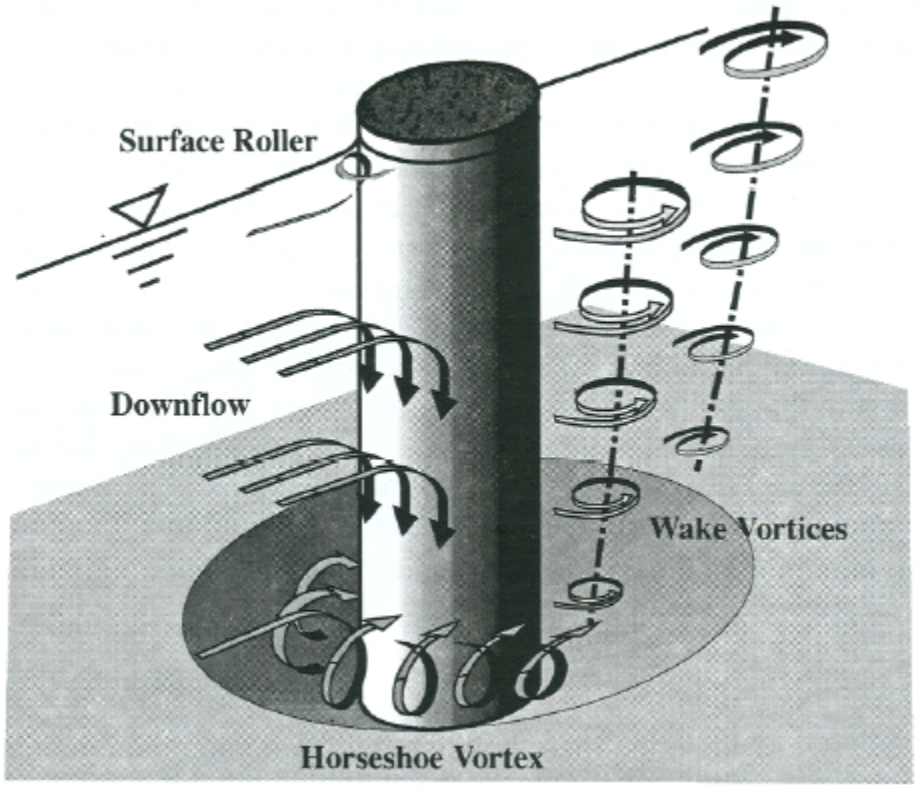


Figure 2.3. Illustration of the flow and scour pattern at a circular pier (Melville & Coleman 2000)

## 2.3 Incipient motion of sediment particles

Knowledge of the hydraulic conditions at which motion of sediment particles of a given size is initiated is of considerable significance in scour-related studies. This condition is referred to as incipient motion or threshold of motion. The maximum scour depth is

achieved at the condition of incipient sediment motion (Breusers and Raudkivi 1991). It is customary to characterise the types of local scour depending on whether the bed sediment upstream of a bridge pier is at rest or not. The threshold of motion condition plays an important role in this regard. This section discusses how the hydraulic flow conditions of incipient motion can be determined using the critical tractive force approach.

*Critical tractive force method*: In this method, the tractive force applied by the flowing water on the channel bed in the flow direction is adjudged the cause of the movement of the sedimentary particles. When the shear stress on the bed is equal to the critical shear stress for a given size of a bed material, individual particles on the bed are said to start moving. The critical tractive force method is the most widely used and, besides, it is also taken to be more rational and reliable than the other approaches (Garde and Ranga-Raju 1985) The critical tractive method is, therefore, described in more detail below.

The major variables that affect the incipient motion of sediment particles on a level bed include: the sediment density ($\rho_s$), water temperature ($T_.$), water density ($\rho$), acceleration due to gravity (g), water viscosity ($\nu$), depth averaged velocity (u), flow depth ($y_o$), grain roughness ($k_s$) and the critical shear stress ($\tau_c$) (Chang 1988). When the shear stress on the bed is equal to the critical shear stress for a given size of a bed material, individual particles on the bed start moving. To find the critical shear stress, the non-dimensional critical shear stress ratio can be obtained from the Shields diagram for the observed condition of temperature, specific gravity and the median size of the sediment material. Shield's diagram is one of the methods for finding the critical shear stress. However, since the Shields diagram has the critical shear stress as an implicit variable that cannot be deduced directly, a parameter in the ASCE Sedimentation Manual (1975) written as

$$\frac{d_{50}}{\upsilon}\left[0.1\left(\frac{\gamma_s}{\gamma}-1\right)gd_{50}\right]^{1/2}$$

can be employed. The parameter appears as a family of parallel lines on the Shields diagram (Chang 1988). From the value of this parameter, the dimensionless stress, $\tau_*$,

can be read directly at the intersection of the line with the Shields curve. The critical shear stress, $\tau_c$, can be calculated using the value of $\tau_*$ obtained, viz.

[2.1] $$\tau_c = \tau_*(\gamma_s - \gamma)d_{50}$$

where $d_{50}$ is the median size of the sediment particle, and $\gamma_s$ and $\gamma$ are the specific weight of the sediment material and water, respectively.

The critical friction velocity, $u_{*c}$, can be calculated using

[2.2] $$u_{*c} = \left(\frac{\tau_c}{\rho}\right)^{1/2}$$

Alternatively, $u_{*c}$ can be determined for the $d_{50}$ size for quartz sand in water at 20ºC using the formulae provided in Melville and Coleman (2000), viz.

[2.3a] $$u_{*c} = 0.0115 + 0.0125 d_{50}^{1.4} \qquad 0.1 \text{ mm} < d_{50} < 1 \text{ mm}$$

[2.3b] $$u_{*c} = 0.0305 d_{50}^{0.5} + 0.0065 d_{50}^{-1} \qquad 1 \text{ mm} < d_{50} < 100 \text{ mm}$$

The corresponding critical velocity, $u_c$, which is dependent on the flow depth, can be determined using the semi-logarithmic average velocity equation for a rough bed given by Chiew and Lim (2000) and Chang (1988) as

[2.4] $$\frac{u_c}{u_{*c}} = 5.75 \log \frac{y_o}{k_s} + 6$$

The shear velocity ratio, $u_*/ u_{*c}$ or $u/u_c$, also known as the flow intensity, demarcates the onset of sediment transport. The symbol, $u_*$, is the shear velocity in this case while u is the mean approach flow velocity. The grain roughness, $k_s$ is taken as equal to $2d_{50}$.

## 2.4 Classification of local scour

Chabert and Engeldinger (1956) identified two main classifications of local scour at piers based on the mode of sediment transport by the approaching stream, namely *clear-water scour* and *live bed scour*. These classifications depend on the ability of the flow approaching the bridge to transport bed material (Chiew and Melville 1987). Clear-water scour is defined as the case where the bed sediment is not moved by the approach flow, or rather where sediment material is removed from the scour hole but not refilled by the approach flow (Melville 1984). Similarly, Raudkivi and Ettema (1983) defined clear-water scour as occurring when the bed material at the upstream side of the pier is not in motion. Live-bed scour, on the other hand, occurs when there is general transportation of the bed material by the flow. Live-bed scour occurs when the scour hole is continually replenished with sediment by the approach flow (Dey 1999).

In clear-water scour, the maximum scour depth is reached when the flow can no longer remove particles from the scour hole (Breusers et al. 1977). In live-bed scour, an equilibrium scour depth is reached when, over a period of time, the quantity of material eroded from the scour hole by the flow equals the quantity of material supplied to the scour hole from upstream (Melville 1984). The temporal development of the maximum scour depth under clear-water and live-bed scour conditions is illustrated in Figure 2.4.

In coarse-grained materials (sands and gravels), an equilibrium local scour condition is rapidly attained with time in live-bed conditions (and then oscillates in response to the passage of bed forms). On the other hand, an equilibrium condition is achieved rather more slowly and asymptotically in clear-water conditions (Raudkivi and Ettema 1983).

Clear-water scour occurs for mean flow velocities up to the threshold velocity for bed sediment entrainment, i.e., $u \leq u_c$ (or $u/u_c \leq 1$) (Melville and Chiew 1999). In contrast, live-bed scour occurs when $u > u_c$ (or $u/u_c > 1$). The maximum scour depth, however, occurs at $u = u_c$. Clear-water scour depth reaches its maximum over a longer period of time than would occur for live-bed condition. Furthermore, local clear-water scour may not reach the maximum depth until after several floods (Richardson and Davies 2001). According to Richardson and Davies, the maximum clear-water pier scour depth is

about 10 percent greater than the equilibrium depth for live-bed pier scour. The time taken for equilibrium scour depth to develop increases rapidly with flow velocity in clear-water conditions but decreases rapidly for live-bed scour (Melville and Chiew 1999). Since an equilibrium clear-water scour depth is reached asymptotically with time, it can take a very long time for the equilibrium scour hole to form.

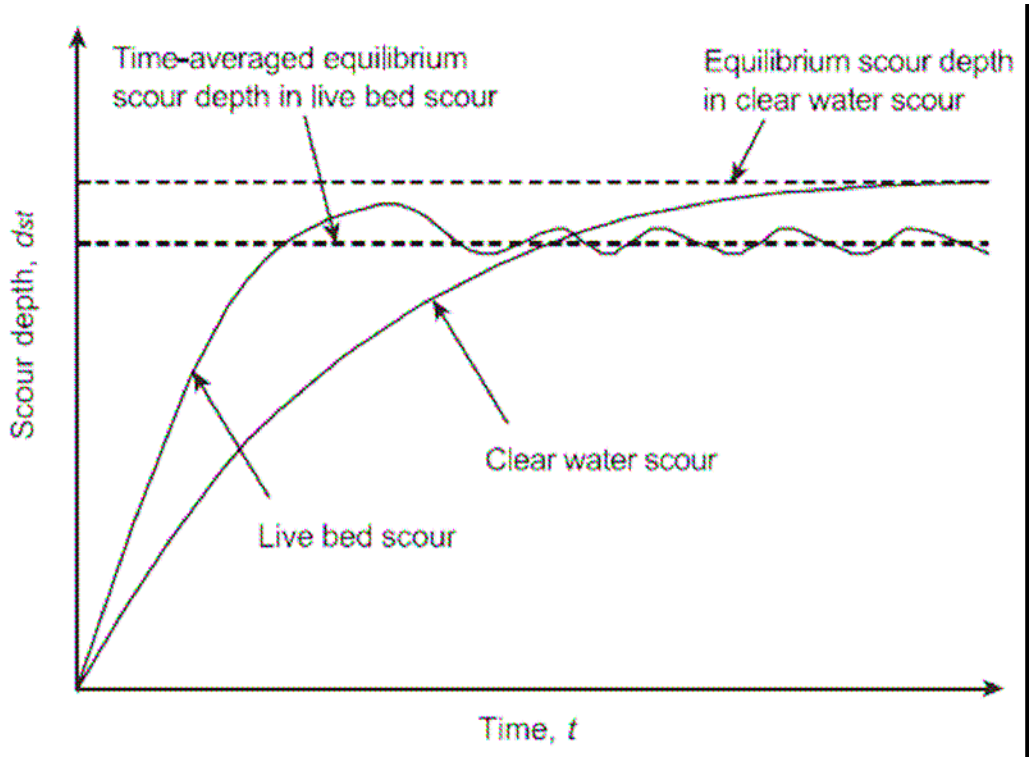


Figure 2.4. Clear-water and live-bed scour conditions (Raudkivi and Ettema 1983)

Richardson and Davies (2001) mentioned that typical clear-water scour situations can be found in (a) coarse-bed material streams, (b) flat gradient streams during low flow, (c) local deposits of larger bed materials that are larger than the biggest fraction being transported by the flow (rock riprap is a special case of this situation), (d) armoured streambeds where the only locations that tractive forces are adequate to penetrate the armour layer are at piers and/or abutments, and (e) vegetated channels or overbank areas.

## 2.5 Classification of scour parameters

Factors which affect the magnitude of the local scour depth at piers as given by Richardson and Davies (1995), Raudkivi and Ettema (1983) and Lagasse et al. (2001) are (1) approach flow velocity, (2) flow depth, (3) pier width, (4) gravitational acceleration, (5) pier length if skewed to the main flow direction, (6) size and gradation of the bed material, (7) angle of attack of the approach flow to the pier, (8) pier shape, (9) bed configuration, and (10) ice or debris jams.

According to Breusers et al. (1977) and Ansari et al. (2002) the parameters listed above can be grouped into four major headings, viz.

- *Approaching stream flow parameters:* Flow intensity, flow depth, shear velocity, mean velocity, velocity distribution and bed roughness.
- *Pier parameters*: Size, geometry, spacing, number and orientation of the pier with respect to the main flow direction (i.e., angle of attack).
- *Bed sediment parameters:* Grain size distribution, mass density, particle shape, angle of repose and cohesiveness of the soil.
- *Fluid parameters*: Mass density, acceleration due to gravity and kinematic viscosity.

Dey (1997) also included the time of scouring as an additional parameter. Also, Oliveto and Hager (2002) and Oliveto and Hager (2005) found that the principal parameter influencing the scour process is the densimetric particle Froude number. The definition of densimetric Froude number as given by Oliveto and Hager (2002) is

[2.5a] $$F_d = \frac{u}{\sqrt{g' d_{50}}}$$

[2.5b] $$g' = \left[\frac{\rho_s - \rho}{\rho}\right] g$$

where g` is the relative gravitational acceleration, $\rho_s$ is the sediment density, $\rho$ is the fluid density (water in this case), u is the approach flow velocity, $d_{50}$ is the median grain size and $F_d$ is densimetric Froude number. A brief summary of the above parameters and their effects is discussed below.

### 2.5.1 Flow intensity

Flow intensity is defined as the ratio of the shear velocity ($u_*$) to the critical shear velocity ($u_{*c}$) or the ratio of the approach mean velocity to the critical mean velocity (Melville and Chiew 1999). Under clear-water conditions, the local scour depth in uniformly-graded sediment increases almost linearly with velocity to a maximum at the threshold velocity (Melville and Coleman 2000). The maximum scour depth is reached when the ratio $u_*/u_{*c} = 1$ and the corresponding maximum scour depth is called the threshold peak. As the velocity exceeds the threshold velocity, the local scour depth in uniform sediment first decreases and then increases again to a second peak, but the threshold peak is not exceeded provided the sediment is uniform. The same trend was observed by Chabert and Engeldinger (1956), Ettema (1980), Raudkivi and Ettema (1983), Laursen and Toch (1956), Breusers et al. (1977) and Chiew (1984). The general conclusion was that the maximum local scour depth in uniform sediments occurs at the threshold condition for clear-water scour conditions.

### 2.5.2 Flow depth

The influence of flow depth on the scour depth has been discussed by many authors (e.g. Chabert and Engeldinger 1956; Laursen and Toch 1956; Dey 1977; Breusers et al. 1977; Breusers and Raudkivi 1991; Hoffmans and Verheij 1997; Ettema 1980; Melville and Coleman 2000). The presence of the pier in the channel causes a surface roller around the pier and a horseshoe vortex at the base of the pier. Flow depth affects local scour depth when the horseshoe vortex is affected by the formation of the surface roller (or bow wave) that forms at the leading edge of the pier. The two rollers, (i.e., the bow wave and the horseshoe vortex) rotate in opposite directions. In principle, as long as

there is no interference between the two rollers, the local scour depth does not depend on the flow depth but depends only on the pier diameter. In such an instance, often called deep flow, the local scour is said to occur at narrow piers. As the flow depth decreases, the surface roller becomes relatively more dominant and causes the horseshoe vortex to be less capable of entraining sediment. Therefore, for shallower flows, the local scour depth is reduced. Subsequently, in a very shallow flow, the local scour is dependent on the flow depth and the local scour is said to occur at a wide pier. Melville and Chiew (1999) claimed that these trends are evident in the laboratory data of many researchers, including Chabert and Engeldinger (1956), Laursen and Toch (1956), Breusers et al. (1977) and Ettema (1980).

The flow shallowness, $D/ y_o$, (where D and $y_o$ are the pier diameter and flow depth, respectively) can be used to classify the influence of the flow depth in relation to the width of the pier (Melville and Coleman 2000). Table 2.1, as adapted from Melville and Coleman, shows a classification of local scour processes at bridge pier foundations.

Table 2.1. Classification of local scour processes at bridge pier foundations

| **Class** | **$D/y_o$** | **Local scour dependence** |
|---|---|---|
| **Narrow** | $D/y_o < 0.7$ | $y_s \alpha D$ |
| **Intermediate width** | $0.7 < D/y_o < 5$ | $y_s \alpha (Dy_o)^{0.5}$ |
| **Wide** | $D/y_o > 5$ | $y_s \alpha y_o$ |

In summary, observations showed that at shallow flow depths the local scour at piers increases with flow depth, but for larger water depth (i.e., deep flow), the scour depth becomes independent of flow depth but depends on the pier diameter.

### 2.5.3 Pier size

Experiments have clearly shown that it is possible to relate the scour depth to the size of the pier (Breusers et al. 1977). This observation, can be explained physically by the fact that scouring is due to the horseshoe vortex system whose dimension is a function of the

diameter of the pier. It has also been observed by Shen et al. (1969) that, the horseshoe vortex, being one of the main scouring agents, is proportional to the pier Reynolds number ($R_b$), ($R_b = uD/\upsilon$), which in turn is a function of the pier diameter. For the same value of mean approach flow velocity, therefore, the scour depth is proportional to the pier width. The influence of pier size on the local scour depth is of interest when data from the laboratory are interpreted for field use (Breusers and Raudkivi 1991). Under clear-water conditions, pier size influences the time taken to reach the ultimate scour depth but not its relative magnitude $y_s/D$, if the influence of relative depth, $y_o/D$, and relative grain size $D/d_{50}$ on the local scour depth are excluded (Breusers and Raudkivi 1991). They also concluded that the volume of the local scour hole formed around the upstream half of the perimeter of the pier is proportional to the cube of the pier diameter (or the projected width of the pier). The larger the pier the larger the scour hole volume and also the longer is the time taken for the development of the scour hole for a given shear stress ratio.

### 2.5.4 Pier shape

Bridge piers are constructed of various shape. The most common shapes used are circular, rectangular, square, rectangular with chamfered end, oblong, lenticular and Joukowski. Figure 2.5 shows a schematic illustration of some pier shapes. The effect of pier shape has been reported by many researchers (e.g. Laursen and Toch 1956, Dey 1997, Breusers 1977, Breusers and Raudkivi 1991, Melville and Coleman 2000). The blunter the pier, the deeper the local scour has been the general conclusion. The shape of the downstream end of the pier is concluded to be of little significance on the maximum scour depth. The pier shape is often accounted for by using a shape factor. Melville and Chiew (2000) cited the work of Mostafa (1994) in which shape factors for uniform piers, that is piers having constant section throughout their depth, was proposed. Mostafa measured the local scour depths for variety of different pier shapes all having the same projected width (140 mm). From his results, a circular pier produced the least scour while a rectangular pier having blunt ends produced the most scour. In practice, shape factors are only significant if axial flow can be maintained

because even a small angle of attack will eliminate any benefit from a streamlined shape (Melville and Chiew 2000). Non-uniform piers include piers with piled foundations, caissons, slab footings and tapered piers. For piers tapered on the upstream and downstream faces, the slope, in elevation, of the leading edge of the pier affects the local scour depth. Downward-tapered piers induce deeper scour than does a circular pier of the same width.

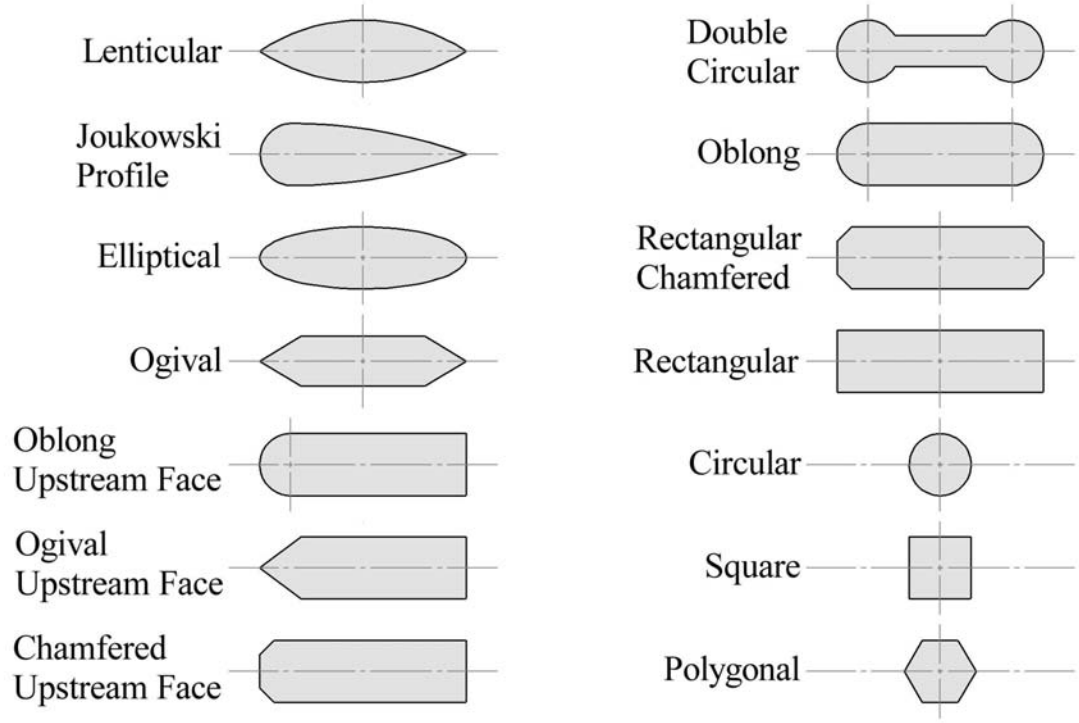


Figure 2.5. Schematic illustration of some common pier shapes

### 2.5.5 Alignment or angle of attack

The effect of alignment, also referred to as the influence of the angle of flow attack, is the effect of the angle between the direction of the bridge pier and the direction of the flow (Hoffmans and Verhejj 1997). The depth of local scour for all shapes of pier is highly dependent on the alignment or orientation of the pier to the flow. However, the exception to this is a circular pier. As the angle of attack increases, the scour depth increases due to the increase in the effective frontal width of the pier (Melville and Coleman 2000). The effect of the pier length is insignificant if the pier is aligned with

the flow. If the pier is skewed to the flow, the pier length has a substantial effect on the scour experienced. For example, Melville and Coleman (2000) demonstrated that the local scour depth at a rectangular pier of an aspect ratio of eight is nearly tripled at an angle of attack of $30^o$ when compared to the same pier aligned with the flow.

The depth of scour has been shown to be functionally related to the projected width of the pier (Breusers and Raudkivi 1991). Here, the projected width of the pier is the width normal to the flow direction. Therefore, the projected width of the pier, which increases with the angle of attack of the flow, is related to the scour depth. As the angle of attack increases, the point of maximum scour depth moves along the exposed side of the pier towards the rear, and the scour depth at the rear becomes greater than at the front face of the pier. Multiplying factors for angle of attack for different pier length-width ratios proposed by Laursen and Toch (1956) are commonly used. In general, angle of attacks greater than $5\text{-}10^o$ are to be avoided (Breusers and Raudkivi 1991). In practice, the angle of attack at bridge crossings may change significantly during floods for braided channels, and it may change progressively over a period of time for meandering channels (Melville and Coleman 2000).

### 2.5.6 Contraction ratio

The equilibrium depth of local scour at a pier is affected by the contraction ratio. For the purpose of experimental investigations, the width of an experimental flume should be at least eight times the pier size for clear-water scour conditions so that blockage effects are minimized (Shen et al. 1969). For live-bed scour, the flume width should be at least 10 times the pier size for scour depths not to be reduced due to bed features being modified as they propagate through the constriction.

### 2.5.7 Sediment coarseness and gradation

The sediment coarseness as defined by Melville and Coleman (2000) is the ratio of the pier width (D) to the mean grain size of the sediment material ($d_{50}$) (i.e. $D/d_{50}$).

According to the authors, the local scour is affected by the sediment size as long as the sediment coarseness ratio $D/d_{50} < 50$. For $D/d_{50} > 50$, the local scour is not influenced by the sediment coarseness. For pier scour, Ettema (1980) explained that, for smaller values of the sediment coarseness ratio, individual grains are large relatively to the groove excavated by the down-flow and erosion is impeded because the porous bed dissipates some of the energy of the down-flow. For $D/d_{50} < 8$, the individual grains are so large relative to the pier that scour is mainly due to entrainment at the flanks of the pier (Melville and Coleman, 2000).

Sediment gradation is usually characterized using the geometric standard deviation of the sand size, $\sigma_g = (d_{84}/d_{16})^{1/2}$. For natural river sand, $\sigma_g$ is about 1.8 while for uniform sand $\sigma_g$ is about 1.3 (Hoffmans and Verhejj 1997). Ettema (1980) studied the effect of sediment gradation on the local scour depth at a circular pier under clear-water scour conditions. He conducted his experiments at the threshold of motion condition for the median size of the sediment material used. The conclusion reached was that the rate of scour hole development and the equilibrium scour depth decreases as the standard deviation of the particle size distribution increases. For a non-uniform sediment material (i.e. at a higher value of $\sigma_g$), armouring occurs on the approach flow bed and at the base of the scour hole around the threshold condition, $u_*/u_{*c} \approx 1$. The armouring at the base of the scour hole leads to a considerable reduction of the local scour depth. However, sediment non-uniformity has only a small effect on the scour depth at a high value of $u_*/u_{*c}$, where the flow is capable of entraining most grain sizes within the non-uniform sediment.

### 2.5.8 Sediment size

The effects of the grain size and the density of the sediment material are often expressed as a function of the critical flow velocity for the initiation of sediment motion. Breusers and Raudkivi (1991) reported on the work of Raudkivi and Ettema (1977a,b) in which the effect of sediment size on local depth of scour at a bridge pier was studied. The experiments were conducted under clear-water conditions and using a pier of diameter

102 mm and a flume 1.5 m in width. It was observed that a sediment size of $d_{50} \leq 0.7$ mm leads to a formation of ripples, whereas sediment size of $d_{50} \geq 0.7$ mm do not cause ripples. It was further stated that the results for grain sizes which lead to the formation of ripples ($d_{50} \leq 0.7$ mm) were different from those for larger grain sizes for which ripples do not form ($d_{50} \geq 0.7$ mm). According to Raudkivi and Ettema, for non-ripple-forming sediments ($d_{50} \geq 0.7$ mm), experiments can be run successfully with a flow condition, $u_* \sim 0.95u_{*c}$, without the upstream bed being disturbed by the approach flow, whereas with finer sands ($d_{50} < 0.7$ mm) a flat bed cannot be maintained for the same flow condition. Therefore, if the sediment is uniform sand with grain size $d_{50} < 0.7$ mm, a flat bed cannot be maintained near the threshold shear stress condition because ripples will develop, with a small amount of general sediment transport taking place so as to replenish some of the sand scoured at the pier. Thus, true clear-water scour conditions cannot be maintained for this case.

It was concluded by Breusers and Raudkivi (1991) that ripples usually developed at shear velocities $u_*$ above $0.6u_{*c}$ for sediment of size, $d_{50} < 0.7$ mm. Thus, clear-water conditions are not maintained long enough for the finer sands to reach the same maximum scour depth that occurs for coarser non-ripple-forming sediments because of the development of live-bed scour after the commencement of the experiment. However, an exception occurs if the geometric standard deviation of the sand size, $\sigma_g \sim 1.3 - 1.5$. In this range of geometric standard deviation, the sediments are not uniform and the coarser grains armour the channel surface but are not large enough to armour the scour hole where the agitation is higher. Then, clear-water scour depths of the same order as observed with non-ripple-forming sediments can be reached.

## 2.6 Development of maximum scour depth with time

Chabert and Engeldinger (1956) described the behavioral pattern of scour at a cylindrical pier with respect to the variation of scour depth with time. In clear-water scour, equilibrium scour depth is approached asymptotically with time, while in live-bed scour the scour develops rapidly and then fluctuates in response to the passage of bed

forms. According to Shen et al. (1969), the equilibrium scour depth in live-bed scour is less than in clear-water scour by 10% (Figure 2.4).

### 2.6.1 Equilibrium scour depth and some definitions of time to equilibrium

Equilibrium scour is said to occur when the scour depth does not change appreciably with time. Equilibrium can also be defined as the asymptotic state of scour reached as the scouring rate becomes very small or insignificant. An equilibrium between the erosive capability of the flow and the resistance to motion of the bed materials is progressively attained through erosion of the flow boundary. The concept of an equilibrium scour condition is widely reported in the literature. Franzetti et al. (1982) made reference to the work of both Baker and Qadar in which the existence of an equilibrium scour condition was confirmed. In this context, Franzetti et al. refer to equilibrium as the state of scour development where no further change occurs with time.

The occurrence of a non-equilibrium condition, however, has also been reported by many researchers. Because an equilibrium clear-water scour condition is approached asymptotically with time, Melville and Chiew (1999) opined that it can take an infinite amount of time for the equilibrium scour hole to develop. They observed that an apparent equilibrium scour hole may continue to deepen at a relatively slow rate long after ‘‘equilibrium conditions” were thought to exist. For an equilibrium scour condition to be achieved in small-scale laboratory experiments of clear-water scour, tests must be run for several days (Melville and Coleman 2000). Melville and Coleman also pointed out that experiments carried out for a shorter period of time, say 10 to 12 hours, can result in a scour depth less than one-half of the equilibrium scour depth.

The definition of time to scour equilibrium adopted for a given test plays an important role in the results obtained and also in the conclusions reached (Franzetti et al. 1982). They also observed that, if care is not taken, the definition of time to equilibrium scour depth can affect the results such that the same experiment carried out under the same experimental conditions but for a different timeframe can yield a different conclusion. Several researchers have come up with different definitions of time to equilibrium scour

depth (e.g. Heidarpour et al. 2003; Zarrati et al. 2004; Mia and Nago 2003; Sheppard et al. 2004). Because it takes a very long time for an equilibrium condition to be attained, it is time demanding to carry out experiments of such long duration. In view of this, the maximum duration of the experiments performed by Bozkus and Osman (2004) was limited to two hours. Although the ultimate equilibrium scour depth was not achieved within two hours, they observed that the rate of increase in the depth of the scour hole was substantially reduced after two hours. Ettema (1980) defined the time to equilibrium scour as the time at which no more than 1 mm of incremental scour was realised within a timeframe of four hours. Sheppard et al. (2004) and Melville and Chiew (1999) stopped their experiments when the change in the scour depth did not exceed 5% of the pier diameter during a 24-hour period. A uniform period of 24 hours was used for all of the tests carried out by Lauchlan (1999). Jones and Sheppard (2000) noted that the duration for many of the experiments reported in the literature was insufficient for the scour depth to have reached an equilibrium condition and, as such, much of the data reported therein may not be useful. They also found that the lack of complete reporting of experimental conditions rendered some data unusable. It may be concluded, therefore, that the whole concept of an experimental equilibrium scour condition warrants further investigation.

### 2.6.2 Temporal development of scour

The process of local scour in the vicinity of bridge piers is time dependent. Time development of scour is the level of maximum scour depth attained in a given time. It is often represented in graphical form by plotting the maximum scour depth against the time. Because of the complexity of the scour process, the majority of the literature is on the determination of the maximum equilibrium scour depth for a given flow and sediment condition and pier geometry. The time development of scour has attracted the attention of many researchers (e.g. Melville and Chiew 1999; Mashair et al. 2004). Dey (1999) was also of the view that time is an important factor in scour studies. The temporal development of scour is dependent on the condition of flow, geometry and sediment parameters (Melville and Chiew 1999).

Melville and Chiew (1999) studied the temporal development of local scour at bridge piers and developed equations for estimating the local scour depth under clear-water flow conditions. Their research was motivated by the fact that a number of investigations in the literature were reporting equilibrium scour depths and drawing conclusions from these values on tests that clearly did not last long enough to reach an equilibrium state. In some cases, the tests were as short as four hours. In an attempt to standardise the criteria for reaching an equilibrium state, Chiew and Melville (1999) collected data from about 35 experiments that covered a wide range of pier diameter, flow depths, and approach flow velocities. Two different sediment diameters in the coarse range were employed. The tests were allowed to run until equilibrium was reached. The authors defined the time to equilibrium as the time when the rate of scour was reduced to five percent of the pier diameter in a 24 hour period. This criterion yielded values of time to equilibrium as high as three days for some cases. The data indicated that, for a given approach flow depth and velocity ratio, the time to equilibrium increases with increasing pier diameter. This result is expected since the size of the scour hole is related to the pier width and a larger hole requires a longer scour time to stabilise. The data also showed that, all other things being equal, the time to an equilibrium scour condition increases with an increase in the velocity ratio.

For bridge piers experiencing clear-water conditions, the equilibrium time scale increases rapidly with flow intensity, reaching a maximum at the threshold condition (Melville and Coleman 2000; Melville and Chiew 1999). The authors observed that there is interdependence between the time required to reach equilibrium scour and the depth of scour at equilibrium. Melville and Chiew (1999) concluded that both the time required to reach equilibrium scour and the depth of scour at equilibrium are influenced similarly by the same set of flow and sediment parameters.

As shown in Figure 2.6, Ettema (1980) noted that, when the depth of scour was plotted versus the logarithm of time, there were three distinct phases of the scour process. He referred to the three phases as the initial phase, the erosion phase, and the equilibrium phase. As shown in the figure, in the initial phase (i.e., region 1), rapid scouring occurs due to the downflow at the pier face impinging on the planar bed. This phase is

characterised by a steep on the graph. The second phase, which is known as the principal eroding phase, starts when the horseshoe vortex starts to dominate the scouring process. The main erosion occurs at the front of the pier. During the erosion phase (i.e., region 2 in Figure 2.6), the scour hole develops as the horseshoe vortex grows in both size and strength. The slope of the line in this phase is considerably less than in the previous phase. In the final stage, called the equilibrium phase (i.e., region 3 in Figure 2.6), the equilibrium depth has been reached and hence no further scour occurs as the horseshoe vortex ceases to excavate further. At this point, the slope of the line is zero.

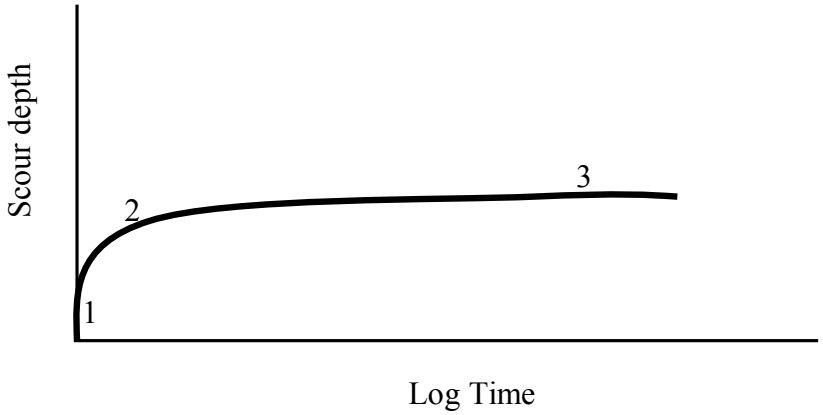


Figure 2.6. Schematic illustration of the three distinct phases of the scour process (Modified from Ettema 1982)

### 2.6.3 Some formulas for describing temporal development of scour depth

Franzetti et al. (1982) studied the influence of test duration on the ultimate scour depth at a circular pier and suggested an exponential function of the form

[2.6] $$y_s = y_{se}\left(1 - \exp\left(-BT^C\right)\right)$$

[2.7] $$T = \frac{ut}{D}$$

where $y_s$ = scour depth; $y_{se}$ = ultimate or equilibrium scour depth; B and C are constants; T = dimensionless time; u = mean velocity of the approach flow; t = time; and D = pier diameter. In order to arrive at the values of the constants, B and C, Franzetti et al. used

their own data for which $d_{50}$ = 2.13 mm (synthetic cohesionless soil), the approach flow velocity ranged from 0.13 – 0.19 m/s, the pier diameter ranged from 26.7 – 48.0 mm, and the critical flow velocity was 0.19 m/s. Franzetti et al. also made use of the data from Chabert and Engeldinger (1956) in which $d_{50}$ value ranged between 0.26 – 0.52 mm, the approach flow velocity ranged from 0.18 – 0.37 m/s, the pier diameter ranged from 50 – 150 mm and the critical flow velocity ranged between 0.21 – 0.38 m/s. Applying the least squares method to the experimental values of each of the tests considered, Franzetti et al. found that the variability of C is small, such that C can be approximated with an average value of 1/3 (i.e. C = 1/3). It was also found that the values of the constant B varied from test to test ($0.021 < B < 0.042$). Franzetti et al. adopted the average value of B = 0.028. The Franzetti et al. equation now becomes

$$[2.8] \qquad y_s = y_{se}\left(1 - \exp\left(-0.028T^{1/3}\right)\right)$$

The concept of an equilibrium scour condition is widely reported in the literature. While an enticing concept, researchers have found it difficult to determine the equilibrium scour condition experimentally. These difficulties have led to the proposal of such expressions that do not include equilibrium scour by some researchers such as Cunha (1975) and Oliveto and Hager (2002). Cunha (1975) gave an expression of the form $y_s = KT^C$, where K has the unit of length, C is a dimensionless constant and T is the dimensionless time.

It was shown by Simarro-Grande and Martin-Vide (2005) that, for a short duration test, no equilibrium scour can be predicted by using the Franzetti et al. (1982) expression. It was also mentioned by Simarro-Grande and Martin-Vide that recourse can be made to the Cunha (1975) expression in such a situation. By comparing the Cunha (1975) expression with that of Franzetti et al. (1982), Simarro-Grande and Martin-Vide found that the value of K can be approximated as $K = y_{se}B$ and also observed that the value of C is approximately equal for each equation. The symbols B and C are as defined in [2.6].

In order to clarify the effect of time on the development of scour at a bridge pier under clear-water conditions, Melville and Chiew (1999) conducted several series of experiments in which the depth of scour was monitored as the scour hole developed. They combined their data with some data from other researchers and developed an equation for predicting the time to reach the clear-water equilibrium scour depth. The combined data were well represented by the following equations:

[2.9] $$\frac{y_s}{y_{se}} = \exp\left\{-0.03\left|\frac{u_c}{u}\mathrm{Ln}\left(\frac{t}{t_e}\right)\right|^{1.6}\right\}$$

[2.10] $$T^* = \frac{ut_e}{D}$$

[2.11] $$T^* = 1.6\mathrm{x}10^6\left(\frac{y_o}{D}\right)^{0.25} \quad \text{for} \quad \frac{y_o}{D} \le 6$$

[2.12] $$T^* = 2.5\mathrm{x}10^6 \quad \text{for} \quad \frac{y_o}{D} > 6$$

where T* is the dimensionless equilibrium time scale and $t_e$ represents the time to the equilibrium scour condition. The critical velocity, $u_c$, which is dependent on the flow depth, was determined using the semi-logarithmic average velocity equation for a rough bed given in [2.4].

On the time development of maximum scour depth, Barkdoll (2000) on the other hand obtained more additional data and compared them with [2.9]. Although the data for circular piers from Barkdoll showed close agreement with that of Melville and Chiew (1999), Barkdoll opined that [2.9] seemed to overpredict the scour depth at a given time. Barkdoll also carried out further experiments on scour using noncircular piers and observed that, while there is some scatter in the data, there is no significant difference in the normalised scour development with time (i.e., $y_s/y_{se}$ vs. $t/t_e$). Barkdoll, therefore, produced a modified form of [2.9] based on a curve fitting to the experimental data. The resulting new equation [2.13] according to Barkdoll fits better to his data when compared with [2.9].

[2.13] $$\frac{y_s}{y_{se}} = \exp\left\{-0.154\left|\frac{u_c}{u}\mathrm{Ln}\left(\frac{t}{t_e}\right)\right|\right\}$$

In his work, Ettema (1980) described the temporal development of local scour around a circular pier with a logarithmic formula given as

$$[2.14] \qquad \frac{y_s}{D} = K_1 \log\left[\left(\frac{d_{50}}{D}\right)\left(\frac{u_* t}{D}\right)\left(\frac{\upsilon}{u_* D}\right)\right] + \log K_2$$

where D = pier diameter; t = time; $y_s$ = scour depth at time t; $u_*$ = shear velocity; $\upsilon$ = kinematic viscosity; and $K_1$ and $K_2$ = coefficients. Ettema obtained the values of $K_1$ and $K_2$ for different values of $d_{50}/D$ and for values of flow intensity, $u_*/u_{*_c}$ equal to 0.90 and 0.95. The general form of [2.14] can be written as

$$[2.15] \qquad \frac{y_s}{D} = K_1 \log X + \log K_2 \quad \text{with } X = \frac{d_{50}\upsilon t}{D^3}$$

where X = non-dimensional parameter that conveys the influence of time on $y_s$.

Sumer et al. (1993) studied the influence of cross-section on wave scour around piles. The equilibrium scour depth and the time scale of the scour process were also investigated. According to Sumer et al., the time variation of the scour depth can be represented approximately in a functional form as

$$[2.16] \qquad y_s = y_{se}\left(1 - \exp\left[\frac{-t}{T_1}\right]\right)$$

where $T_1$ is the time scale. The quantity $T_1$ represents the time period during which the scour depth develops substantially. Sumer et al. stated that the time scale $T_1$ can be predicted from a plot of scour depth vs. time by estimating the slope of the tangent line to the $y_s(t)$ curve at t = 0 as shown in Figure 2.7.

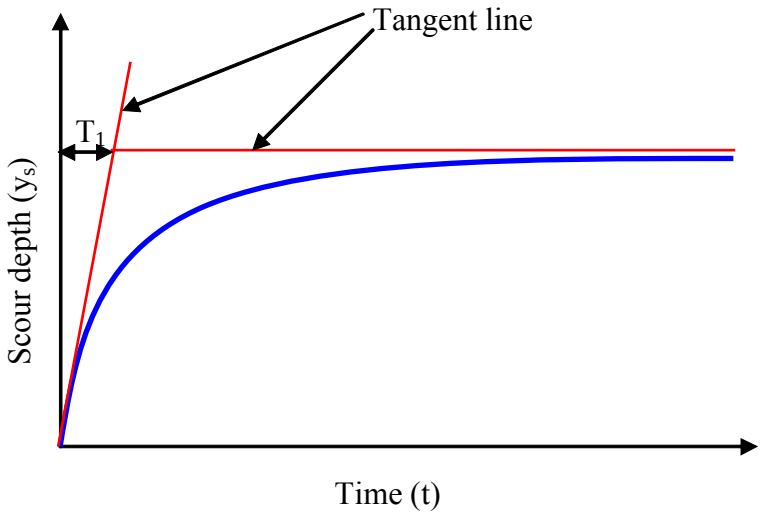


Figure 2.7. Schematic illustration of how to estimate time scale $T_1$ (Sumer et al. 1993)

## 2.7 Equilibrium scour depth prediction equations

Estimation of the depth of scour in the vicinity of bridge piers has been the main concern of engineers for years. While underestimation of the scour depth leads to the design of too shallow a bridge foundation, on the one hand, overestimation leads to uneconomical design on the other (Ting et al. 2001). Therefore, knowledge of the anticipated maximum depth of scour for a given discharge is a significant criterion for the proper design of a bridge pier foundation.

In current practice, the design scour depth is chosen to be the maximum equilibrium scour depth achieved for steady flow under the design flow conditions (Gosselin and Sheppard 1995). A number of studies have been performed with a view to determining the equilibrium scour depth for clear-water scour conditions (e.g. Raudkivi and Ettema 1983). In these studies, the maximum scour depth under steady flow conditions is related to the hydrodynamic and sediment parameters, pier shape, and flow intensity, among others. Empirical equations based on the results of such studies are used in the design of bridge pier by way of computing the expected maximum scour depth for a particular flow condition.

Some of the most common equilibrium scour depth predicting equations are shown in Table 2.2. For a riverine system, the use of equilibrium scour depths is reasonable since,

in many cases, even though the flow is unsteady during storm events, high velocities can persist for long periods of time (Gosselin and Sheppard 1995). "The idea of bed protection and prevention of scour at a pier has attracted a good deal of attention. Reduction of scour depth would mean shallower foundations and reduced cost" (Breusers and Raudkivi 1991).

Table 2.2. Some equilibrium scour depth prediction equations

| Investigator(s) | Equation | Source |
|---|---|---|
| Breusers et al. (1977) [Based on Laursen & Toch (1956) data] | $y_{se} = 1.35K_i b^{0.7} y_o^{0.3}$ where $y_{se}$ = equilibrium scour depth, $K_i$ = 1.0 for circular pier, b = pier width, $y_o$ = flow depth | Hoffmans & Verheij (1997) |
| Neill (1973) | $y_{se} = K_s b$ where $K_s$ = 1.5 for circular pier | Melville & Coleman (2000) |
| Colorado State University (CSU) | $y_{se} = 2.0K_i y_o F_r^{0.43} \left( \frac{b}{y_o} \right)^{0.65}$ where $K_i$ = 1.1 for a circular pier with clear-water scour, $F_r$ = Froude number | Hoffmans & Verheij (1997); HEC-18 |
| Raudkivi & Ettema (1983) | $y_{se} = 2.3bK_\sigma$ where $K = f(\sigma_g) = 1$ for uniform sediment, $\sigma_g$ = geometric standard deviation of the grain size distribution | Dey (1997) |
| Shen et al. (1969) | $y_{se} = 0.000223 R_b^{0.619}$ where $R_b$ = pier Reynolds number | Dey (1997) |

## 2.8 Local scour countermeasures

The purpose of this section of the literature review is to briefly shed light on the various methods available for preventing local scour at a bridge pier. Lagasse et al. (2001) defined countermeasures as "measures incorporated into a highway-stream crossing system to monitor, control, inhibit, change, delay, or minimise stream instability and

bridge scour problems". They further stated that an action plan for monitoring structures during or after flood events can also be considered a countermeasure. Mitigation measures for local scour at bridge piers can be grouped into *armouring techniques* and *flow alteration devices* (Johnson et al. 2001 and Melville and Hadfield 1999).

Armouring techniques are where piers are protected to withstand shear stresses during high flow events while the flow altering device aims to disrupt the flow field around the pier and thereby decrease the erosive strength of the down-flow and horseshoe vortex systems by way of breaking up vortices and reducing the velocity in the vicinity of the piers (Lauchlan 1999). Armoring technique for piers and abutments include riprap, precast concrete units, grout-filled bags, foundation extensions, concrete aprons, and gabions. Armoring devices protect the river bed within the vicinity of the pier against erosive forces. When installed to prevent local scour around a pier, riprap prevents the down-flow and horseshoe vortex systems created by the presence of the pier from removing sediment from the pier face. The use of riprap to deal with pier scour problems is very common in civil engineering practice (Lauchlan 1999).

Flow altering devices at piers include the use of sheet piles and sacrificial piles placed upstream of the pier or circular shields or collars constructed around the piers. Johnson and Niezgoda (2004) identified basically two types of flow altering devices. The first category is used to break up vortices and reduce the high flow velocities, particularly upstream of a pier. Sacrificial piles, such as sill, sheet or cylindrical piles, are common examples of the first category. The second category realigns the flow to prevent local and contraction scour together with bank widening and lateral migration. The common examples of the second category of flow altering devices include vanes and guidebanks. Melville and Hadfield (1999) described sacrificial piles as piles placed upstream of a bridge pier for the purpose of protecting it from local scour. The piles, which themselves may be subject to substantial scour, protect the pier from scour by deflecting the high-velocity flow and creating a wake region behind them. Like sacrificial piles, circular shields or collars placed around the base of the pier can serve the same purpose of breaking up the upstream vortices. Heidarpour et al. (2003) studied the control and

reduction of local scour at bridge pier groups using a slot. In another study, Abdel et al. (2003) were able to reduce scour around bridge piers using internal openings (i.e., slots) through the pier.

In the opinion of Johnson and Niezgoda (2004), "feasibility of and confidence in each of the various countermeasures is a function of many variables which include effectiveness, cost, maintenance, and the ability to detect failure." Therefore, the type of protection that is applicable at a bridge pier depends on the nature of the problem. Lagasse et al. (2001) supplied the design specifications for many of the scour countermeasure techniques.

## 2.9 Application of collars as a countermeasure for local scour at bridge piers

The preceding sections of the chapter have briefly explained the essential terminologies, types of scour and processes germane to the study of local scour at bridge piers and which are also crucial elements needed for greater understanding of the application of collars at bridge piers. This section provides a detailed review of the application of collars for reducing local scour at bridge piers.

### 2.9.1 What are collars?

Melville and Coleman (2000) defined collars as devices attached to the pier at some level usually close to the bed. A collar is in the form of a thin protective disc. A protective disc is a surface which has a negligible thickness, and which is incapable of promoting scour development (Fotherby and Jones 1993). A collar must not be so thick that it causes an obstruction to the flow and advances scour (Whitehouse 1998). A collar extends around the outside edge of the pier with the main objective of protecting the bed from the scouring effect of the down-flow at the pier and the associated vortex action around the base of the pier.

An example of a typical collar and its arrangement for both a rectangular and a circular pier are shown in Figure 2.8. The concept behind a collar as a countermeasure is that the presence of the device will sufficiently inhibit and deflect the local scour

mechanisms so that the scour is reduced. A collar goes by many different names in the literature. A few of the names are a flat plate, horizontal shield and a protective disc.

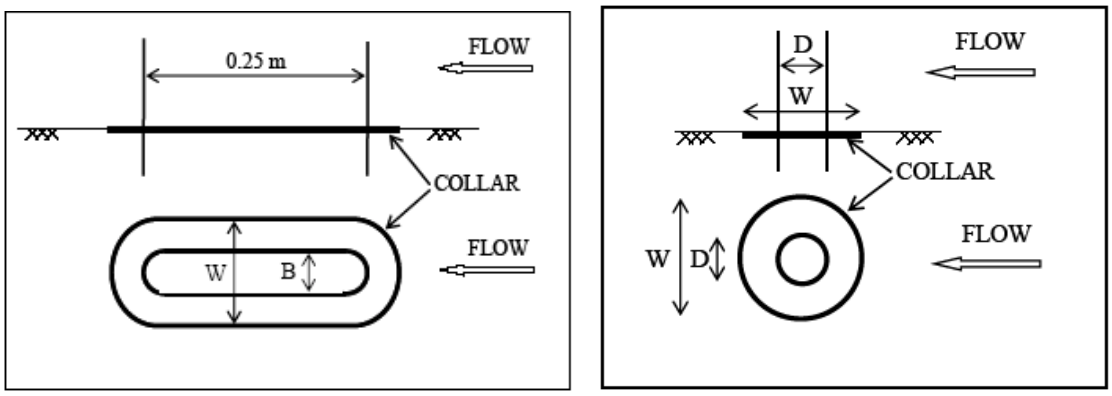


Figure 2.8. Collars positioned around rectangular and circular pier
(Mashahir et al. 2004)

### 2.9.2 Earlier work done and findings on the use of collars

Laursen and Toch (1956) were some of the earlier investigators who worked on the possibility of using a collar-like device for preventing scour at a pier. From their work, it was concluded that such devices may be useful for scour mitigation. However, there was no indication from the author as to the practicability of using collars in the field.

Chabert and Engeldinger (1956) found that a single circular plate placed 0.4D below the original bed elevation and having a diameter of 3D, where D is the pier diameter, could reduce the depth of scour by 60%. No appreciable reduction in scour depth was noticed when an increased number of such plates were tested for various elevations.

Thomas (1967) worked on preventing local scour at a bridge pier and observed that the depth of scour could be reduced by placing a horizontal shield on the pier. The effect of a horizontal shield, which Thomas named "anti-scour", on the depth and extent of the scour at a pier was described. Experiments were conducted using a 50 mm diameter circular pier on which had been fitted a horizontal shield. Two different sizes of shield with W = 100 mm and 150 mm were used. The relative heights of the shield above the channel bed were $y_c/y_o$ = 0.0, 0.18, 0.317, 0.45 and 0.73. The symbol $y_c$ is the distance above the channel bed, while $y_o$ is the flow depth. The shield prevented the vertical flow

at the pier face from reaching the channel bottom. The most effective diameter of the plate recommended by Thomas is three times the pier diameter positioned very close to the channel bed. This result is similar to the observation made by Chabert and Engeldinger (1956).

Tanaka and Yano (1967) also studied the use of a collar to prevent scouring. In their experiment, a fine river sand of median size 0.4 mm, a flow depth of 100 mm and a circular pier of diameter 30 mm were used. A thin circular plate was fitted on the circular pier. The diameters of the plate were, W = 90 mm, 120 mm, 150 mm and 180 mm, and its position on the pier was systematically changed. It was reported that a decrease in the size of the plate led to a decrease in the effect of the plate at reducing the scour depth and vice versa. An increase in the plate elevation with respect to the bed surface also resulted in an increased scour depth. Tanaka and Yano's results are similar to the observations made by Thomas (1967).

Ettema (1980) conducted a series of experiments to ascertain the possibility of using a thin collar to mitigate against local scour at a circular bridge pier. Collars were installed on a circular pier at various elevations on, above and below the channel bed. The parameters of interest were the depth of flow, $y_o$, the collar width, W, the collar elevation relative to the channel bed, $y_c$, and the pier diameter, D. The experiments were conducted in a 0.46 m wide flume using a 45 mm diameter pier. In order for ripples not to form on the flume bed, 1.90 mm diameter coarse sand sediment was used for the experiment. The flow depth was set at 0.20 m while the ratio of $u_*/u_{*c}$ was 0.90. A 0.4 mm thick, circular, brass collar of width two times the pier diameter was installed on the circular pier at four different locations, viz. $y_c/D$ = 0.5, 0, -0.5 and -0.1. The minus sign denotes that the collar was positioned below the channel bed.

It was observed that, when a collar of width twice the size of the pier diameter was installed at an elevation of half the diameter ($y_c/D$ = 0.5) above the channel bed, the collar was not effective at reducing the scour depth. However, the effectiveness of a collar at reducing scour became noticeable when the collar was installed at the channel bed. No scour developed below the collar when the collar was installed at $y_c/D$ = -0.1.

Ettema's (1980) results compared favourably with the results obtained by Tanaka and Yano (1967) and Thomas (1967). The general conclusion was that the influence of the width of the collar on scour increased as the elevation of the collar is decreased.

Dargahi (1990) carried out research on the mechanisms of local scour and how a collar may influence the horseshoe vortex system and ultimately reduce the amount of scour. The experiments were conducted using a uniformly-graded fine sand of median diameter, $d_{50} = 0.36$ mm. A circular pier of diameter 0.15 m was used for each test. The mean flow velocity was 0.26 m/s. The ratio of $u_*/u_{*c}$ was 0.85 while the flow depth was maintained at 0.2 m. In order to study the effect of collar shape on performance, two separate collar shapes were tested: One shape was a thin circular collar of diameter 0.28 m (with W/D = 1.86) and the other was a collar with a Joukowski profile. The shape of a Joukowski profile is shown in Figure 2.5. The Joukowski profile has an airfoil shape that resembles the cross section of an airplane wing. It has a rounded leading edge and a trailing edge that ends in a cusp. A cusp as used here is a point at which two branches of a curve meet such that the tangents of each branch are equal. The Joukowski collar was attached to the circular pier such that its blunt nose faced upstream. The collar was positioned at elevations $y_c/y_o = 0.25$, 0.05, -0.015, and -0.05 relative to the initial channel bed. The total test duration for each experiment was 12 hours. At the end of the test, the scour profiles were measured along the line of symmetry for each collar position.

It was observed that the collar was not effective at hindering the horseshoe vortex formation. It was reported that, irrespective of the collar position and shape, the scour mechanism was similar to the case of a circular pier unprotected with a collar. The maximum reduction in scour depth as a result of the collar occurred at a collar position of $y_c/y_o = -0.015$. At $y_c/y_o = -0.015$, it was found that the maximum reduction of scour depth was 50% and 75% at the upstream and downstream region of the pier, respectively. The collar position $y_c/y_o = 0.25$ did not significantly influence the amount of scour. Similar results were obtained for the two collar shapes tested. It was also reported that, when the ratio of the collar thickness to the pier diameter becomes large, an increase in the effective diameter of the pier resulted, which subsequently caused an

increase in the scour depth. Dargahi, however, cautioned that further research is needed before a practical application of a collar is recommended.

Chiew (1992) experimentally studied the effect of a collar, a slot and a combination of the two in reducing the local scour in the vicinity of a pier. A slot is a hole through the pier to allow the passage of flowing water. The objective of the study was to review existing mitigation approaches and to propose alternative or new devices for mitigating scour in the vicinity of bridge piers. The experiment was conducted using a 32 mm diameter pier and a median particle size of 0.33 mm. The flow intensity, (i.e., $u_*/u_{*c}$) was maintained at 0.9 and the depth of flow was 180 mm. The collar consisted of a 1 mm thick stainless steel plate. Experiments with 2D and 3D wide collars were tested alone and in combination with a pier slot while the positions of the collars were systematically varied. Equilibrium scour depth was defined as the depth attained when there was less than 1 mm change in scour depth in eight hours. Using this criterion, the tests were run for approximately 72 hrs.

The collar alone was found to reduce the scour depth by as much as 20% while no scour occurred when a D/4 slot was used in conjunction with a collar. Similar results were obtained for the two collar diameters tested. When designed and applied with care, Chiew concluded that a combination of collar and slot can be a suitable substitute for the use of riprap as a countermeasure for local scour at bridge piers. These results compared favourably with the results of Ettema (1980) and Tanaka and Yano (1967).

Vittal et al. (1993) studied and compared the scour reduction efficacies of a circular collar on a pier group that was made up of three individual smaller piers. Similar experiment was also performed on a single solid pier. Figure 2.9 shows the schematic illustration of the pier arrangement of their experiments. In the study, a collar fitted to a group of three cylindrical piers angularly spaced at 120º was studied as a scour-reduction device. The particular arrangement of the cylinders is such that any one of them can just pass through the gap between the other two. The sediments used in their experiment were cohesionless natural riverbed sands, with a relative density of 2.65 and geometric mean sizes of 0.775 mm, 1.183 mm, 1.543 mm and 1.844 mm. The flow

intensity ranged between 0.88 and 0.90. In the experiment, the diameter of the solid pier and that of the circumscribing circle of the pier group was 112.5 mm, while the width of the collar was 2.0D. The diameter of the individual three smaller piers that made up the pier group was 34 mm each. The collar was positioned at a height of 15 mm above the channel bed. The full pier group was tested at an orientation of θ = 0º, 15º, 30º, 45º and 60º with respect to the approach flow direction. The duration of each test was six hours. The scour due to the pier group was compared with that of a solid circular pier.

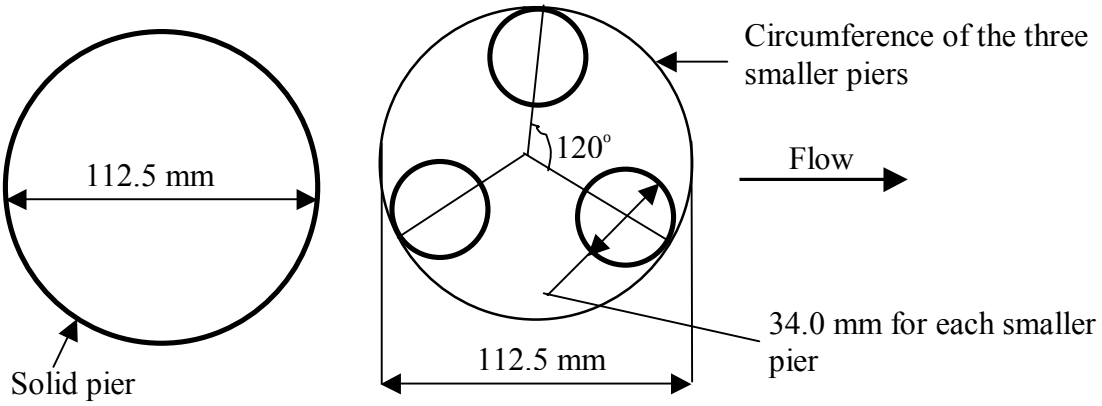


Figure 2.9. Schematic illustration of Vittal et al. experiment (Vittal et al. 1993)

Regarding scour reduction, the full pier group alone without the collar was found to be more effective than a solid cylinder having a full slot of width equal to half the cylinder diameter and as effective as a solid cylinder fitted with a collar of width 3.5 times its diameter. They observed that a collar of 2.0D on a full pier group is equivalent to a collar of more than 6.0D on solid pier. Vittal et al. (1993) concluded that a collar fitted to a pier group is much more effective than the one fitted on a solid pier as far as scour mitigation is concerned.

Fotherby and Jones (1993) studied how effective collars are at reducing scour. The authors recognised the potential usage of both a collar and a footing at reducing scour. According to Fotherby and Jones, footings are seldom considered as countermeasures but they can provide the same type of protection as a collar by interrupting the downflow at the face of the pier. Two different types of footing were identified and

they included a shallow footing and a deep footing. Deep footings and shallow footings both have substantial thickness, but shallow footings are by definition undercut by scour, whereas deep footings extend below the computed maximum depth of scour. Data from earlier studies by Chiew (1992), Schneibe (1951), Tanaka and Yano (1967), and Thomas (1967) were combined and the possible relationships between them were identified. The relationships established were in agreement with the work of other researchers. According to Fotherby and Jones, the parameters influencing the scour mechanism for footings and collars are their height above the channel bed, the width and the thickness. It was concluded that the larger the collar the more its effectiveness at reducing scour and that collar effectiveness reduces when the collar is placed at a greater elevation above the channel bed. Fotherby and Jones pointed out that a collar has been recognised as a conceptual scour countermeasure technique but has not been used in practice.

Kumar et al. (1999) also worked on the use of collars around a cylindrical pier to reduce the scour depth. For the experiment on collar efficacy, five different collar sizes of thickness 3 mm were used (i.e., W = 1.5D, 2.0D, 2.5D, 3.0D and 4.0D). Figure 2.10 shows the collar-pier arrangement used by Kumar et al. in their experiment. It was observed that the width of the collars as well as the relative position of the collars to the bed affected both the depth and location of the maximum scour location. It was also observed that small collars resulted in large scour holes at the upstream pier face, while scour depth was greatest in the wake regions for the larger collars.

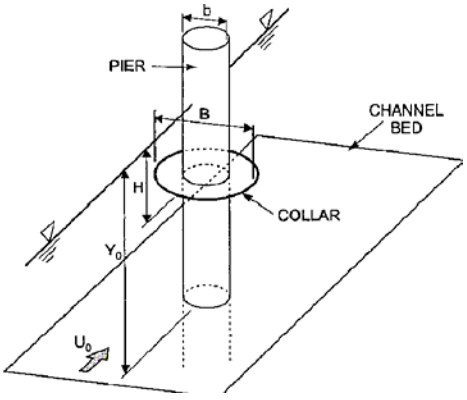


Figure 2.10. Collar installation on the pier above the channel bed (Kumar et al. 1999)

Generally, Kumar et al. (1999) concluded that a large collar placed at a low elevation relative to the bed was most effective at reducing scour. Kumar et al. also worked on the possible combination of collars and slot and found the combination to be very effective at reducing scour. They cautioned, however, that a slot is practically ineffective if the approach flow has a high angle of attack with respect to the slot.

Singh et al. (2001) worked on a collar as a scour protection device around a circular pier. The authors believed that the growth of a vortex can be arrested by retaining the vortex on a rigid surface such as a collar plate. Experiments were conducted in a flume containing fine sediment, $d_{50} = 0.285$ mm and $\sigma_g = 2.51$. The piers tested were of diameters 25 mm and 62 mm and the duration of the test was kept at 300 minutes. It was observed that the efficacy of a collar in preventing scour is a function of its width and its vertical location with respect to the channel bed. It was observed that, as the size of a collar plate increases, the scour decreases. Collar plates of sizes W = 1.5D, 2.0D and 2.5D placed on the channel bed resulted in a reduction of scour by 50%, 68% and 100%, respectively, of an unprotected pier. Collar plates of size W = 2.0D when placed at 0.1D below the bed gave a maximum reduction in scour depth of 91%. However, when the same collar plate was located at 0.5D above the bed, a 25% reduction in scour depth resulted.

Most previous studies on collars have been on circular piers. Recently, however, Zarrati et al. (2004) worked on the application of a collar to control the scouring around rectangular bridge piers having a rounded nose. It was found that collar effectiveness improves as the collar becomes wider and as the level at which it is positioned on the pier becomes lower. They also found that the effectiveness of a collar is reduced as the pier skewness with respect to the flow is increased. On the time of development of the maximum scour depth, Mashahir and Zarrati (2002) and Zarrati et al. (2004) concluded that the time to reach an equilibrium condition is different depending on whether or not the pier is protected with a collar. According to them, it took 20 hrs to reach an equilibrium condition when the pier was unprotected with a collar as compared to 50 hours that was required to reach an equilibrium condition for the pier protected with a collar. Mashahir et al. (2004) also studied the temporal development of scour depth at a

bridge pier. In their experiment, a collar size of three times the pier diameter was used. The sediment material had a median size of 0.95 mm and a geometric standard deviation which was less than 1.2 (i.e., very uniform). While the diameter of the circular pier used in the study was 400 mm, the ratio of the shear velocity to the critical shear velocity was calculated to be 0.92 based on the Shields' criterion. Using a definition of time to equilibrium scour depth for which the change in scour depth was less than 2% of the pier diameter in eight hours, the duration of each experiment was limited to 44 hours. Figure 2.11 shows the temporal development of the scour depth.

As concluded in the study by Mashahir et al. (2004), placing the collar below the channel bed level did not lead to an appreciable increase in the efficacy of the collar. This was so because the depth of the sand sediments above the collar will itself become part of the scour hole as this is swept away very fast by the erosive action of the flow. Comparison of the results for rectangular piers aligned with the flow and the previous experiments on circular piers by Zarrati et al. (2004) and Mashahir et al. showed that a collar of W/D = 3 is more effective at reducing the depth of the scour hole for rectangular piers than for circular piers.

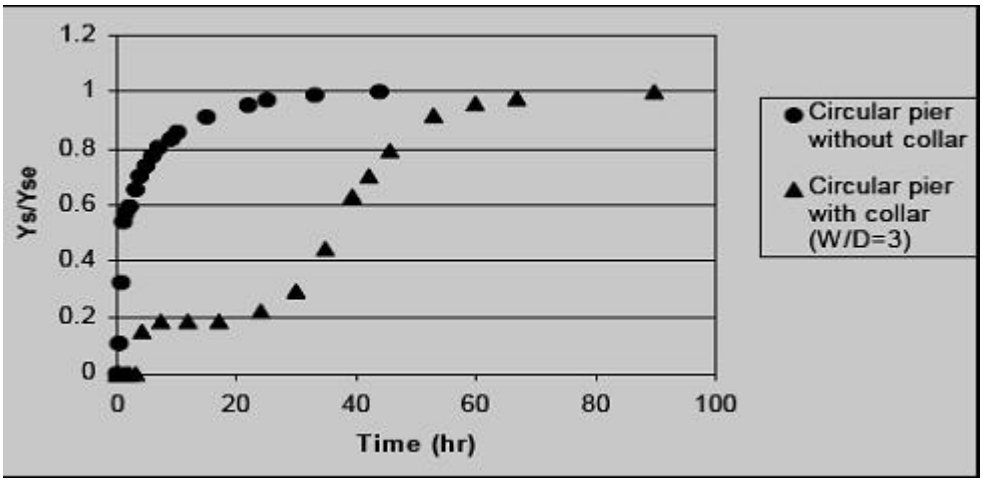


Figure 2.11. Time variation of scour depth at the upstream face of the circular pier with and without a collar (Mashahir et al. 2004)

For a possible application of two collars at the same time, it was reported by Zarrati et al. (2004) that installation of a second collar at an elevation above the channel bed increases the effectiveness of collars. Mashahir et al. (2004) reported that collars not only reduce scour depth but also reduce the scouring rate considerably.

The temporal development of the scour depth for different collar sizes is shown in Figure 2.12. As depicted in the figure, Mashahir et al. (2004) also compared their results with that of Ettema (1980) and concluded that a collar placed on the channel bed and with a width three times the pier diameter or width is more effective than a collar with a size of two times the pier diameter.

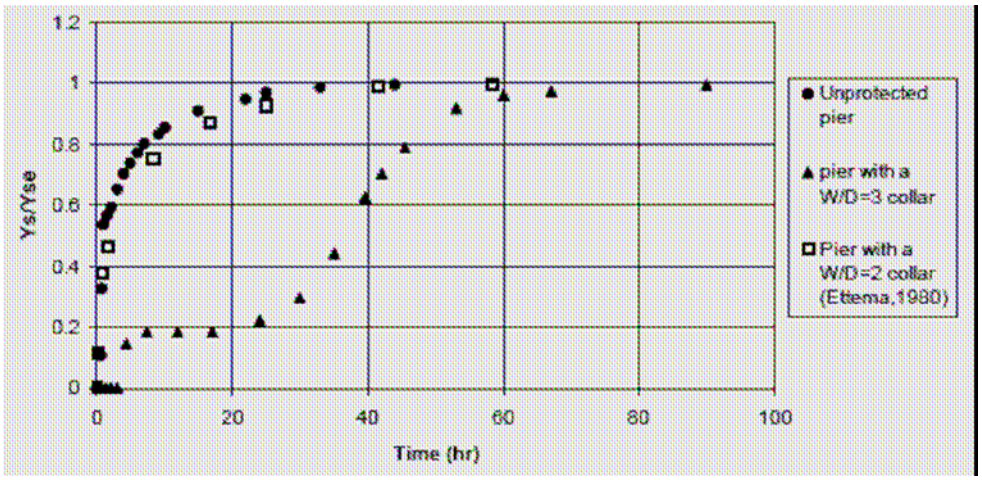


Figure 2.12. Time development of scour for different collars sizes (Mashahir et al. 2004)

Figure 2.13 shows the rate of scour in a pier protected with a collar compared with a pier having a wide foundation. Mashahir et al. (2004) observed that a collar has a better efficiency at reducing the rate of scour than a pier foundation of the same width installed on the same level. When a collar is installed on the pier, the direct impact of the down-flow to the riverbed is prevented. In addition to a reduction of the maximum scour depth, the rate of scouring is also reduced considerably. Reduction in the rate of scouring can reduce the risk of pier failure when the duration of floods is short (Melville and Raudkivi, 1996; Melville and Chiew, 1999).

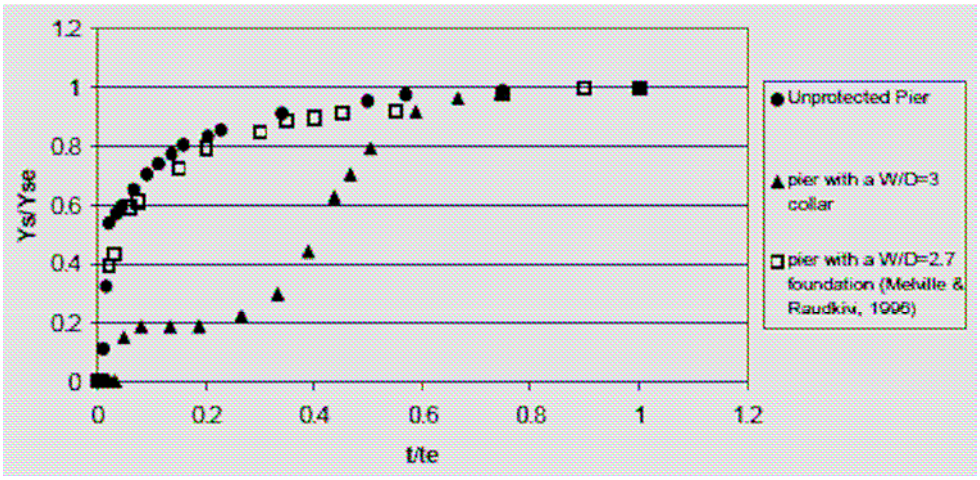


Figure 2.13. Rate of scour in a pier protected with collar compared with a pier with a wide foundation (Mashahir et al. 2004)

Kayaturk et al. (2004) studied the effect of a collar on the temporal development of scour around bridge abutments. The experiments were conducted in a 1.5 m wide flume having a bottom slope of 0.0001. With a flow intensity of 0.90, all of the tests were run under clear-water scour conditions. Operating at a flow depth of 100 mm and a discharge of 0.05 $m^3/s$, each experiment was limited to a duration of six hours. The soil material had a $d_{50}$ = 1.48 mm and geometric standard deviation, $\sigma_g$ = 1.28. In this study, the time development of the local scour around the abutment fitted with and without collar plates was studied. The effects of various sizes of collars fitted at different elevations on the temporal development of scour depth at the abutment were also studied.

Four different collar widths, W = 0.025 m, 0.050 m, 0.075 m and 0.10 m, were tested. Since the effectiveness of the collar on the development of the scour hole is also a function of its vertical location on the abutment, all collar types were tested at various elevations, including at the bed level, 0.025 m and 0.050 m above the bed level, and 0.025 m and 0.050 m below the bed level. Figure 2.14 shows the temporal development of the scour at abutments from the work of Kayaturk et al. The symbol $d_s$ in the figure is the same as $y_s$ while $Z_c$ is the elevation of the collar with respect to the channel bed at the abutment.

As shown by the results in Figure 2.14, the depth of the scour hole reduced because of the collar irrespective of the collar size and vertical position. The experimental results signified that not only did the presence of a collar reduce the scour depth, the rate of temporal development of the scour hole was also reduced. It is also shown that the efficacy of the collar at reducing the scour depth reduces as the vertical distance between the collar plate and the bed level, $Z_c$, increases. However, installation of the collar at elevations below the bed level gave a better result. According to Kayaturk et al. (2004), a 67% reduction in the scour depth was achieved when the collar was positioned at an elevation of 50 mm below the channel bed.

The results of Kayaturk et al. (2004) are in agreement with the other researchers that, as the collar width increases, the scour depth decreases for a given time. They concluded that application of collars at abutments is very effective at reducing the development of scour depth.

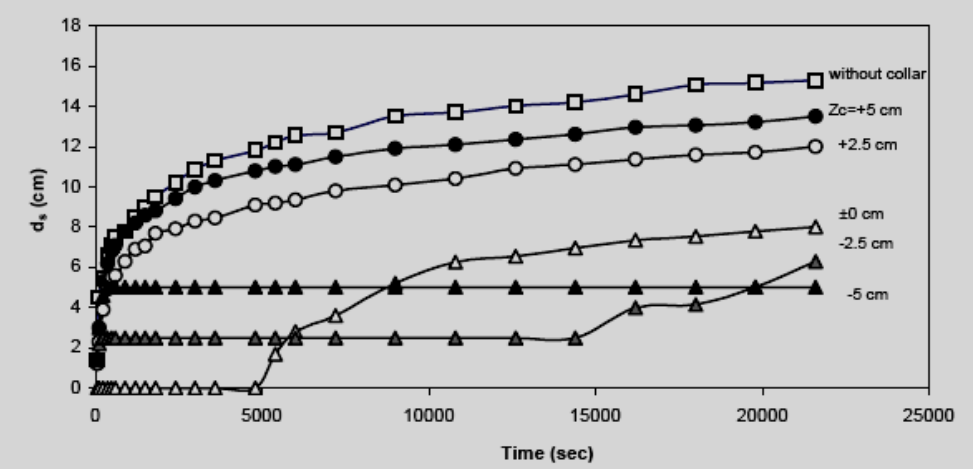


Figure 2.14. Time development of scouring around abutments without and with collar of width 100 mm installed at various elevations $Z_c$ (Kayaturk et al. 2004)

Zarrati et al. (2006) studied the use of independent and continuous pier collars in combination with riprap for reducing local scour around bridge pier groups. Their results showed that with two piers in line, a combination of continuous collars and riprap led to a scour reduction of about 50% and 60% for the front and rear piers, respectively.

In another experiment with two piers in line, independent collars showed better efficiency than a continuous collar around both the pier. It was also observed that the efficiency of collars is more on a rectangular pier aligned to the flow than two piers in line.

Lauchlan (1999), Dey (1997), Whitehouse (1998), Hoffmans and Verheij (1997), and Melville and Coleman (2000) also gave a brief review of the application of a protective collar as a countermeasure for local scour at bridge pier. The general agreement is that a collar can be used to reduce scour depth as well as to reduce the scouring rate.

In summary, based on a variety of experimental studies that have been undertaken using collar techniques, the general agreement appears to be that a reasonably large collar placed at or slightly below the bed level can provide significant scour protection. It should be noted, however, that all of the above studies on collars have been done for clear-water conditions.

## 2.10 Conclusions

As a precursor to this research study, an extensive literature review has been undertaken. The outcome of the review revealed that further work is needed on various aspects of scour, especially in the area of temporal development of scour and the evaluation of the efficacy of a collar as a countermeasure for local scour at a bridge pier. The additional work is needed before a practical application of a collar can be confirmed. The philosophy upon which devices such as collars is based is that their existence will sufficiently prevent and deflect the mechanisms of local scour with the overall effect of reducing the scour depth. Based on the findings reported herein, the use of collars is an effective method for reducing local scour at a bridge pier.

On the basis of model studies, collars are not only very effective at reducing scour but are also much more economical when compared to countermeasure techniques like riprap. It has been concluded that the larger the collar the greater the scour reduction level, and for maximum performance the collar should be placed at or below the channel

bed level. All previous studies on the use of a collar as a countermeasure for local scour at a bridge pier are based on experiments carried out using a physical hydraulic model and as such the practicality of using a collar on the field through a prototype study has not yet been done.

# CHAPTER 3

# EXPERIMENTAL SETUP AND METHODOLOGY

## 3.1 Introduction

In this chapter, the experimental arrangements, hydraulic models, data acquisition system and variables measured in the model study are described. All of the experiments were conducted in the Hydrotechnical Laboratory at the University of Saskatchewan, Saskatoon, Canada.

## 3.2 Flume

The experiment reported herein was conducted in a recirculating flume, 20 m long, 1.22 m wide and 0.61 m deep. The flume has a working section in the form of a recess that is filled with sediment to a uniform thickness of 0.16 m. The sand bed recess is 12.43 m long and is located 5.64 m downstream from the flume inlet section. The working section of the flume is made up of an aluminum bottom and Plexiglas sidewalls along one side for most of its length to facilitate visual observations. The outlet and inlet of the sand bed contain raised sloping ends. The recirculating flow system is served by a 30 hp, variable-speed, centrifugal pump located at the downstream end of the flume. The water discharge is measured by a magnetic flow meter located in the water return pipe at the downstream end of the flume. The magnetic flow meter frequently updates its readings at every few seconds but at a time less than a minute. Each of the readings varies between ±0.02 from the mean reading. Figure 3.1 and Figure 3.2a show a schematic illustration and photograph of the experimental setup, respectively, while the photograph of the magnetic flow meter is shown in Figure 3.2b. The pump takes the water from the reservoir at the downstream end of the flume and returns it to the upstream end via a 223 mm diameter aluminum pipe line which runs directly underneath the flume. The reservoir, which is about 5.34 m long and has the same width as the flume, is located immediately at the downstream end of the flume and is separated from it by the tailgate.

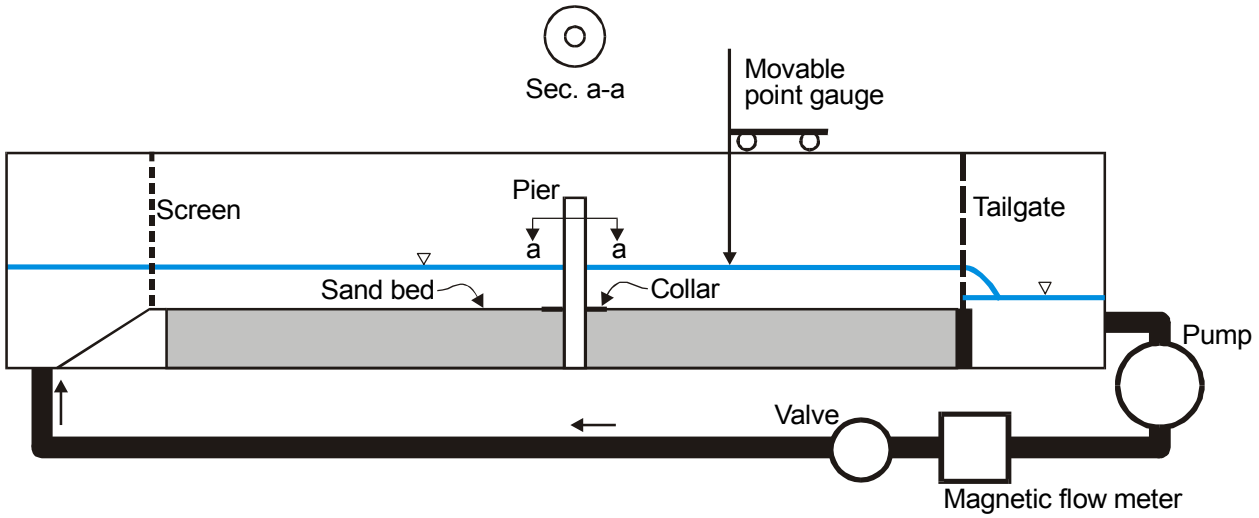


Figure 3.1. Schematic illustration of the experimental setup

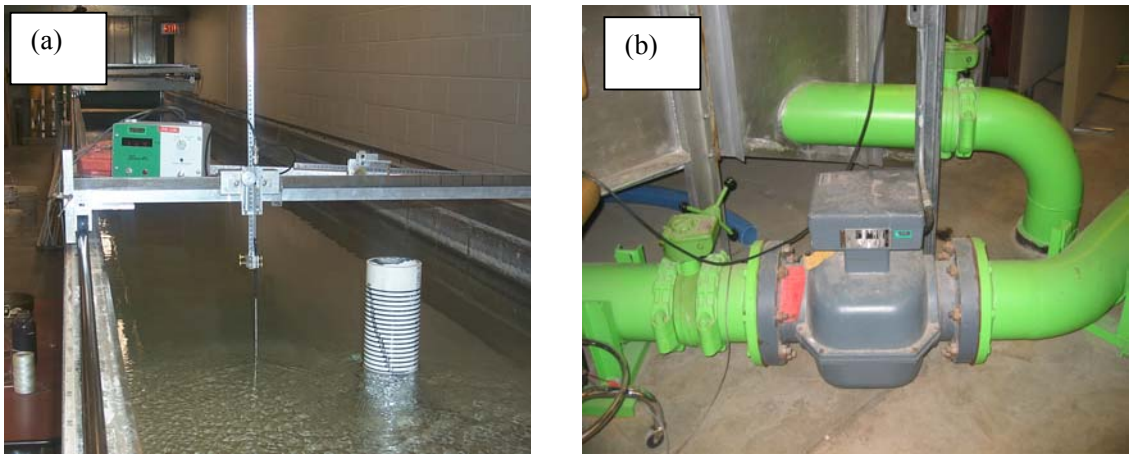


Figure 3.2. Photograph: (a) Experimental setup and (b) Magnetic flow meter

At the upstream end of the flume is installed a head box equipped with a screen to sieve any unwanted particles and debris that might otherwise enter the working section of the flume. To facilitate rapid development of the turbulent boundary layer on the channel bed, the entrance zone upstream of the sand bed was artificially roughened using galvanised wire-mesh of diameter 1.0 mm with each square having a size of 20 mm x 20 mm. While the wire mesh assists in providing excess friction to ensure the existence of fully developed turbulent flow, the screen at the upstream section of the flume also provides baffles for the elimination of eddies that form at the entrance to the flume. A

wooden wave suppressor was also used in the upstream approach section to smooth the flow coming onto the sand bed.

### 3.3 Flow conditions

A Nixon micro-propeller current meter was used for all vertical velocity profiles. The device, which is a member of the Streamflo current velocity flowmeter family, model 403 is a standard low speed velocity probe that measures velocity in the range 2.5 to 150 cm/s. The velocity profile measuring device is shown in Figure 3.3. As shown in Figure 3.3a, each mini-propeller probe consists of a plastic propeller mounted on two jewel bearings. A sensing electrode is located within the inner stem of each probe. As the propeller turns with the flow, the capacitance across the probe is modulated every time that a blade passes close to the sensing terminal. The modulation produces a pulse which is registered by an electronic counter, which then records and displays the number of pulses for a period. As an accessory to the probe is a volt-meter, called a digital indicator, which is capable of giving the mean velocity in terms of frequency either every one second, 10 seconds or continuously (see Figure 3.3b). The frequency thus recorded in Hz can be converted to mean velocity by means of a calibration chart. The accuracy of the device is within ±1% of the true velocity. The operating temperature of the probe ranges between 0 and 50º C.

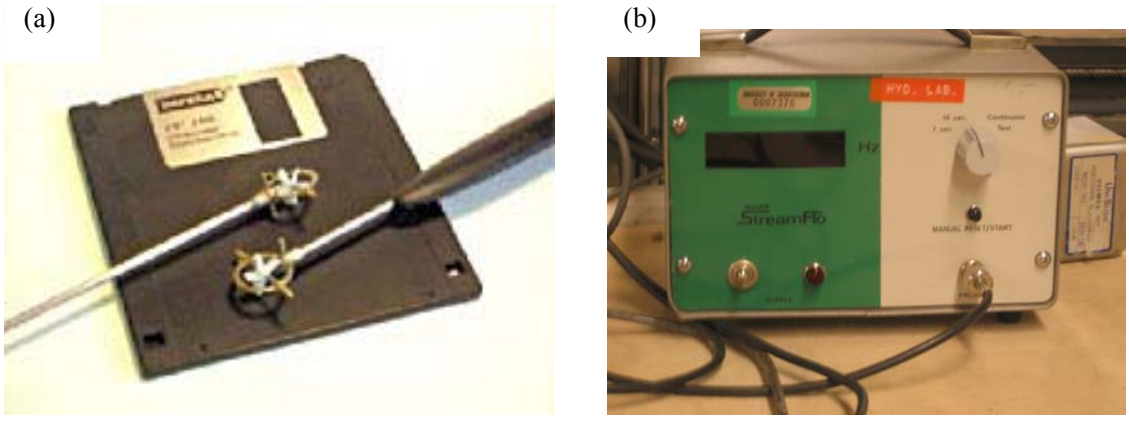


Figure 3.3. Velocity measurement system: (a) Current meter probe, and (b) Digital indicator box

A point gauge having a precision of 0.2 mm was used for the depth measurements. The flow depth was controlled by a vertical-leaf gate that spans the full width of the flume. For all of the tests, the relative flow depth used was twice the pier diameter (i.e., $y_o/D = 2$). The ratio was chosen in order to ensure that the local scour occurs as a narrow pier such that the local scour depth only depends on the pier diameter and not on the flow depth as discussed in Chapter 2.

Measurement of the flow rate was achieved by the use of a model E96T-1A magnetic flowmeter made by Foxboro. The discharge in the flume was controlled by a model 10F-4310 variable speed pump made by S.A. Armstrong Ltd. Control of the pump motor speed was achieved by the use of a Model Y300 Parajust Y AC motor speed controller made by Parametrics.

Water temperature was recorded using an Omega digital thermometer model HH-25TC each time the maximum scour depth was measured throughout each run. Barkdoll (2000) suggested that water temperature, in the form of changes in viscosity and density of water, may exert an influence on the scour development. Melville and Chiew (2000) however, observed otherwise by conducting two experiments which were identical except for the water temperatures, which were at 26.5ºC and 17ºC, respectively. According to Melville and Chiew, no discernible difference in the scour depth development, or equilibrium scour depth, was evident for the two experiments. Despite these contradictions, the operating temperature was monitored for all of the tests. Water level was monitored throughout each test in order to ensure that the water level was kept at the required level. However, for long duration tests, the water level reduced due to evaporation. Therefore, to maintain the same water level, the flume was periodically replenished with water as required (say, two to three days interval). A red dye (Triacrile BR Red 4G 200%) was used to facilitate visual observation of the flow patterns.

### 3.4 Model

The pier model was fabricated from Polyvinyl Chloride (PVC) pipe. Two circular model piers of diameter 115 mm and 73 mm (having a vertical scale of 5 mm marked onto their sides) were used for the study. The purpose of the 5 mm scale around the pier

was to facilitate the measurement of the magnitude of the scour depth. In each case, the pier was placed on the centerline of the flume at the same longitudinal location. Specifically, the coordinates of the centre of the pier along the flume is (15041 mm, 751.4 mm). This coordinate is important in this study especially when measuring the contour profiles of the scour hole as all other measurements were taken with respect to the centre of the pier. The pier was mounted on a base support of thickness 12.25 mm and dimension approximately 250 mm x 250 mm. The collar used in the experiments was 5 mm thick and was made from a transparent Acrylic material. Two different collar widths were used, with one having a width of two times the pier diameter (2D) while the other had a diameter of 3D, where D is the diameter of the pier. Figure 3.4 shows a schematic illustration of a pier fitted with a collar. For all of the tests with a collar, the collar was positioned at the bed level in accordance with the recommendations of earlier researchers (e.g., Ettema 1980; Kumar et al. 1999). The collar thickness of 5 mm used was observed not to have any adverse effect on the flow field. The 5 mm thickness is small enough not to cause any obstruction to the flow through an increase in the effective width of the pier. Dargahi (1990) has observed that, if the ratio of the collar thickness to the cylinder diameter becomes large, the effective pier diameter will increase, causing an increase in the scour depth.

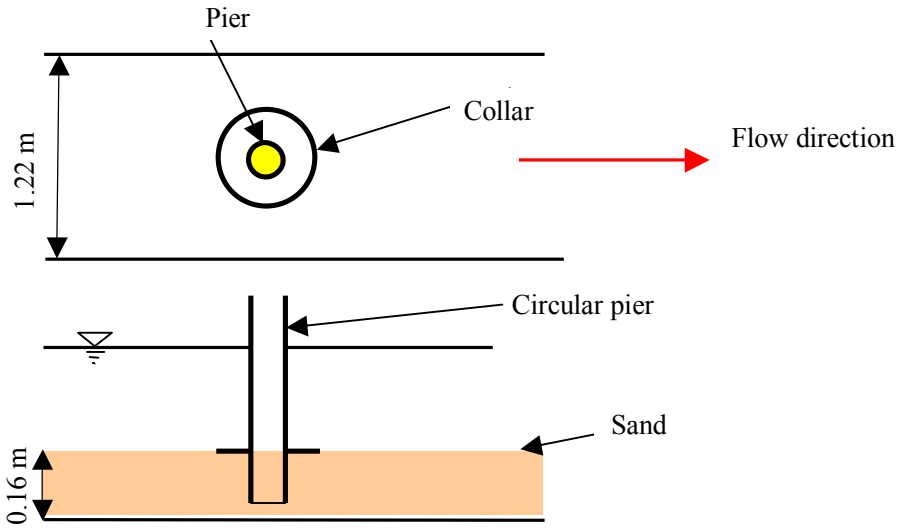


Figure 3.4. Schematic illustration of a pier fitted with a collar

Three pins set at angle of approximately 120°, as shown in Figure 3.5, were used to accurately position the collar in a level orientation precisely at the bed level. The collar was prevented from moving on the pier by the friction fit provided by a rubber O-ring in the collar.

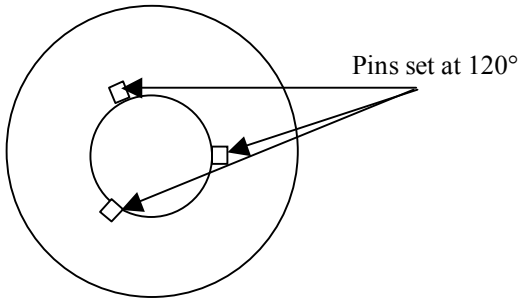


Figure 3.5. The pier, collar and support pin arrangement

The pier diameter was carefully chosen so that there was negligible effect of flume width on the depth of scour. Shen et al. (1969) suggested that, for the purpose of experimental investigations, the width of an experimental flume should be at least eight times the pier size for clear-water scour conditions so that blockage effects, otherwise known as sidewall effects, are minimised. In this study, the flume width to pier diameter ratios are 10.6 and 16.7 for the piers of diameter 115 mm and 73 mm, respectively, which more than satisfies the criterion of Shen et al.

## 3.5 Sand bed

A series of tests were carried out to characterise the sand bed material present in the flume used for the study. The soil tests carried out included a mechanical sieve analysis and a specific gravity test. The results of the tests showed that the bed material consists of cohesionless sand with a median particle size ($d_{50}$) of 0.53 mm and a specific gravity of 2.65. The geometric standard deviation of the sand size, $\sigma_g$, is 1.23, which implies that the sand is of uniform size distribution. The $\sigma_g$ is defined as, $\sigma_g = (d_{84}/d_{16})^{0.5}$. The plot of the grain size distribution (sieve analysis) test is depicted in Figure 3.6. The pier diameter was also carefully chosen so that there was negligible effect of sediment size on the depth of scour. It is known that the bed material grain size does not affect the depth of scour if the pier width to grain size ratio exceeds a value of about 50 (Ettema

1980). For this study, the ratios are about 138 and 217 for the piers of diameter 73 mm and 115 mm, respectively, which more than satisfies the criterion of Ettema.

As depicted in Figure 3.7, the angle of repose of the sand material used in this study was measured to be about 30° using the shear box test.

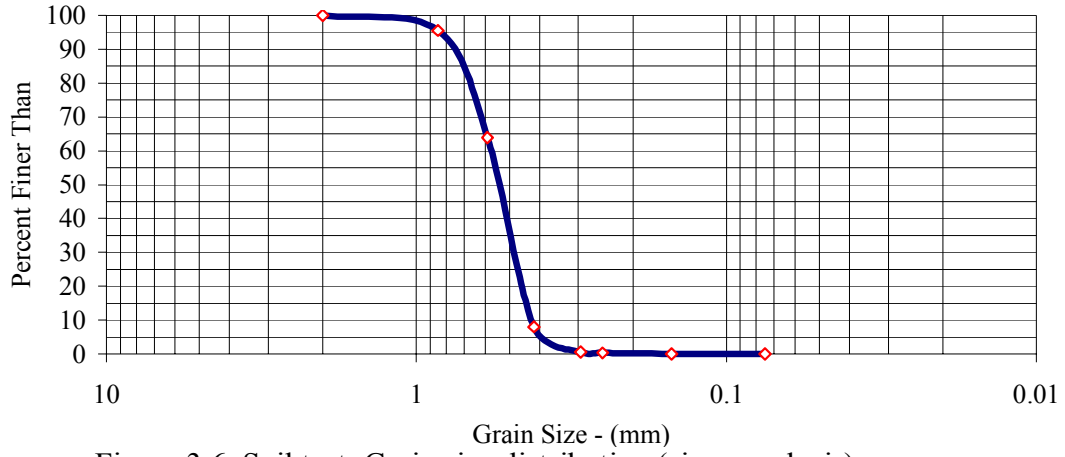


Figure 3.6. Soil test: Grain size distribution (sieve analysis)

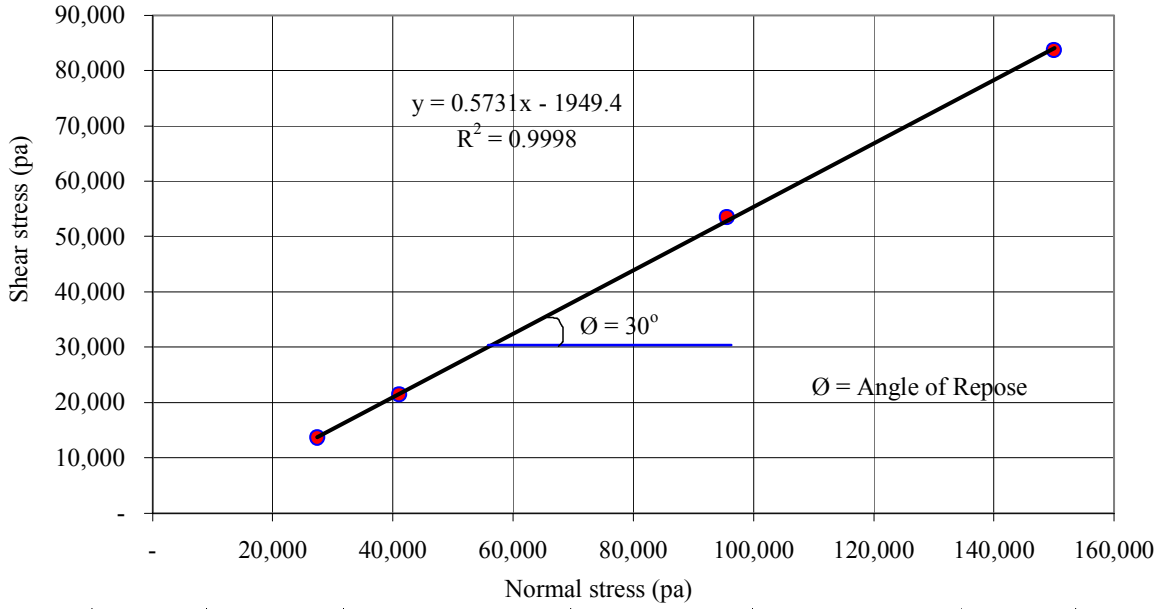


Figure 3.7. Soil test: Angle of repose

## 3.6 Incipient motion of sediment

Knowledge of the hydraulic conditions at which motion of sediment particles is initiated is very significant as far as clear-water scour is concerned. The threshold of bed material motion was determined using the critical tractive force approach and the Shields diagram as described in Chapter 2. A series of calculations was done in this regard, and the Shields parameter, also known as the dimensionless shear stress, was determined to be equal to 0.032. In doing the critical shear stress calculations, Manning's n value was assumed as 0.012. A sample calculation method for the incipient motion of sediment has been itemised in Appendix A-1. The experiments were performed under clear-water conditions at two different flow intensities ($u_*/u_{*c}$) of 0.89 and 0.70, corresponding to a shear stress levels of 80% and 49% of the critical shear stress level based on Shields stress, respectively. The symbols $u_*$ and $u_{*c}$ are the shear velocity and the critical shear velocity, respectively.

## 3.7 Test program

The use of collars has been suggested as a possible pier scour mitigation technique by researchers, largely on the basis of model study results. However, in undertaking model studies of pier scour, and particularly in the case of a pier fitted with a collar, there is some evidence to show that the time required to achieve an equilibrium scour condition needs special attention. The test program was developed to deal with the evaluation of the efficacy of using a collar as a mitigation technique against pier scour, with a major focus on the time required to achieve an equilibrium scour condition. The test program was divided into three series of tests, with each test series representing a complete set of tests. The three series of tests are referred to as Series 1, Series 2, and Series 3. For all of the tests, the collar was positioned at the bed level. A summary of the basic test conditions and flow conditions is shown in Table 3.1.

Table 3.1. Summary of test conditions for Series 1, 2 and 3 tests.

| Tests | Pier diameter (mm) | Flow depth (mm) | Mean velocity (m/s) | Discharge ($m^3/s$) | Froude Number | Flow intensity | Collar size |
|---|---|---|---|---|---|---|---|
| Series 1 | 115 | 230 | 0.249 | 0.070 | 0.166 | 0.89 | 2D |
| Series 2 | 73 | 146 | 0.248 | 0.044 | 0.207 | 0.89 | 2D |
| Series 3 | 115 | 230 | 0.195 | 0.055 | 0.130 | 0.70 | 3D |

***Series 1***

The first series of tests (Series 1) was designed to study the time development of scour as well as the efficacy of using a collar as a countermeasure for scour at a bridge pier. The first test under Series 1 tests was conducted without a collar fitted to the pier. In the second test, a collar of width equal to two times the pier diameter was used. For both tests, a pier of diameter 115 mm was used. The experiments were performed under clear-water conditions at a flow intensity ($u_*/u_{*c}$) of 0.89. Two tests were conducted under Series 1, namely: A test with a plain pier and the other one for a pier fitted with a 2D collar. Some of the tests mentioned above were conducted in duplicate in order to ascertain the repeatability of the results.

***Series 2***

The second series of tests (Series 2) was also conducted for the case where a pier is protected with a collar and the case where it is not. The only difference between the Series 1 and Series 2 tests is the pier diameter, which was 73 mm for the Series 2 tests. For both the Series 1 and 2 tests, the relative flow depth was two times the pier diameter. A summary of the basic test conditions and flow conditions are shown in Table 3.1. The Series 1 and 2 tests were undertaken in order to evaluate the influence of pier diameter on the temporal development of scour and also to evaluate the efficacy of using a collar as a countermeasure for bridge pier scour. Assessment of the occurrence of an equilibrium scour condition, if achieved, or of the implications of not achieving such a condition in respect of interpreting the results obtained from a physical hydraulic model study, was also studied. The effect of adopting some definitions of time to equilibrium scour depth found in the literature on the efficacy of using a collar as a

countermeasure was also undertaken. Two tests were conducted under Series 2, namely: A test with a plain pier and the other one for a pier fitted with a 2D collar.

***Series 3***

The third series of tests (Series 3) comprised of two tests. The first test was run without a collar installed while the second test was conducted with the installation of a collar having a diameter equal to three times that of the pier. The purpose of the Series 3 tests was to evaluate the temporal development of scour with and without a collar while subjected to the same flow conditions. For the Series 3 tests, the bed shear stress was 0.49 times that of the critical shear stress level. It should be noted, however, that these tests were conducted at a lower shear stress level than the Series 1 and 2 tests, where the bed shear stress was 0.80 times the critical shear stress level. Table 3.1 also shows the test conditions and the flow condition for the Series 3 tests.

The purpose of this set of runs was to evaluate the temporal development of scour depth with and without a collar subjected to the conditions shown in Table 3.1. Results from the Series 3 tests were analysed together with some results obtained using a 2D collar fitted to the pier diameter. Two tests were conducted under Series 3, namely: A test with a plain pier and the other one for a pier fitted with a 3D collar. For the Series 3 tests, the contour profile for the case where a collar was not fitted to the pier was compared with the case where a collar was positioned on the pier at the bed level. The longitudinal and transverse scour profiles through the centre of the pier were also plotted using software called Surfer version 8 and the results were discussed for the two tests. Surfer version 8, a software developed by Golden Software is a full-function 3-D surface modelling/mapping program and contouring package. Surfer is capable of quickly and easily converting XYZ data into contour, surface, wireframe, vector, image and shaded relief plots. The data can be randomly dispersed or scattered over the map area; regardless, Surfer's gridding will interpolate the data onto a grid. The Surfer tool was employed to convert the scour hole topographical data into a contour map as well as into a three-dimensional profile of the scour hole region. Surfer is also capable of

calculating the volume of the contour hole using inbuilt trapezoidal and Simpson rules. It can also calculate the surface area of the scour hole.

### 3.8 General experimental procedure and data acquisition

The pier was first installed in the flume at the desired location. For the tests with the collar in place, the collar was also fitted to the pier at the required bed level. Before each test, care was taken to level the sand bed throughout the entire length of the flume and particularly in the vicinity of the pier using a wooden screed that is of the same width as the flume. The screed can be dragged along the flume rails to produce a sand bed having a smooth, uniform surface. Thereafter, any uneven bed surface was levelled using a hand-trowel. By employing the point gauge mounted on a carriage, initial bed elevations were taken randomly to check the levelling of the flume. The sand bed preparation was very key as far as the experiment was concerned. This is because any unevenness or defect in the channel bed can cause premature bed form development.

To start the test, the flume was slowly filled with water to the required depth. It should be noted that extra care is required when filling the flume, especially for tests of this nature where no sediment movement is allowed. Any deformity in the bed surface may trigger the development of ripples or dunes and general movement of the sand if the shear stress on the smooth bed is close to the critical shear stress. The pump was then turned on and its speed slowly increased until the desired flow rate had been achieved. Concurrent with getting the pump up to speed, the tailgate was adjusted so as to maintain the correct depth of flow in the flume.

Throughout the test period, the location and magnitude of the point of maximum scour depth was recorded, with the depth being acquired either using the point gauge or the 5 mm scale marked onto the side of the pier. The 5 mm scale can be read to a precision of approximately 1 mm. The frequency of the measurements varied throughout the test period, with the maximum scour depth readings being taken every few minutes during the first hour or so of the test and less frequently thereafter. It should be noted, however, that the first four hours of each test is very important as frequent readings are

required to be taken in order to properly define the early stage of the graph of maximum scour depth versus time. The required frequency of scour depth measurements decreases as the rate of scouring decreases. Vertical velocity profiles were measured along the length of the flume using the current meter while the development of the scour hole with time was also recorded using an electronic stop watch during each test for the case when a collar was fitted to the pier and the case where no collar was fitted. In additional to a series of lights present in the laboratory, a flood light was put on whenever a reading was being taken. For further visibility of the scour hole, a transparent glass tube was used to facilitate the visual observation of the scour hole development and measurement. The glass tube aided the visibility under the water by clearing the refraction and reflection due to the presence of the flowing water.

A visual record of the important features pertaining to the temporal development of local scour at a cylindrical pier was kept with the aid of photographs and sketches. This record was also accompanied by notes.

At the completion of each test, the pump was stopped to allow the flume to slowly drain without disturbing the scour topography. The flume bed was then allowed to dry, during which time photos of the scour topography around the pier were taken, and the final maximum scour depth was recorded using the point gauge. The contour profile of the scour hole, in the plane of symmetry of the pier and parallel to the flow direction, was taken with the point gauge supported by the mobile carriage of the flume. It should be noted, however, that the contouring of the scour pattern that developed was measured only for the Series 3 tests. The first step in the contouring involved the outlining of the area to be contoured into a grid. Using a grid of 50 mm interval, the three-dimensional co-ordinates of each point within the scour hole and contour area was measured. However, defining the bed topography of the scour hole formed in the vicinity of the pier required more intensive measurements. The maximum scour depth value for each grid point in the scour hole was calculated as the difference between the mean initial bed elevation and the measured scour depth at each grid point around the contoured area. A contour plot as well as the three-dimensional profile of the contour area were created

using computer software called Surfer© version 8. The upstream cone angle, and exit slope cone angle of the scour hole, were determined from the contour profile.

The above procedures were repeated for each test run. It should be noted, however, that in addition to carrying out the routine start-up work for each experiment as discussed above, at the location of the scour hole from a previous test, the sand must be reworked properly so as to remove any "prior history" of scour development.

It should also be noted that the point gauge has a small thickness and as such it is doubtful if the point gauge obstructed the flow to the extent of causing more scour. However, having observed the point gauge as it was slowly lowered toward the sand bed, the sand grains were observed moving in apparent response to the presence of the point gauge. When dealing with 0.5 mm sand grains, the point gauge is no longer particularly "small" in thickness and as such some small disturbances might have occurred but not to the extent of causing more scour than would otherwise be expected.

For all of the tests, no definition of time to equilibrium was adopted per se. The idea behind this was that tests were proposed to run until an equilibrium condition was reached. The existence of an equilibrium condition is doubtful though as observed by other researchers (e.g. Melville and Chew 1999). Nevertheless, tests were stopped only if a form of constraint was encountered in the course of each test. This point is discussed more extensively in Chapter 4.

# CHAPTER 4

# PRESENTATION, ANALYIS AND DISCUSSION OF RESULTS

## 4.1 Introduction

The primary objective of this research program was to study the temporal development of scour at a bridge pier fitted with a collar. Also to be evaluated as part of this study was the efficacy of using a collar as a countermeasure for local scour at a bridge pier. Assessment of the occurrence of an equilibrium scour condition, if achieved, or of the implications of not achieving such a condition in respect of interpreting the results obtained from a physical hydraulic model study was to be carried out. In this chapter, the results obtained from all of the experiments are presented. Also presented are the analyses of the results and discussions pertaining thereto. This research program consists of three series of tests as described in Chapter 3. The general observations made for each series of tests have been summarised in terms of the objectives of the study. The issue of initiation of motion was also experimentally studied vis-à-vis the sediment material used in this study. The evaluation of several equilibrium scour prediction equations described in the literature was also carried out. Some of the results obtained in this study in terms of the temporal development of scour have also been compared with the work of other researchers.

## 4.2 Initiation of sediment motion

For Series 1 and Series 2 tests, it was observed that ripples formed on the sand bed of the flume, starting from the upstream end and progressing downstream toward the pier study area. A photograph showing the ripples as a result of bed movement is shown in Figure 4.1. When the ripples reached the pier study area, it was assumed that clear-water scour conditions no longer prevailed, and the particular test was stopped. The formation and migration of ripples was somewhat surprising given that the tests were being run at a shear stress level corresponding to 80% of that given by the Shields diagram. It appeared as though the formation of ripples was triggered by minor instabilities within the flow due to the entrance conditions to the test section of the

flume and/or due to the undeveloped velocity distribution in the upstream reaches of the flume.

Figure 4.1. Ripple formation at a location far upstream of the pier

In an effort to curb the formation of ripples, several modifications were made to the flume entrance, including the use of a series of baffles and the addition of mesh roughness to the floor of the approach section to the sand bed. Unfortunately, the modifications seemed to do little to prevent the formation of ripples.

Recourse to the literature revealed that, for ripple-forming sediments, which are classified as sediment having $d_{50} < 0.7$ mm, it is seldom possible to maintain a plane bed condition (Breusers and Raudkivi 1991). That this should occur is apparently in spite of the test conditions being below the threshold of motion as determined using the Shields diagram. In fact, Breusers and Raudkivi further noted that ripples can be expected to develop for $u_* > 0.6u_{*c}$ in ripple-forming sediments. Given that the sand used in the current study had a median grain size of 0.53 mm, the implication of this is that ripple

formation should be expected and that clear-water scour conditions could not likely be maintained at high shear stress levels. This is a rather curious finding given that critical or threshold conditions as determined from the Shields diagram presumably mean that bed material motion is incipient and any stress level less than the incipient condition should yield a clear-water flow.

To further evaluate the apparent "real" threshold of motion stress level, a series of tests was run in sequence with successive increases in the applied shear stress being imposed on the system. For this series of tests, the flow depth was set at 230 mm, which corresponds to two diameters of the larger model pier (i.e. $y_o = 2D$). The test sequence was started at a stress level corresponding to $0.55\ u_{*c}$, in which $u_{*c}$ was based on the Shields diagram, and run for 24 hours. When no ripples were observed to have started to form on the bed, the stress level was increased by $0.05u_{*c}$ to $0.60u_{*c}$ by increasing the flow rate and adjusting the tailgate so as to maintain $y_o = 2D$. Again, when no ripples were observed to have started to form after 24 hours of running the test, the stress level was increased by an additional $0.05u_{*c}$. For tests at $u_{*c}$ values of 0.80 or more, the test was allowed to run for 48 hours simply so that any minor tendency for ripple formation could reveal itself before the stress level was again increased. Eventually, ripples were observed to form at a stress level corresponding to $0.85u_{*c}$.

The same exercise was repeated for shallower depths of flow as well (i.e. $y_o = 0.5D$ and $y_o = 0.75D$). It was found that ripples formed more readily at a lower shear stress level shortly after the commencement of the tests when compared with a flow depth of $y_o = 2D$. From this evaluation, it can be concluded that, for the sand material used in this study, ripple formation (hence some form of bed material motion) will begin for a flow condition corresponding to $0.80u_{*c} < \text{Critical} < 0.85u_{*c}$ for a flow depth of 230 mm and a lower proportion of $u_{*c}$ for shallower depths of flow.

It should be borne in mind that the exercise described above was done after carrying out the Series 1 and Series 2 tests and as such the effect of ripples was noticed in all of the tests in these test series. The finding from the exercise influenced the decision to make

use of a lower flow intensity of 70% in the Series 3 tests instead of the 89% flow intensity used in the Series 1 and Series 2 tests.

### 4.3 Velocity distribution

The velocity profiles for each experiment were measured in order to establish if the flow was fully developed at the location of the pier. The variation of the velocity profiles at the upstream reach of the pier was measured and assessed in the flume. For illustration purposes, at the locations shown in Table 4.1, six velocity profiles were measured for the Series 1 test for the case when no collar was fitted to the pier. The approach flow velocity profiles were measured at the centreline of the flume with a mini-propeller current meter at the locations identified in Table 4.1. For each profile, velocities were recorded incrementally from approximately 7 mm near the bed level (but not at the bed) up to the water surface.

The velocity profiles for all of the locations shown in Table 4.1 for the Series 1 test are shown in Figure 4.2. The data for the velocity profiles are found in Appendix B. Similar velocity profiles were measured for all of the other tests carried out in the course of the study. As shown in Figure 4.2, the vertical velocity distribution does change with position along the length of the flume, and judged by visual appearance, the velocity profiles seem to have approached a quasi-equilibrium state just upstream of the pier (e.g., compare $L_1$ and $L_2$). Also, velocity profiles at a location $L_1$ closest to the pier as well as the velocity profiles at locations $L_2$ and $L_3$ are log-linear going by the linear relationships of the curve fitting as shown in Figure 4.3, which implies that the velocity profiles at these locations have approached quasi-equilibrium and as such the flow is somewhat fully developed. The velocity distribution is assumed to be a fully developed turbulent boundary layer when its velocity profile can be approximated by the log-law velocity profiles which is expressed as shown in [2.4]. It should be noted that the velocity profiles shown in the figure for locations $L_1$, $L_2$ and $L_3$ have been included for comparison purposes. Interestingly, the fit for $L_1$ is poorer than $L_2$, the latter of which is located further away from the pier. The plausible reason for this might have been due to the small interference of the flow by the pier at a location $L_1$ through the backwater

effect behind the pier. Another reason for this may be due to some uncertainties associated with the velocity measurement using the current meter.

Table 4.1. Positions for the measurement of velocity profiles relative to the pier location

| Position | Distance upstream from pier | Remarks |
|---|---|---|
| $L_1$ | About 1 m | The closest location to the pier |
| $L_2$ | 2 m | |
| $L_3$ | 3 m | |
| $L_4$ | 4 m | |
| $L_5$ | 5 m | |
| $L_6$ | 7 m | The farthest location from the pier |

In order to compare the discharge, Q, from the velocity profile measurements with the discharge from the magnetic flow meter during the course of the Series 1 tests, the velocity profile at a location 1.0 m upstream from the pier as shown in Figure 4.2 was integrated using the trapezoidal rule to get the corresponding discharge. The result is shown in Table 4.2. It is shown that the difference in the magnetic flow meter discharge and the discharge determined through the integration of the velocity profile is small. The close agreement of the two discharge values increases the confidence in the velocity measurement. It should be noted, however, that the integration of the 2-D velocity profile measured along the centreline of the flume only gave approximately the discharge per unit width. Accounting for the width of the flume gave the discharge value. That discharge value was then compared against the value from the magnetic flow meter. Of course, such a procedure does not account for the lateral variation in velocity. This coupled with the uncertainty associated with the instrumentation and measurement technique as well as the trapezoidal integration rule, which is only an approximation technique, among others are the reasons why there is a difference in the discharge values shown in Table 4.2.

Table 4.2. Discharges as determined from velocity profile and magnetic flow meter

| | **Discharge ($m^3/s$)** |
|---|---|
| Discharge from the velocity profile at $L_1$ | 0.068 |
| Magnetic flow meter discharge | 0.070 |

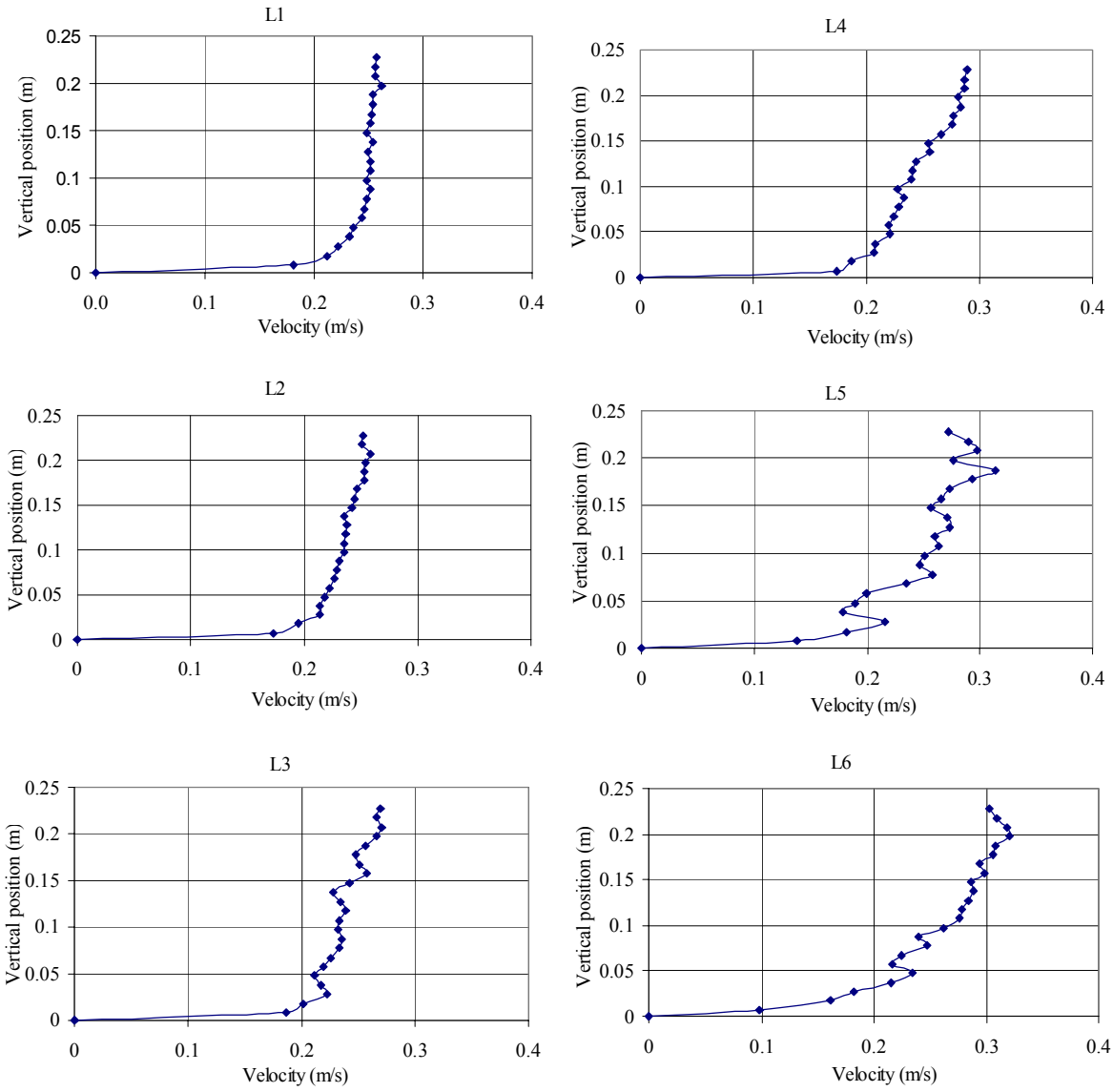


Figure 4.2. Velocity profiles of the approach flow at the centreline of the flume at various longitudinal locations (locations described in Table 4.1)

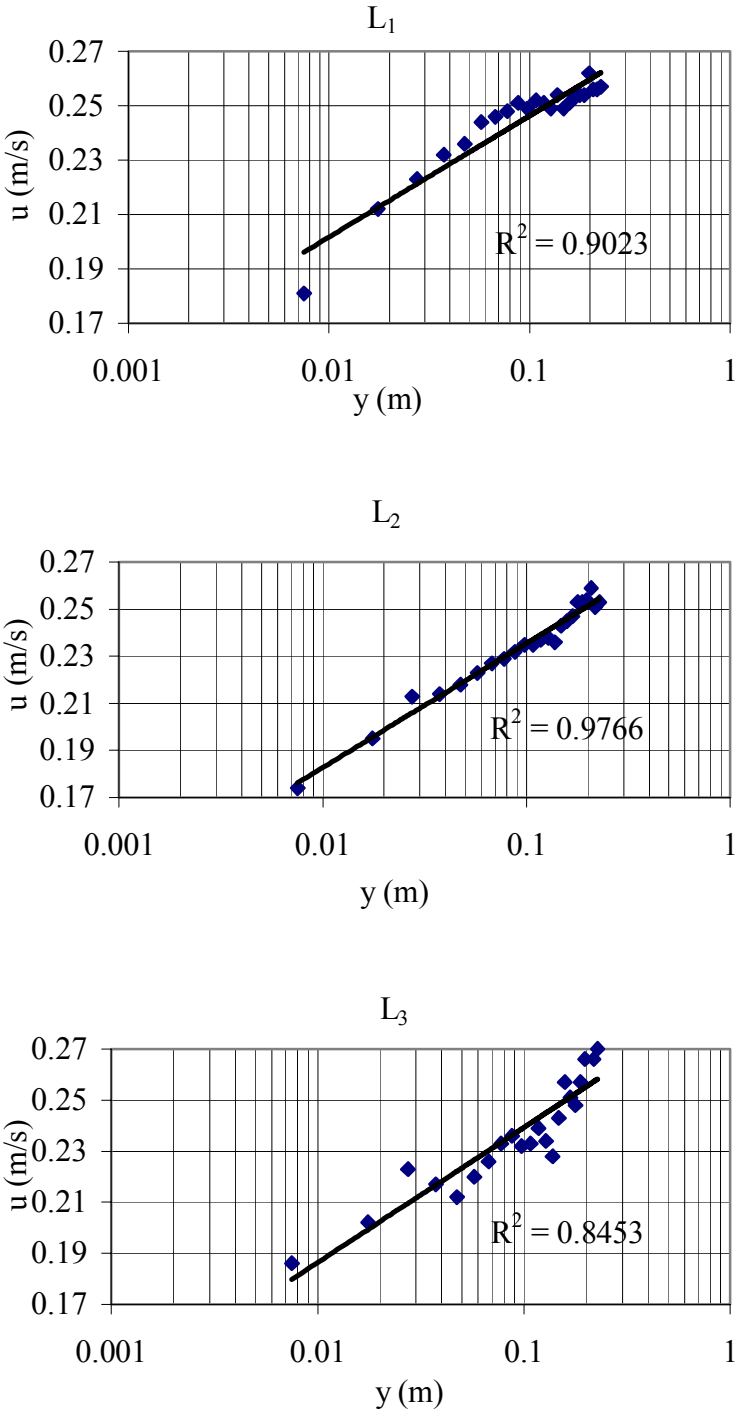


Figure 4.3. Log-linear velocity profiles for location $L_1$, $L_2$ and $L_3$

The shear velocity computation from the velocity profiles for the Series 1 test data were also compared with the actual shear velocity and the result is depicted in Table 4.3. The shear velocity computation from the velocity profile data gives an approximation of the actual shear velocity obtained from the Shields criterion for the flow conditions and sediment material. The close agreement (90%) of the computed shear velocity with the expected or actual value further increases the confidence in the measured velocity profiles. An illustrative example of computing the shear velocity and the bed shear stress from the velocity profiles is shown in Appendix A-2.

Table 4.3. Shear velocity computation from the velocity profiles

| | **Shear velocity (m/s)** |
|---|---|
| Shear velocity from velocity profile at $L_1$ | 0.0130 |
| Expected shear velocity based on the test conditions | 0.0148 |

## 4.4 Scour test results: Series 1 tests

In the Series 1 tests, the time development of scour as well as the efficacy of using a collar as a countermeasure was studied. For the Series 1 tests, a 115 mm pier diameter was used for the case where no collar was fitted to the pier and for the case where a 2D collar was used. The tests were conducted under clear-water conditions at a flow intensity ($u_*/u_{*c}$) of 0.89. As mentioned in section 4.2, the flow intensity of 0.89 had been used for the Series 1 and Series 2 tests before the discovery of the idea that it is hard to maintain a clear-water flow for a long time for the fine sediment used in the study. The tests had initially been run at a flow intensity of 0.89 with the expectation that a clear-water condition would occur for a flow intensity below 100%. It should be noted that the Shields criterion was used in the study for the calculation of the point of incipient motion. The test conditions are summarised in Table 3.1.

### 4.4.1 Pier without a collar: 115 mm diameter pier (flow intensity = 0.89)

For this test, the effect of the scouring process was noticed immediately upon starting the test. Figure 4.4 shows a schematic illustration of the scour hole development pattern

with time. The scour started first at the sides of the pier (i.e., region 1 in Figure 4.4a), and eventually propagated rather rapidly around the pier perimeter from both sides toward the centerline of the pier at the upstream face (i.e., region 2). At this stage, there was a ring-like groove formed by the scouring process around the upstream half of the pier between regions 1 and 2. Ripple formation was noticed in the wake region after 15 minutes of running the test. There was also the deposition of sediment in the wake region (i.e., region 3) due to the transport of eroded sediment from the scour hole. After one hour of running the test, the deposited sediment initially found very close to the back of the pier was observed to be moving downstream. At this point, a scour hole became noticeable immediately behind the pier within the wake region (i.e., region A in Figure 4.4b).

In due course, the point of maximum scour, which was initially located at the side of the pier (i.e., region 1), migrated to the upstream face of the pier (i.e. region 2). As the scour process continued, the scoured sand material was deposited in the wake region immediately downstream from the pier and the ripples continued to migrate further downstream of the pier (i.e., region 4). The overall scour pattern, which was symmetrical, consisted of a hole situated in front of the pier, a mound of deposited sand located a short distance downstream from the pier, and an alternate formation of depressions and mounds and a series of ripples fanning out from the pier in the downstream direction. The point of maximum scour depth was located immediately in front of the pier for most of the test duration.

Figure 4.5 shows the time development of the maximum scour for the 115 mm diameter pier. The data plotted in the figure are presented in a tabular format in Appendix C- 1. As the results show, the maximum scour depth increases with time. However, an equilibrium scour condition was not reached before the test was stopped at about 80 hours. The test was stopped because the scour was about to penetrate through the thickness of the sand layer in the flume. The log-log plot of the temporal development of scour depth has been included to show that the equilibrium scour is not being approached as indicated by the continuous increase of the slope of the plot in Figure 4.5(b).

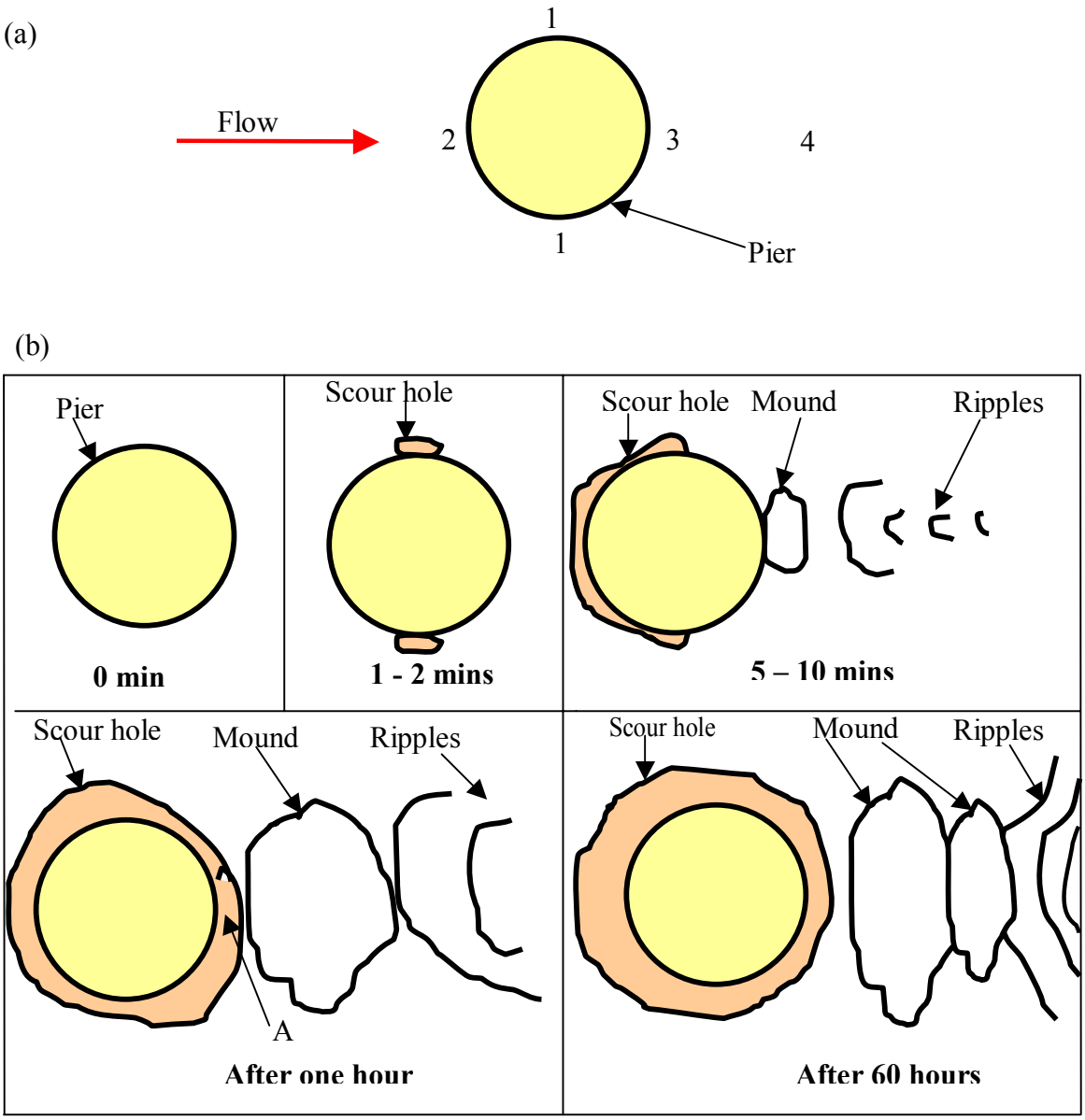


Figure 4.4. Schematic illustration of the scour hole development for the plain pier: (a) Scour pattern, and (b) Sketches of scour hole with time

The scour rate versus time for the test is shown in Figure 4.6. The scour rate is defined as the change in scour depth per change in time (mm/hour). Even though equilibrium was not attained, the rate of scour is low by the end of the test. The scour rate, which was 240 mm/hr during the first three minutes of the test, was drastically reduced to about 0.2 mm/hr by the end of the test as depicted in Figure 4.6. The slope of a straight

line fitted to the figure is 0.833. Being a negative slope denotes that the scour rate decreases with time. After the 80-hour test duration, the maximum scour depth was 140 mm. As the data show, about 70% of the maximum depth of scour was attained within the first 12 hours, which corresponds to approximately 15% of the total test duration.

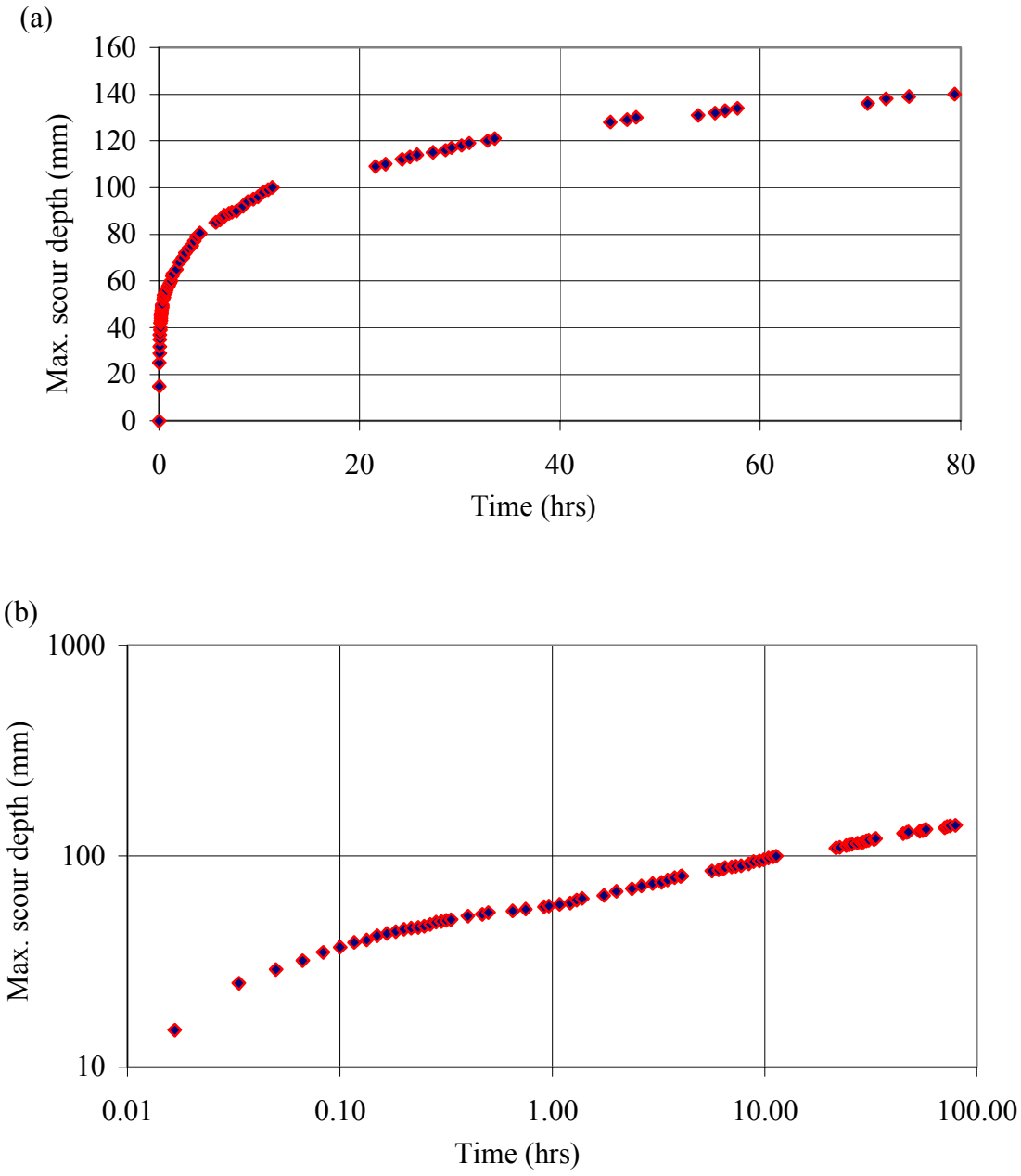


Figure 4.5. Temporal development of scour depth for the 115 mm pier without a collar: (a) Arithmetic scale, and (b) Log-log scale

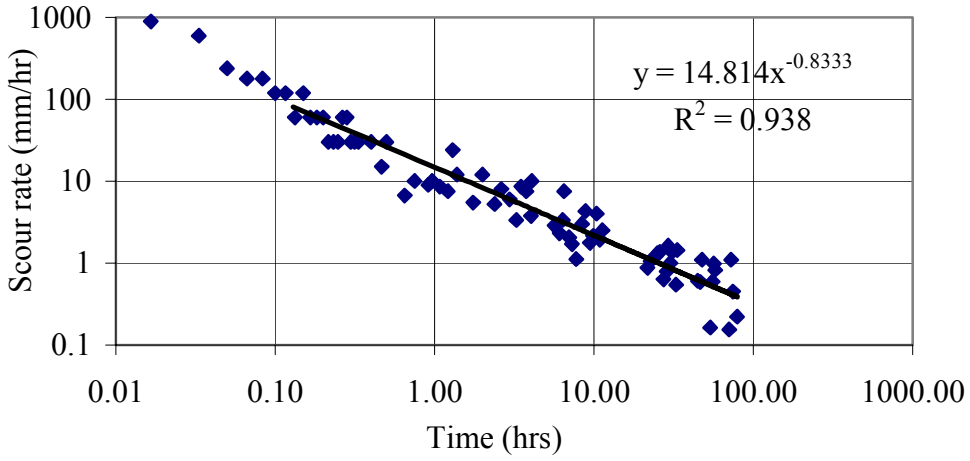


Figure 4.6. Scour rate with time for the 115 mm pier without a collar

### 4.4.2 Pier fitted with a collar: 115 mm diameter pier (flow intensity = 0.89)

For this test, a 2D collar was positioned at the level of the channel bed in accordance with the recommendations of earlier researchers (e.g., Ettema 1980; Kumar et al. 1999). Figure 4.7 shows the schematic illustration of the scour development pattern with time. Scour was first noticed to occur at the edge of the collar on either side of the collar toward the downstream portion of the collar (i.e, region 1 in Figure 4.7a). During the first few minutes of the test, a groove was observed to form on either side of the collar at the interface with the sand bed. As the test proceeded, the grooves extended toward the upstream side of the collar, eventually meeting at the centerline (i.e., region 2). In due course, the scour pattern at the upstream side of the collar progressed below the collar and eventually to the upstream face of the pier (i.e., region P). After 20 hours of running the test, the location of maximum scour shifted to being adjacent to the front face of the pier. Figure 4.8 shows a photograph of the scour hole at a point during the test. As sediment material was being removed from beneath the collar at the upstream side of the pier, deposition was taking place in the grooves that had formed around the periphery of the collar. Some of the material was also deposited in the wake region (i.e., region 3, Figure 4.7a). Ripple formation was noticed at the wake region. The ripples continued to migrate further downstream of the collar (i.e., region 4). Consequently, the grooves hitherto formed in regions 1 became shallower with time. The maximum scour

depth, which had been located within the grooves, gradually decreased as more sediment material was scoured from below the collar.

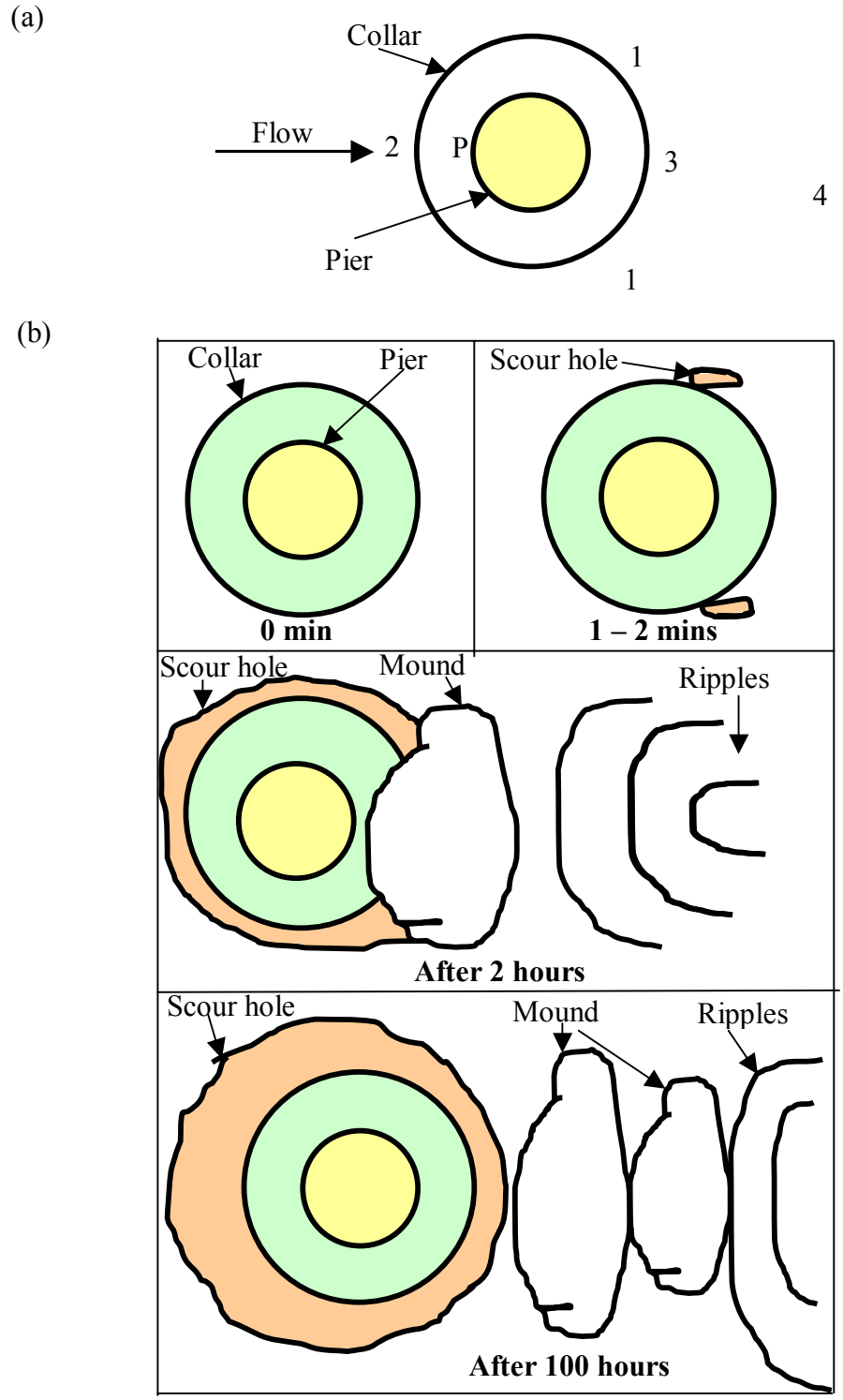


Figure 4.7. Schematic illustration of the scour hole development for pier with a collar: Scour pattern, and (b) Sketches of scour hole with time

Figure 4.8. Photograph of scour hole at the middle of the Series 1 test with a 2D collar

Figure 4.9 shows the temporal development of scour for the test. The data plotted in the figure are also listed in Appendix C-2. There was a temporary equilibrium during an early stage of the test (because of the deposition of sediment material on the grooves), during which time the maximum depth of scour was constant, as shown in Figure 4.9. A similar observation was made by Ettema (1980). Eventually, the development of the scour hole resumed, and the scour phenomenon behaved in a way similar to what was observed when the test was carried out without the collar installed. The test was run for 194 hours. An equilibrium scour condition was not achieved by the end of the test. The test was stopped because the scour was about to penetrate through the thickness of the sand layer.

The scour rate with time for the 115 mm pier fitted with a 2D collar is shown in Figure 4.10. Similar to the data indicated in Figure 4.6, the rate of scour decreases with time. As shown in Figure 4.10, the rate of increase of the scour depth had reduced from 138 mm/hr during the first three minutes of the test to 0.3 mm/hr by the end of the test. The figure has a similar pattern and trend with that of Figure 4.6. Similarly, a slope of a straight line fitted to the curve in Figure 4.10 is 0.753 and when compared with the slope shown in Figure 4.6 for the case of a plain pier, it is seen that they both have a negative slope and that there is a reduced slope in case of a test involving a 2D collar. The collar acts as an obstacle against the down-flow and the down-flow loses its strength on

impingement at the collar thereby reducing the rate at which sediment is removed. It should be noted, as evident in Figure 4.9, that some negative scour rates were experienced but Figure 4.10 shows no such evidence. The negative values of the scour rate were not plotted in Figure 4.10 because negative values cannot be plotted on log-log scale. In part, however, the matter of negative scour rates is an issue of measurement resolution rather than the actual depth of the scour getting larger and smaller.

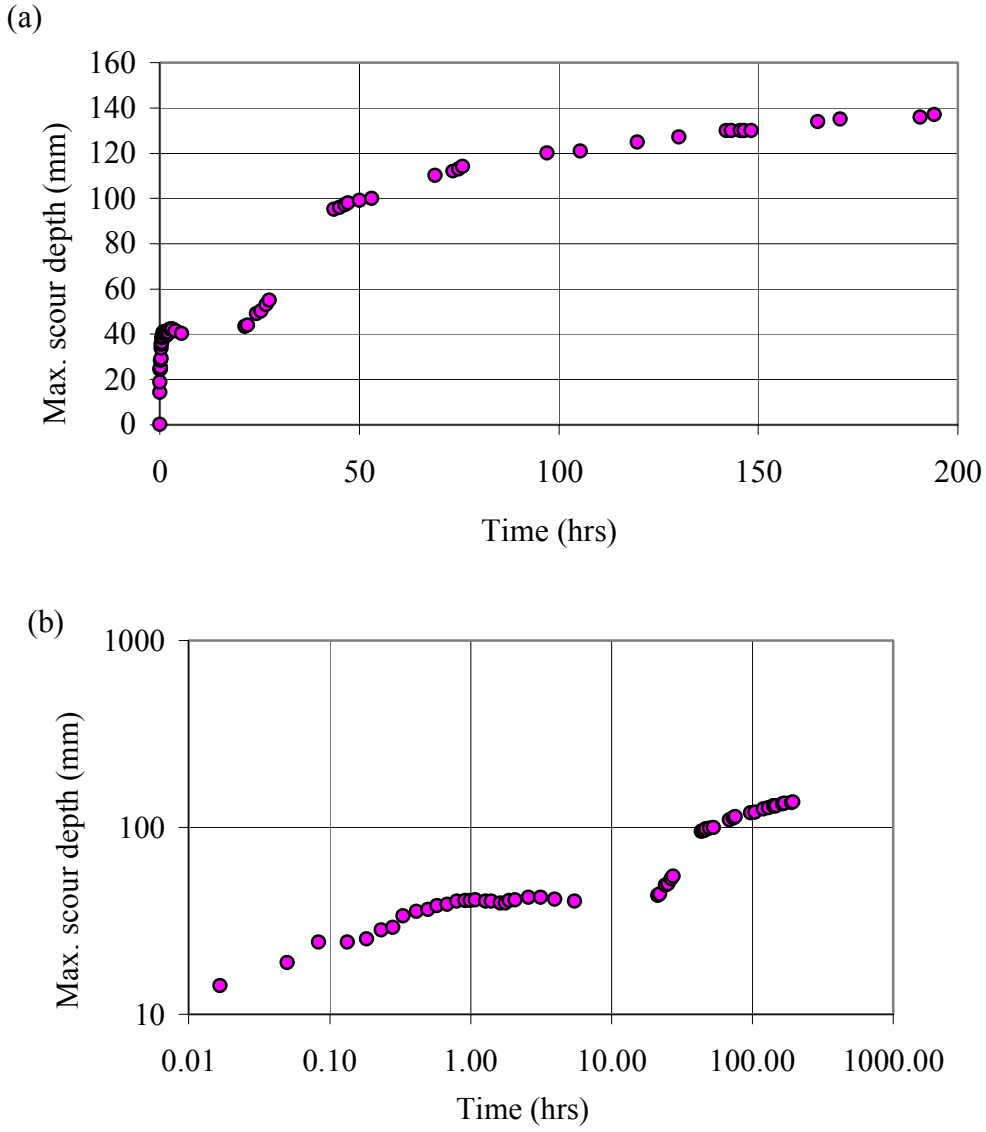


Figure 4.9. Temporal development of scour depth for the 115 mm pier with a 2D collar: (a) Arithmetic scale, and (b) Log-log scale

The maximum scour depth reached was 137 mm. About 70% of the measured maximum depth of scour occurred within the first 45 hours, which is equivalent to 23% of the total test time.

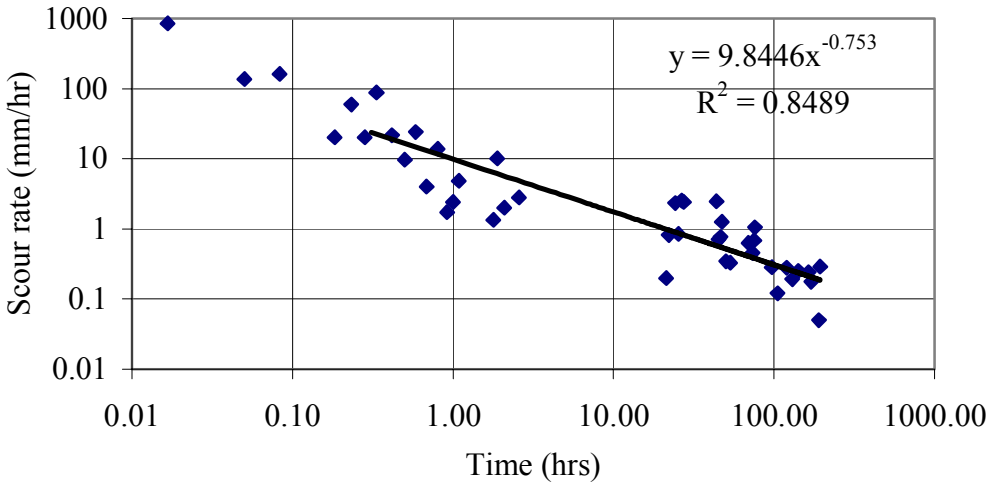


Figure 4.10. Scour rate with time for the 115 mm pier with a 2D collar

To further compare the data set in the Series 1 tests, the time development of the maximum scour depth for the model pier with a 2D collar and the case where a plain pier was used is shown in Figure 4.11. In Figure 4.11, the data indicated in Figure 4.5 were plotted together with that of Figure 4.9 for easy comparison. As shown in Figure 4.11, the time development of local scour can vary depending on whether a collar has been fitted to the pier or not. For the two tests, it can be seen that the time history of the scour is different. For example, after 22 hours, the maximum measured depths were 44 mm and 109 mm, respectively, for the pier protected with a 2D collar and the one without a collar.

Ettema (1980) identified three phases of the development of local scour at a cylindrical pier. They are the initial phase, the principal erosion phase, and the equilibrium phase. As defined by Ettema, only the first two phases have been experienced in the Series 1 tests. An equilibrium phase was not reached. Ettema defined the time to equilibrium scour as the time at which no more than 1 mm of incremental scour was realised within a timeframe of four hours. Since the test durations reported here are greater than some of those reported by Ettema (less than six days), it would seem doubtful if an

equilibrium phase is attainable. Therefore, the idea of equilibrium scour condition being achieved within that time frame as reported by Ettema might have been misreported in the literature.

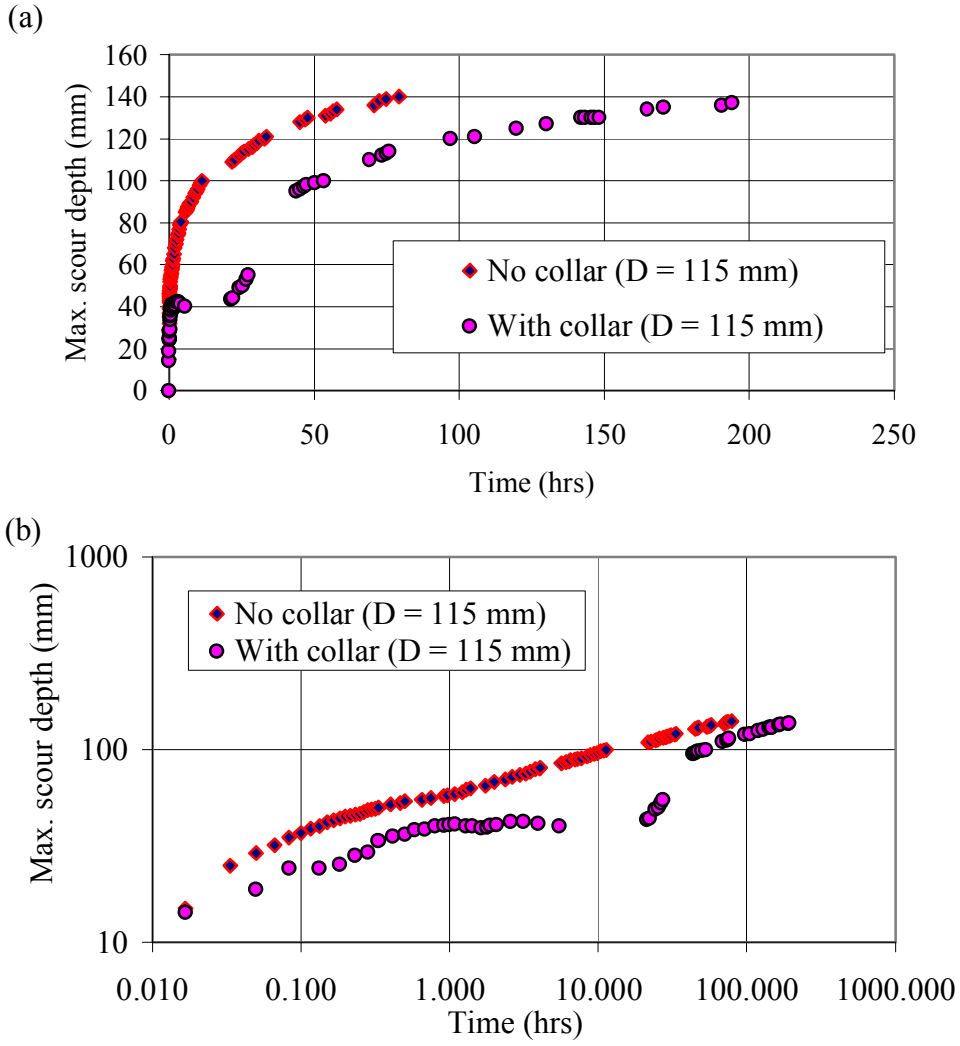


Figure 4.11. Combined temporal development of scour depth for the Series 1 tests: (a) Arithmetic scale and (b) Log-log scale

In summary, the time development of scour for a 115 mm diameter pier was studied in the Series 1 tests for the case where a 2D collar was fitted to the pier and for the plain pier case where no collar was fitted to the pier. It was observed that as the time increased the scour depth also increased. It was observed that the rate of scour decreased as the time increased. The results are in agreement with the work of other

researchers such as Ettema (1980), Tanaka and Yano (1967), Chabert and Engeldinger (1956), Thomas (1967) and Chiew and Melville (1992). It was noted that the efficacy of a collar as a countermeasure decreased as the test duration increased. An equilibrium condition was not achieved in the Series 1 tests.

## 4.5 Scour test results: Series 2 tests

The Series 2 tests are a little the same as the Series 1 tests but with a few differences. The basic difference is that, in the Series 2 tests, the pier diameter was 73 mm instead of 115 mm. The Series 2 tests were also operated at a flow intensity of 89%. Since the flow depth for the tests was set at two times the pier diameter, the approach flow velocity and flow rate for the Series 2 tests are different from the Series 1 tests. The flow conditions are as shown in Table 3.1.

### 4.5.1 Pier without a collar: 73 mm diameter pier (flow intensity = 0.89)

The same observations presented above for the case of 115 mm diameter pier were also noticed for the 73 mm diameter pier. The scour started at the sides of the pier (i.e., region 1 in Figure 4.4a). The resulting scour hole rapidly propagated around the pier perimeter shortly after the commencement of the test, eventually coinciding at the upstream centerline of the pier (i.e., region 2 in Figure 4.4a). At a time of five minutes after the commencement of the test, the maximum scour depth at the sides (region 1) and immediate back of the pier (region 3) was 38 mm and 10 mm, respectively. The height of the sediment mound at the backside of the pier at this time was about 30 mm. At about 22 minutes after the commencement of the test, the point of maximum scour depth shifted to the upstream face of the pier (region 2, Figure 4.4a). The corresponding scour depth at the backside of the pier was 20 mm while the height of the mound was 40 mm. The ripples that formed at the backside of the pier migrated rapidly downstream (Region 4). Figure 4.12 shows the temporal development of the maximum scour depth for the 73 mm diameter pier. The data plotted in the figure are also presented in Appendix D-1.

As the results of the test show in the figure, an equilibrium scour condition was not attained before the test was ended at about 49 hours. As with the pier of diameter 115 mm, the scour depth increases with time. The relatively short test duration of about 49 hours was due to the development of bed material transport in the form of ripples advancing from the upstream end of the flume. About 70% of the measured depth of scour was achieved at about 6.5 hours, which corresponds to approximately 13% of the total test duration.

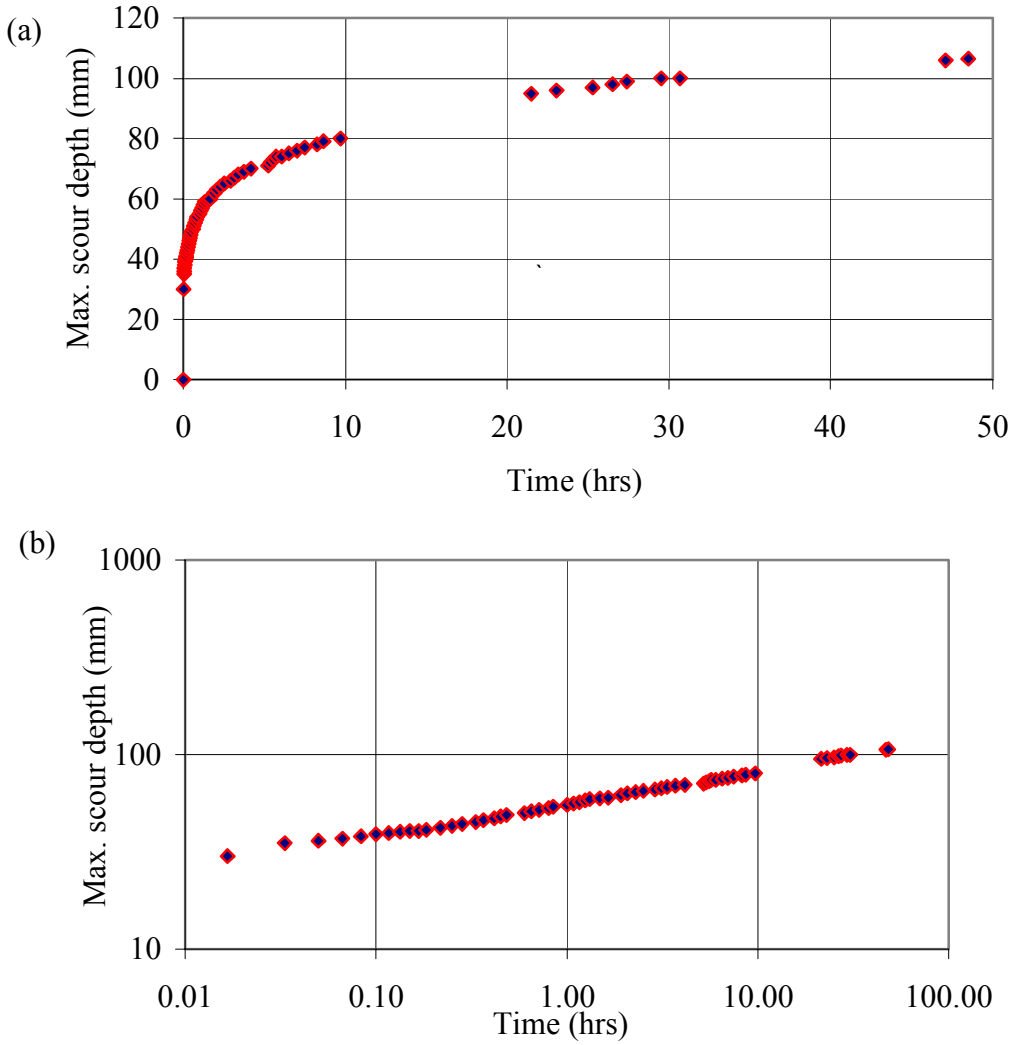


Figure 4.12. Temporal development of scour depth for the 73 mm pier without a collar: (a) Arithmetic scale and (b) Log-log scale

The maximum scour depth was about 107 mm by the time the test was stopped. The test was stopped because of the general bed material motion. Figure 4.13 shows the scour

rate with time for the test. The rate of scouring, which was 60 mm/hr after only three minutes into the test, was reduced to 0.4 mm/hr by the time that the test was stopped. Figure 4.13 follows the same trend as Figure 4.6 and Figure 4.10. For instance, the slope of a line of best fit to Figure 4.13 is 0.828, which is approximately equal to a slope of 0.833 obtained from Figure 4.6.

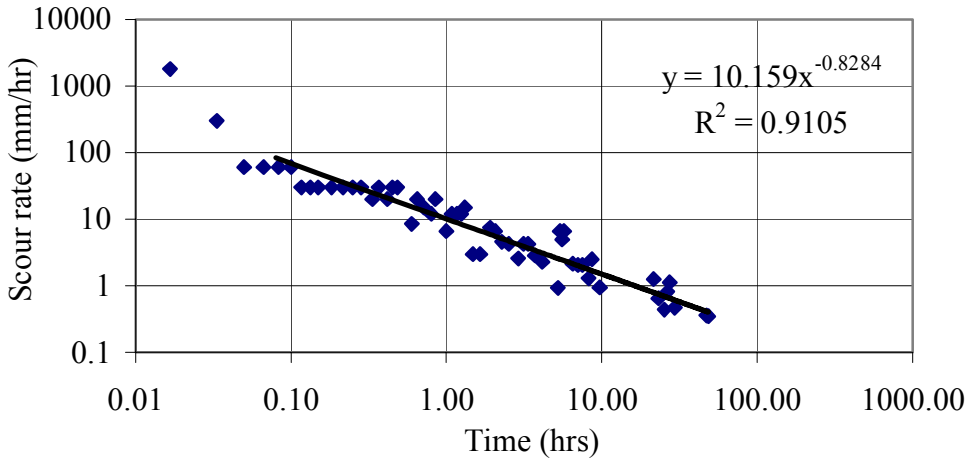


Figure 4.13. Scour rate with time for the 73 mm pier without a collar

### 4.5.2 Pier fitted with a collar: 73 mm diameter pier (flow intensity = 0.89)

The same observations made in the case of the 115 mm diameter pier with a 2D collar were observed for the 73 mm diameter pier fitted with a 2D collar. The scour started at both sides of the collar (i.e., region 1, Figure 4.7a), reaching the upstream face of the collar (region 2) after 43 minutes of running the test. At that time, the maximum scour depth at the sides of the collar and at the upstream face of the collar were about 28 mm and 5 mm, respectively. Within about 48 minutes of starting the test, the sediment deposit at the backside of the collar (region 3) was 18 mm high while the maximum scour depth at the upstream face and sides of the collar was 15 mm and 29 mm, respectively. As was also observed for a pier of diameter 115 mm fitted with a 2D collar, ripples formed at the backside of the collar as the test progressed (region 4, Figure 4.7a). For instance, the ripples propagated downstream a distance of about 450 mm relative to the pier position after a time of 59 minutes, while at a time of 124 minutes the ripples had spread to about 850 mm.

It was observed that the position of the maximum scour depth was sometimes located under the collar at the upstream face. For example, Figure 4.14 shows the location of the point of maximum scour depth beneath the collar at a time of 144 minutes of running the test. At this time, the maximum scour depth was located at about 5 mm from the edge of the collar circumference at the upstream face as depicted in Figure 4.14.

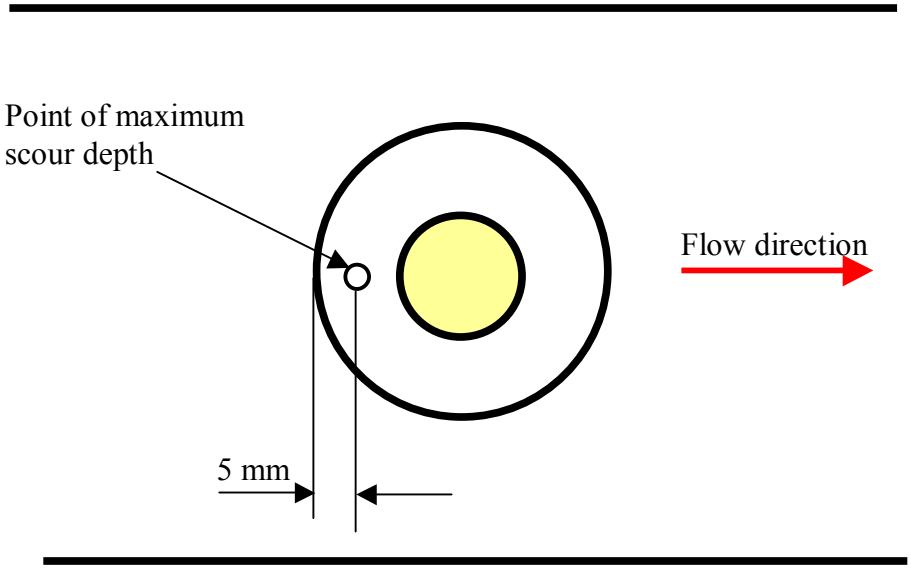


Figure 4.14. Location of point of maximum scour depth found beneath the collar

When the point of maximum scour depth was located under the collar, the scour depth was estimated relative to the reading from the point gauge measurement taken outside the collar position at the upstream face and also relative to the reading from the scale around the pier. An estimate of the maximum scour depth was achieved by using these two related measurements as a reference.

As the test proceeded, there was alternate formation of depressions and mounds in the region downstream from the pier. After about two and a half hours of running the test, the mound, which had a maximum height of 30 mm, was located at the backside of the collar at a distance of 200 mm from the centre of the pier.

Figure 4.15 show the temporal development of scour for the pier of diameter 73 mm fitted with a collar. The data plotted in the figure are also presented in Appendix D-2. As shown in the figure, there was an irregular growth in the scour depth during an early stage of the test (say 3 hours) because of the deposition of sediment material removed from beneath the collar on the grooves as shown in figure. Therefore, there was an alternate decrease and increase of the scour depth with time during the initial phase of the scour process. The collar acts as an obstacle against the down-flow and the down-flow loses its strength on impingement at the collar thereby reducing the rate at which sediment is removed. The test was run for about 59 hours. An equilibrium scour condition was not reached as the test was stopped because of the cascade of ripples that enveloped the flume. The maximum scour depth attained was 83 mm. About 70% of the measured maximum scour depth occurred during the first 15 hours of the test, representing about 26% of the total test duration.

Figure 4.16 shows the scour rate with time for the 73 mm pier with a 2D collar. As with the other tests, the rate of increase of the scour depth reduces with time. For example the scour rate reduced from 60 mm/hr during the first six minutes of the test to about 0.2 mm/hr at the end of the test. The slope of the power law equation fitted to the figure is 0.809, which is slightly lower than the slope for a plain pier shown in Figure 4.13.

Figure 4.17 shows the temporal development of scour for the tests in Series 2 plotted together. The reason for doing this is for comparison purposes as explained above for the case of Series 1 tests. It is shown that the temporal development of the maximum scour depth is similar in trend to that of the 115 mm pier. Moreover, it is apparent that an equilibrium scour condition was not achieved. It is also found that the temporal development of the scour with and without a protective collar in place is different, with the collar providing for a delay in the scour development.

In summary, it is seen that the same trend that was noticed in the Series 1 tests was also observed in these tests. The scour depth increased with time and the scour rate reduced with time. An equilibrium condition was not also attained in the Series 2 tests. Based on the Series 1 and 2 tests, it can be said that for the same flow intensity of 0.89, the

slope of the line of best fit to the scour rate versus time is higher for the case of a plain pier when compared with a pier fitted with a collar.

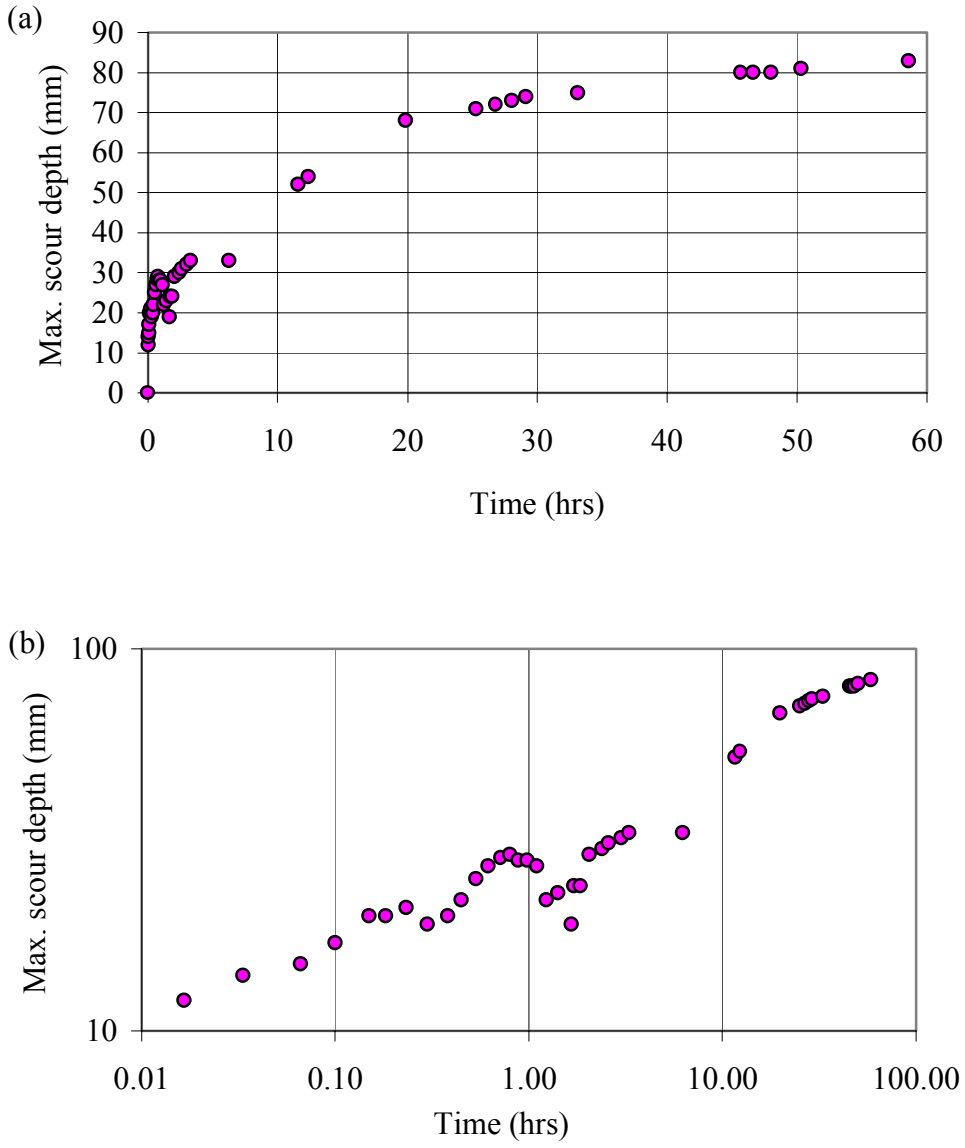


Figure 4.15. Temporal development of scour depth for the 73 mm pier with a 2D collar: (a) Arithmetic scale and (b) Log-log scale

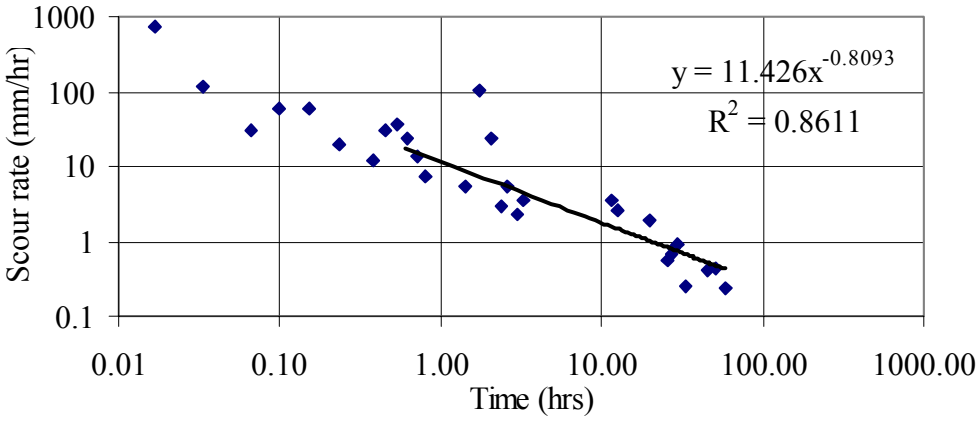


Figure 4.16. Scour rate with time for the 73 mm pier with a 2D collar

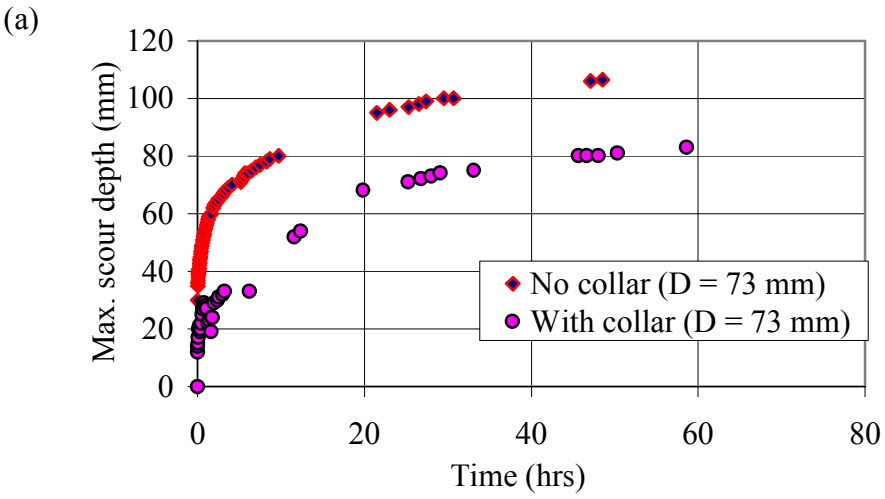


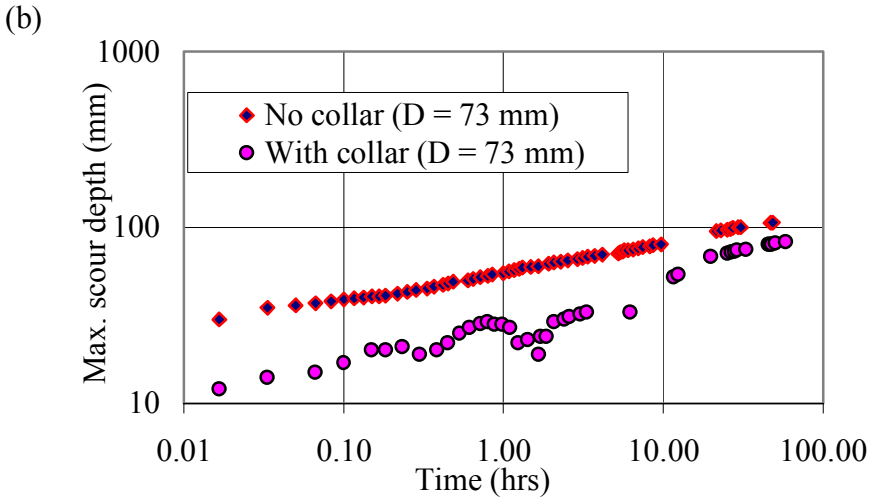


Figure 4.17. Combined temporal development of scour depth for the Series 2 tests: (a) Arithmetic scale and (b) Log-log scale

### 4.5.3 Repeatability of tests

In hydrotechnical engineering, running duplicate tests in order to ensure data quality and integrity is sometimes not done. What is typically being done is to carry out several series of tests under systematically selected experimental conditions such that any outlier among the tests can easily be detected. Duplicate tests were run as part of the study in order to clarify the issue of repeatability of tests. The results of such tests helped to ascertain whether it is possible to repeat a test. To demonstrate the repeatability of a test and for the purpose of an illustration, the results of the two tests carried out using a 73 mm diameter pier for the same experimental conditions (Table 3.1) is presented in Figure 4.18. As can be seen in the figure, the temporal development of maximum scour depth for the two tests, A and B, collapsed to form almost a single function. It may not be necessary, therefore, to run a duplicate test for a test of this nature especially when the cost and time of doing so are taken into consideration. It should be noted that Series 1 tests were also repeated and they were found to be reproducible.

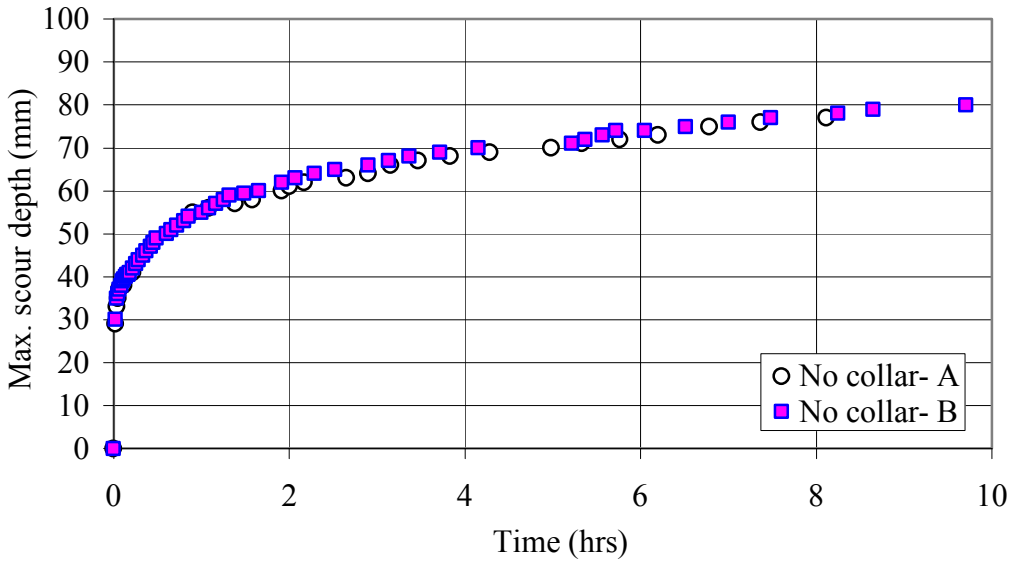


Figure 4.18. Time development of scour for the repeated test: Series 2 test without collar

## 4.6 Scour test results: Series 3 tests

The Series 3 tests comprised of two tests. A 115 mm diameter pier was used for both tests. The first test was run without a collar installed on the pier, while in the second test a 3D collar was fitted to the pier. In the Series 3 tests, an evaluation of the temporal development of the maximum scour depth for the flow conditions shown in Table 3.1 was carried out. For these tests, the flow intensity was 0.70. This is a lower flow intensity than for the Series 1 and 2 tests where the flow intensity was 0.89. As shown in Section 4.2, a clear-water flow cannot be maintained for a longer time at a higher flow intensity for the sediment size used in these tests. Therefore, a lower flow intensity was used in the Series 3 tests.

### 4.6.1 Pier without a collar: 115 mm diameter pier (flow intensity = 0.70)

The effect of the scouring process was noticed immediately upon starting the test as indicated by the removal of sand particles in the vicinity of the pier. The scour started first at the sides of the pier (i.e., region 1, Figure 4.4a), and eventually propagated rather rapidly around the pier perimeter from both sides toward the centerline of the pier at the upstream face (region 2, Figure 4.4a). At this stage, there was a ring-like groove formed by the scouring process around the upstream half of the pier (i.e., between regions 1 and 2). The point of maximum scour, which was initially located at the side of the pier, migrated to the upstream face of the pier after about six hours of starting the test. As the scour process continued, the scoured sand material was deposited in the wake region immediately downstream from the pier (region 3) and the formation of ripples became evident (region 4). The deposited sediment in the wake region, which was initially found very close to the backside of the pier, was observed to move downstream while a scour hole became noticeable immediately behind the pier.

Photographs of the final scour pattern are as shown in Figures 4.19 and 4.20. The overall scour pattern, which was symmetrical, consisted of a hole situated in front of the pier, a mound of deposited sand located a short distance downstream from the pier, and an alternate formation of depressions and mounds and a series of ripples fanning out from the pier in the downstream direction. The point of maximum scour depth, which

was first noticed at the immediate upstream face of the pier after about six hours, remained at the upstream face of the pier for most of the test duration of about 531 hours. The test was stopped because the scour was about to penetrate through the thickness of the sand layer in the flume. It was apparent from the test that the maximum depth of scour and the maximum height of the mound continued to increase with time. It was also evident that the location of the mound moved downstream as time increased. At the end of the test, the shape of the scour hole around the pier could be approximated by the shape of an inverted cone, as shown in the photographs. The upstream half of the scour hole can be approximated as that of half an inverted frustum of a right circular cone. The cone angle of the frustum at the upstream face of the pier was estimated to be equal to the angle of repose of the sediment (i.e., 30˚)

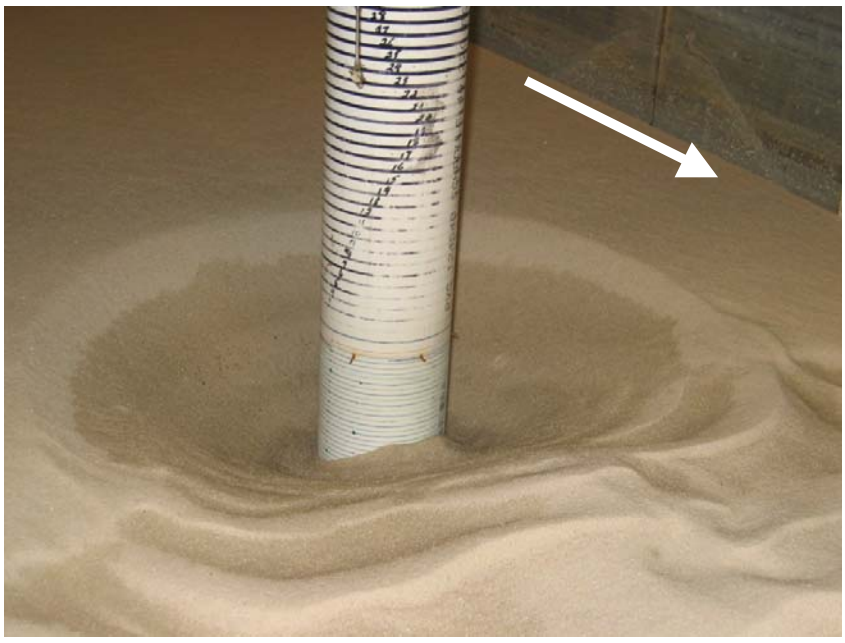

Figure 4.19. Photograph of scour hole at the end of the Series 3 test: No collar

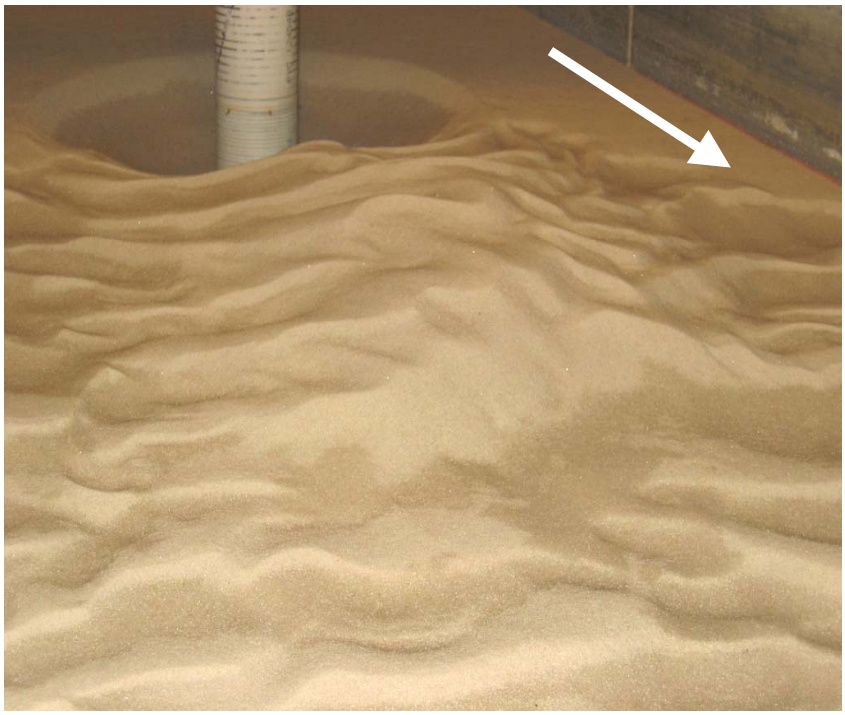

Figure 4.20. Photograph of mounds and depressions at the end of the Series 3 test: No collar (Note the scour hole at the pier)

The result of the test carried out for the pier not protected with a collar is shown in Figure 4.21. The data plotted in the figure are also presented in Appendix E-1(a). The results show that the maximum scour depth increases with time and that the rate of increase of scour depth decreases as the time increases. An equilibrium condition was not reached in this test. The scour rate with time for this test is shown in Figure 4.22.

The rate of scouring, which was 180 mm/hr after only three minutes into the test, was reduced to 0.1 mm/hr by the time that the test was stopped. At that point, the maximum scour depth was about 140 mm. As shown in Figure 4.22, the plot shows the same trend and pattern with that of Figure 4.6 even though they are of different test conditions. The slope of the power equation fitted to Figure 4.22 (i.e., 0.7635), however, is lower than that of Figure 4.6 and Figure 4.13. The reason for this lower slope might be due to a lower flow intensity used in the case of the test results shown in Figure 4.22.

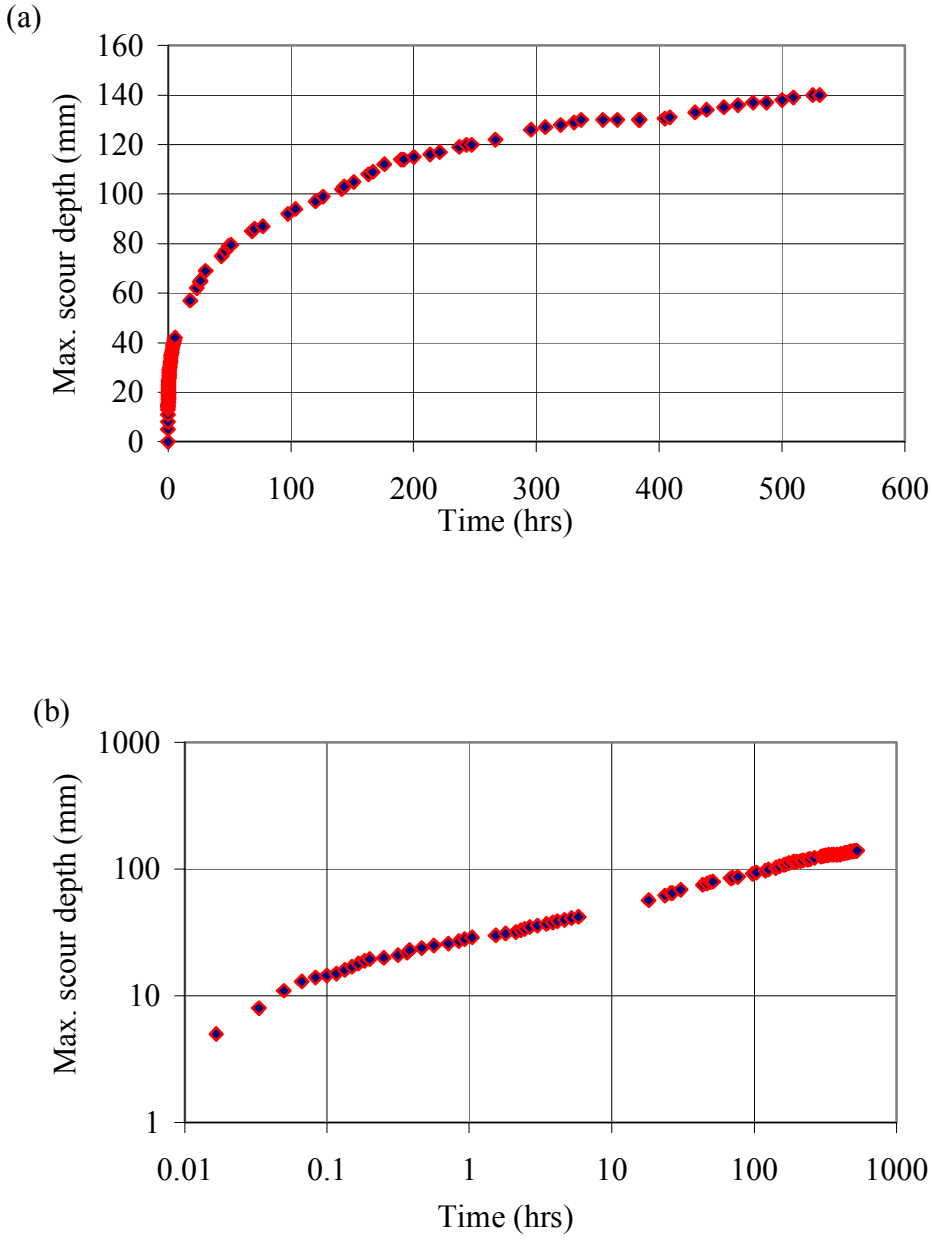


Figure 4.21. Temporal development of scour depth for the Series 3 test without a collar: (a) Arithmetic scale and (b) Log-log scale

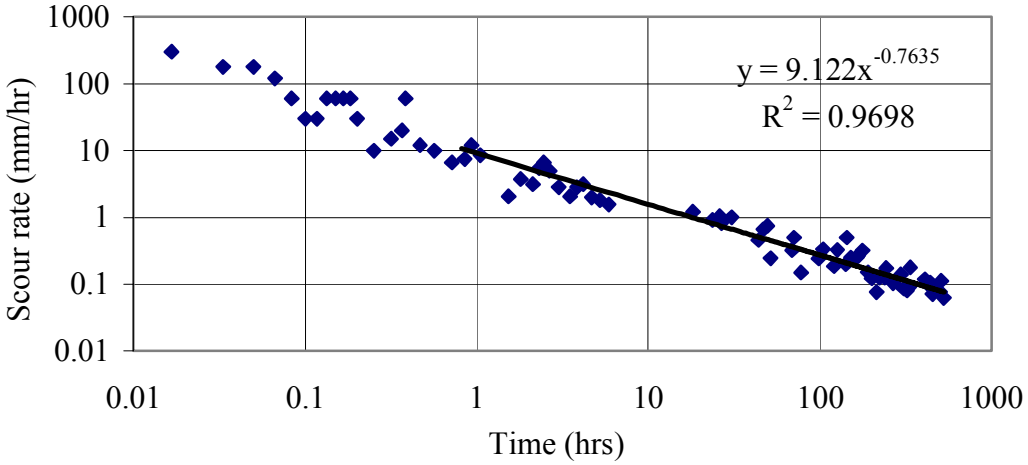


Figure 4.22. Scour rate with time for the 115 mm pier without a 3D collar (Series 3 test)

#### 4.6.1.1 Scour hole contour for Series 3 tests without a collar

The contour map and the 3-D map of the scour hole at the end of the test are as shown in the Figures 4.23 and 4.24, respectively. The data plotted in the figures are given in tabular format in Appendix E-1(b). As shown, apart from the scour hole, there was also the alternate formation of mounds and depressions. Also, the scour hole is predominant at the upstream face of the pier. The maximum scour depth is also located at the upstream face of the pier. The maximum scour depth is shown by a contour line of about 14 cm while the maximum height of the mound is about 7 cm.

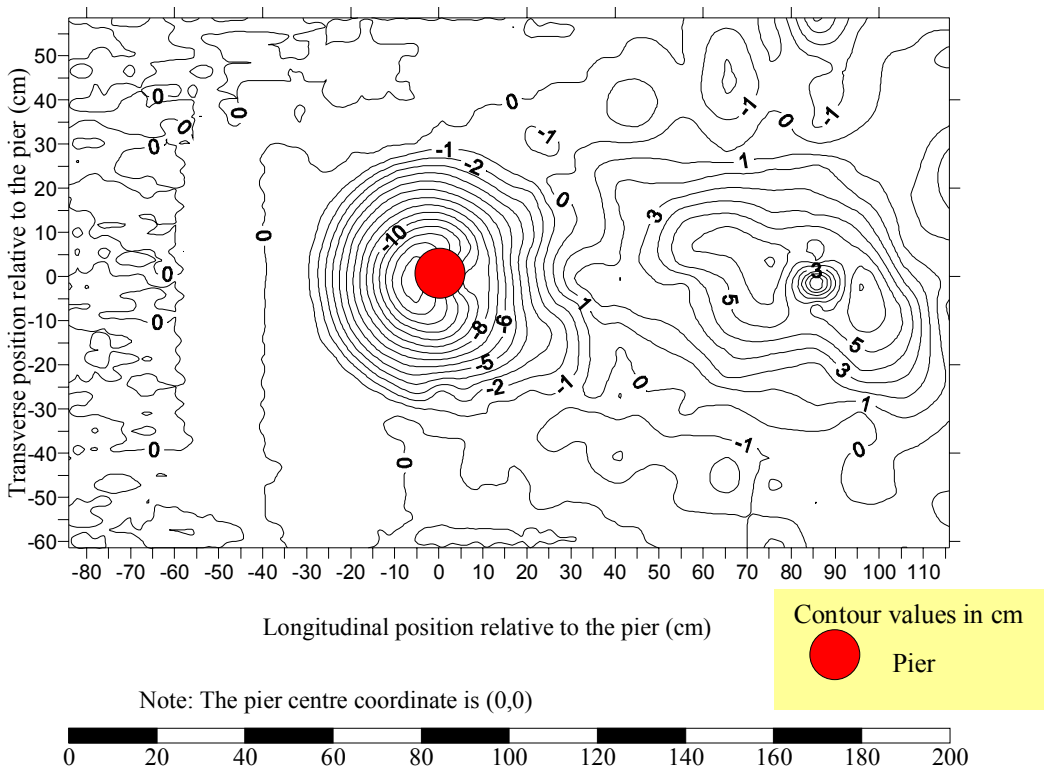


Figure 4.23. Contour map of the scour for the Series 3 test: No collar

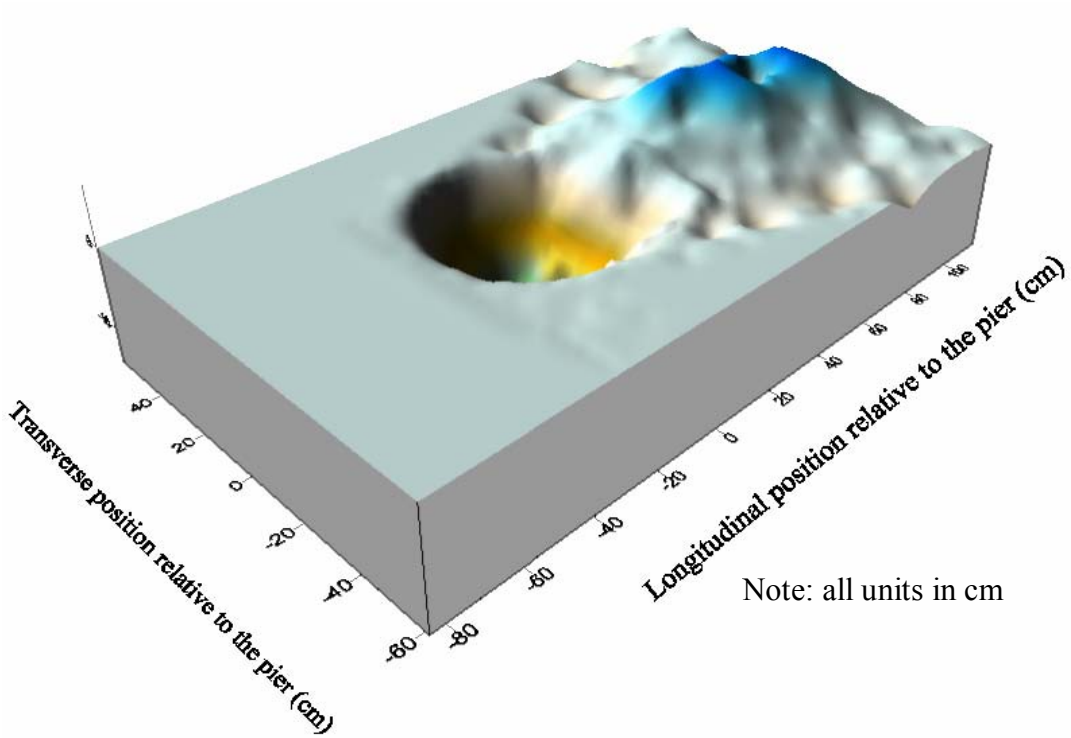


Figure 4.24. Oblique 3-D map of the scour for the Series 3 test: No collar

#### 4.6.1.2 Longitudinal scour profile for Series 3 test for a plain pier

The longitudinal profile of the scour along the centreline of the channel is plotted in Figure 4.25. Since an equilibrium scour condition has not been reached, the scour process at this stage is still at the erosion phase as defined by Ettema (1980). The data plotted in the figure are given in tabular format in Appendix E 1(c). The (0,0) reference point is at the original bed level at the centreline of the pier. As shown, the deepest portion of the scour hole occurred at the upstream face of the pier. After a distance of 115 cm downstream of the pier, there was a series of ripples fanning out and occupying the entire width of the flume. The maximum height of the mound at the wake is about 54% of the maximum scour depth.

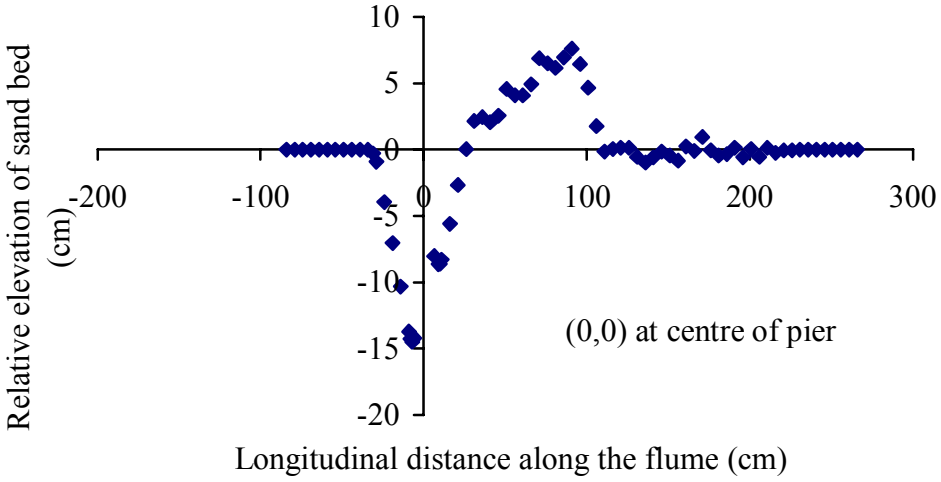


Figure 4.25. Longitudinal scour profile at the centreline of the plain pier: Series 3 test

#### 4.6.1.3 Transverse scour profile for Series 3 test for a plain pier

Figure 4.26 shows the lateral profile of the scour hole through the centreline of the pier. The data plotted in the figure are given in tabular format in Appendix E-1(d). The (0,0) reference point is at the original bed level at the centerline of the pier. As shown in Figure 4.26, the scour profile is symmetrical about the pier. For instance, it is shown that the scour hole extended to a distance of approximately 300 mm away from either side of the pier. It is also shown that the maximum scour depth at the side of the pier is about 126 mm, which is less than the 140 mm maximum scour depth observed at the upstream face of the pier.

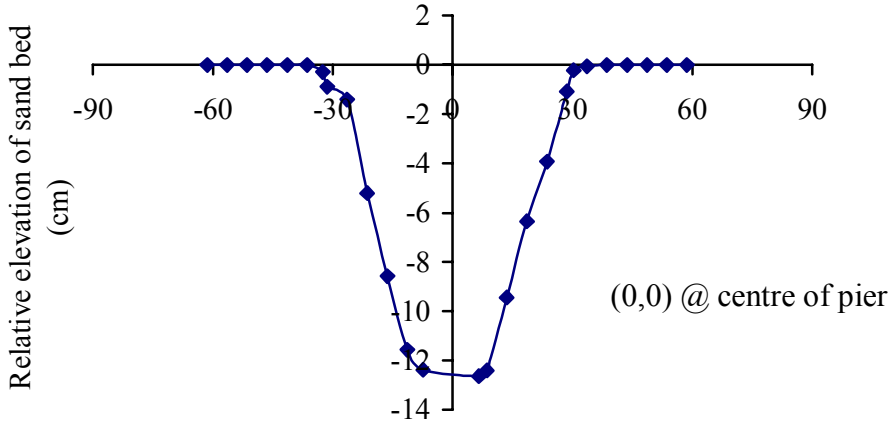


Figure 4.26. Transverse section of scour profile across the plain pier centre: Series 3 test

### 4.6.2 Pier fitted with a collar: 115 mm diameter pier (flow intensity = 0.70)

For the test with a 3D collar fitted to the pier, scour was first noticed to occur at the backside of the collar on either side of the pier toward the downstream region as shown in Figure 4.27a. At about 20 minutes after starting the test, no scour had yet occurred at the side and upstream face of the collar, however, a small amount of sediment was deposited on top of the collar at the backside. As the test progressed, the scour hole on either side of the backside (regions A and B in Figure 4.27a) started expanding in size towards the downstream region away from the collar. It took about 313 hours into the test before the scour hole started migrating toward the side of the collar, but surprisingly only at one side of the collar as depicted in Figure 4.27b. Thus, the scour was asymmetrical around the collar perimeter. It is to be noted, however, that the scour penetrated beneath the collar towards the pier as shown in Figure 4.27b.

As the test proceeded, the groove, which was formed at only one side of the collar, began to extend toward the upstream side, eventually reaching to the centreline of the collar (see Figure 4.27b). In due course, the scour pattern at the upstream side of the collar progressed below the collar and eventually to the other side of the collar as shown in Figure 4.27c. For this test, the points of maximum scour were located at regions A and B as shown in Figure 4.27c. The test was stopped after 955 hours.

The location of the maximum scour depth with time is shown in Figure 4.28. The data plotted in the figure are given in tabular format in Appendix E-2(a). For illustration purposes, the term t[419] as shown in the legend of the figure denotes the time of the test in hours, while the corresponding symbol shows the location of the maximum scour depth at that time. As shown, the point of maximum scour depth hovered around the backside of the collar.

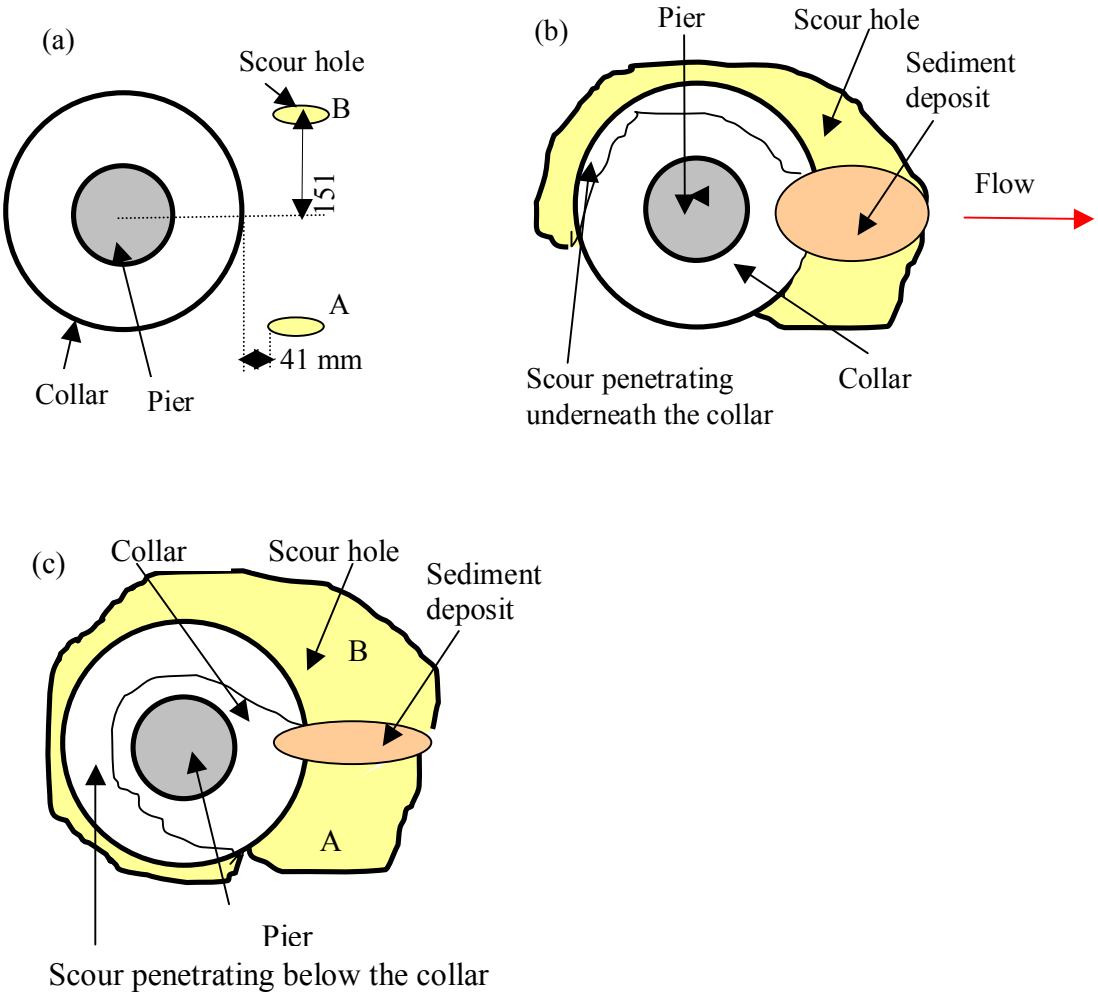


Figure 4.27. Schematic illustration of the scour hole patterns for the Series 3 test with a 3D collar: (a) First few minutes, (b) about 13 days, and (c) 28 days

The photographs in Figures 4.29, 4.30 and 4.31 show the scour pattern at the end of the test. As shown in Figure 4.29, the scour hole was most pronounced immediately

downstream from the collar. There were deposits of sediment in the region downstream of the collar as depicted in Figure 4.30. As shown in Figure 4.31, ripples formed further downstream of the collar.

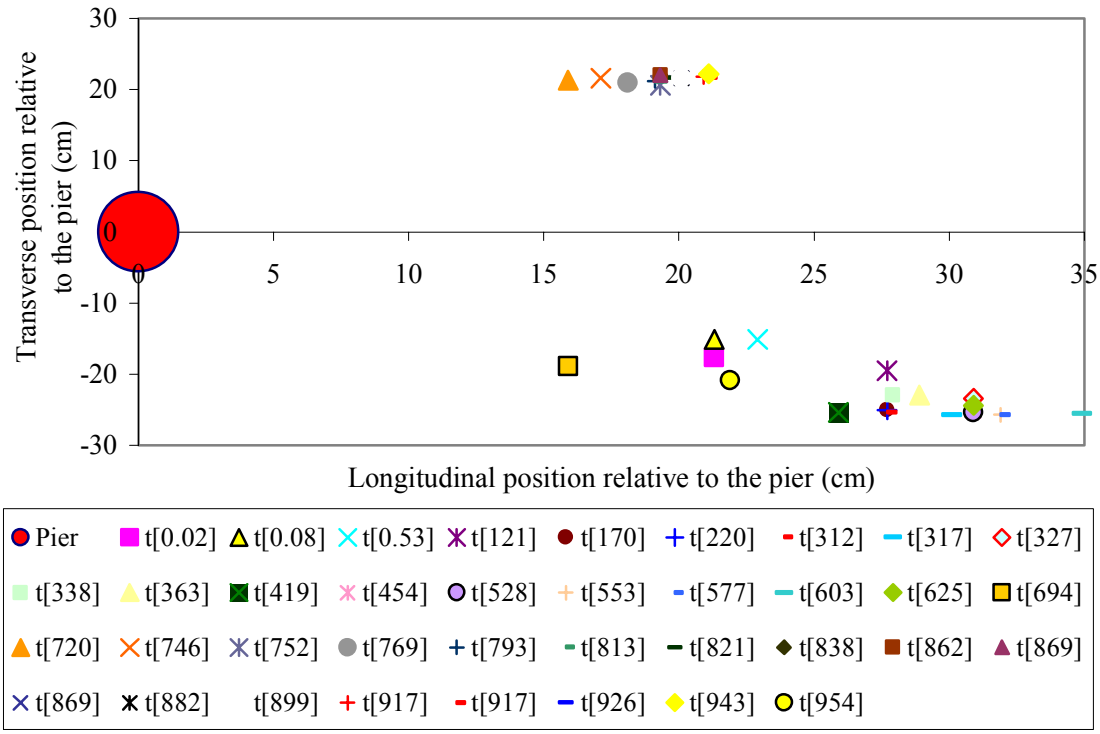


Figure 4.28. Locations of maximum scour depth with time: Series 3 test with a 3D collar

Figure 4.29. Scour pattern before the removal of the 3D collar at the end of the test

Figure 4.30. Scour pattern after removing the 3D collar at the end of the test

Figure 4.31. Scour pattern with mounds, depressions and ripples at the end of the test

The temporal development of the scour for the pier protected with a 3D collar is shown in Figure 4.32. The data plotted in the figure are given in tabular format in Appendix E 2(b). As shown, the scour depth increased with time. An equilibrium scour condition was not attained before the test was stopped due to a faulty pump controller. It should be pointed out here, however, that the test was being contemplated to be stopped just before this pump controller developed a fault. The test was taking a longer time than was anticipated. The test was ended after about 955 hours of its commencement.

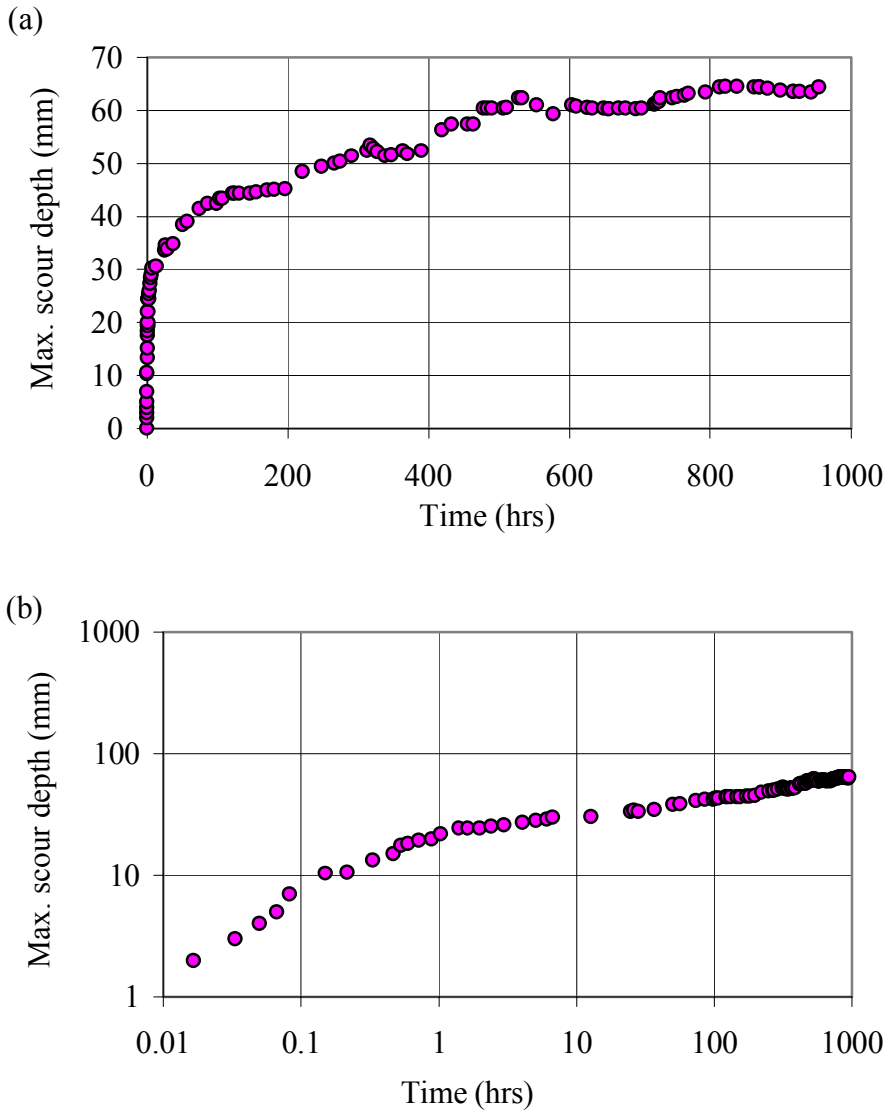


Figure 4.32. Temporal development of scour depth for the Series 3 test with a 3D collar: (a) Arithmetic scale and (b) Log-log scale

Figure 4.33 shows the scour rate with time for this test. As shown, the rate of scour decreases with time. For instance, the rate of increase of scour depth, which was 60 mm/hr during the first three minutes of the test, decreased drastically to about 0.1 mm/hr by the end of the test. Although, Figure 4.33 and Figure 4.22 show the same trend, the slope of the power law equation fitted to the former (i.e., 0.6995), is lower than that of the latter. Also, the slope as shown in Figure 4.33 is lower than the ones shown in Figures 4.10 and 4.16. The reason for the lower slope in Figure 4.33 might be due to a lower shear flow intensity under which the test was carried out and also because

of a larger size of collar used. The collar acts as an obstacle against the down-flow and the down-flow loses its strength on impingement at the collar thereby reducing the rate at which sediment is removed.

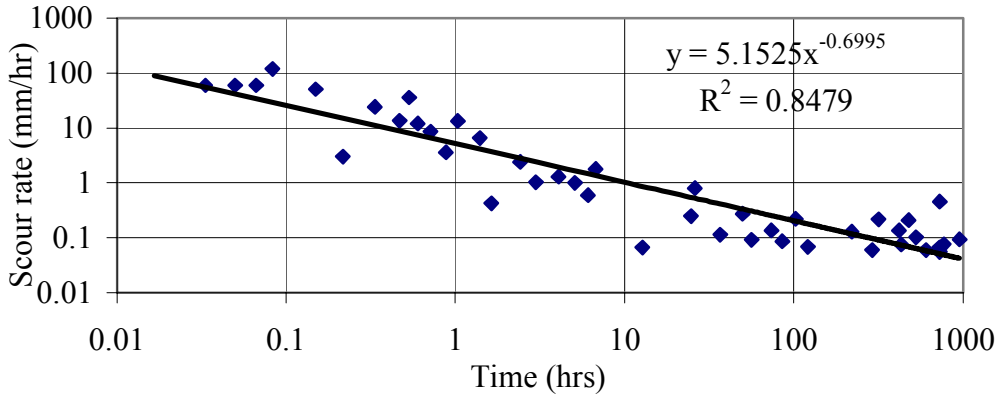


Figure 4.33. Scour rate with time for the 115 mm pier with a 3D collar (Series 3 test)

#### 4.6.2.1 Scour hole contour for Series 3 tests for a pier fitted with a collar

Figure 4.34 shows the contour map of the scour hole at the end of the test while Figure 4.35 shows the 3-D map of the scour hole. The data plotted in the figure are given in tabular format in Appendix E-2(c). The maximum scour depth is about 6 cm while the maximum height of the mound is about 5 cm. From the figures, it is shown that the point of deepest scour is located immediately downstream from the collar. This observation is different from the case for the plain pier in which the point of maximum scour depth was located at the upstream face of the pier. Similar observations were made by Kumar et al. (1999) for a larger size collar. However, it is not clear if in the longer term the position of the deepest scour would have shifted to the upstream face.

As shown in Figure 4.35, the scour hole did not reach the immediate vicinity of the pier after about 40 days of running the test, although the scour depth was increasing marginally, albeit at a slow rate at the time the test was stopped. This finding is in contrast to the test without a collar fitted to the pier (Figure 4.24) in which the position of the maximum scour depth was found at the immediate front face of the pier after about six hours of running the test. The reason for this is that the collar was able to curtail the action of the down-flow and the horseshoe vortex, thereby reducing the extent

of the scour. A similar observation that the scour did not extend to the immediate area of the pier was made by Mashahir and Zarrati (2002) after conducting an experiment for a duration of 52 hours also using a 3D collar. However, it may be speculated that there is the possibility of the scour hole reaching the immediate front face of the pier if the test had been allowed to run for a longer period of time. The logical question is for how long? This has remained unknown in the course of this study. It should be noted that little was done with the 3-D plots in Figure 4.24 and Figure 4.35, although the former at least gives a visual impression of the scour pattern, the latter figure does not really represent any type of an end condition, so it is less useful.

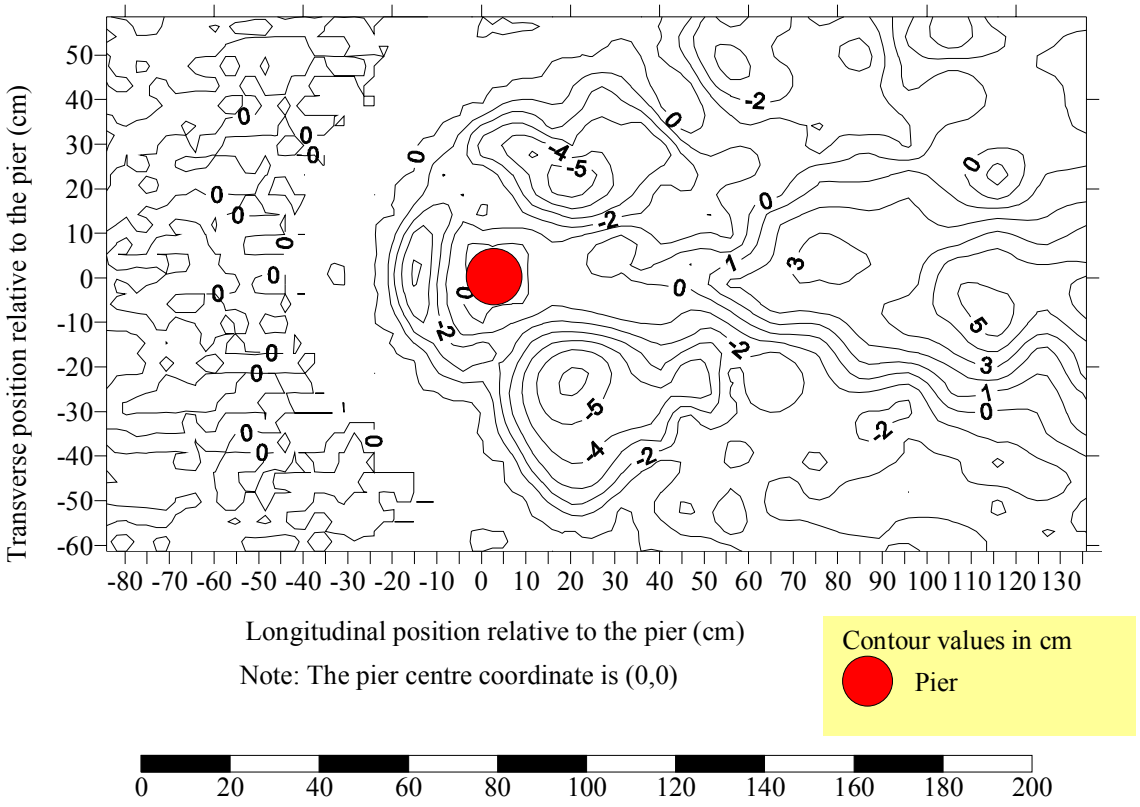


Figure 4.34. Contour map of the scour for the Series 3 test: With a 3D collar

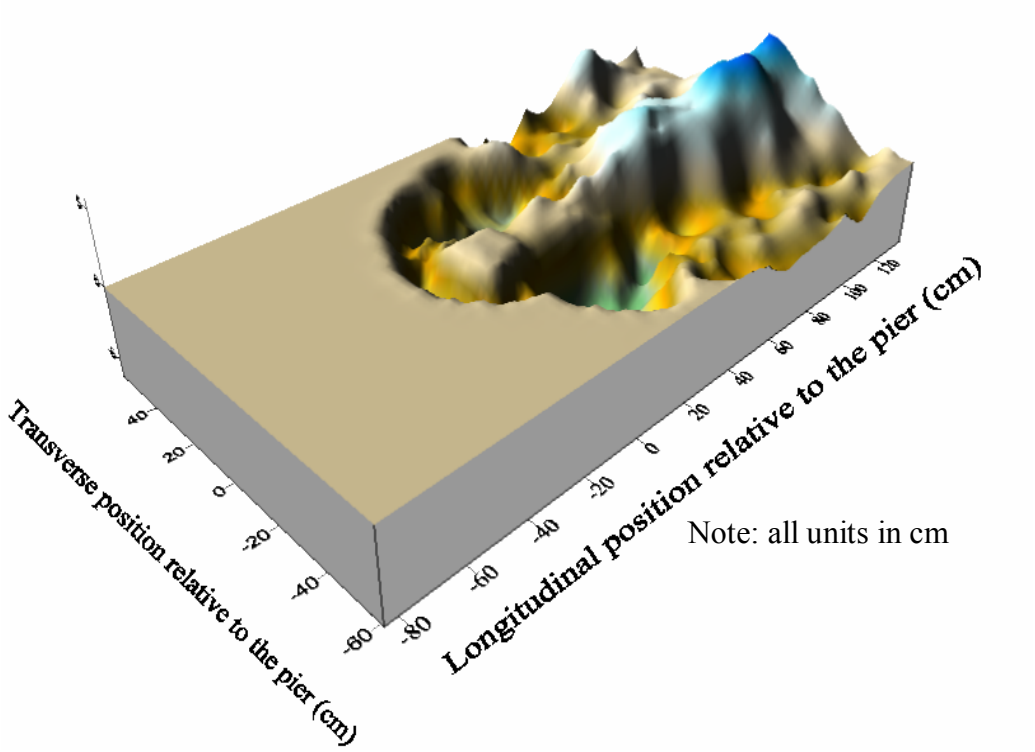


Figure 4.35. Oblique 3-D map of the scour for the Series 3 test: With a 3D collar

#### 4.6.2.2 Longitudinal scour profile for Series 3 test with a collar

The longitudinal scour profile along the centreline of the channel for this test is shown in Figure 4.36. The data plotted in the figure are given in tabular format in Appendix E 2(d). It can be seen that there was a limited amount of scour along the longitudinal centre of the pier in the region downstream from the collar. For instance, the maximum scour depth at the backside of the collar (labeled as C) in the Figure 4.36 was about 3.4 mm whereas at the upstream face of the collar (labeled as D), the maximum scour depth was 43 mm. As shown in Figure 4.36, there was an alternate formation of mounds and depressions at the region downstream from the collar. The same observation pertaining to the mounds and depressions was made for the case where the pier was unprotected with a 3D collar. The only difference is that the mounds and depressions occurred further downstream of the collar for the test with a 3D collar. The mounds and the depressions occurred in response to the deposition of the scoured sediment.

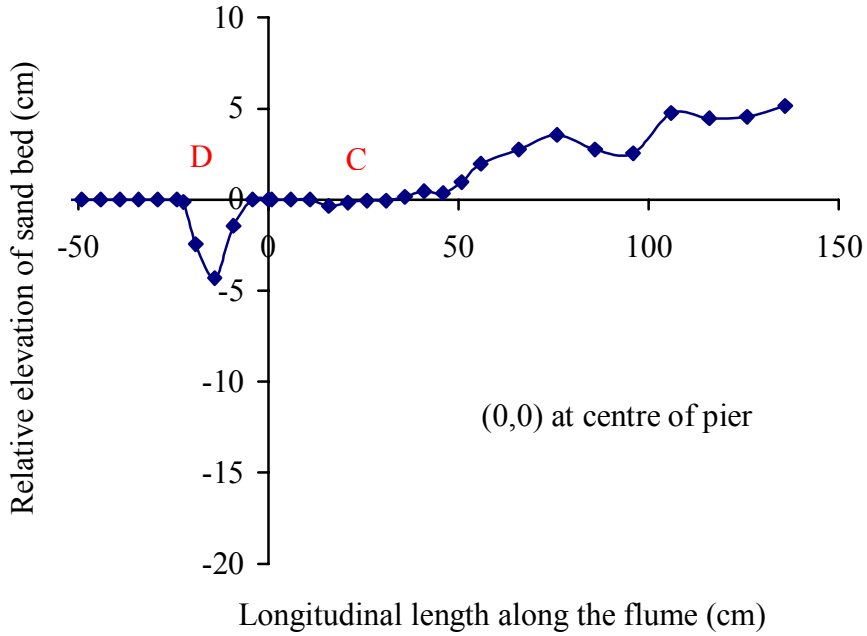


Figure 4.36. Longitudinal scour profile along the pier centre: Series 3 test with a 3D collar

#### 4.6.2.3 Transverse scour profile for Series 3 test with a collar

The transverse section of the scour hole through the centre of the pier and across the flume width is shown in Figure 4.37. The data plotted in the figure are given in tabular format in Appendix E-2(e). In this test, it was discovered that the scour hole profile at the two sides of the collar in the transverse direction was not similar. As shown in Figure 4.37, the scour depth at the side labelled E was 36.4 mm whereas at the side labelled F the scour depth was only 26.4 mm. Therefore, there was a 27.5% difference in the maximum scour depth between the two sides of the collar. The only plausible reason that could be given to the dissimilarity in the maximum scour depth is that there may have been a minor disturbance or disequilibrium in the course of conducting the test. When the result in Figure 4.37 is compared with the result of the test for the plain pier (Figure 4.26), an approximately equal depth of scour was observed at both sides of the pier instead of the dissimilarity in scour depth observed when a 3D collar was fitted to the pier. It is shown in Figures 4.36 and 4.37 that the scour hole did not reach the pier.

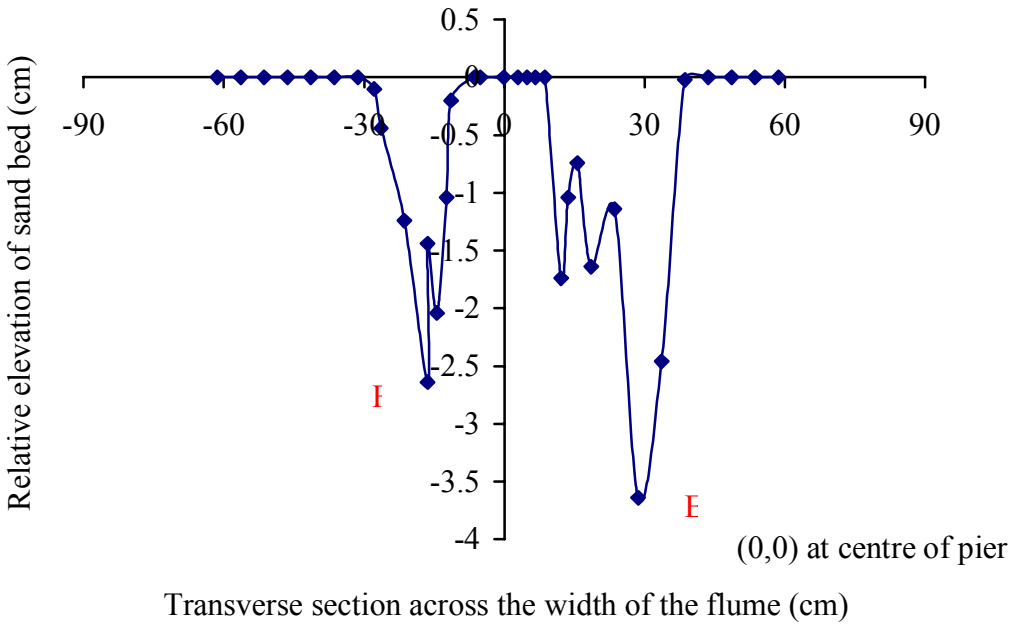


Figure 4.37. Transverse section of scour profile across the pier centre: Series 3 test with a 3D collar

### 4.6.3 Scour depth with time for the Series 3 tests (flow intensity = 0.70)

The temporal development of scour for the case where a 3D collar was fitted to the pier is compared with the case of a plain pier. Figure 4.38 shows the temporal development of scour for the two cases for a flow intensity of 70%. It is shown that the time history of the scour for the two cases is different. Also, there is an apparent reduction in the scour depth when a 3D collar was used to protect the pier against scour. The results in Figure 4.38 showed that a 3D collar may be very effective at reducing the maximum scour depth as well as the scour rate. It is shown that the 3D collar was able to reduce the maximum scour depth by about 58% after a test duration of 955 hours. It is also observed that an equilibrium scour condition has not been reached. Therefore, the 58% reduction in the scour depth due to the installation of the 3D collar cannot be said with a full conviction as the two tests were not run to an equilibrium stage.

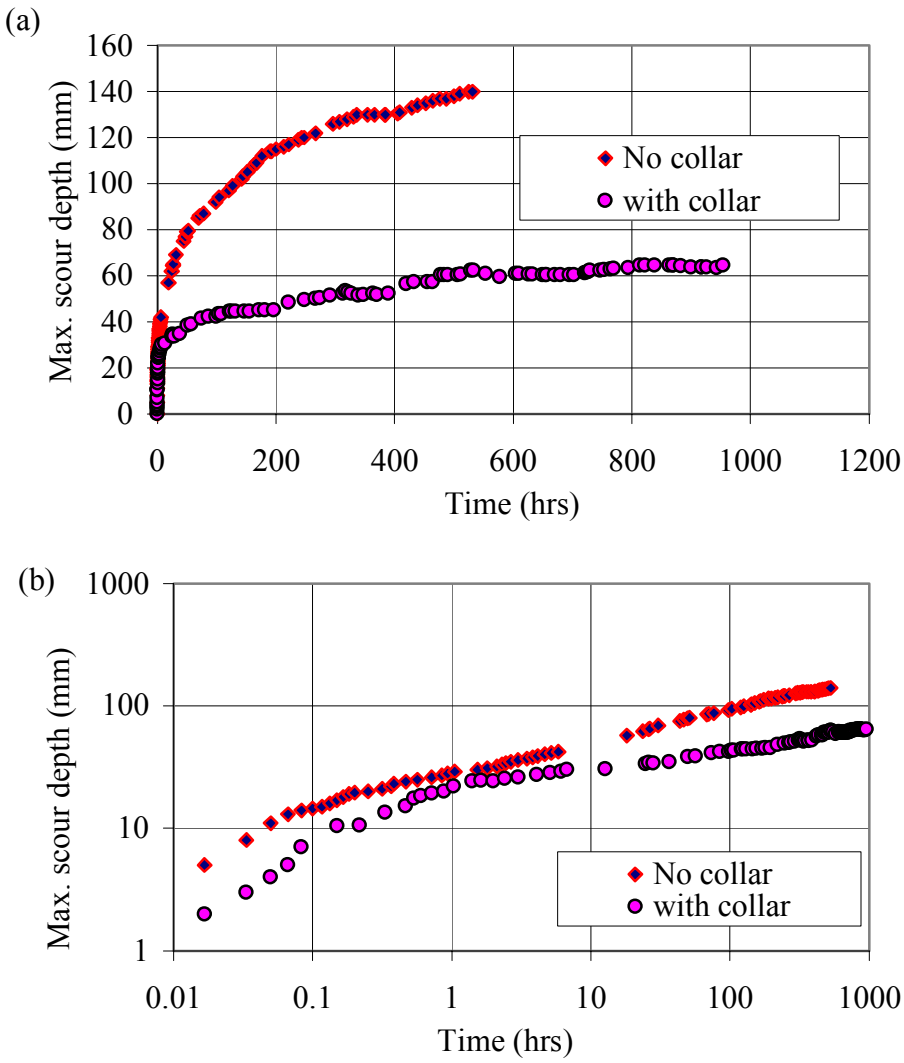


Figure 4.38. Combined time development of maximum scour depth for the Series 3 test: (a) Arithmetic scale and (b) Log-log scale

The following points can be concluded within the scope of the Series 3 tests:

- For a test duration of about 22 days, the maximum scour depth was observed at the upstream face of the pier for an unprotected pier while the position of the maximum scour depth for a pier protected with a 3D collar was found within the region immediately downstream of the collar over a test duration of about 40 days.
- There was a reduction in the scour depth when a 3D collar was used to protect the pier when compared with a plain pier.

- The scour rate was lower for the case of a test with a 3D collar than when no collar was attached (see Figures 4.22 and 4.33). Also, the slope of the power law fitted to the scour rate versus time graph is a bit flatter in the Series 3 tests when compared to the Series 1 and Series 2 tests.

### 4.6.4 Maximum scour at the pier versus maximum scour elsewhere within the flow field

For a fair assessment of the efficacy of using a collar as a countermeasure against the pier scour, it is pertinent to compare the time development of maximum scour for scour occurring immediately adjacent to the pier and that elsewhere within the flow field. The term flow field as used here means any location within the flume. The maximum scour elsewhere in the flow field is the greatest scour at any location within the flow field aside the pier immediate face where the maximum scour depth has been observed to occur. The data from the Series 3 tests and those from the Series 1 tests were used for this analysis. The results of the run in the Series 3 tests with a 3D collar are shown in Figure 4.39. It is noted that, after 955 hours of running the test, the scour has not reached the immediate vicinity of the pier. The implication of this is that, for a short duration storm, the effect of the scour may not be felt near the pier and the risk of failure may be small.

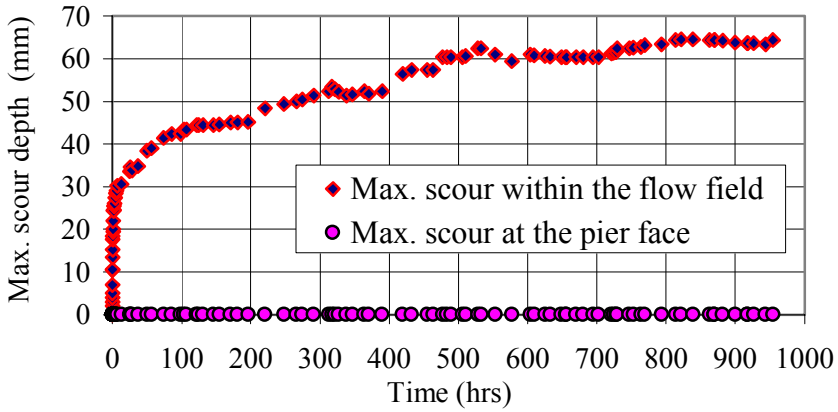


Figure 4.39. Comparison of the temporal development of the maximum scour occurring at the pier face and within the flow field for a pier fitted with a 3D collar only

The temporal development of maximum scour at the pier face for the test where a 3D collar was fitted to the pier and the test involving a plain pier is depicted in Figure 4.40. As shown, when using a 3D collar, no scour was experienced at the pier after 955 hours of running the test, whereas for the plain pier, a scour depth of about 140 mm was reached after 530 hours. It is seen that a collar efficacy at reducing pier scour can be appreciated because of non-occurrence of scour at the immediate pier face when a 3D collar was used.

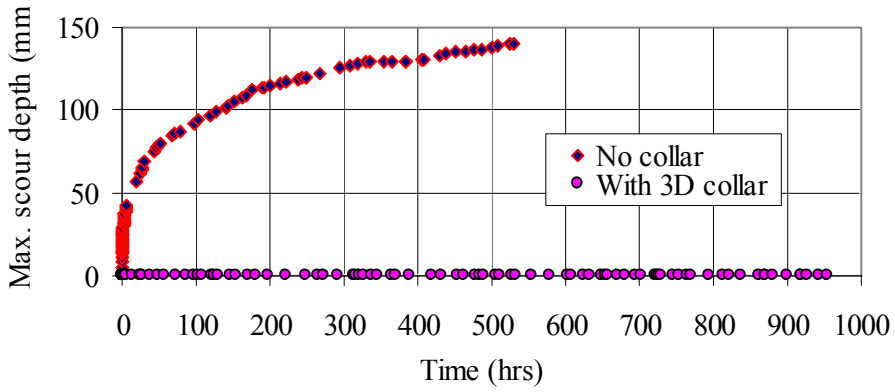


Figure 4.40. Temporal development of maximum scour at the pier face for Series 3 tests

With a test involving a 2D collar in the Series 1 test, as shown in Figure 4.41, the scour hole did not reach the immediate face of the pier until between 6 to 21 hours into the test. Comparison of Figure 4.41 with Figure 4.40 shows that a 3D collar protected the pier better than a 2D collar. As shown in Figures 4.39 and 4.40, even after a period of over 900 hours, the scour hole was yet to reach the immediate face of the pier for a 3D collar whereas at a duration of between 6 to 21 hours, the scour hole was at the face of the pier for a pier protected with a 2D collar (Figure 4.41).

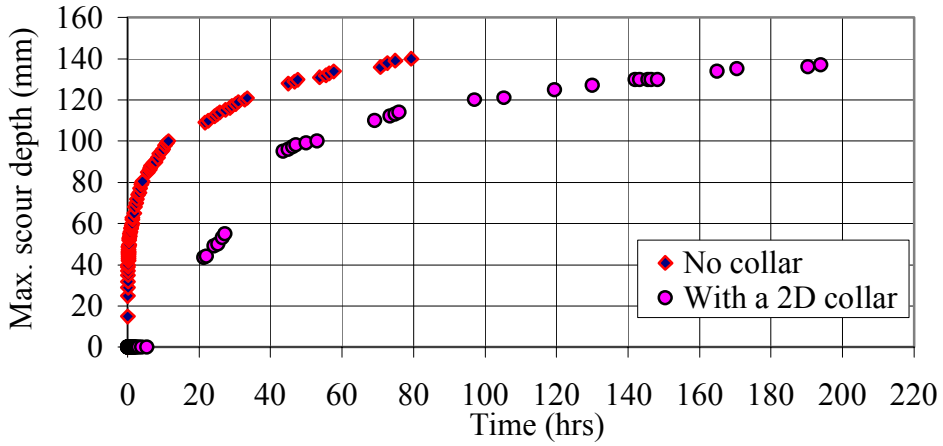


Figure 4.41. Temporal development of maximum scour at the pier face for Series 1 tests

A similar observation made for the cases of the Series 3 and 1 tests was made for the Series 2 tests as depicted in Figure 4.42. As shown in the figure, the scour hole did not reach the pier face until after about three hours into the test.

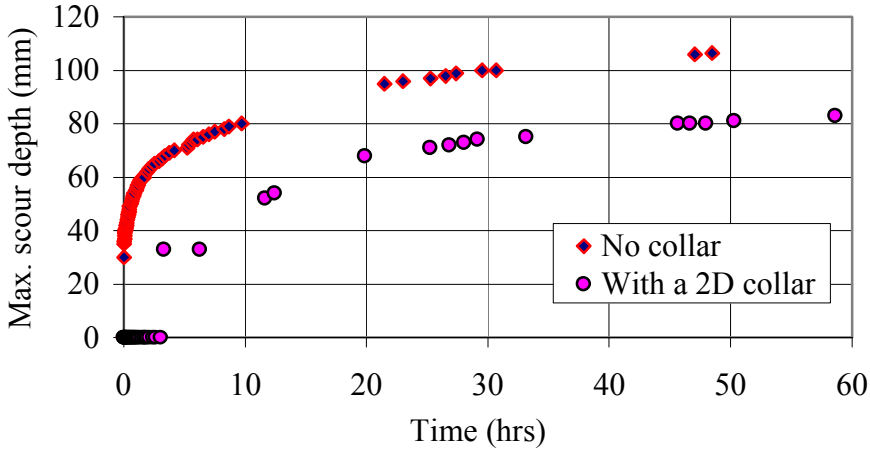


Figure 4.42. Temporal development of maximum scour at pier face for the Series 2 tests

## 4.7 Implications of the definition of time development of local scour

The difference in the time development of local scour for tests having different physical setups (e.g., collar vs. no collar) has significant implications for those studies in which the test is stopped after a finite, pre-determined length of time (e.g., 2 hrs., 24 hrs., etc.). That is, while the ultimate or equilibrium scour condition for two situations may be the

same, the time history to the equilibrium point can vary significantly, as illustrated by the data shown in Figure 4.11. For the case where the collar was not used to protect the pier against scour, a maximum scour depth of 140 mm was reached in about 80 hours. When a 2D collar was installed at the channel bed, it took some 194 hours to accomplish a maximum scour depth of 137 mm. In essence, this means that nearly the same maximum scour depth was achieved in both cases, with the only difference being the time required for scour development. Zarrati et al. (2004) made a similar finding for scour at a rectangular pier in respect of the time for scour development.

Using the data given in Figure 4.11, one can easily demonstrate that wrong conclusions may be reached if a test is stopped short of an equilibrium state. For example, if the tests had been stopped at, say, 40 hours, a different conclusion would have been reached than if the test had been stopped at 60 hours. For example, in the case of the 115 mm pier shown in Figure 4.11, it is evident that the apparent reduction in the maximum scour depth with the collar at 24 hours is 56%, whereas if the results had been assessed at a test time of two hours the reduction in maximum scour depth would have been 40%. Other examples of this assessment are shown in Table 4.4.

Table 4.4. Time variation in the apparent efficacy of the 2D collar pier scour countermeasure for the 115 mm pier (data from Figure 4.11)

| Time (hrs) | Max. scour depth: No collar (mm) | Max. scour depth: With collar (mm) | Apparent reduction in scour depth (%) |
|---|---|---|---|
| 20 | 108 | 42 | 61 |
| 40 | 125 | 93 | 26 |
| 60 | 135 | 104 | 23 |
| 80 | 140 | 118 | 16 |

A similar analysis of the apparent efficacy of a collar was also done using the various definitions of the equilibrium condition as published in the literature. The results of this analysis are shown in Table 4.5. As shown in the table, the conclusion that one might reach on the apparent efficacy of a collar varies considerably, depending on what definition of equilibrium scour is used. Even though an equilibrium scour condition was

not achieved in the current study, it is also shown that most of the definitions given in the table are pointing to the fact that an equilibrium condition has been achieved.

As such, there is some apparent cause for concern and further indication of the need to continue the search for improved understanding of the scour process and the need for global definition of equilibrium scour condition.

Table 4.5. Effect of definition of time to equilibrium scour on the conclusion of efficacy of using collar as a countermeasure for pier scour (Figure 4.11 data)

| **Definitions of time to equilibrium scour** | **Source** | **Equilibrium scour depth: Test without collar (mm)** | **Equilibrium scour depth: Test with collar (mm)** | **Apparent reduction in scour depth (%)** |
|---|---|---|---|---|
| The time at which the rate of increase of scour depth does not exceed 5% of the pier diameter over a 24-hour period | Melville and Chiew (1999) | 140 | 130 | 7 |
| The time at which the increase in scour depth does not exceed 1 mm within an 8-hour period | Zaratti et al. (2004) | 140 | 121 | 14 |
| The time at which the increase in scour depth does not exceed 1 mm within a 3-hour period | Kurmar et al. (1999) | 140 | 100 | 29 |
| Scour depth at the point of deepest scour adjacent to the pier face were recorded for 24 hours period. | Lauchlan (1999) | 112 | 49 | 56 |
| Stoppage time for Series 1 tests | Present study | 140 | 137 | 2 |

## 4.8 Equilibrium scour depth from common prediction equations

In an effort to analyse the data from this study further, several of the common equilibrium scour depth prediction equations as published in the literature were used to compute the equilibrium scour depth to be expected for the test conditions applicable to the 115 mm pier for the case of no collar protection (i.e. data from Figure 4.11). The reason for the analysis is to evaluate the usefulness of some of the renowned equations in the literature with a view of testing how reasonably they can predict the equilibrium scour depth based on the flow and sediment conditions used in this study. The results of this analysis are shown in Table 4.6 (same as Table 2.2 but with the results incorporated).

Table 4.6. Predicted equilibrium scour depth for the 115 mm pier using several equilibrium scour depth prediction equations (data from Figure 4.11)

| Investigator(s) | Equation | Source | Predicted equilibrium scour depth (mm) |
|---|---|---|---|
| Breusers et al. (1977) [Based on Laursen & Toch (1956) data] | $y_{se} = 1.35K_i b^{0.7} y_o^{0.3}$ where $y_{se}$ = equilibrium scour depth, $K_i$ = 1.0 for circular pier, b = pier width, $y_o$ = flow depth | Hoffmans & Verheij (1997) | 191 |
| Neill (1973) | $y_{se} = K_s b$ where $K_s$ = 1.5 for circular pier | Melville & Coleman (2000) | 173 |
| Colorado State University (CSU) | $y_{se} = 2.0K_i y_o F_r^{0.43} \left( \frac{b}{y_o} \right)^{0.65}$ where $K_i$ = 1.1 for a circular pier with clear-water scour, $F_r$ = Froude number | Hoffmans & Verheij (1997); HEC-18 | 150 |
| Raudkivi & Ettema (1983) | $y_{se} = 2.3bK_\sigma$ where $K = f(\sigma_g) = 1$ for uniform sediment, $\sigma_g$ = geometric standard deviation of the grain size distribution | Dey (1997) | 265 |
| Shen et al. (1969) | $y_{se} = 0.000223 R_b^{0.619}$ where $R_b$ = pier Reynolds number | Dey (1997) | 109 |

Perhaps not surprisingly, there is a wide variation in the predicted equilibrium scour depth. Moreover, even though an equilibrium scour condition was not achieved in the current study, one of the prediction equations shown in Table 4.6 yields an equilibrium scour depth less than the 140 mm reached in the test (i.e., under-prediction). As such, there is some apparent cause for concern and further indication of the need to continue the search for improved understanding of the scour process and the development of better scour prediction tools.

## 4.9 Effect of pier size on the temporal development of scour

For the analysis of the effect of pier diameter on the temporal development of the maximum scour depth, the data from the Series 1 and Series 2 tests for the case where a collar has not been fitted to the pier was used. It should be recalled that, in the Series 1 tests, the pier diameter used was 115 mm while in the Series 2 tests the diameter of the pier was 73 mm. Figure 4.43 shows the temporal development of the maximum scour depth for the pair of tests. As the results show, greater depth of maximum scour occurred for the larger diameter pier (D = 115 mm) when compared with the smaller pier of diameter 73 mm. Also, the scour depth increased with time for each case. Thus, the smaller the size of the pier the longer it takes to reach a given value of the scour depth. The same observation was made by Ettema (1980).

The reason for the trends in Figure 4.43 is that a greater disturbance to the flow due to a larger pier size can cause a greater acceleration of the flow with an implication of a greater entrainment of the bed sediment by the action of the downflow. The overall effect is a much greater scour depth with time for a larger diameter pier when compared with a smaller pier. The same observations on the effect of pier diameter on scour as shown in Figure 4.43 were also observed by Chabert and Engeldinger (1956), Raudikivi and Ettema (1983) and Franzetti et al. (1982). As depicted in Figure 4.43, the actual difference in the maximum scour depth between the two piers increases with time.

(a)

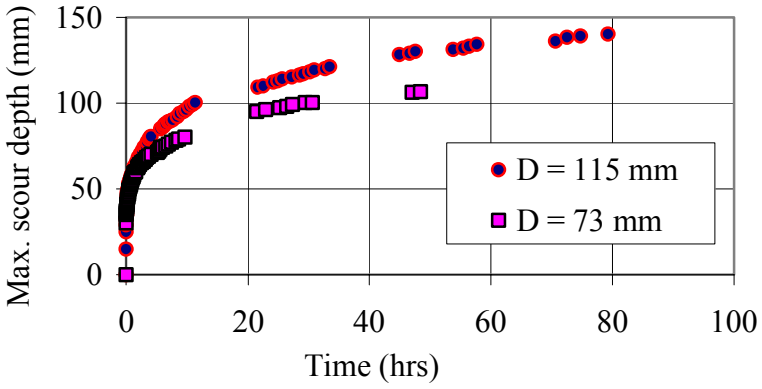


(b)

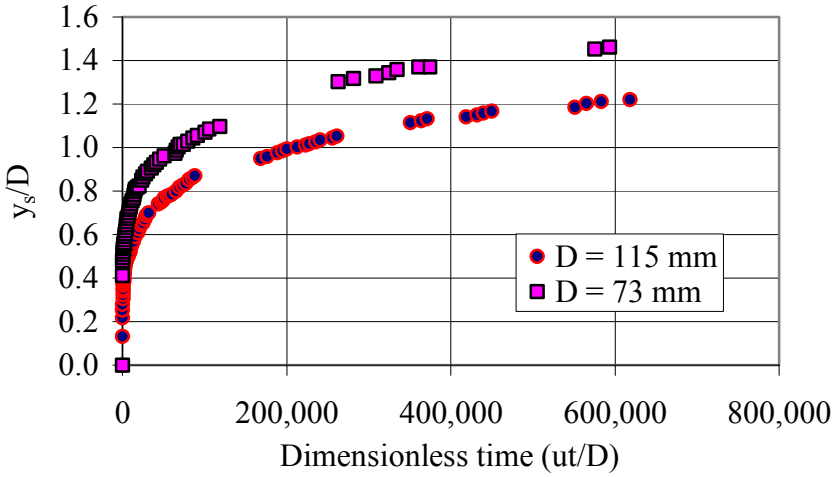


(c)

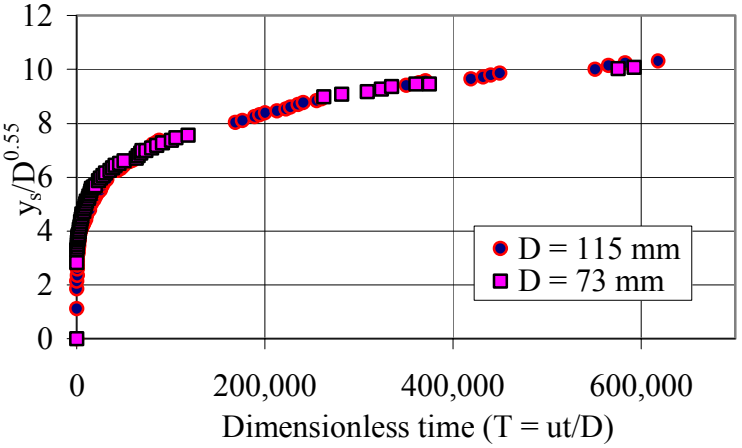


Figure 4.43. Temporal development of maximum scour depth (effect of pier size): (a) Arithmetic scale, (b) Dimensionless form, and (c) Dimensional form

Melville and Coleman (2000) found that, for a narrow pier in which the ratio of the pier diameter to the flow depth is less than 0.7, the scour depth will depend only on the pier diameter (D). Since this ratio is equal to 0.5 for the two tests shown in Figure 4.43(a), it is pertinent to show the dimensionless scour depth with respect to the pier diameter (D) as shown in Figure 4.43(b). As shown in Figure 4.43(b), it can be seen that the relative scour depth, $y_s/D$, increased with time and is larger for a smaller pier diameter. As depicted in Figure 4.43(b), one would have expected the data for the two piers to collapse into a single relationship but they did not. That this does not occur indicates that there is a scale effect or that there is a wrong scaling parameter.

The formulation of a relationship to describe the temporal development of local scour at the pier is very complex because of the complex nature of the evolution of the scour mechanisms. The number of influencing parameters as described in Chapter 2 is so numerous that it is difficult to say categorically the reason for the scale effect observed in the data trends given in Figure 4.43(b). However, Figure 4.43(c) shows the dimensional scour depth with time for the same set of data shown in Figures 4.43(a) and 4.43(b). Perhaps the correcting scaling parameter is $D^n$ for $n < 1$ as shown by the collapse of the data to a single relationship in Figure 4.43(c) when the value of $n = 0.55$. The essence of using dimensional scaling parameter, $D^n$, is to be able to find the scour depth for a given flow condition and for a given pier diameter.

The effect of pier diameter on the temporal development of scour for the case of a pier with a 2D collar for the Series 1 and Series 2 tests is shown in Figure 4.44. The results show that the scour depth increased with time and that a greater scour depth was observed with time for the 115 mm pier when compared with the 73 mm pier.

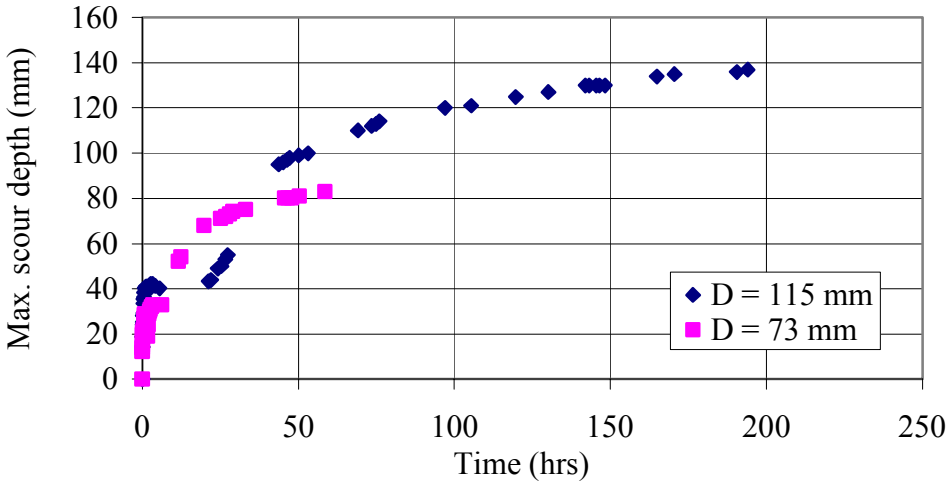


Figure 4.44. Temporal development of maximum scour depth for the pier protected with a 2D collar (effect of pier size)

## 4.10 Effect of flow intensity

The variation of flow intensity on the temporal development of scour was also considered. For this evaluation, the data collected under the Series 1 and Series 3 tests for the plain pier were used. It should be noted that the Series 2 data have not been analysed as part of this section because a different pier size (73 mm) was used. As depicted in Figure 4.45, it can be seen that the higher the flow intensity the deeper the scour depth at a given time. The reason for this is related to the fact that at higher flow intensity there is a greater acceleration of the flow within the vicinity of the pier, and thus the intensity of the downflow and the horseshoe vortex is greater. The same trend was observed by Raudikivi and Ettema (1983), Breusers et al. (1977) and Chiew (1984). It was noted that it takes more time to achieve the same level of scour depth for the lower flow intensity (i.e. $u_*/u_{*c} = 0.70$) when compared with a higher flow intensity (i.e. $u_*/u_{*c} = 0.89$). To be precise, it takes over six times as long to achieve the same level of maximum scour depth for the case of the flow intensity of 70% when compared with a flow intensity of 89%. It should be noted, however, that the scour process was still at the erosion phase of the scour process by the time the tests referred to here were stopped since equilibrium condition was not reached.

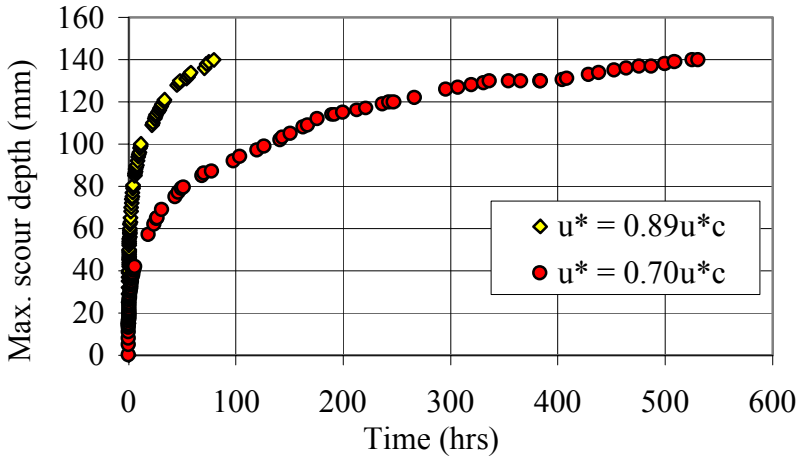


Figure 4.45. Temporal development of maximum scour depth (flow intensity effect)

## 4.11 Temporal development of scour depth: Comparison with existing formulas

The scour that occurs at a bridge pier has been analysed by many researchers. A number of approaches relating to the quantitative description of the time development of scour at a bridge pier exist in the literature. This section is devoted to comparing the test data to several of the equations that are found in the literature to describe the time evolution of scour at a bridge pier. The Series 3 and Series 1 test data from the present study for the case where the pier is unprotected with a collar are used for the comparison. The equations used for the basis of the comparison include: Franzetti et al. (1982), Melville and Chiew (1999), Barkdoll (2000), Ettema (1980) and Sumer et al. (1993). Also discussed in this section is the application of the Franzetti et al. (1982) equation to a case where a pier has been fitted with a collar.

### 4.11.1 Franzetti et al. (1982) comparison: For plain pier

Franzetti et al. (1982) suggested an exponential function in the form of [2.6] to be well suited to describing the evolution of scour with time. The data from the present study were compared with the Franzetti et al. equation [2.6]. In making the comparison, the data obtained from the Series 1 and Series 3 tests for the plain pier were used. Since none of the tests reported in this work reached an equilibrium state, a regression analysis was performed on the data obtained from the Series 1 and 3 tests in order to

independently calculate the values of $y_{se}$ and constants B and C in [2.6]. Thus, the average values of B and C as suggested by Franzetti et al. in [2.8] were not used. The reason for this was that, when an attempt was made to use a regression analysis to calculate the value of $y_{se}$ using [2.8], the value of $y_{se}$ obtained was even less than the scour depth that had been observed in these tests even though an equilibrium condition had not yet been attained. Thus, the general form of the Franzetti et al. equation was used as shown in [2.6]. A regression analysis was performed on the data in order to obtain the values of $y_{se}$ and constants B and C.

Looking at the data set for the Series 1 and 3 tests, it is evident the frequency of the measurements varied throughout the test period, with the maximum scour depth readings being taken every few minutes during the first hour or so of the test and less frequently thereafter. Since most of the data are clustered around the beginning of the test period, there is a weighting issue to consider when carrying out the regression analysis. Simply, weighting is a way of varying the amount that each point 'counts' or is significant in the data distribution. The regression procedure treats each point of the data equally, and thus the use of many points during the first hour or so of testing and relatively few points thereafter inherently biases the outcome to the early stages of the test period. The purpose of the weighting is to allow the regression analysis to be adjusted to better represent the data. As regards the temporal development of scour, if the weighting is not considered, therefore, the results of the regression analysis will be heavily based by the early stages of the scour process. An adjustment needs to be made, therefore, to account for the weighting. In this study, the weighting problem has been handled by simply removing some of the data from the beginning of the test since the SPSS tools used for the regression analysis do not have the capability of doing a weighting of individual points. The criterion for determining which data to remove is simply by locating the point of discontinuity of the supposedly linear relationship of the log-log plot of the temporal development of scour and deleting the test data up to that point. To demonstrate this approach, Figure 4.46 shows a schematic illustration of the log-log plot of the temporal development of scour, with the point W in the figure being the point of discontinuity and the data to be removed are those from S to W. For the

purpose of long term prediction of $y_{se}$, the data for the latter part of the linear relationship (i.e., data between W and V) after deleting the first linear part are then made use of. It should also be realised that the application of the regression analysis to the data between W and V only minimises the weighting problem but the problem is not totally eradicated. In this study, no other method apart from the method described above was found to address the weighting problem.

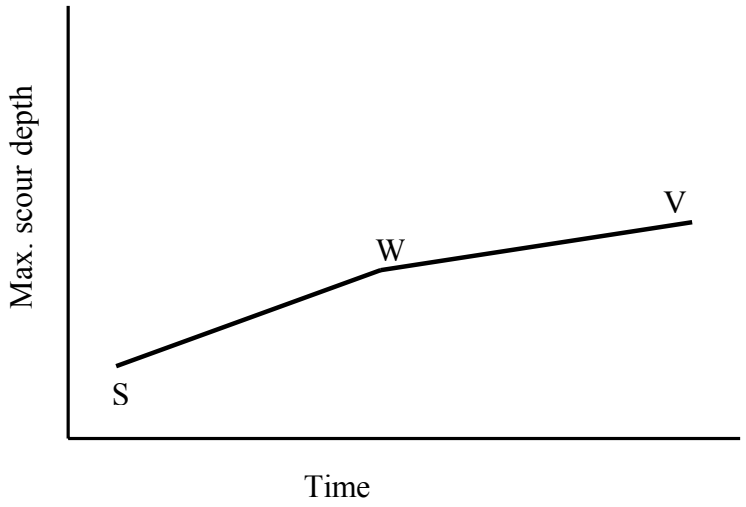


Figure 4.46. Schematic illustration of the log-log plot of the temporal development of scour for a plain pier

The distribution of the data plotted in Figure 4.5b for the Series 1 test and Figure 4.21b for the Series 3 test revealed that there were many measurements during the early stages of the test and few measurements later on. In SPSS, which was the regression analysis tool used in this study, this will influence the curve fit because there are so many data points measured near to t = 0, which will affect the coefficients B and C in Franzetti et al. (1982) equation. Referring to Figure 4.5b and Figure 4.21b, it is observed that there is discontinuity in the linear relationship in the log-log plots, thus, dividing the plot into two log-linear parts. For the Series 1 test, the point of discontinuity is located at a time of one hour into the test (Figure 4.5b) while in the Series 3 test, as shown in Figure 4.21b, the point of discontinuity is located at a time in which the test had been run for about six hours. Interestingly, the point of discontinuity referred to here seems to coincide with the shift in maximum scour depth location to the front of the pier.

When a regression analysis was performed on the data from the Series 1 and Series 3 tests, the values of the constants obtained from the analysis are as shown in Table 4.7. As the results show, the equilibrium scour depth for the Series 1 test was 248 mm while that of the Series 3 test was 197 mm.

Table 4.7. Regression analysis results using Franzetti et al. (1982) equation

| Variable | Series 1 | Series 3 |
|---|---|---|
| $y_{se}$ | 248 mm | 197 mm |
| B | 0.026 | 0.0043 |
| C | 0.259 | 0.379 |
| Regression Statistics ($R^2$) | 0.9972 | 0.9972 |

Employing the values of constants B and C given in Table 4.7, it is obvious that the resulting curves using the general form of the Franzetti et al. equation displayed a good correlation with the data for the Series 1 and Series 3 tests as shown in Figure 4.47 and Figure 4.48, respectively. From the figures, the Franzetti et al. (1982) equation fits well to the data in the present study and the corresponding $R^2 = 0.9972$. Even though [2.6] fits well to the data of the present study, the associated coefficients B and C seem to be related to specific data (i.e. flow conditions, pier geometry and sediment parameters).

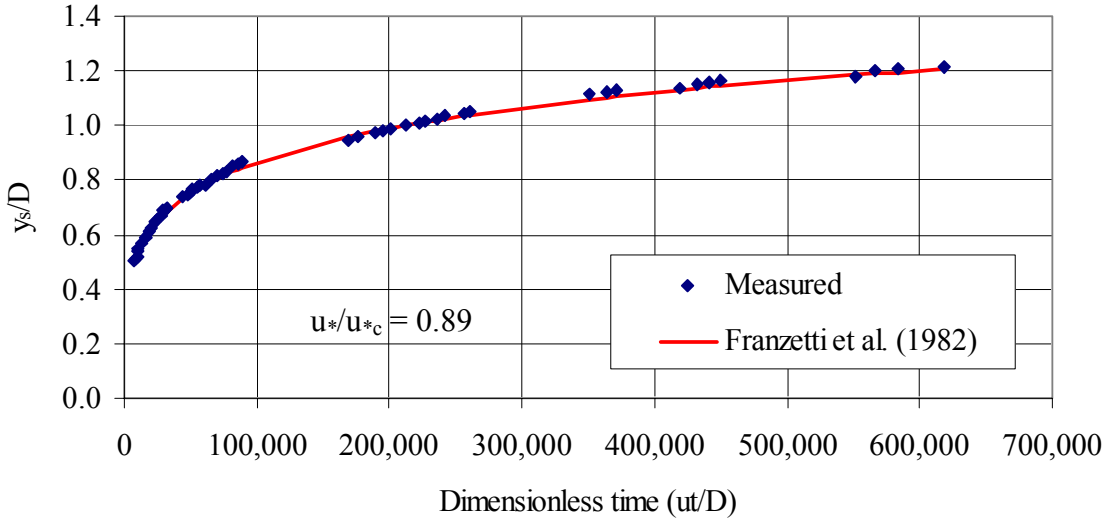


Figure 4.47. Series 1 data and Franzetti et al. (1982) prediction line

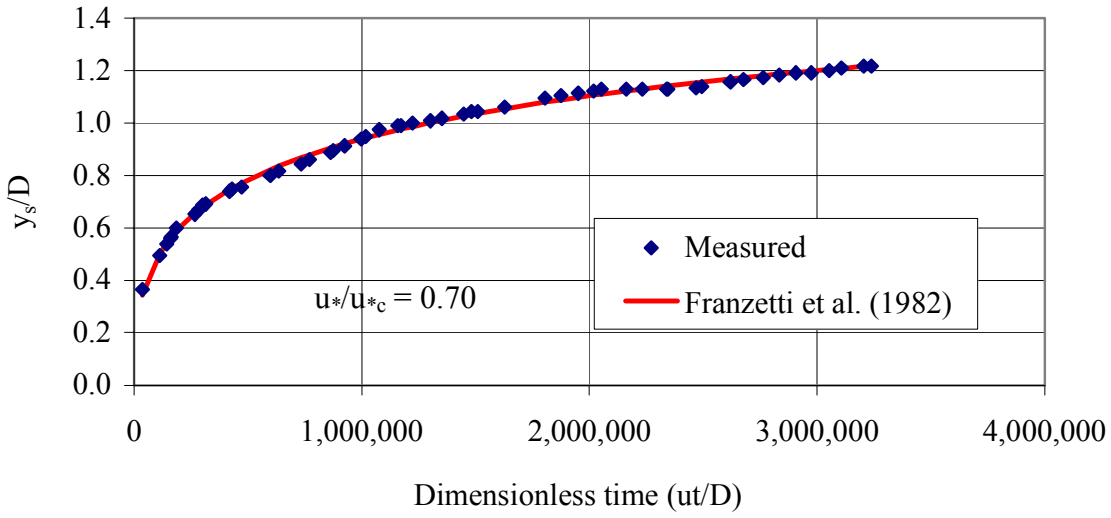


Figure 4.48. Series 3 data and Franzetti et al. (1982) prediction line

Alternatively, it was also found from Whitebread et al. (2000) that [4.1] can be used in place of [2.7], viz.

[4.1] $$T = \frac{ut}{(Dy_o)^{0.5}}$$

When [4.1] was used in the analysis of the Series 3 test, it yielded the same value of $y_{se}$ = 197 mm. Equation [4.1] specifically takes into account the flow depth, $y_o$ and being one of the parameters influencing the scour mechanism, it does provide an alternative method of determining the dimensionless time, T.

In order to calculate the time that a significant portion of the equilibrium scour depth of 197 mm would have been reached for the Series 3 test, a 90% asymptote as suggested by Cunha (1975) was adopted. The 90% asymptote was adopted because it is not mathematically possible to determine the time to infinity at which an equilibrium scour depth is purported to be achieved based on the form of the Franzetti et al. (1982) relationship (i.e., using equation 2.6 and values in Table 4.7). From the calculation, it was estimated that it will take about 7 months to achieve 90% of the equilibrium scour depth, which amounts to 177 mm. This duration is long and casts doubt on whether an equilibrium condition can be achieved within the context of a laboratory experiment.

It may not be economically feasible to carry out experiments of such a long duration in the laboratory.

Even though Franzetti et al. (1982) observed that the value of the constant B varied between 0.021 and 0.042, the value of B for the Series 3 test shown in Table 4.7 falls outside this range but not by a significant amount. Also, the values of the constant C shown in the table are also pretty close to the average value of 1/3 given by Franzetti et al. The reason for the very little differences seen may be due to the difference in the flow conditions and/or sediment properties that were used for the tests upon which the Franzetti et al. findings were based and the ones used for the present study. It is to be noted also that the average values of B and C given in [2.8] were based on experimental results by Chabert and Engeldinger (1956) and Franzetti et al. (1982). The longest duration of those tests was about 234 hours. The test reported under Series 3 was run for about 531 hours. This might be the reason why there was a significant difference in the values of B as given by Franzetti et al. and that given in Series 3 of the present study. Therefore, average values of the constants B and C as suggested by Franzetti et al. should be used with caution.

In order to contest further the idea of using the average values of B and C in [2.8], $y_s/y_{se}$ was plotted against the dimensionless time, T, using [2.8] and values of B and C in [4.2] as given in Table 4.7. The resulting figure is as shown in Figure 4.49. It should be noted that the Series 3 data have been used for illustration only.

[4.2] $$\frac{y_s}{y_{se}} = \left[1 - \exp\left(-0.00425T^{0.379}\right)\right]$$ (Present study, Series 3 test)

As shown in Figure 4.49, it can be seen that at a dimensionless time of 3,200,000 with an equivalent experimental duration of about 531 hours, the equilibrium depth of scour attained was 71% and 98%, respectively, for the Series 3 test (i.e., equation [4.2]) and by using the Franzetti et al. (1982) average values of B and C (i.e., equation [2.8]). It is uncertain if 98% of the equilibrium scour depth would have been achieved within the 531 hours of the Series 3 test going by the fact that equilibrium condition was not reached in the course of this test. The 71% of the equilibrium scour depth which

corresponded to a scour depth of about 140 mm seems more reasonable a value as far as this test is concerned.

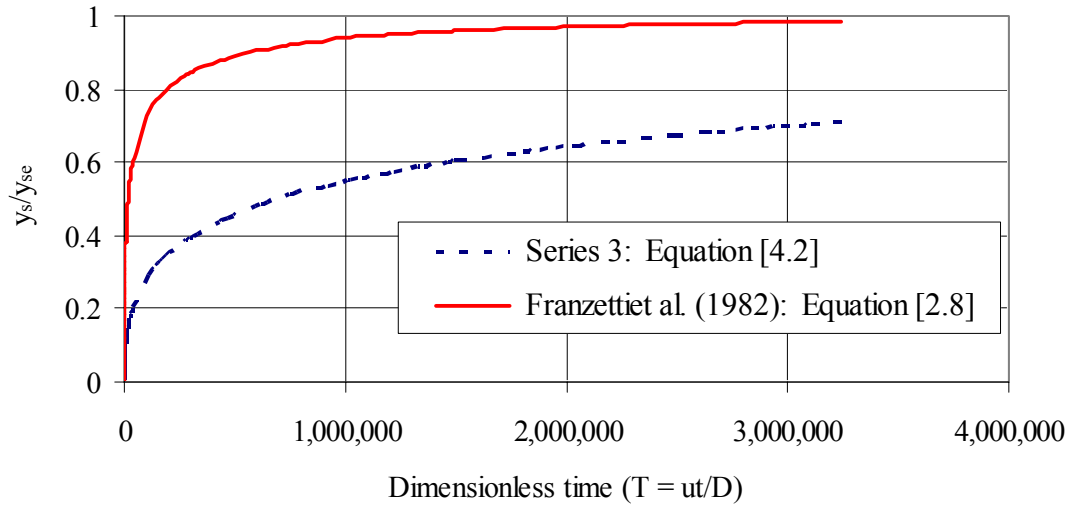


Figure 4.49. The scour depth, $y_s$, relative to equilibrium scour depth, $y_{se}$, as a function of dimensionless time, T

### 4.11.2 Melville and Chiew (1999) and Barkdoll (2000) comparison

The comparison of the present study data with [2.9] and [2.13] is given in Figure 4.50. For this comparison, [4.2], which best described the data set for the Series 3 test, was used. It should be noted, however, that the coefficients for [4.2] were obtained from the regression analysis performed on the Series 3 test data. Equation [4.2] has been used in place of the measured data in the Series 3 test for two reasons. The first reason is that [4.2] describes the Series 3 data set very well and, secondly, the Series 3 data is obtained from a test which was run for only a duration of 22 days, and for a good comparison with the work of Melville and Chiew (1999) and Barkdoll (2000) the experimental duration should be very long. Therefore, since no equilibrium was reached in the Series 3 test, the equilibrium scour depth obtained by regression analysis using [4.2] was employed. Since the time to equilibrium scour was at infinity using the equation, a 90% asymptote as explained before was used. At 90% of the equilibrium condition, the scour depth was 177 mm and the corresponding time to reach the 90% asymptote was 5,040

hours. The time to equilibrium scour, $t_e$, was assumed to be equal to 5,040 hours while the corresponding equilibrium scour depth was also taken as 177 mm.

As shown in Figure 4.50, the Series 3 data set is well described by the Melville and Chiew (1999) equation when compared with the equation given by Barkdoll (2000). The reason for the near-fit may be connected with the fact that the Melville and Chiew equation was developed from a data set wholly for a circular pier whereas the Barkdoll equation was developed from a combined data set for both circular and noncircular piers. The reason why the plots, as shown in Figure 4.50, did not collapse into a single relationship may be due to the fact that [2.9] and [2.13] were developed from a pool of data obtained from various flow conditions, geometry and sediment parameters. In conclusion, the Melville and Chiew equation described the present Series 3 test data better than the Barkdoll (2000) equation.

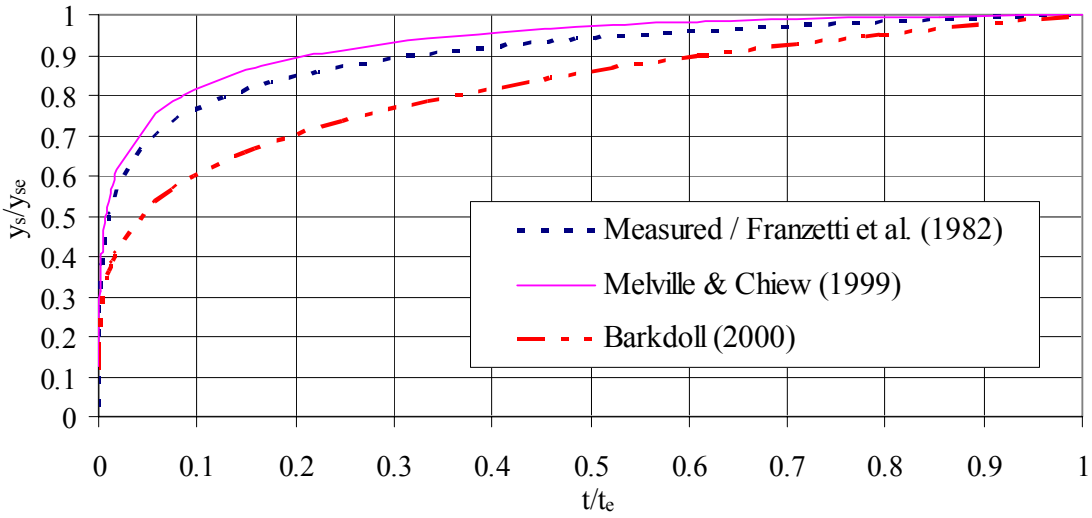


Figure 4.50. Comparison of scour depth with time: Melville & Chiew (1999) and Barkdoll (2000) equations for flow intensity of 0.70

### 4.11.3 Ettema (1980) equation comparison

In order to determine if [2.15] can be fitted to the Series 3 data, a regression analysis was performed to determine the coefficients $K_1$ and $K_2$. For the tests in this study, the average value of the water temperature was 20°C. The corresponding value of viscosity,

$\upsilon = 1.00 \times 10^{-6}$ m$^2$/s, was used in calculating X. The results of the regression analysis showed that the values of $K_1$ and $K_2$ are 290 and 1147, respectively, for the Series 3 data with $R^2 = 0.94$. The comparison of the Series 3 test data to [2.15] is given in Figure 4.51. As shown in the figure, the trend of the Series 3 test data is the same as that of Ettema's equation. Even though the trend is the same, it can be seen that the scour depth is overpredicted by Ettema's equation before the time of 167 hours and underpredicted thereafter. In conclusion, Ettema's equation does not represent the Series 3 test data very well.

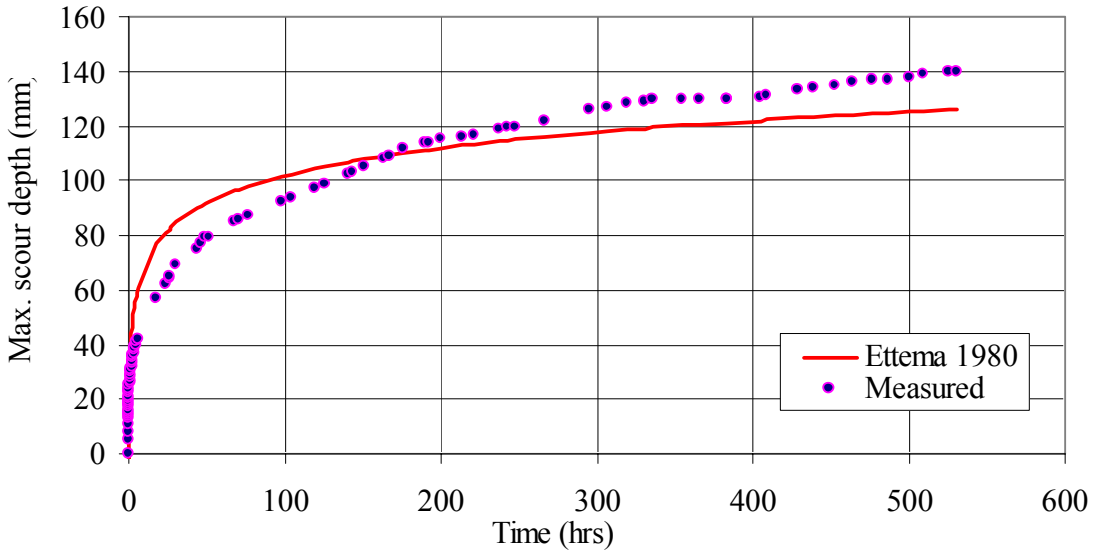


Figure 4.51. Comparison of measured Series 3 scour depth versus time with Ettema (1980) equation

### 4.11.4 Sumer et al. (1993) comparison

In order to compare the Series 3 test data with [2.16], the time scale ($T_1$) for the data was estimated to be approximately 20 hours in accordance with the Sumer et al. (1993) approach. By regression analysis using the Series 3 data and [2.16], the value of the equilibrium scour depth, $y_{se}$, was found to be 117 mm. This is a poor correlation as the value of the equilibrium scour depth is even smaller than the 140 mm maximum scour depth reached in the Series 3 test even though an equilibrium scour depth was not reached. Therefore, the expression given by Sumer et al. (1993) does not fit the Series 3

test data. The regression analysis performed on the data with the Sumer et al. approach gave an $R^2 = 0.86$.

An adjustment to the Sumer et al. equation in the present study gave rise to an equation that fitted well to the data. The adjusted equation was re-written in the form of [2.9] as

$$[4.3] \qquad y_s = y_{se}\left(1 - \exp - G\left(\frac{t}{T_1}\right)^F\right)$$

It was noted that by introducing new coefficients, G and F, in [2.16], a new form of the equation as shown in [4.3] fitted well to the Series 3 test data. The value of the time scale for the Series 3 data analysis was still $T_1 = 20$ hours, as mentioned above. The results of the regression analysis yielded the value of equilibrium scour depth, which is the same as that obtained from the Franzetti et al. (1982) equation. Specifically, the equilibrium scour depth, $y_{se}$, is 196 mm. A plot showing the comparison of the measured scour depth versus time with the Sumer et al. (1993) equation and the adjusted Sumer et al. (1993) equation is shown in Figure 4.52. It is shown that the Sumer et al. (1993) equation did not describe the Series 3 test data. It is shown by Sumer et al.'s equation that the equilibrium condition has been reached at a scour depth of 117 mm even though, the Series 3 test data did not show any equilibrium condition as the scour depth was still increasing at the time the test was stopped. Equation [2.16] was used to describe the time evolution of scour around circular vertical piles by waves in marine environments.

That the equation did not correlate well with the Series 3 data may be due to the fact that this present study has been conducted for a steady flow rather than under a steady current and wave action that are associated with a flow in which [2.16] was applied. However, the adjusted Sumer et al. (1993) equation aligns well with the Series 3 data as shown in Figure 4.52.

In summary, for the studies in which no collar was fitted to the pier, it was noted that the form of an equation that fits the experimental data was the one given by Fanzetti et al. (1982). The equation is given as:

$$y_s = y_{se}(1 \quad \exp(\ BT^C))$$

However, there is every reason to be cautious of the use of the average values of B and C given by Franzetti et al. The adjusted Sumer et al. (1993) equation aligns well with the data though it is recognised that it is a form of Franzetti et al. (1982) equation.

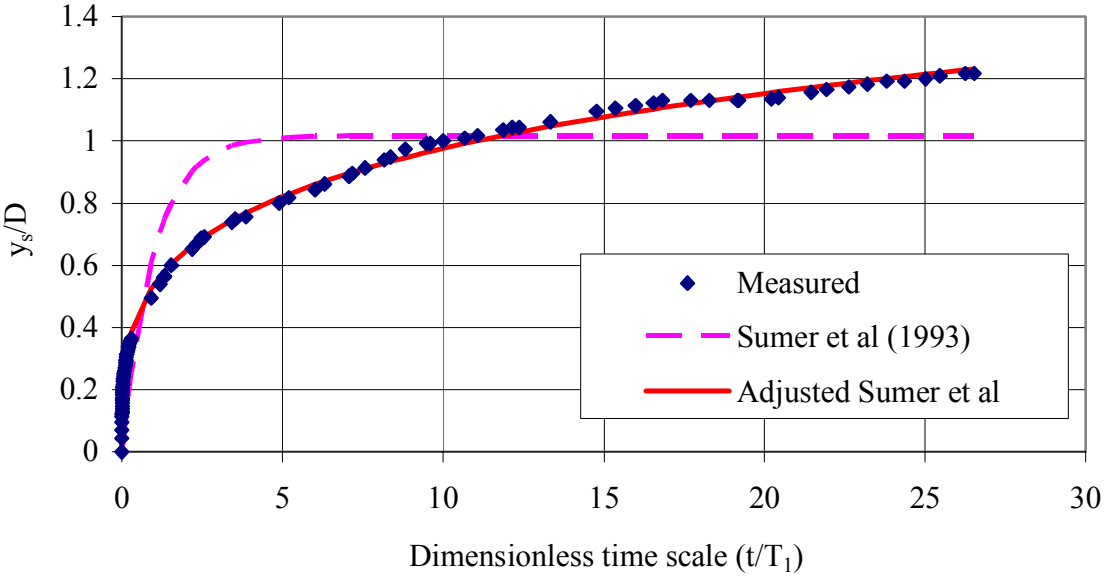


Figure 4.52. Comparison of measured scour depth with time: Sumer et al. (1993) and the adjusted Sumer et al. (1993) equations

### 4.11.5 Application of Franzetti et al. (1982) equation to a pier fitted with a collar

Having successfully applied the form of Franzetti et al. (1982) equation to describe the temporal development of scour depth for the case of a plain pier, the same idea was extended to a case where a collar was fitted to a pier. With a collar in place, the idea is to integrate a delay factor into the curve fitting analysis using the regression analysis technique together with the form of Franzetti et al. (1982) equation. An attempt was made to simply apply the Franzetti et al. equation and the regression analysis technique to Series 1 and Series 2 test data for the case in which a 2D collar was fitted to the pier. Figure 4.53 shows the schematic illustration of temporal development of scour for a pier fitted with a collar (point J to M). This figure is similar in trend to that of Figure 4.9 and Figure 4.15. By incorporating such a delay factor, it is meant that the data between point L and M as shown in Figure 4.53, which show the same trend as that of a test with

a plain pier are only used for the purpose of the curve fitting analysis. It is like truncating the data between J and L. However, the point L for the purpose of the analysis still retained it original coordinates in both (x,y).

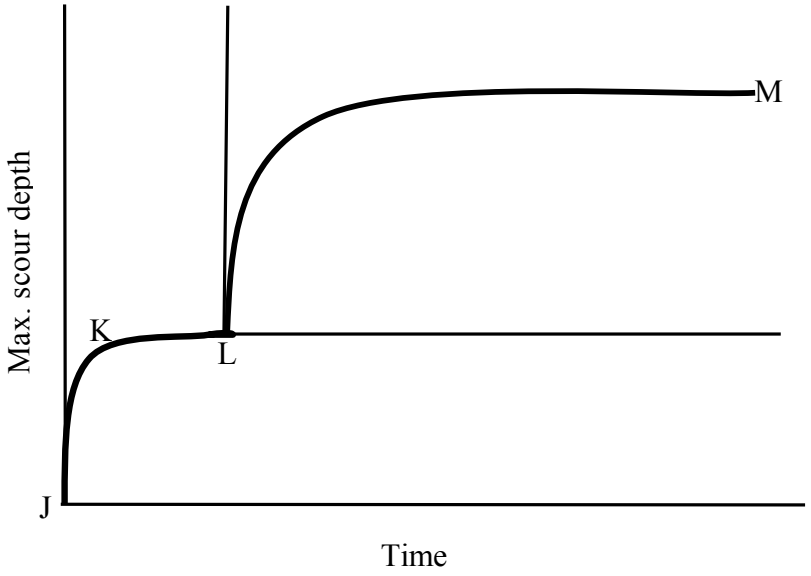


Figure 4.53. Schematic illustration of the temporal development of scour for a pier fitted with a collar

The results of the regression analysis are shown in Table 4.8 and Figure 4.54. As shown in the table the resulting equilibrium scour depths predicted from the regression analysis for the Series 1 test are smaller than the maximum scour depths obtained at the end of the test. The result, therefore, is not meaningful. In case of Series 2 test, however, the resulting equilibrium scour depth from the analysis is a little more than the maximum scour depth obtained when the test was stopped. It is known that the equilibrium condition has not been reached as the test was stopped abruptly because of ripple formation as explained earlier. That the equilibrium condition is obtained to be 87 mm from the regression analysis may not be correct. Can a delay factor be simply incorporated into the form of Franzetti e al. (1982) relationship such that the equation fits well to the data? The answer is yes, but the resulting equilibrium scour depth from this approach is not correct and therefore, the approach may not be useful for the case where a collar has been fitted to the pier. However, the application of Franzetti et al. equation for a case where a collar is fitted to a pier can be a potential research area in which a further work is required.

(a)

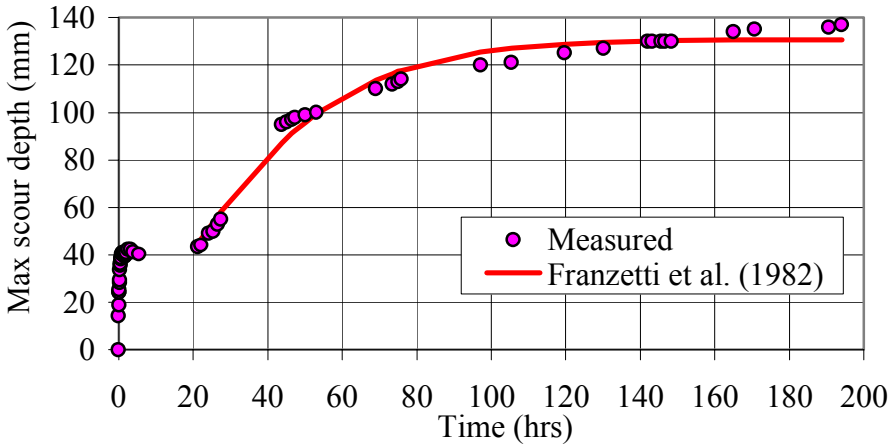


(b)

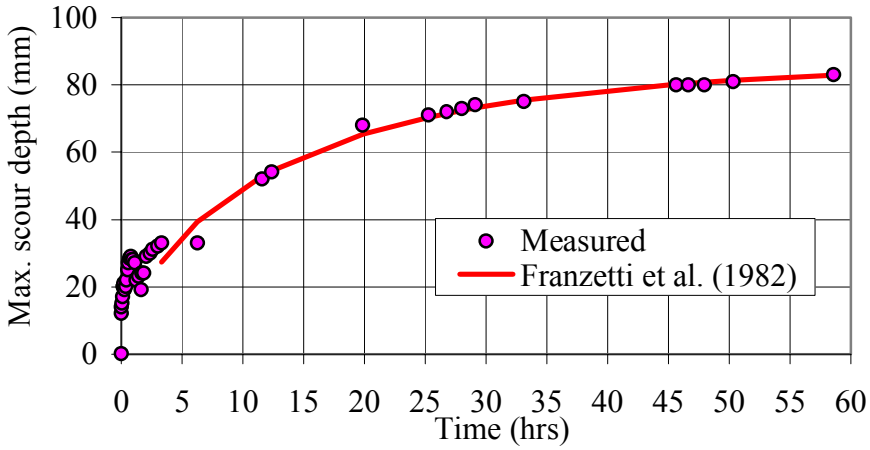


Figure 4.54. Test data and Franzetti et al. (1982) prediction line for a pier with a 2D collar: (a) Series 1 test, and (b) Series 2 test

Table 4.8. Regression analysis results using Franzetti et al. (1982) equation for a pier fitted with a 2D collar

| Variable | Series 1 | Series 2 |
|---|---|---|
| $y_{se}$ | 131 mm | 87 mm |
| B | 4.16E-8 | 2.38E-4 |
| C | 1.342 | 0.726 |
| $y_s$ when test ended | 137 mm | 83 mm |

# CHAPTER 5

# SUMMARY, CONCLUSIONS AND RECOMMENDATIONS

## 5.1 Summary

The scour that occurs around a circular pier founded in erodible bed material is a complex three-dimensional phenomenon. Notwithstanding the considerable effort that has been invested in the study of local scour by many researchers, an understanding of the mechanics of local scour around a bridge pier remains far from complete. This is reflected by the wide range of relationships available to the designer for the estimation of the depth of local scour around a bridge pier. There are also various methods that have been proposed to prevent local scour at bridge piers. Among others, the use of collars has been suggested as a possible mitigation technique, largely on the basis of model study results. Peak flood flows may last for only a few hours or days in the field. For short duration floods, the duration of the flood may be insufficient for achieving an equilibrium scour depth. In such instances, the actual scour depth may only be a small percentage of the equilibrium scour depth, which could take weeks or months to fully develop. In this regard, reducing the rate of scour can serve to limit the risk of pier failure when short duration floods occur. When a collar is installed on a pier, the direct impact of the downflow to the riverbed is prevented, which serves to reduce the depth of scour that can take place. In addition to reducing the depth of maximum scour, the rate of scour is also reduced considerably. Therefore, the capability of a collar at reducing the rate of scour can play a significant role at slowing down the development of scour and, hence, reducing the impact of scour at a bridge pier.

In this work, the temporal development of scour at a circular pier fitted with or without a collar was experimentally studied using a physical hydraulic model. The study was performed under clear-water conditions using a uniform cohesionless bed material and a circular pier. The principal objective of this study is to carry out a much longer test than found in the literature with a view to evaluating the time development of the local scour at a bridge pier that has been fitted with a protective collar for the purpose of mitigating the scour. Subsidiary objectives also included the evaluation of the effectiveness of a

pier collar for mitigating the depth of scour that would otherwise occur at a bridge pier, and the assessment of the occurrence of an equilibrium scour condition, if achieved, or of the implications of not achieving such a condition in respect of interpreting the results obtained from a physical hydraulic model study. Also to be assessed as part of this study are some of the equilibrium scour depth prediction equations as well as some definitions of equilibrium scour depth found in the literature.

In addressing the objectives, a series of tests was designed to study the time development of scour as well as the efficacy of using a collar as a countermeasure for the scour at a bridge pier. Tests were conducted using two different pier diameters so as to determine the effect of pier diameter on the temporal development of scour. Also investigated was the effect of collar size on the time development of scour and its efficacy at preventing scour at a bridge pier. The effect of flow intensity on temporal development of scour was also studied. The time development of the scour hole around the model pier with and without a collar installed was also compared with similar studies on bridge piers. Several equations for the temporal development of scour depth and those for the prediction of the equilibrium scour depth were tested as part of this study. Based on the results obtained, the objectives of the current study were successfully achieved.

## 5.2 Conclusions

The results of the model study indicated that the depth of scour is highly dependent on time. The depth of the scour hole increases as the time increases. The extent of scour observed downstream of the pier also increases as time increases. It was found that the temporal development of the scour hole at a pier is dependent on whether or not the pier is fitted with a collar placed at the bed level. The pathway to equilibrium depth is different depending on whether the pier is fitted with a collar or not. There were two bends in the scour depth-time curve for a case where a collar was fitted to the pier when compared with a single kink in case of a plain pier. With a collar in place, the development of the scour hole is considerably delayed.

Further, it was also found that:

- A 2D collar delays the development of the scour hole. However, its usage may provide little long-term benefit at reducing the maximum scour depth. Based on 40 days test duration and results, a 3D collar may be very effective at reducing both the scour depth and the scour rate when compared with a 2D collar. Having run one of the tests in the present study for as long as about 40 days, the conclusion that can be drawn is that the scour still did not extend to the vicinity of the pier when a 3D collar was fitted to it, although the scour depth continued to increase at a very low rate.

- As regards the temporal development of scour depth and for the tests in which no collar was fitted to the pier, it was noted that the form of equation that fits the experimental data well was the one given by Franzetti et al. (1982). The equation is given as:

  [2.6] $$y_s = y_{se}\left(1 - \exp\left(-BT^C\right)\right)$$

  However, there is every reason to be cautious of the use of the average values of B and C given by Franzetti et al.

  With a collar in place and with an integration of a delay factor into the curve fitting analysis using the regression analysis technique together with the form of Franzetti et al. (1982) equation, the resulting equilibrium scour depth seems to be questionable and thus may not be correct. Therefore, the application of the Franzetti et al. equation may not work for the case where a collar has been fitted to the pier.

- A modification to the Sumer et al. (1993) equation made the modified equation fit well to the data from the present study when compared with the original equation. The adjusted equation was re-written as

  [4.3] $$y_s = y_{se}\left(1 - \exp\left[-G\left(\frac{t}{T_1}\right)^F\right]\right)$$

The adjusted Sumer et al. (1993) equation shares a great resemblance to the Franzetti et al. (1982) equation, but the method of obtaining the time scale, $T_1$, is different.

- Based on the limited amount of testing done as part of this study and some of the results reported in the literature, it appears that one benefit of using a collar at a pier is to delay the development of the scour hole. However, the use of a collar may provide little long-term benefit at reducing the maximum scour depth. It was also noted that collar efficacy increases with increasing collar diameter.
- A truly equilibrium scour condition is not readily attainable and was not achieved in the work reported herein. Given that many scour tests reported in the literature have been undertaken for test durations considerably less than that used in this work, it is speculated that the occurrence of an equilibrium scour condition may be widely misreported in the literature.
- From the regression analysis and using the form of equation given by Fanzetti et al. (1982), it was estimated that, for a test with a plain pier, it will take about seven months to achieve 90% of the equilibrium scour depth. This duration is long and tends to cast doubt on whether an equilibrium condition can be achieved within the context of a laboratory experiment. This point is supported by the finding from the study herein in which no equilibrium scour condition was reached despite running a long test.
- From this study, it was demonstrated that wrong conclusions may be reached if a test is stopped short of an equilibrium state. An equilibrium scour depth determined based on some definitions of an equilibrium scour condition reported in the literature may not be correct as shown from the results of the present study. Furthermore, it is possible to reach a variety of conclusions about the efficacy of using collars as a pier scour countermeasure technique, depending on which definition of time to equilibrium scour is adopted.
- In addition to experimental testing, several suggested empirical equations by researchers were used as predictors for the maximum depth of clear-water scour.

When compared to the test data, these equations give a wide range of values. Therefore, the performance of many scour prediction formulas in the literature may need to be further evaluated. As such, there is some apparent cause for concern and further indication of the need to continue the search for improved understanding of the scour process and the development of better scour prediction tools.

In the course of the work, the following conclusions also became evident:

- For the case where a collar was not fitted to the pier, the overall scour pattern, which was symmetrical, consisted of a hole situated in front of the pier, a mound of deposited sand located a short distance downstream from the pier, and the alternate formation of depressions and mounds and a series of ripples fanning out from the pier in the downstream direction. The point of maximum scour depth was found immediately in front of the pier for most of the test duration.
- From this study and based on some work of other researchers, it can be concluded that the time taken to reach any given scour depth decreases as the flow intensity increases.
- Shields criterion for the initiation of sediment motion needs to be interpreted with caution. Bed material motion may occur for flow conditions apparently below Shields' threshold of motion condition. For a sand bed having $d_{50}$ = 0.53 mm, the incipient motion condition for clear-water scour would appear to occur in the range $0.80u_{*c}$ - $0.85u_{*c}$ for a flow depth of 230 mm and a lower $u_{*c}$ condition for shallower depths of flow. In this, $u_{*c}$ was defined using the Shields diagram.

## 5.3 Recommendations

Recommendations regarding possible future work in relation to the current research project are as follows:

- Since a river usually carries debris, particularly during flood conditions, a study of the effect of debris on the performance of a collar and on the temporal

development of scour could be investigated in order to gain more knowledge or insight as to the use of a collar.

- All previous studies on the use of a collar as a countermeasure for local scour at a bridge pier are based on experiments carried out using a physical hydraulic model. It would be useful to investigate the practicality of using a collar on the field through a prototype study.
- All previous studies on the use of a collar as a countermeasure for local scour at a bridge pier have been confined to cohesionless material and clear-water flow conditions. Since local scour other than under a clear-water scour condition is possible at a bridge pier, it could be useful if the use of a collar under a live-bed scour condition were studied. Also, since a bridge pier can be located on a soil other than cohesionless soil, studying the performance of a collar as well as the temporal development of scour in a cohesive soil will give valuable clues to the behaviour of a collar under this circumstance.
- Having run one of the tests in the present study for as long as about 40 days, the conclusion that can be drawn is that the scour still did not extend to the vicinity of the pier when a 3D collar was fitted to it, although the scour depth continued to increase at a reduced rate. As a further piece of research work, perhaps the test could be run for a much longer time to investigate if the scour hole would eventually extend to the vicinity of the pier.
- What is common in the literature is the description of flow mechanism causing local scour at a plain pier. Since no work has been done to describe the flow behaviour with a collar in place, a research study in this area will address a deficiency in the understanding of such a flow mechanism.
- Even though the general form of the equation given by Franzetti et al. (1982) fits well to the data of the present study as well as some of the data of other researchers, the associated coefficients contained in the formulae seem to be data specific (i.e., flow conditions and sediment parameters). Therefore, the dependence of those coefficients on some other parameters that are related to the

evolution of scour may be a potential area of further research. As regards this point, more tests relating to different flow intensity, sediment material, collar and pier diameters and flow depth are needed to properly define the coefficients and also the time scour relationship for the case where a collar is not fitted to the pier and the case where it is.

# REFERENCES


Abdel, R.M., Abdel, M.M. and Bayoumy, M. 2003. Scour reduction around bridge piers using internal openings through the pier. Proceedings, XXX IAHR Congress, Thessaloniki, Greece, August 24-29, 8 p.

Ahmed, F. and Rajaratnam, N. 1998. Flow around bridge piers. Journal of Hydraulic Engineering, ASCE, 124(3): 288-300.

Ansari, S.A., Kothyari, U.C. and Ranga Raju, K.G. 2002. Influence of cohesion on scour around bridge piers. Journal of Hydraulic Research, IAHR, 40(6): 717-729.

Ariathurai, R. and Arulanandan, K. 1978. Erosion rates of cohesive soils. Journal of Hydraulic Engineering, ASCE, 104(2): 279-283.

Barkdoll, B.B. 2000. Time scale for local scour at bridge piers. Journal of Hydraulic Engineering, ASCE, 126(10): 793-794.

Bozkus, Z. and Osman, Y. 2004. Effects of inclination of bridge piers on scouring depth. Journal of Hydraulic Engineering, ASCE, 130(8): 827-832.

Breusers, H.N.C., Nicollet, G. and Shen, H.W. 1977. Local scour around cylindrical piers. Journal of Hydraulic Research, 15(3): 211-252.

Breusers, H.N.C. and Raudkivi, A.J. 1991. Scouring - Hydraulic structures design manual. IAHR, A.A. Balkema, Rotterdam, 143 p.

Briaud, J.L., Ting, F.C.K., Chen, H.C., Gudavalli, R. and Perugu, S. 1999(a). SRICOS: prediction of scour rate in cohesive soils at bridge piers. Journal of Geotechnical and Geoenvironmental Engineering, ASCE, 125(4): 237-246.

Briaud, J.L., Ting, F.C.K., Chen, H.C., Cao, Y., Han, S.W., and Kwak, K.W. 1999b. Erosion function apparatus for scour rate predictions. Journal of Geotechnical and Geoenvironmental Engineering, ASCE, 127(2): 105-113.

Chabert, J. and Engeldinger, P. 1956. Etude des affouillements autour des piles de points (Study of scour at bridge piers). Bureau Central d'Etudes les Equipment d'Outre-Mer, Laboratoire National d'Hydraulique, France.

Chang, H.H. 1988. Fluvial processes in river engineering. John Wiley & Sons, 432 p.

Cheremisinoff, P.N., Cheremisinoff, N.P. and Cheng, S.L. 1987. Hydraulic mechanics 2. Civil Engineering Practice, Technomic Publishing Company, Inc., Lancaster, Pennsylvania, U.S.A. 780 p.

Chiew, Y.M. and Melville, B.M. 1987. Local scour around bridge piers. Journal of Hydraulic Research, IAHR, 25(1): 15-26.

Chiew, Y.M. 1992. Scour protection at bridge piers. Journal of Hydraulic Engineering, ASCE, 118(9): 1260-1269.

Chiew Y.M. 1995. Mechanics of riprap failure at bridge piers. Journal of Hydraulic Engineering, ASCE, 121(9): 635-643.

Chiew, Y.M. and Lim, F.H. 2000. Failure behaviour of riprap layers at bridge piers under live-bed conditions. Journal of Hydraulic Engineering, ASCE, 126(1): 43-55.

Chiew, Y. and Lim, S. 2003. Protection of bridge piers using a sacrificial sill. Water & Maritime Engineering Journal, Proceedings of the Institution of Civil Engineers, Thomas Telford Journals, London, 156(1): 53-62, Paper 12722, March.

Chiew, Y.M. 2004. Local scour and riprap stability at bridge piers in a degrading channel. Journal of Hydraulic Engineering. ASCE, 130(3): 218-226.

Cunha, L.V. 1975. Time evolution of local scour. Proceedings, 16th IAHR Congress, Sao Paulo, Brazil, July 27 – August 1, pp. 285-299.

Dargahi, B. 1990. Controlling mechanism of local scouring. Journal of Hydraulic Engineering, ASCE, 116(10): 1197-1214.

Dey, S. 1997. Local scour at piers, part 1: A review of development of research. International Journal of Sediment Research, IJSH, 12(2): 23-46.

Dey, S. 1999. Time-variation of scour in the vicinity of circular piers. Water & Maritime Engineering Journal, Proceedings of the Institution of Civil Engineers, Thomas Telford Journals, London, 136(2): 67-75, Paper 11426, June.

Dey, S. and Barbhuiya, A.K. 2004. Clear-water scour at abutments in thinly armoured beds. Journal of Hydraulic Engineering, ASCE, 130(7): 622-634.

Ettema, R. 1980. Scour at bridge piers. PhD Thesis, Auckland University, Auckland, New Zealand.

Ettema, R., Arndt, R., Robert, P. and Wahl, T. 2000. Hydraulic modelling concepts and practice. ASCE Manuals and Reports on Engineering Practice No. 97, Sponsored by the Environmental and Water Resources Institute of the ASCE, ASCE, 390 p.

Fanzetti, S., Larcan, E. and Mignosa, P. 1982. Influence of tests duration on the evaluation of ultimate scour around circular piers. International Conference on the Hydraulic Modelling of Civil Engineering Structures, Organised and Sponsored by BHRA Fluid Engineering, University of Warwick, Coventry, England, September 22-24, 16 p.

Federico, F., Silvagni, G. and Volpi, F. 2003. Scour vulnerability of river bridge piers. Journal of Geotechnical and Geoenvironmental Engineering, ASCE, 129(10): 890-899.

Fotherby, L.M. and Jones, J.S. 1993. The influence of exposed footings on pier scour depths. Proceeding of Hydraulics Conference, ASCE, New York: 922-927.

Garde, R.J. and Ranga-Raju, K.G. 1985. Mechanics of sediment transportation and alluvial stream problems. John Wiley & Sons, 618 p.

Gosselin, M.S. and Sheppard, M. 1995. Time rate of local scour. Proceedings, 1st International Conference on Water Resources Engineering, San Antonio, Texas, 1: 775-779.

Heidarpour, M., Khodarahmi, Z. and Mousavi, S.F. 2003. Control and reduction of local scour at bridge pier groups using slot. Proceedings, XXX IAHR Congress, Thessaloniki, Greece, August 24 - 29, 7 p.

Hoffmans, G.J.C.M. and Verheij, H.J. 1997. Scour manual. A.A. Balkema, Rotterdam, Netherlands, 205 p.

Jia, Y., Xu, Y. and Wang, S.Y. 2002. Numerical simulation of local scouring around a cylindrical pier. Proceedings of First International Conference on Scour of Foundations, Texas A & M University, College Station, Texas, USA, November 17-20; pp. 1181-1187.

Johnson, P.A., Hey, R.D., Tessier, M. and Rosgen, D.L. 2001. Use of vanes for control of scour at vertical wall abutments. Journal of Hydraulic Engineering, ASCE, 127(9): 772-778.

Johnson, P.G. and Niezgoda, S.L. 2004. Risk-based method for selecting bridge scour countermeasures. Journal of Hydraulic Engineering, ASCE, 130(2): 121-128.

Jones, J.S. and Sheppard, D.M. 2000. Scour at wide bridge piers. Joint Conference on Water Resources Engineering and Water Resources Planning and Management, ASCE, July 30 – August 2, 2000, Minneapolis, Minnesota, U.S., 10 p.

Kayaturk, S.Y., Kokpinar, M.A. and Gogus, M. 2004. Effect of collar on temporal development of scour around bridge abutments. 2nd International Conference on scour and erosion, IAHR, Singapore, 14-17 November, 7 p.

Kobus, H. 1980. Hydraulic modelling. German Association for Water Resources and Land Management, Bulletin 7, Issued in cooperation with IAHR, 323 p.

Kumar, V., Ranga Raju, K.G. and Vittal, N. 1999. Reduction of local scour around bridge piers using slots and collars. Journal of Hydraulic Engineering, ASCE, 125(12): 1302-1305.

Kuti, E.O. and Yen, C. 1976. Scouring of cohesive soils. Journal of Hydraulic Research, IAHR, 14(3): 195-206.

Lagasse, P.F., Zevenbergen, L.W., Schall, J.D. and Clopper, P.E. 2001. Bridge scour and stream instability countermeasures: Experience, selection, and design guidelines. FHWA NHI 01-003: Federal Highway Administration, Hydraulic Engineering Circular No. 23, 2nd ed., U.S. Department of Transportation, Washington, D.C.

Lagasse, P.F. and Richardson, E.V. 2001. ASCE compendium of stream stability and bridge scour papers. Journal of Hydraulic Engineering, ASCE, 127(7): 531-533.

Lauchlan, C.S. 1999. Pier scour countermeasures. PhD Thesis, Department of Civil and Resources Engineering, University of Auckland, Auckland, New Zealand.

Lauchlan, C.S. and Melville, B.W. 2001. Riprap protection at bridge piers. Journal of Hydraulic Engineering, ASCE, 121(9): 635-643.

Laursen, E.M. and Toch, A. 1956. Scour around bridge piers and abutments. Iowa Highway Research Board, Bulletin # 4, Bureau of Public Roads, Iowa.

Lim, F.H. and Chiew, Y.M. 2001. Parametric study of riprap failure around bridge piers. Journal of Hydraulic Research, IAHR, 39(1): 61-189.

Link, O. and Zanke, U. 2004. On the time-dependent scour-hole volume evolution at a circular pier in uniform coarse sand. 2nd International conference on scour and erosion, IAHR, Singapore, 14-17 November, 8 p.

Mashair, M.B. and Zarrati, A.R. 2002. Effect of collar on time development of scouring around rectangular bridge piers. 5th International Conference on Hydroscience and Engineering, Warsaw, Poland, 9 p.

Mashair, M.B., Zarrati, A.R. and Rezayi, A.R. 2004. Time development of scouring around a bridge pier protected by collar. 2nd International Conference on Scour and Erosion, ICSE-2, Singapore, 8 p.

Melville, B.W. and Raudkivi, A.J. 1977. Flow characteristics in local scour at bridge piers. Journal of Hydraulic Research. IAHR, 15(1):373-380.

Melville, B.W. 1984. Live bed scour at bridge piers. Journal of Hydraulic Engineering, ASCE, 110(9): 1234-1247.

Melville, B.W. and Raudkivi, A.J. 1996. Effect of foundation geometry on bridge pier scour. Journal of Hydraulic Engineering, ASCE, 114(10): 203-209.

Melville, B.W. and Hadfield, A.C. 1999. Use of sacrificial piles as pier scour countermeasures. Journal of Hydraulic Engineering, ASCE, 125(11): 1221-1224.

Melville, B.W. and Chiew, Y.M. 1999. Time scale for local scour at bridge piers. Journal of Hydraulic Engineering, ASCE, 125(1): 59-65.

Melville, B.W. and Coleman, S.E. 2000. Bridge scour. Water Resources Publications, LLC, Colorado, U.S.A., 550 p.

Muzzammil, M., Gangadharaiah, T. and Gupta, A. K. 2004. An experimental investigation of a horseshoe vortex induced by a bridge pier. Water Management Journal, Proceedings of the Institution of Civil Engineers, Thomas Telford Journals, London.157 (2): 109-119. Paper 13904, June 2004.

Neill, C.R. 1973. Guide to bridge hydraulics. Project Committee on Bridge Hydraulics, Roads and Transportation Association of Canada. University of Toronto Press, Toronto and Buffalo, 191 p.

Oliveto, G. and Hager, W.H. 2002. Temporal evolution of clear-water pier and abutment scour. Journal of Hydraulic Engineering, ASCE. 128(9): 811-820.

Oliveto, G. and Hager, W.H. 2005. Further results to time-dependent local scour at bridge elements. Journal of Hydraulic Engineering, ASCE. 131(2): 97-105.

Posey, C.J. 1974. Tests of scour protection for bridge piers. Journal of Hydraulics Division, ASCE, 100(12): 1773-1783.

Raudkivi,A.J. and Ettema, R. 1977a. Effect of sediment gradation on clear-water scour and measurement of scour depth. Proc. 17th Congress IAHR, Baden-Baden 4, pp. 521-527.

Raudkivi,A.J. and Ettema, R. 1977b. Effect of sediment gradation on clear-water scour and measurement of scour depth. Journal of the Hydraulics Division, ASCE, 103 (HY10): 1209-1213.

Raudkivi, A.J. and Ettema, R. 1983. Clear-water scour at cylindrical piers. Journal of Hydraulic Engineering, ASCE, 109(3): 339-350.

Raudkivi, A.J. 1998. Loose boundary hydraulics. 4th Edition. Rotterdam ; Brookfield, VT : Balkema. 496 p.

Richardson, E.V. and Davies, S.R. 1995. Evaluating scour at bridges. Rep. No. FHWA-IP-90-017 (HEC 18), Federal Administration, U.S. Department of Transportation, Washington, D.C.

Schneibe, D.E. 1951. An investigation on the effect of bridge pier shape on the relative depth of scour. Msc. Thesis, State University of Iowa.

Shen, H.W. and Schneider, V.R. 1969. Local scour around bridge piers. Journal of the Hydraulics Division, Proceedings of the American Society of Civil Engineers, 95(6): 1919-1941.

Sheppard, D.M., Odeh, M. and Glasser, T. 2004. Large scale clear-water local scour experiments. Journal of Hydraulic Engineering, ASCE, 130(10): 957-963.

Simarro-Grande, G. and Martin-Vide, J.P. (2005). Exponential expression for time evolution in local scour. Journal of Hydraulic Research, IAHR, 42(6):663-65.

Singh, C.P., Setia, B. and Verma, D.V.S. 2001. Collar-sleeve combination as a scour protection device around a circular pier. Proceedings of Theme D, 29th Congress on Hydraulics of Rivers, Water Works and Machinery, Chinese Hydraulic Engineering Society, Beijing, China. September 16-21, 202-209.

Sumer, B.M., Christiansen, N. and Fredsoe, J. 1993. Influence of cross-section on wave scour around piles. Journal of Waterway, Port, Coastal, and Ocean Engineering. ASCE, 119(5): 477-495.

Tanaka, S. and Yano, M. 1967. Local scour around a circular cylinder. Proceedings, 12th IAHR Congress, Colorado State University, Colorado, U.S.A., Published by IAHR, Delft, The Netherlands. Vol. 3, September 11-14.

Thomas, Z. 1967. An interesting hydraulic effect occurring at local scour. Proceedings, 12th IAHR Congress, Colorado State University, Colorado, U.S.A., Published by IAHR, Delft, The Netherlands, Vol. 3, September 11-14.

Ting, F.C.K., Briaud, J.L., Chen, H.C., Gudavalli, R. and Perugu, S. 2001. Flume tests for scour in clay at circular piers. Journal of Hydraulic Engineering, ASCE, 127(11): 969-978.

Vittal, N., Kothyari, U.C. and Haghighat, M. 1993. Clear-water scour around bridge pier group. Journal of Hydraulic Engineering, ASCE, 120(11): 1309-1318.

Wardhana, K. and Hadipriono, F.C. 2003. Analysis of recent bridge failures in the United States. Journal of Performance of Constructed Facilities, ASCE, 17(3): 144-150.

Whitebread, J. E., Benn, J. R. and Hailes, J. M. 2000. Cost-effective management of scour-prone bridges. Transport Journal, Proceedings of the Institution of Civil Engineers, London. 141(2): 79-86. Paper 10752, May 2000.

Whitehouse, R.J.S. 1998. Scour at marine structures : A manual for practical applications. Thomas Telford publications, Thomas Telford Ltd, 1 Heron Quay, London, United Kingdom. 198 p.

www.pepevasquez.com

Yanmaz, A.M. and Altinbilek, H.D. 1991. Study of time-dependent local scour around bridge pier. Journal of Hydraulic Engineering, ASCE, 117(10): 1247-1268.

Zarrati, A.M., Gholami, H. and Mashahir, M.B. 2004. Application of collar to control scouring around rectangular bridge piers. Journal of Hydraulic Research, IAHR, 42(1): 97-103.

Zarrati, A.M., Nazariha, M. and Mashahir, M.B. 2006. Reduction of local scour in the vicinity of bridge pier groups using collars and riprap. Journal of Hydraulic Engineering, ASCE, 132(2): 154-162.

# APPENDICES

# APPENDIX A Calculation of incipient motion condition and the bed shear stress

## Appendix A-1

### Calculation of incipient motion condition.

A condition of incipient motion is the hydraulic condition at which motion is initiated in sediment particles (of a given size). The requirement for a clear-water condition is that the shear stress in the upstream reach of the flume be equal to or less than the critical shear stress of the bed material. The calculation example given below illustrates the procedure for using Shields diagram and the tractive force approach for calculating the point of incipient motion in a flume bed.

An experiment is being designed in a flume to convey clear-water to a pier located downstream of the flume. The design calls for a strict adherence to a flow depth, $y_o$ = 230 mm. The width of the flume is 1.22 m. The flume bed material consists of sediment of median size of 0.53 mm and its specific gravity (G.S.) is 2.65. Clear-water is admitted to the flume channel and it is imperative that no material be scoured from the channel bottom at the upstream of the pier. To be on the side of safety, the experiment is being designed to be conducted at a shear stress of 80% of the critical shear stress in order to ensure that no scour or ripple formation is expected on the flume channel prior to reaching the pier location. Determine the flow conditions to achieve these requirements. Assume a temperature of 10°C and a corresponding kinematic viscosity, $\upsilon = 1.306 \times 10^{-6} m^2/s$.

**Solution**

By using the approach described in Section 2.3 of Chapter 2, the steps below can be used to determine conditions of incipient motion.

Step 1: Find the third dimensionless parameter using

$$\frac{d_{50}}{\upsilon}\left[0.1\left(\frac{\gamma_s}{\gamma}-1\right)gd_{50}\right]^{1/2} \quad \text{or} \quad \frac{d_{50}}{\upsilon}\left[0.1(G.S-1)\gamma g d_{50}\right]^{1/2}$$

The value of the parameter for this example is equal to 11.89

Step 2: Determine the dimensionless shear stress $\tau_*$ from the Shields diagram using the dimensionless parameter from Step 1 (i.e, 11.89)

Hence, $\tau_* = 0.032$

Step 3: Find the critical shear stress $\tau_c$, from

$$\tau_c = \tau_*(\gamma_s - \gamma)d_{50} \quad \text{or} \quad \tau_c = \tau_*(G.S-1)\gamma d_{50}$$

$$\tau_c = 0.275 \text{ N/m}^2$$

Step 4: Calculate the critical shear velocity, $u_{*c}$, from

$$u_{*c} = \left( \frac{\tau_c}{\rho} \right)^{1/2} \qquad [\rho = 1000 \text{ kg/m}^3]$$

$u_{*c} = 0.0166$ m/s

Step 5: Determine the actual shear stress, $\tau_a$, expected to prevent ripple formation using the percentage of critical shear stress expected (i.e., 80%)

$\tau_a = 80\% \, \tau_c = 0.220 \text{ N/m}^2$

Similarly, as in step 4, the actual shear velocity $u_* = 0.0148$ m/s

and $u_*/u_{*c} = 0.89$

Step 6: Calculate the friction slope, $S_f$, using the relationship

$\tau_a = \gamma y_o S_f$

$S_f = 9.74 \times 10^{-5}$ m/m

Step 7: Calculate the mean approach velocity, u, by employing the Manning's formula with $S_o$ known and assuming the value of Manning's n, n = 0.012. The symbol R is the hydraulic radius.

$$u = \frac{R^{2/3} S_f^{1/2}}{n}$$

$u = 0.249$ m/s

Step 8: The flow discharge, Q, can then be determined using the continuity equation

$Q = Au$

$Q = 0.070 \text{ m}^3/\text{s}$

**Note**

$\gamma$ – Specific weight of water

$\gamma_s$ – Specific weight of sediment

Note: In doing the critical shear stress calculations, Manning's n value was assumed as 0.012.

## Appendix A-2

### Calculation of bed shear stress

As part of experiments conducted in the Hydrotechnical Laboratory at the University of Saskatchewan, Saskatoon, Canada, the velocity distribution in the central portion of a recirculating flume, 20 m long, 1.22 m wide and 0.61 m deep was measured. The flume has a working section in the form of a recess that is filled with sediment to a uniform thickness of 0.16 m. The data is given in the table below for the location identified as $L_1$ in Section 4.3. Compute the bed shear velocity and the corresponding bed shear stress.

| Flow depth (y) (m) | Velocity (u) (m/s) |
|---|---|
| 0.0075 | 0.181 |
| 0.0175 | 0.212 |
| 0.0275 | 0.223 |
| 0.0375 | 0.232 |
| 0.0475 | 0.236 |
| 0.0575 | 0.244 |
| 0.0675 | 0.246 |
| 0.0775 | 0.248 |
| 0.0875 | 0.251 |
| 0.0975 | 0.249 |
| 0.1075 | 0.252 |
| 0.1175 | 0.251 |
| 0.1275 | 0.249 |
| 0.1375 | 0.254 |
| 0.1475 | 0.249 |
| 0.1575 | 0.251 |
| 0.1675 | 0.253 |
| 0.1775 | 0.254 |
| 0.1875 | 0.254 |
| 0.1975 | 0.262 |
| 0.2075 | 0.256 |
| 0.2175 | 0.256 |
| 0.2275 | 0.257 |

**Solution**

Step 1: Plot velocity, u, versus y

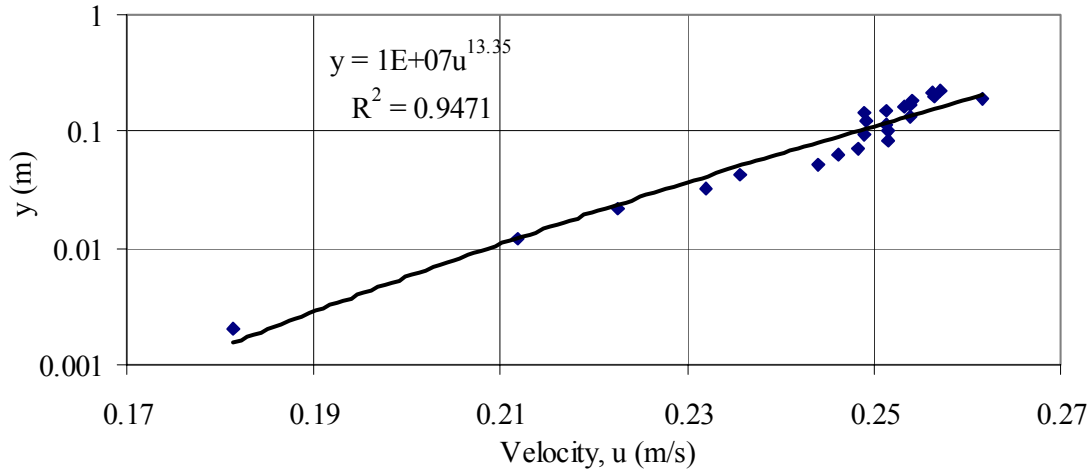


Step 2: From the plot, fit a straight line equation of best fit to the data, i.e.

[1] $y = 1E + 07u^{13.35}$

Which implies, for the plot shown, the slope = 13.35

Step 3: The semi-logarithmic average velocity equation for a bed given by Chiew and Lim (2000) and Chang (1988) is:

[2] $\frac{u}{u_*} = 5.75\log\left(5.53\frac{y}{d_{50}}\right)$ [where $u_*$ is the shear velocity]

Recall,

[3] mx + c [Equation of a straight line]

If [2] is expressed in the form of [3], then

[4] $\text{Log}(y) = \frac{u}{5.75u_*} \log\frac{5.53}{d_{50}}$ [where $d_{50}$ is the median grain size]

Step 4: By comparing the slopes of [1] and [4], the shear velocity, $u_*$ can be determined.

[5] $13.35 = \frac{1}{5.75u_*}$

By solving [5], the shear velocity,

$u_* = 0.013$ m/s

Step 5: The bed shear stress, $\tau$, can be determined by using:

[6] $\tau = u_*^2\rho$ [$\rho = 1000$ kg/m$^3$]

# APPENDIX B Data for the velocity profiles

## Appendix B

Table B shows the velocity profile data which were analysed in Section 4.3.

Table B. Data for the velocity profiles

| $L_1$ | | $L_2$ | | $L_3$ | | $L_4$ | | $L_5$ | | $L_6$ | |
|---|---|---|---|---|---|---|---|---|---|---|---|
| **y (m)** | **u (m/s)** | **y (m)** | **u (m/s)** | **y (m)** | **u (m/s)** | **y (m)** | **u (m/s)** | **y (m)** | **u (m/s)** | **y (m)** | **u (m/s)** |
| 0.0000 | 0.000 | 0.0000 | 0.000 | 0.0000 | 0.000 | 0.0000 | 0.000 | 0.0000 | 0.000 | 0.0000 | 0.000 |
| 0.0075 | 0.181 | 0.0075 | 0.174 | 0.0075 | 0.186 | 0.0075 | 0.173 | 0.0075 | 0.138 | 0.0075 | 0.099 |
| 0.0175 | 0.212 | 0.0175 | 0.195 | 0.0175 | 0.202 | 0.0175 | 0.187 | 0.0175 | 0.182 | 0.0175 | 0.162 |
| 0.0275 | 0.223 | 0.0275 | 0.213 | 0.0275 | 0.223 | 0.0275 | 0.206 | 0.0275 | 0.216 | 0.0275 | 0.183 |
| 0.0375 | 0.232 | 0.0375 | 0.214 | 0.0375 | 0.217 | 0.0375 | 0.208 | 0.0375 | 0.179 | 0.0375 | 0.215 |
| 0.0475 | 0.236 | 0.0475 | 0.218 | 0.0475 | 0.212 | 0.0475 | 0.221 | 0.0475 | 0.189 | 0.0475 | 0.234 |
| 0.0575 | 0.244 | 0.0575 | 0.223 | 0.0575 | 0.220 | 0.0575 | 0.220 | 0.0575 | 0.199 | 0.0575 | 0.216 |
| 0.0675 | 0.246 | 0.0675 | 0.227 | 0.0675 | 0.226 | 0.0675 | 0.225 | 0.0675 | 0.235 | 0.0675 | 0.225 |
| 0.0775 | 0.248 | 0.0775 | 0.229 | 0.0775 | 0.233 | 0.0775 | 0.228 | 0.0775 | 0.258 | 0.0775 | 0.247 |
| 0.0875 | 0.251 | 0.0875 | 0.232 | 0.0875 | 0.236 | 0.0875 | 0.232 | 0.0875 | 0.247 | 0.0875 | 0.240 |
| 0.0975 | 0.249 | 0.0975 | 0.235 | 0.0975 | 0.232 | 0.0975 | 0.227 | 0.0975 | 0.252 | 0.0975 | 0.262 |
| 0.1075 | 0.252 | 0.1075 | 0.235 | 0.1075 | 0.233 | 0.1075 | 0.239 | 0.1075 | 0.263 | 0.1075 | 0.277 |
| 0.1175 | 0.251 | 0.1175 | 0.237 | 0.1175 | 0.239 | 0.1175 | 0.240 | 0.1175 | 0.260 | 0.1175 | 0.278 |
| 0.1275 | 0.249 | 0.1275 | 0.238 | 0.1275 | 0.234 | 0.1275 | 0.244 | 0.1275 | 0.273 | 0.1275 | 0.284 |
| 0.1375 | 0.254 | 0.1375 | 0.236 | 0.1375 | 0.228 | 0.1375 | 0.256 | 0.1375 | 0.271 | 0.1375 | 0.288 |
| 0.1475 | 0.249 | 0.1475 | 0.243 | 0.1475 | 0.243 | 0.1475 | 0.255 | 0.1475 | 0.257 | 0.1475 | 0.287 |
| 0.1575 | 0.251 | 0.1575 | 0.245 | 0.1575 | 0.257 | 0.1575 | 0.266 | 0.1575 | 0.266 | 0.1575 | 0.299 |
| 0.1675 | 0.253 | 0.1675 | 0.247 | 0.1675 | 0.251 | 0.1675 | 0.276 | 0.1675 | 0.273 | 0.1675 | 0.294 |
| 0.1775 | 0.254 | 0.1775 | 0.253 | 0.1775 | 0.248 | 0.1775 | 0.277 | 0.1775 | 0.293 | 0.1775 | 0.306 |
| 0.1875 | 0.254 | 0.1875 | 0.253 | 0.1875 | 0.257 | 0.1875 | 0.283 | 0.1875 | 0.314 | 0.1875 | 0.309 |
| 0.1975 | 0.262 | 0.1975 | 0.254 | 0.1975 | 0.266 | 0.1975 | 0.281 | 0.1975 | 0.277 | 0.1975 | 0.320 |
| 0.2075 | 0.256 | 0.2075 | 0.259 | 0.2075 | 0.271 | 0.2075 | 0.287 | 0.2075 | 0.297 | 0.2075 | 0.318 |
| 0.2175 | 0.256 | 0.2175 | 0.251 | 0.2175 | 0.266 | 0.2175 | 0.287 | 0.2175 | 0.290 | 0.2175 | 0.310 |
| 0.2275 | 0.257 | 0.2275 | 0.253 | 0.2275 | 0.270 | 0.2275 | 0.289 | 0.2275 | 0.272 | 0.2275 | 0.303 |
| 0.2300 | 0.202 | 0.2300 | 0.211 | 0.2300 | 0.216 | 0.2300 | 0.204 | 0.2300 | 0.212 | 0.2300 | 0.178 |

**Note**
y – Position within the vertical
u – Approach mean velocity

# APPENDIX C Data for the Series 1 tests

## APPENDIX C-1

The data presented in this appendix refer to the Series 1 test without a collar and the combination of pier and flow conditions that are given in Table 3.1. The data are analysed in Section 4.4.1.

Table C-1. Data for temporal development of scour depth for the 115 mm pier without a collar (Flow intensity = 0.89)

| Time (hrs) | Max. scour depth ( $y_s$) (mm) | Temp. ($^oC$) | Scour rate (mm/hr) | | Time (hrs) | Max. scour depth ( $y_s$) (mm) | Temp. ($^oC$) | Scour rate (mm/) |
|---|---|---|---|---|---|---|---|---|
| 0.000 | 0 | 12.1 | | | 4.033 | 80 | 14.3 | 3.8 |
| 0.017 | 15 | 12.1 | 900.0 | | 4.083 | 80.5 | 14.3 | 10.0 |
| 0.033 | 25 | 12.1 | 600.0 | | 5.650 | 85 | 14.4 | 2.9 |
| 0.050 | 29 | 12.1 | 240.0 | | 6.083 | 86 | 15 | 2.3 |
| 0.067 | 32 | 12.1 | 180.0 | | 6.383 | 87 | 15.1 | 3.3 |
| 0.083 | 35 | 12.1 | 180.0 | | 6.517 | 88 | 15.1 | 7.5 |
| 0.100 | 37 | 12.2 | 120.0 | | 7.005 | 89 | 15.3 | 2.0 |
| 0.117 | 39 | 12.2 | 120.0 | | 7.300 | 89.5 | 15.4 | 1.7 |
| 0.133 | 40 | 12.2 | 60.0 | | 7.750 | 90 | 15.5 | 1.1 |
| 0.150 | 42 | 12.3 | 120.0 | | 8.417 | 92 | 15.6 | 3.0 |
| 0.167 | 43 | 12.3 | 60.0 | | 8.883 | 94 | 15.8 | 4.3 |
| 0.183 | 44 | 12.3 | 60.0 | | 9.450 | 95 | 15.9 | 1.8 |
| 0.200 | 45 | 12.3 | 60.0 | | 9.917 | 96 | 16 | 2.1 |
| 0.217 | 45.5 | 12.3 | 30.0 | | 10.417 | 98 | 16.1 | 4.0 |
| 0.233 | 46 | 12.4 | 30.0 | | 10.933 | 99 | 16.2 | 1.9 |
| 0.250 | 46.5 | 12.4 | 30.0 | | 11.333 | 100 | 16.3 | 2.5 |
| 0.267 | 47.5 | 12.4 | 60.0 | | 21.650 | 109 | 18.4 | 0.9 |
| 0.283 | 48.5 | 12.4 | 60.0 | | 22.600 | 110 | 18.5 | 1.1 |
| 0.300 | 49 | 12.5 | 30.0 | | 24.250 | 112 | 18.5 | 1.2 |
| 0.317 | 49.5 | 12.5 | 30.0 | | 25.017 | 113 | 18.5 | 1.3 |
| 0.333 | 50 | 12.5 | 30.0 | | 25.750 | 114 | 18.9 | 1.4 |
| 0.400 | 52 | 12.5 | 30.0 | | 27.333 | 115 | 19 | 0.6 |
| 0.467 | 53 | 12.6 | 15.0 | | 28.600 | 116 | 19.1 | 0.8 |
| 0.500 | 54 | 12.6 | 30.0 | | 29.217 | 117 | 19.1 | 1.6 |
| 0.650 | 55 | 12.8 | 6.7 | | 30.217 | 118 | 19.2 | 1.0 |
| 0.750 | 56 | 12.9 | 10.0 | | 30.950 | 119 | 19.3 | 1.4 |
| 0.917 | 57.5 | 13 | 9.0 | | 32.800 | 120 | 19.4 | 0.5 |
| 0.967 | 58 | 13 | 10.0 | | 33.500 | 121 | 19.4 | 1.4 |
| 1.083 | 59 | 13.1 | 8.6 | | 45.033 | 128 | 20.1 | 0.6 |
| 1.217 | 60 | 13.2 | 7.5 | | 46.733 | 129 | 20.3 | 0.6 |
| 1.300 | 62 | 13.2 | 24.0 | | 47.650 | 130 | 20.3 | 1.1 |
| 1.383 | 63 | 13.2 | 12.0 | | 53.800 | 131 | 20.3 | 0.2 |
| 1.750 | 65 | 13.4 | 5.5 | | 55.483 | 132 | 20.3 | 0.6 |
| 2.000 | 68 | 13.5 | 12.0 | | 56.500 | 133 | 20.3 | 1.0 |
| 2.383 | 70 | 13.7 | 5.2 | | 57.717 | 134 | 20.3 | 0.8 |
| 2.633 | 72 | 13.8 | 8.0 | | 70.750 | 136 | 20.9 | 0.2 |
| 2.967 | 74 | 13.9 | 6.0 | | 72.583 | 138 | 20.8 | 1.1 |
| 3.267 | 75 | 14 | 3.3 | | 74.817 | 139 | 20.8 | 0.4 |
| 3.500 | 77 | 14.1 | 8.6 | | 79.367 | 140 | 20.8 | 0.2 |
| 3.767 | 79 | 14.2 | 7.5 | | | | | |

## APPENDIX C-2

The data presented in this appendix refer to the Series 1 test with a 2D collar and the combination of pier and flow conditions that are given in Table 3.1. The data are analysed in Section 4.4.2.

Table C-2. Data for temporal development of scour depth for the 115 mm pier with a 2D collar (Flow intensity = 0.89)

| Time (hrs) | Max. scour depth ( $y_s$) (mm) | Temp. ($^oC$) | Scour rate (mm/hr) | Time (hrs) | Max. scour depth ( $y_s$) (mm) | Temp. ($^oC$) | Scour rate (mm/hr) |
|---|---|---|---|---|---|---|---|
| 0.000 | 0.00 | 13.70 | | 50.083 | 99.00 | 21.00 | 0.3 |
| 0.017 | 14.27 | 13.70 | 856.0 | 53.133 | 100.00 | 21.00 | 0.3 |
| 0.050 | 18.87 | 13.70 | 138.0 | 69.100 | 110.00 | 21.30 | 0.6 |
| 0.083 | 24.27 | 13.70 | 162.0 | 73.500 | 112.00 | 21.40 | 0.5 |
| 0.133 | 24.27 | 13.70 | 0.0 | 74.967 | 113.00 | 21.40 | 0.7 |
| 0.183 | 25.27 | 13.70 | 20.0 | 75.917 | 114.00 | 21.40 | 1.1 |
| 0.233 | 28.27 | 13.70 | 60.0 | 97.083 | 120.00 | 21.40 | 0.3 |
| 0.283 | 29.27 | 13.70 | 20.0 | 105.417 | 121.00 | 21.10 | 0.1 |
| 0.333 | 33.67 | 13.70 | 88.0 | 119.667 | 125.00 | 21.20 | 0.3 |
| 0.417 | 35.47 | 13.70 | 21.6 | 130.083 | 127.00 | 20.90 | 0.2 |
| 0.500 | 36.27 | 13.70 | 9.6 | 142.050 | 130.00 | 21.10 | 0.3 |
| 0.583 | 38.27 | 14.00 | 24.0 | 143.250 | 130.00 | 21.10 | 0.0 |
| 0.683 | 38.67 | 14.00 | 4.0 | 145.583 | 130.00 | 21.10 | 0.0 |
| 0.800 | 40.27 | 14.00 | 13.7 | 146.583 | 130.00 | 21.10 | 0.0 |
| 0.917 | 40.47 | 14.10 | 1.7 | 148.333 | 130.00 | 21.10 | 0.0 |
| 1.000 | 40.67 | 14.10 | 2.4 | 164.917 | 134.00 | 21.10 | 0.2 |
| 1.083 | 41.07 | 14.20 | 4.8 | 170.583 | 135.00 | 21.10 | 0.2 |
| 1.283 | 40.27 | 14.30 | -4.0 | 190.583 | 136.00 | 21.30 | 0.1 |
| 1.417 | 40.27 | 14.40 | 0.0 | 194.050 | 137.00 | 21.20 | 0.3 |
| 1.633 | 39.27 | 14.50 | -4.6 | | | | |
| 1.783 | 39.47 | 14.50 | 1.3 | | | | |
| 1.883 | 40.47 | 14.50 | 10.0 | | | | |
| 2.083 | 40.87 | 14.50 | 2.0 | | | | |
| 2.583 | 42.27 | 15.00 | 2.8 | | | | |
| 3.150 | 42.27 | 15.00 | 0.0 | | | | |
| 3.967 | 41.27 | 15.50 | -1.2 | | | | |
| 5.483 | 40.27 | 15.90 | -0.7 | | | | |
| 21.267 | 43.40 | 19.60 | 0.2 | | | | |
| 22.000 | 44.00 | 19.30 | 0.8 | | | | |
| 24.150 | 49.00 | 19.50 | 2.3 | | | | |
| 25.333 | 50.00 | 19.60 | 0.8 | | | | |
| 26.517 | 53.00 | 19.70 | 2.5 | | | | |
| 27.350 | 55.00 | 19.80 | 2.4 | | | | |
| 43.667 | 95.00 | 21.00 | 2.5 | | | | |
| 45.083 | 96.00 | 21.00 | 0.7 | | | | |
| 46.383 | 97.00 | 21.00 | 0.8 | | | | |
| 47.183 | 98.00 | 21.00 | 1.3 | | | | |

# APPENDIX D Data for the Series 2 tests

## APPENDIX D-1

The data presented in this appendix refer to the Series 2 test without a collar and the combination of pier and flow conditions that are given in Table 3.1. The data are analysed in Section 4.5.1.

Table D-1. Data for temporal development of scour depth for the73 mm pier without a collar (Flow intensity = 0.89)

| Time (hrs) | Max. scour depth ( $y_s$) (mm) | Temp. ($^oC$) | Scour Rate (mm/hr) | Time (hrs) | Max. scour depth ( $y_s$) (mm) | Temp ($^oC$) | Scour rate (mm/hr) |
|---|---|---|---|---|---|---|---|
| 0.00 | 0.0 | 9.0 | | 3.72 | 69.0 | 12.6 | 2.9 |
| 0.02 | 30.0 | 9.0 | 1800.0 | 4.15 | 70 | 12.9 | 2.3 |
| 0.03 | 35.0 | 9.0 | 300.0 | 5.22 | 71 | 13.4 | 0.9 |
| 0.05 | 36.0 | 9.0 | 60.0 | 5.37 | 72 | 13.5 | 6.7 |
| 0.07 | 37.0 | 9.0 | 60.0 | 5.57 | 73 | 13.5 | 5.0 |
| 0.08 | 38.0 | 9.0 | 60.0 | 5.72 | 74 | 13.6 | 6.7 |
| 0.10 | 39.0 | 9.1 | 60.0 | 6.05 | 74 | 13.8 | 0.0 |
| 0.12 | 39.5 | 9.1 | 30.0 | 6.52 | 75 | 13.9 | 2.1 |
| 0.13 | 40.0 | 9.2 | 30.0 | 7.00 | 76 | 14 | 2.1 |
| 0.15 | 40.5 | 9.3 | 30.0 | 7.48 | 77 | 14.5 | 2.1 |
| 0.17 | 40.5 | 9.3 | 0.0 | 8.25 | 78 | 14.7 | 1.3 |
| 0.18 | 41.0 | 9.4 | 30.0 | 8.65 | 79 | 14.8 | 2.5 |
| 0.22 | 42.0 | 9.4 | 30.0 | 9.70 | 80 | 15 | 1.0 |
| 0.25 | 43.0 | 9.5 | 30.0 | 21.50 | 95 | 18 | 1.3 |
| 0.28 | 44.0 | 9.6 | 30.0 | 23.03 | 96 | 18.3 | 0.7 |
| 0.33 | 45.0 | 9.6 | 20.0 | 25.28 | 97 | 18.5 | 0.4 |
| 0.37 | 46.0 | 9.7 | 30.0 | 26.50 | 98 | 18.6 | 0.8 |
| 0.42 | 47.0 | 9.7 | 20.0 | 27.38 | 99 | 18.7 | 1.1 |
| 0.45 | 48.0 | 9.8 | 30.0 | 29.50 | 100 | 18.9 | 0.5 |
| 0.48 | 49.0 | 9.9 | 30.0 | 30.67 | 100 | 19 | 0.0 |
| 0.60 | 50.0 | 10.1 | 8.6 | 47.08 | 106 | 19.8 | 0.4 |
| 0.65 | 51.0 | 10.1 | 20.0 | 48.50 | 106.5 | 19.9 | 0.4 |
| 0.72 | 52.0 | 10.3 | 15.0 | | | | |
| 0.80 | 53.0 | 10.3 | 12.0 | | | | |
| 0.85 | 54.0 | 10.4 | 20.0 | | | | |
| 1.00 | 55.0 | 10.7 | 6.7 | | | | |
| 1.08 | 56.0 | 10.8 | 12.0 | | | | |
| 1.17 | 57.0 | 10.9 | 12.0 | | | | |
| 1.25 | 58.0 | 10.9 | 12.0 | | | | |
| 1.32 | 59.0 | 11.0 | 15.0 | | | | |
| 1.48 | 59.5 | 11.2 | 3.0 | | | | |
| 1.65 | 60.0 | 11.4 | 3.0 | | | | |
| 1.92 | 62.0 | 11.5 | 7.5 | | | | |
| 2.07 | 63.0 | 11.6 | 6.7 | | | | |
| 2.28 | 64.0 | 11.7 | 4.6 | | | | |
| 2.52 | 65.0 | 11.8 | 4.3 | | | | |
| 2.90 | 66.0 | 12.2 | 2.6 | | | | |
| 3.13 | 67.0 | 12.3 | 4.3 | | | | |
| 3.37 | 68.0 | 12.4 | 4.3 | | | | |

## APPENDIX D-2

The data presented in this appendix refer to the Series 2 test with a 2D collar and the combination of pier and flow conditions that are given in Table 3.1. The data are analysed in Section 4.5.2.

Table D-2. Data for temporal development of scour depth for the 73 mm pier with a 2D collar (Flow intensity = 0.89)

| Time (hrs) | Max. scour depth ( $y_s$) (mm) | Temp. ($^oC$) | Scour rate (mm/hr) | Time (hrs) | Max. scour depth ( $y_s$) (mm) | Temp. ($^oC$) | Scour rate (mm/hr) |
|---|---|---|---|---|---|---|---|
| 0.00 | 0.0 | 9.9 | | 48.00 | 80.0 | 19.3 | 0.0 |
| 0.02 | 12.0 | | 720.0 | 50.33 | 81.0 | 19.4 | 0.4 |
| 0.03 | 14.0 | | 120.0 | 58.60 | 83.0 | 19.4 | 0.2 |
| 0.07 | 15.0 | | 30.0 | | | | |
| 0.10 | 17.0 | | 60.0 | | | | |
| 0.15 | 20.0 | | 60.0 | | | | |
| 0.18 | 20.0 | 9.7 | 0.0 | | | | |
| 0.23 | 21.0 | | 20.0 | | | | |
| 0.30 | 19.0 | | -30.0 | | | | |
| 0.38 | 20.0 | | 12.0 | | | | |
| 0.45 | 22.0 | | 30.0 | | | | |
| 0.53 | 25.0 | | 36.0 | | | | |
| 0.62 | 27.0 | | 24.0 | | | | |
| 0.72 | 28.4 | | 14.0 | | | | |
| 0.80 | 29.0 | | 7.2 | | | | |
| 0.88 | 28.0 | | -12.0 | | | | |
| 0.98 | 28.0 | | 0.0 | | | | |
| 1.10 | 27.0 | | -8.6 | | | | |
| 1.23 | 22.0 | 11.1 | -37.5 | | | | |
| 1.42 | 23.0 | | 5.5 | | | | |
| 1.67 | 19.0 | | -16.0 | | | | |
| 1.72 | 24.0 | | 100.0 | | | | |
| 1.85 | 24.0 | | 0.0 | | | | |
| 2.07 | 29.0 | 11.7 | 23.1 | | | | |
| 2.40 | 30.0 | 11.7 | 3.0 | | | | |
| 2.58 | 31.0 | 11.9 | 5.5 | | | | |
| 3.02 | 32.0 | 12.1 | 2.3 | | | | |
| 3.30 | 33.0 | 12.3 | 3.5 | | | | |
| 6.25 | 33.0 | 13.5 | 0.0 | | | | |
| 11.62 | 52.0 | 15.2 | 3.5 | | | | |
| 12.38 | 54.0 | 15.2 | 2.6 | | | | |
| 19.87 | 68.0 | 17.1 | 1.9 | | | | |
| 25.25 | 71.0 | 17.7 | 0.6 | | | | |
| 26.78 | 72.0 | 17.9 | 0.7 | | | | |
| 28.03 | 73.0 | 18.0 | 0.8 | | | | |
| 29.12 | 74.0 | 18.1 | 0.9 | | | | |
| 33.12 | 75.0 | 18.2 | 0.3 | | | | |
| 45.65 | 80.0 | 19.3 | 0.4 | | | | |
| 46.65 | 80.0 | 19.3 | 0.0 | | | | |

# APPENDIX E Data for the Series 3 tests

## APPENDIX E-1(a)

The data presented in this appendix refer to the Series 3 test without a collar and the combination of pier and flow conditions that are given in Table 3.1. The data are analysed in Section 4.6.1.

Table E-1(a). Data for temporal development of scour depth for the 115 mm pier without a collar (Flow intensity = 0.70)

| Time (hrs) | Max. scour depth ( $y_s$) (mm) | Temp. ($^oC$) | Scour rate (mm/hr) | | Time (hrs) | Max. scour depth ( $y_s$) (mm) | Temp. ($^oC$) | Scour rate (mm/hr) |
|---|---|---|---|---|---|---|---|---|
| 0.000 | 0.0 | 8.4 | | | 30.567 | 69.0 | 17.9 | 1.0 |
| 0.017 | 5.0 | | 300.0 | | 43.667 | 75.0 | 19.0 | 0.5 |
| 0.033 | 8.0 | | 180.0 | | 46.667 | 77.0 | 19.1 | 0.7 |
| 0.050 | 11.0 | | 180.0 | | 49.333 | 79.0 | 19.1 | 0.7 |
| 0.067 | 13.0 | | 120.0 | | 51.383 | 79.5 | 19.2 | 0.2 |
| 0.083 | 14.0 | | 60.0 | | 68.417 | 85.0 | 19.6 | 0.3 |
| 0.100 | 14.5 | | 30.0 | | 70.417 | 86.0 | 19.6 | 0.5 |
| 0.117 | 15.0 | | 30.0 | | 77.167 | 87.0 | 19.6 | 0.1 |
| 0.133 | 16.0 | | 60.0 | | 97.833 | 92.0 | 19.6 | 0.2 |
| 0.150 | 17.0 | | 60.0 | | 103.833 | 94.0 | 19.5 | 0.3 |
| 0.167 | 18.0 | 10.0 | 60.0 | | 120.000 | 97.0 | 19.5 | 0.2 |
| 0.183 | 19.0 | | 60.0 | | 126.167 | 99.0 | 19.6 | 0.3 |
| 0.200 | 19.5 | | 30.0 | | 141.333 | 102.0 | 19.8 | 0.2 |
| 0.250 | 20.0 | 9.9 | 10.0 | | 143.333 | 103.0 | 19.9 | 0.5 |
| 0.317 | 21.0 | | 15.0 | | 151.333 | 105.0 | 19.7 | 0.3 |
| 0.367 | 22.0 | | 20.0 | | 163.167 | 108.0 | 20.1 | 0.3 |
| 0.383 | 23.0 | | 60.0 | | 166.917 | 109.0 | 20.0 | 0.3 |
| 0.467 | 24.0 | | 12.0 | | 176.333 | 112.0 | 20.0 | 0.3 |
| 0.567 | 25.0 | | 10.0 | | 189.667 | 114.0 | 20.2 | 0.2 |
| 0.717 | 26.0 | 10.2 | 6.7 | | 192.000 | 114.0 | 20.3 | 0.0 |
| 0.850 | 27.0 | | 7.5 | | 200.167 | 115.0 | 20.2 | 0.1 |
| 0.933 | 28.0 | | 12.0 | | 213.333 | 116.0 | 20.5 | 0.1 |
| 1.050 | 29.0 | 10.4 | 8.6 | | 221.333 | 117.0 | 21.0 | 0.1 |
| 1.533 | 30.0 | 10.7 | 2.1 | | 237.167 | 119.0 | 21.1 | 0.1 |
| 1.800 | 31.0 | | 3.8 | | 242.917 | 120.0 | 21.4 | 0.2 |
| 2.117 | 32.0 | | 3.2 | | 247.333 | 120.0 | 21.6 | 0.0 |
| 2.300 | 33.0 | | 5.5 | | 266.667 | 122.0 | 21.2 | 0.1 |
| 2.450 | 34.0 | 11.2 | 6.7 | | 295.500 | 126.0 | 21.2 | 0.1 |
| 2.650 | 35.0 | | 5.0 | | 307.167 | 127.0 | 20.5 | 0.1 |
| 3.000 | 36.0 | | 2.9 | | 319.667 | 128.0 | 20.4 | 0.1 |
| 3.483 | 37.0 | | 2.1 | | 330.667 | 129.0 | 20.0 | 0.1 |
| 3.833 | 38.0 | | 2.9 | | 336.333 | 130.0 | 20.3 | 0.2 |
| 4.150 | 39.0 | 12.0 | 3.2 | | 354.167 | 130.0 | 20.5 | 0.0 |
| 4.650 | 40.0 | | 2.0 | | 365.667 | 130.0 | 20.7 | 0.0 |
| 5.200 | 41.0 | | 1.8 | | 383.167 | 130.0 | 20.5 | 0.0 |
| 5.833 | 42.0 | 12.7 | 1.6 | | 384.000 | 130.0 | 20.5 | 0.0 |
| 18.167 | 57.0 | 16.1 | 1.2 | | 404.417 | 130.5 | 20.6 | 0.0 |
| 23.633 | 62.0 | 17.1 | 0.9 | | 408.667 | 131.0 | 20.3 | 0.1 |
| 26.017 | 64.5 | 17.4 | 1.0 | | 429.167 | 133.0 | 20.8 | 0.1 |
| 26.617 | 65.0 | | 0.8 | | 438.667 | 134.0 | 20.7 | 0.1 |

Table E-1(a) **Continued**

| Time (hrs) | Max. scour depth ( $y_s$) (mm) | Temp-Erature ($^oC$) | Scour rate (mm/hr) |
|---|---|---|---|
| 452.667 | 135.0 | 20.8 | 0.1 |
| 464.167 | 136.0 | 20.9 | 0.1 |
| 476.167 | 137.0 | 20.9 | 0.1 |
| 487.167 | 137.0 | 20.1 | 0.0 |
| 500.167 | 138.0 | 21.2 | 0.1 |
| 509.167 | 139.0 | 21.1 | 0.1 |
| 525.167 | 140.0 | | 0.1 |
| 530.667 | 140.0 | 22.0 | 0.0 |
| 452.667 | 135.0 | 20.8 | 0.1 |
| 464.167 | 136.0 | 20.9 | 0.1 |
| 476.167 | 137.0 | 20.9 | 0.1 |
| 487.167 | 137.0 | 20.1 | 0.0 |
| 500.167 | 138.0 | 21.2 | 0.1 |
| 509.167 | 139.0 | 21.1 | 0.1 |
| 525.167 | 140.0 | 21.2 | 0.1 |
| 530.667 | 140.0 | 21.2 | 0.0 |

**APPENDIX E-1(b)**

The data for the scour hole contour for the Series 3 test without a collar are shown in Table E-(b). The data are plotted and analysed in Section 4.6.1.1.

Table E-1(b). Scour hole contour data for Series 3 test without a collar

| Longitudinal position relative to the pier (cm) | Transverse position relative to the pier (cm) | Scour depth (cm) | | Longitudinal position relative to the pier (cm) | Transverse position relative to the pier (cm) | Scour depth (cm) |
|---|---|---|---|---|---|---|
| -84.1 | -61.4 | 0.00 | | -79.1 | 13.6 | 0.00 |
| -84.1 | -56.4 | 0.00 | | -79.1 | 18.6 | 0.00 |
| -84.1 | -51.4 | 0.00 | | -79.1 | 23.6 | 0.00 |
| -84.1 | -46.4 | 0.00 | | -79.1 | 28.6 | 0.00 |
| -84.1 | -41.4 | 0.00 | | -79.1 | 33.6 | 0.00 |
| -84.1 | -36.4 | 0.00 | | -79.1 | 38.6 | 0.00 |
| -84.1 | -31.4 | 0.00 | | -79.1 | 43.6 | 0.00 |
| -84.1 | -26.4 | 0.00 | | -79.1 | 48.6 | 0.00 |
| -84.1 | -21.4 | 0.00 | | -79.1 | 53.6 | 0.00 |
| -84.1 | -16.4 | 0.00 | | -79.1 | 58.6 | 0.00 |
| -84.1 | -11.4 | 0.00 | | -74.1 | -61.4 | 0.00 |
| -84.1 | -6.4 | 0.00 | | -74.1 | -56.4 | 0.00 |
| -84.1 | -1.4 | 0.00 | | -74.1 | -51.4 | 0.00 |
| -84.1 | 3.6 | 0.00 | | -74.1 | -46.4 | 0.00 |
| -84.1 | 8.6 | 0.00 | | -74.1 | -41.4 | 0.00 |
| -84.1 | 13.6 | 0.00 | | -74.1 | -36.4 | 0.00 |
| -84.1 | 18.6 | 0.00 | | -74.1 | -31.4 | 0.00 |
| -84.1 | 23.6 | 0.00 | | -74.1 | -26.4 | 0.00 |
| -84.1 | 28.6 | 0.00 | | -74.1 | -21.4 | 0.00 |
| -84.1 | 33.6 | 0.00 | | -74.1 | -16.4 | 0.00 |
| -84.1 | 38.6 | 0.00 | | -74.1 | -11.4 | 0.00 |
| -84.1 | 43.6 | 0.00 | | -74.1 | -6.4 | 0.00 |
| -84.1 | 48.6 | 0.00 | | -74.1 | -1.4 | 0.00 |
| -84.1 | 53.6 | 0.00 | | -74.1 | 3.6 | 0.00 |
| -84.1 | 58.6 | 0.00 | | -74.1 | 8.6 | 0.00 |
| -79.1 | -61.4 | 0.00 | | -74.1 | 13.6 | 0.00 |
| -79.1 | -56.4 | 0.00 | | -74.1 | 18.6 | 0.00 |
| -79.1 | -51.4 | 0.00 | | -74.1 | 23.6 | 0.00 |
| -79.1 | -46.4 | 0.00 | | -74.1 | 28.6 | 0.00 |
| -79.1 | -41.4 | 0.00 | | -74.1 | 33.6 | 0.00 |
| -79.1 | -36.4 | 0.00 | | -74.1 | 38.6 | 0.00 |
| -79.1 | -31.4 | 0.00 | | -74.1 | 43.6 | 0.00 |
| -79.1 | -26.4 | 0.00 | | -74.1 | 48.6 | 0.00 |
| -79.1 | -21.4 | 0.00 | | -74.1 | 53.6 | 0.00 |
| -79.1 | -16.4 | 0.00 | | -74.1 | 58.6 | 0.00 |
| -79.1 | -11.4 | 0.00 | | -69.1 | -61.4 | 0.00 |
| -79.1 | -6.4 | 0.00 | | -69.1 | -56.4 | 0.00 |
| -79.1 | -1.4 | 0.00 | | -69.1 | -51.4 | 0.00 |
| -79.1 | 3.6 | 0.00 | | -69.1 | -46.4 | 0.00 |
| -79.1 | 8.6 | 0.00 | | -69.1 | -41.4 | 0.00 |

Table E-1(b) Continued

| Longitudinal position relative to the pier (cm) | Transverse position relative to the pier (cm) | Scour depth (cm) | | Longitudinal position relative to the pier (cm) | Transverse position relative to the pier (cm) | Scour depth (cm) |
|---|---|---|---|---|---|---|
| -69.1 | -36.4 | 0.00 | | -64.1 | 38.6 | 0.00 |
| -69.1 | -31.4 | 0.00 | | -64.1 | 43.6 | 0.00 |
| -69.1 | -26.4 | 0.00 | | -64.1 | 48.6 | 0.00 |
| -69.1 | -21.4 | 0.00 | | -64.1 | 53.6 | 0.00 |
| -69.1 | -16.4 | 0.00 | | -64.1 | 58.6 | 0.00 |
| -69.1 | -11.4 | 0.00 | | -59.1 | -61.4 | 0.00 |
| -69.1 | -6.4 | 0.00 | | -59.1 | -56.4 | 0.00 |
| -69.1 | -1.4 | 0.00 | | -59.1 | -51.4 | 0.00 |
| -69.1 | 3.6 | 0.00 | | -59.1 | -46.4 | 0.00 |
| -69.1 | 8.6 | 0.00 | | -59.1 | -41.4 | 0.00 |
| -69.1 | 13.6 | 0.00 | | -59.1 | -36.4 | 0.00 |
| -69.1 | 18.6 | 0.00 | | -59.1 | -31.4 | 0.00 |
| -69.1 | 23.6 | 0.00 | | -59.1 | -26.4 | 0.00 |
| -69.1 | 28.6 | 0.00 | | -59.1 | -21.4 | 0.00 |
| -69.1 | 33.6 | 0.00 | | -59.1 | -16.4 | 0.00 |
| -69.1 | 38.6 | 0.00 | | -59.1 | -11.4 | 0.00 |
| -69.1 | 43.6 | 0.00 | | -59.1 | -6.4 | 0.00 |
| -69.1 | 48.6 | 0.00 | | -59.1 | -1.4 | 0.00 |
| -69.1 | 53.6 | 0.00 | | -59.1 | 3.6 | 0.00 |
| -69.1 | 58.6 | 0.00 | | -59.1 | 8.6 | 0.00 |
| -64.1 | -61.4 | 0.00 | | -59.1 | 13.6 | 0.00 |
| -64.1 | -56.4 | 0.00 | | -59.1 | 18.6 | 0.00 |
| -64.1 | -51.4 | 0.00 | | -59.1 | 23.6 | 0.00 |
| -64.1 | -46.4 | 0.00 | | -59.1 | 28.6 | 0.00 |
| -64.1 | -41.4 | 0.00 | | -59.1 | 33.6 | 0.00 |
| -64.1 | -36.4 | 0.00 | | -59.1 | 38.6 | 0.00 |
| -64.1 | -31.4 | 0.00 | | -59.1 | 43.6 | 0.00 |
| -64.1 | -26.4 | 0.00 | | -59.1 | 48.6 | 0.00 |
| -64.1 | -21.4 | 0.00 | | -59.1 | 53.6 | 0.00 |
| -64.1 | -16.4 | 0.00 | | -59.1 | 58.6 | 0.00 |
| -64.1 | -11.4 | 0.00 | | -54.1 | -61.4 | 0.00 |
| -64.1 | -6.4 | 0.00 | | -54.1 | -56.4 | 0.00 |
| -64.1 | -1.4 | 0.00 | | -54.1 | -51.4 | 0.00 |
| -64.1 | 3.6 | 0.00 | | -54.1 | -46.4 | 0.00 |
| -64.1 | 8.6 | 0.00 | | -54.1 | -41.4 | 0.00 |
| -64.1 | 13.6 | 0.00 | | -54.1 | -36.4 | 0.00 |
| -64.1 | 18.6 | 0.00 | | -54.1 | -31.4 | 0.00 |
| -64.1 | 23.6 | 0.00 | | -54.1 | -26.4 | 0.00 |
| -64.1 | 28.6 | 0.00 | | -54.1 | -21.4 | 0.00 |
| -64.1 | 33.6 | 0.00 | | -54.1 | -16.4 | 0.00 |

Table E-1(b) Continued

| Longitudinal position relative to the pier (cm) | Transverse position relative to the pier (cm) | Scour depth (cm) | | Longitudinal position relative to the pier (cm) | Transverse position relative to the pier (cm) | Scour depth (cm) |
|---|---|---|---|---|---|---|
| -54.1 | -16.4 | 0.00 | | -49.1 | 58.6 | 0.00 |
| -54.1 | -11.4 | 0.00 | | -44.1 | -61.4 | 0.00 |
| -54.1 | -6.4 | 0.00 | | -44.1 | -56.4 | 0.00 |
| -54.1 | -1.4 | 0.00 | | -44.1 | -51.4 | 0.00 |
| -54.1 | 3.6 | 0.00 | | -44.1 | -46.4 | 0.00 |
| -54.1 | 8.6 | 0.00 | | -44.1 | -41.4 | 0.00 |
| -54.1 | 13.6 | 0.00 | | -44.1 | -36.4 | 0.00 |
| -54.1 | 18.6 | 0.00 | | -44.1 | -31.4 | 0.00 |
| -54.1 | 23.6 | 0.00 | | -44.1 | -26.4 | 0.00 |
| -54.1 | 28.6 | 0.00 | | -44.1 | -21.4 | 0.00 |
| -54.1 | 33.6 | 0.00 | | -44.1 | -16.4 | 0.00 |
| -54.1 | 38.6 | 0.00 | | -44.1 | -11.4 | 0.00 |
| -54.1 | 43.6 | 0.00 | | -44.1 | -6.4 | 0.00 |
| -54.1 | 48.6 | 0.00 | | -44.1 | -1.4 | 0.00 |
| -54.1 | 53.6 | 0.00 | | -44.1 | 3.6 | 0.00 |
| -54.1 | 58.6 | 0.00 | | -44.1 | 8.6 | 0.00 |
| -49.1 | -61.4 | 0.00 | | -44.1 | 13.6 | 0.00 |
| -49.1 | -56.4 | 0.00 | | -44.1 | 18.6 | 0.00 |
| -49.1 | -51.4 | 0.00 | | -44.1 | 23.6 | 0.00 |
| -49.1 | -46.4 | 0.00 | | -44.1 | 28.6 | 0.00 |
| -49.1 | -41.4 | 0.00 | | -44.1 | 33.6 | 0.00 |
| -49.1 | -36.4 | 0.00 | | -44.1 | 38.6 | 0.00 |
| -49.1 | -31.4 | 0.00 | | -44.1 | 43.6 | 0.00 |
| -49.1 | -26.4 | 0.00 | | -44.1 | 48.6 | 0.00 |
| -49.1 | -21.4 | 0.00 | | -44.1 | 53.6 | 0.00 |
| -49.1 | -16.4 | 0.00 | | -44.1 | 58.6 | 0.00 |
| -49.1 | -11.4 | 0.00 | | -39.1 | -61.4 | 0.00 |
| -49.1 | -6.4 | 0.00 | | -39.1 | -56.4 | 0.00 |
| -49.1 | -1.4 | 0.00 | | -39.1 | -51.4 | 0.00 |
| -49.1 | 3.6 | 0.00 | | -39.1 | -46.4 | 0.00 |
| -49.1 | 8.6 | 0.00 | | -39.1 | -41.4 | 0.00 |
| -49.1 | 13.6 | 0.00 | | -39.1 | -36.4 | 0.00 |
| -49.1 | 18.6 | 0.00 | | -39.1 | -31.4 | 0.00 |
| -49.1 | 23.6 | 0.00 | | -39.1 | -26.4 | 0.00 |
| -49.1 | 28.6 | 0.00 | | -39.1 | -21.4 | 0.00 |
| -49.1 | 33.6 | 0.00 | | -39.1 | -16.4 | 0.00 |
| -49.1 | 38.6 | 0.00 | | -39.1 | -11.4 | 0.00 |
| -49.1 | 43.6 | 0.00 | | -39.1 | -6.4 | 0.00 |
| -49.1 | 48.6 | 0.00 | | -39.1 | -1.4 | 0.00 |
| -49.1 | 53.6 | 0.00 | | -39.1 | 3.6 | 0.00 |

Table E-1(b) Continued

| Longitudinal position relative to the pier (cm) | Transverse position relative to the pier (cm) | Scour depth (cm) | | Longitudinal position relative to the pier (cm) | Transverse position relative to the pier (cm) | Scour depth (cm) |
|---|---|---|---|---|---|---|
| -39.1 | 8.6 | 0.00 | | -31.1 | -41.4 | -0.20 |
| -39.1 | 13.6 | 0.00 | | -31.1 | -36.4 | -0.24 |
| -39.1 | 18.6 | 0.00 | | -31.1 | -31.4 | -0.22 |
| -39.1 | 23.6 | 0.00 | | -31.1 | -26.4 | -0.24 |
| -39.1 | 28.6 | 0.00 | | -31.1 | -21.4 | -0.28 |
| -39.1 | 33.6 | 0.00 | | -31.1 | -16.4 | -0.34 |
| -39.1 | 38.6 | 0.00 | | -31.1 | -11.4 | -0.28 |
| -39.1 | 43.6 | 0.00 | | -31.1 | -6.4 | -0.38 |
| -39.1 | 48.6 | 0.00 | | -31.1 | -1.4 | -0.44 |
| -39.1 | 53.6 | 0.00 | | -31.1 | 0 | -0.46 |
| -39.1 | 58.6 | 0.00 | | -31.1 | 3.6 | -0.44 |
| -34.1 | -61.4 | 0.00 | | -31.1 | 8.6 | -0.38 |
| -34.1 | -56.4 | 0.00 | | -31.1 | 13.6 | -0.26 |
| -34.1 | -51.4 | -0.04 | | -31.1 | 18.6 | -0.14 |
| -34.1 | -46.4 | -0.02 | | -31.1 | 23.6 | 0.00 |
| -34.1 | -41.4 | 0.00 | | -31.1 | 28.6 | 0.00 |
| -34.1 | -36.4 | -0.18 | | -31.1 | 33.6 | 0.00 |
| -34.1 | -31.4 | -0.20 | | -31.1 | 38.6 | 0.00 |
| -34.1 | -26.4 | -0.20 | | -31.1 | 43.6 | 0.00 |
| -34.1 | -21.4 | -0.22 | | -31.1 | 48.6 | 0.00 |
| -34.1 | -16.4 | -0.24 | | -31.1 | 53.6 | 0.00 |
| -34.1 | -11.4 | -0.24 | | -31.1 | 58.6 | 0.00 |
| -34.1 | -6.4 | -0.24 | | -29.1 | -61.4 | 0.00 |
| -34.1 | -1.4 | -0.24 | | -29.1 | -56.4 | 0.00 |
| -34.1 | 3.6 | -0.16 | | -29.1 | -51.4 | 0.00 |
| -34.1 | 8.6 | -0.30 | | -29.1 | -46.4 | 0.00 |
| -34.1 | 13.6 | -0.20 | | -29.1 | -41.4 | -0.24 |
| -34.1 | 18.6 | -0.18 | | -29.1 | -36.4 | -0.14 |
| -34.1 | 23.6 | -0.14 | | -29.1 | -31.4 | -0.20 |
| -34.1 | 28.6 | 0.00 | | -29.1 | -26.4 | -0.34 |
| -34.1 | 33.6 | 0.00 | | -29.1 | -21.4 | -0.20 |
| -34.1 | 38.6 | 0.00 | | -29.1 | -16.4 | -0.30 |
| -34.1 | 43.6 | 0.00 | | -29.1 | -11.4 | -0.54 |
| -34.1 | 48.6 | 0.00 | | -29.1 | -9.4 | -0.54 |
| -34.1 | 53.6 | 0.00 | | -29.1 | -6.4 | -0.64 |
| -34.1 | 58.6 | 0.00 | | -29.1 | -1.4 | -1.09 |
| -31.1 | -61.4 | 0.00 | | -29.1 | 3.6 | -1.12 |
| -31.1 | -56.4 | -0.14 | | -29.1 | 8.6 | -0.54 |
| -31.1 | -51.4 | -0.18 | | -29.1 | 13.6 | -0.40 |
| -31.1 | -46.4 | -0.14 | | -29.1 | 18.6 | -0.14 |

Table E-1(b) Continued

| Longitudinal position relative to the pier (cm) | Transverse position relative to the pier (cm) | Scour depth (cm) | | Longitudinal position relative to the pier (cm) | Transverse position relative to the pier (cm) | Scour depth (cm) |
|---|---|---|---|---|---|---|
| -29.1 | 18.6 | -0.14 | | -19.1 | -41.4 | 0.00 |
| -29.1 | 23.6 | -0.06 | | -19.1 | -36.4 | -0.24 |
| -29.1 | 28.6 | 0.00 | | -19.1 | -31.4 | -0.12 |
| -29.1 | 33.6 | 0.00 | | -19.1 | -26.4 | -0.34 |
| -29.1 | 38.6 | 0.00 | | -19.1 | -23.9 | -0.46 |
| -29.1 | 43.6 | 0.00 | | -19.1 | -21.4 | -1.48 |
| -29.1 | 48.6 | 0.00 | | -19.1 | -16.4 | -3.84 |
| -29.1 | 53.6 | 0.00 | | -19.1 | -11.4 | -5.70 |
| -29.1 | 58.6 | 0.00 | | -19.1 | -6.4 | -6.84 |
| -24.1 | -61.4 | 0.00 | | -19.1 | -1.4 | -7.24 |
| -24.1 | -56.4 | -0.06 | | -19.1 | 3.6 | -6.84 |
| -24.1 | -51.4 | -0.02 | | -19.1 | 8.6 | -6.24 |
| -24.1 | -46.4 | -0.06 | | -19.1 | 13.6 | -4.50 |
| -24.1 | -41.4 | -0.26 | | -19.1 | 18.6 | -2.44 |
| -24.1 | -36.4 | -0.24 | | -19.1 | 23.6 | -0.36 |
| -24.1 | -31.4 | -0.14 | | -19.1 | 28.6 | 0.00 |
| -24.1 | -26.4 | -0.20 | | -19.1 | 33.6 | 0.00 |
| -24.1 | -21.4 | -0.34 | | -19.1 | 38.6 | 0.00 |
| -24.1 | -18.4 | -0.68 | | -19.1 | 43.6 | 0.00 |
| -24.1 | -16.4 | -1.30 | | -19.1 | 48.6 | 0.00 |
| -24.1 | -11.4 | -2.70 | | -19.1 | 53.6 | 0.00 |
| -24.1 | -6.4 | -3.60 | | -19.1 | 58.6 | 0.00 |
| -24.1 | -1.4 | -4.10 | | -14.1 | -61.4 | 0.00 |
| -24.1 | 3.6 | -3.88 | | -14.1 | -56.4 | 0.00 |
| -24.1 | 8.6 | -3.00 | | -14.1 | -51.4 | -0.10 |
| -24.1 | 13.6 | -1.86 | | -14.1 | -46.4 | 0.00 |
| -24.1 | 18.6 | -0.68 | | -14.1 | -41.4 | -0.14 |
| -24.1 | 19.1 | -0.56 | | -14.1 | -36.4 | -0.10 |
| -24.1 | 23.6 | 0.00 | | -14.1 | -31.4 | -0.12 |
| -24.1 | 28.6 | 0.00 | | -14.1 | -27.4 | -0.34 |
| -24.1 | 33.6 | 0.00 | | -14.1 | -26.4 | -0.84 |
| -24.1 | 38.6 | 0.00 | | -14.1 | -21.4 | -3.54 |
| -24.1 | 43.6 | 0.00 | | -14.1 | -16.4 | -6.04 |
| -24.1 | 48.6 | 0.00 | | -14.1 | -11.4 | -7.94 |
| -24.1 | 53.6 | 0.00 | | -14.1 | -6.4 | -9.68 |
| -24.1 | 58.6 | 0.00 | | -14.1 | -1.4 | -10.54 |
| -19.1 | -61.4 | 0.00 | | -14.1 | 3.6 | -10.24 |
| -19.1 | -56.4 | -0.04 | | -14.1 | 8.6 | -8.64 |
| -19.1 | -51.4 | -0.02 | | -14.1 | 13.6 | -6.74 |
| -19.1 | -46.4 | 0.00 | | -14.1 | 18.6 | -4.64 |

Table E-1(b) Continued

| Longitudinal position relative to the pier (cm) | Transverse position relative to the pier (cm) | Scour depth (cm) | | Longitudinal position relative to the pier (cm) | Transverse position relative to the pier (cm) | Scour depth (cm) |
|---|---|---|---|---|---|---|
| -14.1 | 23.6 | -1.88 | | -6.1 | -36.4 | 0.00 |
| -14.1 | 27.1 | -0.08 | | -6.1 | -31.4 | -0.06 |
| -14.1 | 28.6 | 0.04 | | -6.1 | -26.4 | -3.00 |
| -14.1 | 33.6 | 0.16 | | -6.1 | -21.4 | -5.44 |
| -14.1 | 38.6 | 0.00 | | -6.1 | -16.4 | -8.10 |
| -14.1 | 43.6 | 0.00 | | -6.1 | -11.4 | -11.04 |
| -14.1 | 48.6 | 0.00 | | -6.1 | -6.4 | -13.96 |
| -14.1 | 53.6 | 0.00 | | -6.1 | -1.4 | -14.48 |
| -14.1 | 58.6 | 0.00 | | -6.1 | 3.6 | -14.20 |
| -9.1 | -61.4 | 0.00 | | -6.1 | 8.6 | -12.16 |
| -9.1 | -56.4 | 0.00 | | -6.1 | 13.6 | -9.14 |
| -9.1 | -51.4 | 0.00 | | -6.1 | 18.6 | -6.42 |
| -9.1 | -46.4 | 0.00 | | -6.1 | 28.6 | -0.54 |
| -9.1 | -41.4 | 0.00 | | -6.1 | 29.6 | -0.04 |
| -9.1 | -36.4 | 0.00 | | -6.1 | 33.6 | 0.00 |
| -9.1 | -31.4 | 0.00 | | -6.1 | 38.6 | 0.00 |
| -9.1 | -29.9 | -0.20 | | -6.1 | 43.6 | 0.00 |
| -9.1 | -26.4 | -2.30 | | -6.1 | 48.6 | 0.00 |
| -9.1 | -21.4 | -4.94 | | -6.1 | 53.6 | 0.00 |
| -9.1 | -16.4 | -7.54 | | -6.1 | 58.6 | 0.00 |
| -9.1 | -11.4 | -10.34 | | -4.1 | -61.4 | 0.00 |
| -9.1 | -6.4 | -12.68 | | -4.1 | -56.4 | 0.00 |
| -9.1 | -1.4 | -14.00 | | -4.1 | -51.4 | 0.00 |
| -9.1 | 3.6 | -13.10 | | -4.1 | -46.4 | 0.00 |
| -9.1 | 8.6 | -10.94 | | -4.1 | -41.4 | 0.00 |
| -9.1 | 13.6 | -8.40 | | -4.1 | -36.4 | 0.00 |
| -9.1 | 18.6 | -6.06 | | -4.1 | -31.4 | -0.34 |
| -9.1 | 23.6 | -3.38 | | -4.1 | -26.4 | -3.20 |
| -9.1 | 28.6 | -0.14 | | -4.1 | -21.4 | -5.36 |
| -9.1 | 33.6 | 0.06 | | -4.1 | -16.4 | -8.44 |
| -9.1 | 38.6 | 0.00 | | -4.1 | -11.4 | -11.58 |
| -9.1 | 43.6 | 0.00 | | -4.1 | -6.4 | -13.88 |
| -9.1 | 48.6 | 0.00 | | -4.1 | -5.4 | -13.94 |
| -9.1 | 53.6 | 0.00 | | -4.1 | 4.7 | -14.00 |
| -9.1 | 58.6 | 0.00 | | -4.1 | 6.6 | -13.64 |
| -6.1 | -61.4 | 0.00 | | -4.1 | 8.6 | -12.48 |
| -6.1 | -56.4 | 0.00 | | -4.1 | 13.6 | -9.48 |
| -6.1 | -51.4 | 0.00 | | -4.1 | 18.6 | -6.58 |
| -6.1 | -46.4 | 0.00 | | -4.1 | 23.6 | -3.96 |
| -6.1 | -41.4 | 0.00 | | -4.1 | 28.6 | -0.84 |

Table E-1(b) Continued

| Longitudinal position relative to the pier (cm) | Transverse position relative to the pier (cm) | Scour depth (cm) | | Longitudinal position relative to the pier (cm) | Transverse position relative to the pier (cm) | Scour depth (cm) |
|---|---|---|---|---|---|---|
| -4.1 | 30.1 | -0.02 | | 5.9 | -33.4 | -0.34 |
| -4.1 | 33.6 | 0.00 | | 5.9 | -31.4 | -1.18 |
| -4.1 | 38.6 | 0.00 | | 5.9 | -26.4 | -2.88 |
| -4.1 | 43.6 | 0.00 | | 5.9 | -21.4 | -4.74 |
| -4.1 | 48.6 | 0.00 | | 5.9 | -16.4 | -7.62 |
| -4.1 | 53.6 | 0.00 | | 5.9 | -11.4 | -9.74 |
| -4.1 | 58.6 | 0.00 | | 5.9 | -6.4 | -10.44 |
| 0 | 0 | | | 5.9 | -1.4 | -8.24 |
| 0.9 | -61.4 | 0.00 | | 5.9 | 3.6 | -9.68 |
| 0.9 | -56.4 | 0.00 | | 5.9 | 6.1 | -10.74 |
| 0.9 | -51.4 | 0.00 | | 5.9 | 8.6 | -10.34 |
| 0.9 | -46.4 | 0.00 | | 5.9 | 13.6 | -8.02 |
| 0.9 | -41.4 | 0.00 | | 5.9 | 18.6 | -5.44 |
| 0.9 | -36.4 | 0.00 | | 5.9 | 23.6 | -3.08 |
| 0.9 | -32.5 | -0.28 | | 5.9 | 28.6 | -1.02 |
| 0.9 | -31.4 | -0.88 | | 5.9 | 30.35 | -0.34 |
| 0.9 | -26.4 | -1.40 | | 5.9 | 33.6 | 0.00 |
| 0.9 | -21.4 | -5.20 | | 5.9 | 38.6 | 0.00 |
| 0.9 | -16.4 | -8.58 | | 5.9 | 43.6 | 0.00 |
| 0.9 | -11.4 | -11.56 | | 5.9 | 48.6 | 0.00 |
| 0.9 | -7.4 | -12.38 | | 5.9 | 53.6 | 0.00 |
| 0.9 | 6.6 | -12.64 | | 5.9 | 58.6 | 0.00 |
| 0.9 | 8.6 | -12.40 | | 10.9 | -61.4 | 0.00 |
| 0.9 | 13.6 | -9.44 | | 10.9 | -56.4 | 0.00 |
| 0.9 | 18.6 | -6.34 | | 10.9 | -51.4 | 0.00 |
| 0.9 | 23.6 | -3.92 | | 10.9 | -46.4 | 0.00 |
| 0.9 | 28.6 | -1.08 | | 10.9 | -41.4 | -0.34 |
| 0.9 | 30.3 | -0.22 | | 10.9 | -36.4 | -0.26 |
| 0.9 | 33.6 | -0.05 | | 10.9 | -35 | -0.44 |
| 0.9 | 38.6 | 0.00 | | 10.9 | -33.4 | -0.46 |
| 0.9 | 43.6 | 0.00 | | 10.9 | -31.4 | -0.98 |
| 0.9 | 48.6 | 0.00 | | 10.9 | -26.4 | -1.08 |
| 0.9 | 53.6 | 0.00 | | 10.9 | -21.4 | -4.28 |
| 0.9 | 58.6 | 0.00 | | 10.9 | -16.4 | -6.44 |
| 5.9 | -61.4 | 0.00 | | 10.9 | -11.4 | -7.44 |
| 5.9 | -56.4 | 0.00 | | 10.9 | -6.4 | -8.24 |
| 5.9 | -51.4 | 0.00 | | 10.9 | -1.4 | -8.42 |
| 5.9 | -46.4 | 0.00 | | 10.9 | 3.6 | -8.38 |
| 5.9 | -41.4 | 0.00 | | 10.9 | 8.6 | -7.54 |
| 5.9 | -36.4 | 0.00 | | 10.9 | 13.6 | -6.24 |

Table E-1(b) Continued

| Longitudinal position relative to the pier (cm) | Transverse position relative to the pier (cm) | Scour depth (cm) | | Longitudinal position relative to the pier (cm) | Transverse position relative to the pier (cm) | Scour depth (cm) |
|---|---|---|---|---|---|---|
| 10.9 | 18.6 | -4.16 | | 20.9 | -41.4 | -0.14 |
| 10.9 | 23.6 | -2.10 | | 20.9 | -36.4 | -0.74 |
| 10.9 | 28.6 | -0.54 | | 20.9 | -31.4 | -0.10 |
| 10.9 | 33.6 | -0.20 | | 20.9 | -29.4 | -1.28 |
| 10.9 | 38.6 | 0.00 | | 20.9 | -27.4 | -0.24 |
| 10.9 | 43.6 | 0.00 | | 20.9 | -26.4 | -0.84 |
| 10.9 | 48.6 | 0.00 | | 20.9 | -21.4 | -2.44 |
| 10.9 | 53.6 | 0.00 | | 20.9 | -16.4 | -3.38 |
| 10.9 | 58.6 | 0.00 | | 20.9 | -11.4 | -3.60 |
| 15.9 | -61.4 | 0.00 | | 20.9 | -6.4 | -3.12 |
| 15.9 | -56.4 | 0.00 | | 20.9 | -1.4 | -2.74 |
| 15.9 | -51.4 | 0.00 | | 20.9 | 3.6 | -2.44 |
| 15.9 | -46.4 | 0.00 | | 20.9 | 8.6 | -3.44 |
| 15.9 | -41.4 | 0.00 | | 20.9 | 13.6 | -3.04 |
| 15.9 | -36.4 | -0.54 | | 20.9 | 18.6 | -2.38 |
| 15.9 | -32.2 | -0.40 | | 20.9 | 23.6 | -0.34 |
| 15.9 | -31.4 | -0.48 | | 20.9 | 25.6 | -0.08 |
| 15.9 | -26.4 | -1.44 | | 20.9 | 28.6 | -1.04 |
| 15.9 | -21.4 | -3.20 | | 20.9 | 31.6 | -1.34 |
| 15.9 | -16.4 | -5.00 | | 20.9 | 33.6 | -1.14 |
| 15.9 | -11.4 | -5.74 | | 20.9 | 38.6 | -0.04 |
| 15.9 | -6.4 | -5.54 | | 20.9 | 43.6 | 0.00 |
| 15.9 | -1.4 | -5.56 | | 20.9 | 48.6 | 0.00 |
| 15.9 | 3.6 | -5.08 | | 20.9 | 53.6 | 0.00 |
| 15.9 | 8.6 | -5.24 | | 20.9 | 58.6 | 0.00 |
| 15.9 | 13.6 | -4.64 | | 25.9 | -61.4 | 0.00 |
| 15.9 | 18.6 | -2.74 | | 25.9 | -56.4 | 0.00 |
| 15.9 | 23.6 | -1.04 | | 25.9 | -51.4 | 0.00 |
| 15.9 | 27.6 | -0.18 | | 25.9 | -46.4 | -0.24 |
| 15.9 | 28.6 | -0.14 | | 25.9 | -41.4 | -0.56 |
| 15.9 | 33.6 | -0.24 | | 25.9 | -36.4 | -2.02 |
| 15.9 | 38.6 | 0.00 | | 25.9 | -31.4 | -0.84 |
| 15.9 | 43.6 | 0.00 | | 25.9 | -26.4 | -1.04 |
| 15.9 | 48.6 | 0.00 | | 25.9 | -21.4 | -2.14 |
| 15.9 | 53.6 | 0.00 | | 25.9 | -16.4 | -2.84 |
| 15.9 | 58.6 | 0.00 | | 25.9 | -11.4 | -3.04 |
| 20.9 | -61.4 | 0.00 | | 25.9 | -6.4 | -1.24 |
| 20.9 | -56.4 | 0.00 | | 25.9 | -1.4 | -0.24 |
| 20.9 | -51.4 | 0.00 | | 25.9 | 3.6 | -0.04 |
| 20.9 | -46.4 | 0.00 | | 25.9 | 8.6 | -0.74 |

Table E-1(b) Continued

| Longitudinal position relative to the pier (cm) | Transverse position relative to the pier (cm) | Scour depth (cm) | | Longitudinal position relative to the pier (cm) | Transverse position relative to the pier (cm) | Scour depth (cm) |
|---|---|---|---|---|---|---|
| 25.9 | 13.6 | -1.06 | | 35.9 | -41.4 | -1.76 |
| 25.9 | 18.6 | 0.06 | | 35.9 | -36.4 | -0.96 |
| 25.9 | 22.1 | 0.46 | | 35.9 | -31.4 | -1.20 |
| 25.9 | 23.6 | -0.24 | | 35.9 | -26.4 | 0.42 |
| 25.9 | 28.6 | -1.38 | | 35.9 | -21.4 | 0.62 |
| 25.9 | 33.6 | -0.64 | | 35.9 | -16.4 | 0.64 |
| 25.9 | 38.6 | -0.14 | | 35.9 | -11.4 | 0.76 |
| 25.9 | 43.6 | 0.00 | | 35.9 | -6.4 | 2.10 |
| 25.9 | 48.6 | 0.00 | | 35.9 | -1.4 | 2.60 |
| 25.9 | 53.6 | 0.00 | | 35.9 | 3.6 | 1.92 |
| 25.9 | 58.6 | 0.00 | | 35.9 | 8.6 | 0.66 |
| 30.9 | -61.4 | 0.00 | | 35.9 | 13.6 | 0.46 |
| 30.9 | -56.4 | 0.00 | | 35.9 | 18.6 | 0.68 |
| 30.9 | -51.4 | 0.00 | | 35.9 | 23.6 | 1.16 |
| 30.9 | -46.4 | 0.00 | | 35.9 | 28.6 | 0.36 |
| 30.9 | -41.4 | -0.04 | | 35.9 | 33.6 | -0.44 |
| 30.9 | -36.4 | -1.14 | | 35.9 | 38.6 | -0.24 |
| 30.9 | -31.4 | -1.54 | | 35.9 | 43.6 | -0.10 |
| 30.9 | -26.4 | -0.04 | | 35.9 | 48.6 | 0.00 |
| 30.9 | -21.4 | -1.24 | | 35.9 | 53.6 | 0.00 |
| 30.9 | -16.4 | -1.44 | | 35.9 | 58.6 | 0.00 |
| 30.9 | -11.4 | -1.14 | | 40.9 | -61.4 | 0.00 |
| 30.9 | -6.4 | -0.42 | | 40.9 | -56.4 | 0.00 |
| 30.9 | -1.4 | 2.16 | | 40.9 | -51.4 | -0.14 |
| 30.9 | 3.6 | 1.46 | | 40.9 | -46.4 | -1.14 |
| 30.9 | 8.6 | 0.26 | | 40.9 | -41.4 | -2.14 |
| 30.9 | 13.6 | -0.04 | | 40.9 | -36.4 | -1.84 |
| 30.9 | 18.6 | 0.16 | | 40.9 | -31.4 | -0.74 |
| 30.9 | 23.6 | -0.04 | | 40.9 | -26.4 | -1.14 |
| 30.9 | 28.6 | 0.00 | | 40.9 | -21.4 | -0.30 |
| 30.9 | 33.6 | -0.94 | | 40.9 | -16.4 | -0.14 |
| 30.9 | 38.6 | -0.24 | | 40.9 | -11.4 | 0.66 |
| 30.9 | 43.6 | 0.00 | | 40.9 | -6.4 | 2.06 |
| 30.9 | 48.6 | 0.00 | | 40.9 | -1.4 | 1.88 |
| 30.9 | 53.6 | 0.00 | | 40.9 | 3.6 | 1.96 |
| 30.9 | 58.6 | 0.00 | | 40.9 | 8.6 | 1.86 |
| 35.9 | -61.4 | 0.00 | | 40.9 | 13.6 | 1.96 |
| 35.9 | -56.4 | 0.00 | | 40.9 | 18.6 | 2.36 |
| 35.9 | -51.4 | 0.00 | | 40.9 | 23.6 | 1.76 |
| 35.9 | -46.4 | -0.54 | | 40.9 | 28.6 | 0.40 |

Table E-1(b) Continued

| Longitudinal position relative to the pier (cm) | Transverse position relative to the pier (cm) | Scour depth (cm) | | Longitudinal position relative to the pier (cm) | Transverse position relative to the pier (cm) | Scour depth (cm) |
|---|---|---|---|---|---|---|
| 40.9 | 33.6 | -0.74 | | 55.9 | -6.4 | 2.82 |
| 40.9 | 38.6 | -2.04 | | 55.9 | -1.4 | 2.72 |
| 40.9 | 43.6 | -1.14 | | 55.9 | 3.6 | 5.86 |
| 40.9 | 48.6 | 0.00 | | 55.9 | 8.6 | 5.76 |
| 45.9 | -61.4 | 0.00 | | 55.9 | 13.6 | 4.86 |
| 45.9 | -56.4 | 0.00 | | 55.9 | 18.6 | 2.82 |
| 45.9 | -51.4 | -0.24 | | 55.9 | 23.6 | 1.26 |
| 45.9 | -46.4 | -0.44 | | 55.9 | 28.6 | 0.66 |
| 45.9 | -41.4 | -1.28 | | 55.9 | 33.6 | 0.56 |
| 45.9 | -36.4 | -1.34 | | 55.9 | -60.4 | -0.24 |
| 45.9 | -31.4 | -1.04 | | 55.9 | 43.6 | -0.34 |
| 45.9 | -26.4 | 0.02 | | 55.9 | 48.6 | 0.08 |
| 45.9 | -21.4 | 0.26 | | 55.9 | 53.6 | -0.02 |
| 45.9 | -16.4 | 0.46 | | 55.9 | 58.6 | 0.00 |
| 45.9 | -11.4 | 1.48 | | 65.9 | -61.4 | 0.00 |
| 45.9 | -6.4 | 2.60 | | 65.9 | -56.4 | -0.54 |
| 45.9 | -1.4 | 2.46 | | 65.9 | -51.4 | -1.44 |
| 45.9 | 3.6 | 3.16 | | 65.9 | -46.4 | -2.64 |
| 45.9 | 8.6 | 2.76 | | 65.9 | -41.4 | -2.14 |
| 45.9 | 13.6 | 2.30 | | 65.9 | -36.4 | -0.84 |
| 45.9 | 18.6 | 2.16 | | 65.9 | -31.4 | -0.44 |
| 45.9 | 23.6 | 1.76 | | 65.9 | -26.4 | 0.56 |
| 45.9 | 28.6 | 0.60 | | 65.9 | -21.4 | 2.66 |
| 45.9 | 33.6 | -0.90 | | 65.9 | -16.4 | 3.10 |
| 45.9 | 38.6 | -1.74 | | 65.9 | -11.4 | 4.56 |
| 45.9 | 43.6 | -1.14 | | 65.9 | -6.4 | 5.00 |
| 45.9 | 48.6 | -0.44 | | 65.9 | -1.4 | 5.00 |
| 45.9 | 53.6 | 0.00 | | 65.9 | 3.6 | 5.76 |
| 45.9 | 58.6 | 0.00 | | 65.9 | 8.6 | 6.82 |
| 55.9 | -61.4 | 0.00 | | 65.9 | 13.6 | 5.26 |
| 55.9 | -56.4 | 0.00 | | 65.9 | 18.6 | 3.46 |
| 55.9 | -51.4 | -1.48 | | 65.9 | 23.6 | 2.00 |
| 55.9 | -46.4 | -1.04 | | 65.9 | 28.6 | -0.22 |
| 55.9 | -41.4 | -1.24 | | 65.9 | 33.6 | -0.54 |
| 55.9 | -36.4 | -1.20 | | 65.9 | 38.6 | -1.84 |
| 55.9 | -31.4 | 0.16 | | 65.9 | 43.6 | -2.24 |
| 55.9 | -26.4 | -0.04 | | 65.9 | 48.6 | -2.10 |
| 55.9 | -21.4 | 0.24 | | 65.9 | 53.6 | -1.84 |
| 55.9 | -16.4 | 1.56 | | 65.9 | 58.6 | -0.38 |
| 55.9 | -11.4 | 2.26 | | 75.9 | -61.4 | -2.54 |

Table E-1(b) Continued

| Longitudinal position relative to the pier (cm) | Transverse position relative to the pier (cm) | Scour depth (cm) | | Longitudinal position relative to the pier (cm) | Transverse position relative to the pier (cm) | Scour depth (cm) |
|---|---|---|---|---|---|---|
| 75.9 | -56.4 | -1.44 | | 85.9 | 18.6 | 2.96 |
| 75.9 | -51.4 | -0.34 | | 85.9 | 23.6 | 2.76 |
| 75.9 | -46.4 | 0.36 | | 85.9 | 28.6 | 0.56 |
| 75.9 | -41.4 | -1.00 | | 85.9 | 33.6 | -1.14 |
| 75.9 | -36.4 | -0.44 | | 85.9 | 38.6 | -1.04 |
| 75.9 | -31.4 | 0.56 | | 85.9 | 43.6 | -1.24 |
| 75.9 | -26.4 | 0.76 | | 85.9 | 48.6 | -0.60 |
| 75.9 | -21.4 | 1.96 | | 85.9 | 53.6 | -2.44 |
| 75.9 | -16.4 | 3.28 | | 85.9 | 58.6 | -4.48 |
| 75.9 | -11.4 | 5.08 | | 95.9 | -61.4 | -0.03 |
| 75.9 | -6.4 | 5.96 | | 95.9 | -56.4 | -0.44 |
| 75.9 | -1.4 | 6.58 | | 95.9 | -51.4 | -0.04 |
| 75.9 | 3.6 | 7.26 | | 95.9 | -46.4 | 0.96 |
| 75.9 | 8.6 | 5.56 | | 95.9 | -41.4 | 0.56 |
| 75.9 | 13.6 | 4.16 | | 95.9 | -36.4 | -0.44 |
| 75.9 | 18.6 | 3.12 | | 95.9 | -31.4 | -0.34 |
| 75.9 | 23.6 | 2.32 | | 95.9 | -26.4 | 1.86 |
| 75.9 | 28.6 | 0.24 | | 95.9 | -21.4 | 4.06 |
| 75.9 | 33.6 | 0.72 | | 95.9 | -16.4 | 5.00 |
| 75.9 | 38.6 | -0.10 | | 95.9 | -11.4 | 6.26 |
| 75.9 | 43.6 | -0.64 | | 95.9 | -6.4 | 6.90 |
| 75.9 | 48.6 | 0.08 | | 95.9 | -1.4 | 7.36 |
| 75.9 | 53.6 | 0.44 | | 95.9 | 3.6 | 5.76 |
| 75.9 | 58.6 | 0.24 | | 95.9 | 8.6 | 4.26 |
| 85.9 | -61.4 | -0.64 | | 95.9 | 13.6 | 3.16 |
| 85.9 | -56.4 | -0.34 | | 95.9 | 18.6 | 1.76 |
| 85.9 | -51.4 | -1.04 | | 95.9 | 23.6 | 0.86 |
| 85.9 | -46.4 | -0.74 | | 95.9 | 28.6 | 0.76 |
| 85.9 | -41.4 | -1.04 | | 95.9 | 33.6 | 0.06 |
| 85.9 | -36.4 | -0.24 | | 95.9 | 38.6 | -0.68 |
| 85.9 | -31.4 | 0.76 | | 95.9 | 43.6 | -0.68 |
| 85.9 | -26.4 | 1.36 | | 95.9 | 48.6 | -0.74 |
| 85.9 | -21.4 | 1.38 | | 95.9 | 53.6 | -0.64 |
| 85.9 | -16.4 | 2.96 | | 95.9 | 58.6 | -1.14 |
| 85.9 | -11.4 | 4.46 | | 105.9 | -61.4 | 0.06 |
| 85.9 | -6.4 | 5.36 | | 105.9 | -56.4 | -1.04 |
| 85.9 | -1.4 | -2.90 | | 105.9 | -51.4 | 0.00 |
| 85.9 | 3.6 | 6.16 | | 105.9 | -46.4 | -0.24 |
| 85.9 | 8.6 | 6.06 | | 105.9 | -41.4 | -0.28 |
| 85.9 | 13.6 | 4.06 | | 105.9 | -36.4 | 0.50 |

Table E-1(b) Continued

| Longitudinal position relative to the pier (cm) | Transverse position relative to the pier (cm) | Scour depth (cm) |
|---|---|---|
| 105.9 | -31.4 | 1.08 |
| 105.9 | -26.4 | 2.26 |
| 105.9 | -21.4 | 3.26 |
| 105.9 | -16.4 | 4.12 |
| 105.9 | -11.4 | 4.86 |
| 105.9 | -6.4 | 4.56 |
| 105.9 | -1.4 | 2.86 |
| 105.9 | 3.6 | 1.48 |
| 105.9 | 8.6 | 0.56 |
| 105.9 | 13.6 | 0.52 |
| 105.9 | 18.6 | 0.16 |
| 105.9 | 23.6 | 0.66 |
| 105.9 | 28.6 | 0.86 |
| 105.9 | 33.6 | 0.96 |
| 105.9 | 38.6 | 0.88 |
| 105.9 | 43.6 | 0.66 |
| 105.9 | 48.6 | 0.86 |
| 105.9 | 53.6 | -0.66 |
| 105.9 | 58.6 | -0.26 |
| 115.9 | -61.4 | -0.52 |
| 115.9 | -56.4 | 0.06 |
| 115.9 | -51.4 | 0.34 |
| 115.9 | -46.4 | -0.24 |
| 115.9 | -41.4 | -1.00 |
| 115.9 | -36.4 | -0.34 |
| 115.9 | -31.4 | 0.10 |
| 115.9 | -26.4 | 0.76 |
| 115.9 | -21.4 | 0.80 |
| 115.9 | -16.4 | 0.36 |
| 115.9 | -11.4 | 0.06 |
| 115.9 | -6.4 | -0.34 |
| 115.9 | -1.4 | 0.86 |
| 115.9 | 3.6 | 0.16 |
| 115.9 | 8.6 | 0.06 |
| 115.9 | 13.6 | -0.86 |
| 115.9 | 18.6 | -1.24 |
| 115.9 | 23.6 | -1.54 |
| 115.9 | 28.6 | -1.14 |
| 115.9 | 33.6 | -0.04 |
| 115.9 | 38.6 | 0.16 |
| 115.9 | 43.6 | 0.06 |
| 115.9 | 48.6 | 1.34 |
| 115.9 | 53.6 | 0.86 |
| 115.9 | 58.6 | -1.02 |

## APPENDIX E-1(c)

Table E-1(c) shows the data for the longitudinal profile of the scour hole across the centre of the pier for a Series 3 test for a pier without a collar. The data are plotted and analysed in Section 4.6.1.2.

Table E-1(c). Data for the longitudinal scour profile along the centreline of the pier for Series 3 test: No collar

| Longitudinal position relative to the pier (cm) | Scour depth (cm) | | Longitudinal position relative to the pier (cm) | Scour depth (cm) |
|---|---|---|---|---|
| -84.1 | 0.00 | | 85.9 | 6.96 |
| -79.1 | 0.00 | | 90.9 | 7.60 |
| -74.1 | 0.00 | | 95.9 | 6.46 |
| -69.1 | 0.00 | | 100.9 | 4.66 |
| -64.1 | 0.00 | | 105.9 | 1.76 |
| -59.1 | 0.00 | | 110.9 | -0.14 |
| -54.1 | 0.00 | | 115.9 | 0.06 |
| -49.1 | 0.00 | | 120.9 | 0.16 |
| -44.1 | 0.00 | | 125.9 | 0.14 |
| -39.1 | 0.00 | | 130.9 | -0.54 |
| -34.1 | -0.02 | | 135.9 | -0.98 |
| -31.1 | -0.28 | | 140.9 | -0.56 |
| -29.1 | -0.90 | | 145.9 | -0.14 |
| -24.1 | -3.94 | | 150.9 | -0.44 |
| -19.1 | -7.04 | | 155.9 | -0.84 |
| -14.1 | -10.32 | | 160.9 | 0.24 |
| -9.1 | -13.72 | | 165.9 | -0.10 |
| -8.1 | -14.28 | | 170.9 | 0.96 |
| -7.1 | -14.50 | | 175.9 | -0.04 |
| -6.1 | -14.24 | | 180.9 | -0.44 |
| -5.7 | -14.20 | | 185.9 | -0.32 |
| 6.3 | -8.04 | | 190.9 | 0.16 |
| 8.9 | -8.64 | | 195.9 | -0.58 |
| 9.9 | -8.62 | | 200.9 | 0.06 |
| 10.9 | -8.30 | | 205.9 | -0.54 |
| 15.9 | -5.58 | | 210.9 | 0.12 |
| 20.9 | -2.66 | | 215.9 | -0.24 |
| 25.9 | 0.04 | | 220.9 | -0.06 |
| 30.9 | 2.16 | | 225.9 | -0.04 |
| 35.9 | 2.44 | | 230.9 | 0.00 |
| 40.9 | 2.06 | | 235.9 | 0.00 |
| 45.9 | 2.56 | | 240.9 | 0.00 |
| 50.9 | 4.56 | | 245.9 | 0.00 |
| 55.9 | 4.10 | | 250.9 | 0.00 |
| 60.9 | 4.08 | | 255.9 | 0.00 |
| 65.9 | 4.94 | | 260.9 | 0.00 |
| 70.9 | 6.88 | | 265.9 | 0.00 |
| 75.9 | 6.52 | | | |
| 80.9 | 6.16 | | | |

## APPENDIX E-1(d)

The data for the transverse profile of the scour hole across the centre of the pier for the Series 3 test for a pier without a collar are shown in Table E-1(d). The data are plotted and analysed in Section 4.6.1.3.

Table E-1(d). Data for the transverse scour profile along the centreline of the pier for Series 3 test: No collar

| **Transverse position relative to the pier (cm)** | **Scour depth (cm)** |
|---|---|
| -61.4 | 0.0 |
| -56.4 | 0.0 |
| -51.4 | 0.0 |
| -46.4 | 0.0 |
| -41.4 | 0.0 |
| -36.4 | 0.0 |
| -32.5 | -0.3 |
| -31.4 | -0.9 |
| -26.4 | -1.4 |
| -21.4 | -5.2 |
| -16.4 | -8.6 |
| -11.4 | -11.6 |
| -7.4 | -12.4 |
| 6.6 | -12.6 |
| 8.6 | -12.4 |
| 13.6 | -9.4 |
| 18.6 | -6.3 |
| 23.6 | -3.9 |
| 28.6 | -1.1 |
| 30.3 | -0.2 |
| 33.6 | -0.1 |
| 38.6 | 0.0 |
| 43.6 | 0.0 |
| 48.6 | 0.0 |
| 53.6 | 0.0 |
| 58.6 | 0.0 |

## APPENDIX E-2 (a)

The appendix represents the data for the locations of maximum scour depth with time for the Series 3 test for a pier fitted with a 3D collar. The data are plotted and analysed in Section 4.6.2.

Table E-2(a). Data for locations of maximum scour depth with time for Series 3 test with a 3D collar

| **Time (hrs)** | 0.00 | 0.02 | 0.08 | 0.53 | 121.33 | 170.83 | 220.83 | 312.50 |
|---|---|---|---|---|---|---|---|---|
| **X (cm)** | 0.0 | 21.3 | 21.3 | 22.9 | 27.7 | 27.7 | 27.7 | 27.7 |
| **Z (cm)** | 0.0 | -17.6 | -15.1 | -15.1 | -19.5 | -25.0 | -25.0 | -25.4 |
| **$y_s$ (mm)** | 0.0 | 0.0 | 2.0 | 7.0 | 17.6 | 44.4 | 45.0 | 48.4 |

| **Time (hrs)** | 317.08 | 327.00 | 338.17 | 363.83 | 419.00 | 454.83 | 528.33 | 553.08 |
|---|---|---|---|---|---|---|---|---|
| **X (cm)** | 30.1 | 30.9 | 27.9 | 28.9 | 25.9 | 30.9 | 30.9 | 31.9 |
| **Z (cm)** | -25.7 | -23.4 | -22.9 | -22.9 | -25.4 | -25.2 | -25.4 | -25.7 |
| **$y_s$ (mm)** | 52.4 | 53.4 | 52.2 | 51.4 | 52.4 | 56.4 | 57.4 | 62.4 |

| **Time (hrs)** | 577.17 | 603.83 | 625.25 | 694.33 | 720.83 | 746.58 | 752.75 | 769.08 |
|---|---|---|---|---|---|---|---|---|
| **X (cm)** | 31.9 | 34.9 | 30.9 | 15.9 | 15.9 | 17.1 | 19.3 | 18.1 |
| **Z (cm)** | -25.7 | -25.5 | -24.4 | -18.9 | 21.3 | 21.6 | 20.6 | 21.0 |
| **$y_s$ (mm)** | 61.0 | 59.4 | 61.0 | 60.6 | 60.3 | 61.2 | 62.4 | 62.6 |

| **Time (hrs)** | 793.67 | 813.75 | 821.83 | 838.75 | 862.75 | 869.83 | 879.83 | 882.00 |
|---|---|---|---|---|---|---|---|---|
| **X (cm)** | 19.1 | 19.1 | 19.7 | 19.3 | 19.3 | 19.3 | 20.1 | 20.1 |
| **Z (cm)** | 21.2 | 21.2 | 21.6 | 22.0 | 22.0 | 22.0 | 21.6 | 21.6 |
| **$y_s$ (mm)** | 63.2 | 63.4 | 64.4 | 64.5 | 64.5 | 64.4 | 64.4 | 64.4 |

| **Time (hrs)** | 899.92 | 917.58 | 917.67 | 926.67 | 943.75 | 954.42 |
|---|---|---|---|---|---|---|
| **X (cm)** | 20.1 | 20.9 | 20.9 | 21.1 | 21.1 | 21.9 |
| **Z (cm)** | 21.6 | 21.8 | 21.8 | 22.1 | 22.2 | -20.9 |
| **$y_s$ (mm)** | 64.2 | 63.8 | 63.6 | 63.6 | 63.6 | 63.4 |

**Note**:
X - Longitudinal position relative to the pier

Z - Transverse position relative to the pier

$y_s$ - Maximum scour depth

## APPENDIX E-2(b)

The data presented in this appendix refer to the Series 3 test with a 3D collar and the combination of pier and flow conditions that are given in Table 3.1. The data are analysed in Section 4.6.2.

Table E-2(b). Data for temporal development of scour depth for the 115 mm pier with a 3D collar (Flow intensity = 0.70)

| Time (hrs) | Max. scour depth ( $y_s$) (mm) | Temp- ($^oC$) | Scour rate (mm/hr) | Time (hrs) | Max. scour depth ( $y_s$) (mm) | Temp- ($^oC$) | Scour rate (mm/hr) |
|---|---|---|---|---|---|---|---|
| 0.000 | 0.0 | 17.0 | | 121.333 | 44.4 | 20.5 | 0.1 |
| 0.017 | 2.0 | 17.0 | 120.0 | 124.000 | 44.4 | 20.2 | 0.0 |
| 0.033 | 3.0 | 17.0 | 60.0 | 130.833 | 44.4 | 20.4 | 0.0 |
| 0.050 | 4.0 | 17.0 | 60.0 | 145.833 | 44.4 | 20.6 | 0.0 |
| 0.067 | 5.0 | 17.0 | 60.0 | 154.833 | 44.6 | | 0.0 |
| 0.083 | 7.0 | 17.0 | 120.0 | 170.833 | 45.0 | 20.9 | 0.0 |
| 0.150 | 10.4 | 17.0 | 51.0 | 180.833 | 45.1 | 20.9 | 0.0 |
| 0.217 | 10.6 | 17.0 | 3.0 | 196.167 | 45.2 | 21.2 | 0.0 |
| 0.333 | 13.4 | 17.1 | 24.0 | 220.833 | 48.4 | 21.3 | 0.1 |
| 0.467 | 15.2 | 17.1 | 13.5 | 248.000 | 49.4 | 21.1 | 0.0 |
| 0.533 | 17.6 | 17.1 | 36.0 | 266.000 | 50.0 | 21.2 | 0.0 |
| 0.600 | 18.4 | 17.1 | 12.0 | 274.167 | 50.4 | 22.5 | 0.0 |
| 0.717 | 19.4 | 17.1 | 8.6 | 290.833 | 51.4 | 21.8 | 0.1 |
| 0.883 | 20.0 | 17.1 | 3.6 | 312.500 | 52.4 | 21.0 | 0.0 |
| 1.033 | 22.0 | | 13.3 | 317.083 | 53.4 | 22.5 | 0.2 |
| 1.400 | 24.4 | | 6.5 | 321.333 | 52.9 | 22.2 | -0.1 |
| 1.633 | 24.5 | | 0.4 | 327.000 | 52.2 | 21.8 | -0.1 |
| 2.000 | 24.4 | | -0.3 | 338.167 | 51.4 | 21.7 | -0.1 |
| 2.417 | 25.4 | 17.4 | 2.4 | 346.833 | 51.6 | 23.0 | 0.0 |
| 3.000 | 26.0 | 17.6 | 1.0 | 363.833 | 52.4 | 21.9 | 0.0 |
| 4.083 | 27.4 | | 1.3 | 370.167 | 51.8 | 23.4 | -0.1 |
| 5.083 | 28.4 | | 1.0 | 389.833 | 52.4 | 24.1 | 0.0 |
| 6.083 | 29.0 | 18.0 | 0.6 | 419.000 | 56.4 | | 0.1 |
| 6.750 | 30.2 | | 1.8 | 432.250 | 57.4 | 25.5 | 0.1 |
| 12.750 | 30.6 | 18.8 | 0.1 | 454.833 | 57.4 | 26.3 | 0.0 |
| 24.750 | 33.6 | 19.8 | 0.3 | 463.333 | 57.4 | | 0.0 |
| 26.000 | 34.6 | 19.9 | 0.8 | 477.583 | 60.4 | 26.2 | 0.2 |
| 28.000 | 33.8 | 20.0 | -0.4 | 483.333 | 60.4 | 26.6 | 0.0 |
| 36.750 | 34.8 | 20.1 | 0.1 | 489.333 | 60.4 | 26.5 | 0.0 |
| 49.833 | 38.4 | 20.5 | 0.3 | 506.167 | 60.4 | 26.6 | 0.0 |
| 56.333 | 39.0 | 20.5 | 0.1 | 510.833 | 60.6 | 26.5 | 0.0 |
| 73.833 | 41.4 | 20.4 | 0.1 | 528.333 | 62.4 | 26.6 | 0.1 |
| 85.333 | 42.4 | 20.2 | 0.1 | 532.583 | 62.4 | 26.5 | 0.0 |
| 98.333 | 42.4 | 20.5 | 0.0 | 553.083 | 61.0 | 26.6 | -0.1 |
| 102.833 | 43.4 | | 0.2 | 577.167 | 59.4 | 26.5 | -0.1 |
| 106.833 | 43.4 | 20.4 | 0.0 | 603.833 | 61.0 | 25.9 | 0.1 |

**APPENDIX E-2(b) continued**

| Time (hrs) | Max. scour depth ( $y_s$) (mm) | Temp-erature ($^oC$) | Scour rate (mm/hr) |
|---|---|---|---|
| 609.333 | 60.8 | 26.3 | 0.0 |
| 625.250 | 60.6 | 26.0 | 0.0 |
| 632.333 | 60.5 | 26.0 | 0.0 |
| 648.833 | 60.4 | 25.9 | 0.0 |
| 654.833 | 60.3 | 26.0 | 0.0 |
| 655.833 | 60.3 | | 0.0 |
| 669.750 | 60.4 | | 0.0 |
| 679.833 | 60.4 | | 0.0 |
| 694.333 | 60.3 | | 0.0 |
| 702.333 | 60.4 | | 0.0 |
| 720.833 | 61.2 | 21.2 | 0.0 |
| 723.833 | 61.4 | | 0.1 |
| 727.417 | 61.6 | 21.1 | 0.1 |
| 729.167 | 62.4 | 21.1 | 0.5 |
| 746.583 | 62.4 | 21.3 | 0.0 |
| 752.750 | 62.6 | 21.4 | 0.0 |
| 763.833 | 62.8 | 21.6 | 0.0 |
| 769.083 | 63.2 | 21.6 | 0.1 |
| 793.667 | 63.4 | 21.5 | 0.0 |
| 813.750 | 64.4 | 21.5 | 0.0 |
| 821.833 | 64.5 | 21.5 | 0.0 |
| 838.750 | 64.5 | 21.6 | 0.0 |
| 862.750 | 64.4 | 21.7 | 0.0 |
| 869.833 | 64.4 | 21.6 | 0.0 |
| 869.833 | 64.4 | 21.2 | 0.0 |
| 882.000 | 64.2 | 21.0 | 0.0 |
| 899.917 | 63.8 | 21.1 | 0.0 |
| 917.583 | 63.6 | 21.1 | 0.0 |
| 917.667 | 63.6 | 21.1 | 0.0 |
| 926.667 | 63.6 | 21.2 | 0.0 |
| 943.750 | 63.4 | 21.3 | 0.0 |
| 954.417 | 64.4 | 21.4 | 0.1 |

## APPENDIX E-2(c)

The data for the Scour hole contour for the Series 3 test with a 3D collar are shown in Table E- 2(c). The data are plotted and analysed in Section 4.6.2.1.

Table E-2(c). Data for the scour hole contour for Series 3 tests with a 3D collar

| Longitudinal position relative to the pier (cm) | Transverse position relative to the pier (cm) | Scour depth (cm) | | Longitudinal position relative to the pier (cm) | Transverse position relative to the pier (cm) | Scour depth (cm) |
|---|---|---|---|---|---|---|
| -84.1 | -61.4 | 0.00 | | -79.1 | 13.6 | 0.00 |
| -84.1 | -56.4 | 0.00 | | -79.1 | 18.6 | 0.00 |
| -84.1 | -51.4 | 0.00 | | -79.1 | 23.6 | 0.00 |
| -84.1 | -46.4 | 0.00 | | -79.1 | 28.6 | 0.00 |
| -84.1 | -41.4 | 0.00 | | -79.1 | 33.6 | 0.00 |
| -84.1 | -36.4 | 0.00 | | -79.1 | 38.6 | 0.00 |
| -84.1 | -31.4 | 0.00 | | -79.1 | 43.6 | 0.00 |
| -84.1 | -26.4 | 0.00 | | -79.1 | 48.6 | 0.00 |
| -84.1 | -21.4 | 0.00 | | -79.1 | 53.6 | 0.00 |
| -84.1 | -16.4 | 0.00 | | -79.1 | 58.6 | 0.00 |
| -84.1 | -11.4 | 0.00 | | -74.1 | -61.4 | 0.00 |
| -84.1 | -6.4 | 0.00 | | -74.1 | -56.4 | 0.00 |
| -84.1 | -1.4 | 0.00 | | -74.1 | -51.4 | 0.00 |
| -84.1 | 3.6 | 0.00 | | -74.1 | -46.4 | 0.00 |
| -84.1 | 8.6 | 0.00 | | -74.1 | -41.4 | 0.00 |
| -84.1 | 13.6 | 0.00 | | -74.1 | -36.4 | 0.00 |
| -84.1 | 18.6 | 0.00 | | -74.1 | -31.4 | 0.00 |
| -84.1 | 23.6 | 0.00 | | -74.1 | -26.4 | 0.00 |
| -84.1 | 28.6 | 0.00 | | -74.1 | -21.4 | 0.00 |
| -84.1 | 33.6 | 0.00 | | -74.1 | -16.4 | 0.00 |
| -84.1 | 38.6 | 0.00 | | -74.1 | -11.4 | 0.00 |
| -84.1 | 43.6 | 0.00 | | -74.1 | -6.4 | 0.00 |
| -84.1 | 48.6 | 0.00 | | -74.1 | -1.4 | 0.00 |
| -84.1 | 53.6 | 0.00 | | -74.1 | 3.6 | 0.00 |
| -84.1 | 58.6 | 0.00 | | -74.1 | 8.6 | 0.00 |
| -79.1 | -61.4 | 0.00 | | -74.1 | 13.6 | 0.00 |
| -79.1 | -56.4 | 0.00 | | -74.1 | 18.6 | 0.00 |
| -79.1 | -51.4 | 0.00 | | -74.1 | 23.6 | 0.00 |
| -79.1 | -46.4 | 0.00 | | -74.1 | 28.6 | 0.00 |
| -79.1 | -41.4 | 0.00 | | -74.1 | 33.6 | 0.00 |
| -79.1 | -36.4 | 0.00 | | -74.1 | 38.6 | 0.00 |
| -79.1 | -31.4 | 0.00 | | -74.1 | 43.6 | 0.00 |
| -79.1 | -26.4 | 0.00 | | -74.1 | 48.6 | 0.00 |
| -79.1 | -21.4 | 0.00 | | -74.1 | 53.6 | 0.00 |
| -79.1 | -16.4 | 0.00 | | -74.1 | 58.6 | 0.00 |
| -79.1 | -11.4 | 0.00 | | -69.1 | -61.4 | 0.00 |
| -79.1 | -6.4 | 0.00 | | -69.1 | -56.4 | 0.00 |
| -79.1 | -1.4 | 0.00 | | -69.1 | -51.4 | 0.00 |
| -79.1 | 3.6 | 0.00 | | -69.1 | -46.4 | 0.00 |
| -79.1 | 8.6 | 0.00 | | -69.1 | -41.4 | 0.00 |

Table E-2(c) Continued

| Longitudinal position relative to the pier (cm) | Transverse position relative to the pier (cm) | Scour depth (cm) | | Longitudinal position relative to the pier (cm) | Transverse position relative to the pier (cm) | Scour depth (cm) |
|---|---|---|---|---|---|---|
| -69.1 | -36.4 | 0.00 | | -64.1 | 38.6 | 0.00 |
| -69.1 | -31.4 | 0.00 | | -64.1 | 43.6 | 0.00 |
| -69.1 | -26.4 | 0.00 | | -64.1 | 48.6 | 0.00 |
| -69.1 | -21.4 | 0.00 | | -64.1 | 53.6 | 0.00 |
| -69.1 | -16.4 | 0.00 | | -64.1 | 58.6 | 0.00 |
| -69.1 | -11.4 | 0.00 | | -59.1 | -61.4 | 0.00 |
| -69.1 | -6.4 | 0.00 | | -59.1 | -56.4 | 0.00 |
| -69.1 | -1.4 | 0.00 | | -59.1 | -51.4 | 0.00 |
| -69.1 | 3.6 | 0.00 | | -59.1 | -46.4 | 0.00 |
| -69.1 | 8.6 | 0.00 | | -59.1 | -41.4 | 0.00 |
| -69.1 | 13.6 | 0.00 | | -59.1 | -36.4 | 0.00 |
| -69.1 | 18.6 | 0.00 | | -59.1 | -31.4 | 0.00 |
| -69.1 | 23.6 | 0.00 | | -59.1 | -26.4 | 0.00 |
| -69.1 | 28.6 | 0.00 | | -59.1 | -21.4 | 0.00 |
| -69.1 | 33.6 | 0.00 | | -59.1 | -16.4 | 0.00 |
| -69.1 | 38.6 | 0.00 | | -59.1 | -11.4 | 0.00 |
| -69.1 | 43.6 | 0.00 | | -59.1 | -6.4 | 0.00 |
| -69.1 | 48.6 | 0.00 | | -59.1 | -1.4 | 0.00 |
| -69.1 | 53.6 | 0.00 | | -59.1 | 3.6 | 0.00 |
| -69.1 | 58.6 | 0.00 | | -59.1 | 8.6 | 0.00 |
| -64.1 | -61.4 | 0.00 | | -59.1 | 13.6 | 0.00 |
| -64.1 | -56.4 | 0.00 | | -59.1 | 18.6 | 0.00 |
| -64.1 | -51.4 | 0.00 | | -59.1 | 23.6 | 0.00 |
| -64.1 | -46.4 | 0.00 | | -59.1 | 28.6 | 0.00 |
| -64.1 | -41.4 | 0.00 | | -59.1 | 33.6 | 0.00 |
| -64.1 | -36.4 | 0.00 | | -59.1 | 38.6 | 0.00 |
| -64.1 | -31.4 | 0.00 | | -59.1 | 43.6 | 0.00 |
| -64.1 | -26.4 | 0.00 | | -59.1 | 48.6 | 0.00 |
| -64.1 | -21.4 | 0.00 | | -59.1 | 53.6 | 0.00 |
| -64.1 | -16.4 | 0.00 | | -59.1 | 58.6 | 0.00 |
| -64.1 | -11.4 | 0.00 | | -54.1 | -61.4 | 0.00 |
| -64.1 | -6.4 | 0.00 | | -54.1 | -56.4 | 0.00 |
| -64.1 | -1.4 | 0.00 | | -54.1 | -51.4 | 0.00 |
| -64.1 | 3.6 | 0.00 | | -54.1 | -46.4 | 0.00 |
| -64.1 | 8.6 | 0.00 | | -54.1 | -41.4 | 0.00 |
| -64.1 | 13.6 | 0.00 | | -54.1 | -36.4 | 0.00 |
| -64.1 | 18.6 | 0.00 | | -54.1 | -31.4 | 0.00 |
| -64.1 | 23.6 | 0.00 | | -54.1 | -26.4 | 0.00 |
| -64.1 | 28.6 | 0.00 | | -54.1 | -21.4 | 0.00 |
| -64.1 | 33.6 | 0.00 | | -54.1 | -16.4 | 0.00 |

Table E-2(c) Continued

| Longitudinal position relative to the pier (cm) | Transverse position relative to the pier (cm) | Scour depth (cm) | | Longitudinal position relative to the pier (cm) | Transverse position relative to the pier (cm) | Scour depth (cm) |
|---|---|---|---|---|---|---|
| -54.1 | -16.4 | 0.00 | | -49.1 | 58.6 | 0.00 |
| -54.1 | -11.4 | 0.00 | | -44.1 | -61.4 | 0.00 |
| -54.1 | -6.4 | 0.00 | | -44.1 | -56.4 | 0.00 |
| -54.1 | -1.4 | 0.00 | | -44.1 | -51.4 | 0.00 |
| -54.1 | 3.6 | 0.00 | | -44.1 | -46.4 | 0.00 |
| -54.1 | 8.6 | 0.00 | | -44.1 | -41.4 | 0.00 |
| -54.1 | 13.6 | 0.00 | | -44.1 | -36.4 | 0.00 |
| -54.1 | 18.6 | 0.00 | | -44.1 | -31.4 | 0.00 |
| -54.1 | 23.6 | 0.00 | | -44.1 | -26.4 | 0.00 |
| -54.1 | 28.6 | 0.00 | | -44.1 | -21.4 | 0.00 |
| -54.1 | 33.6 | 0.00 | | -44.1 | -16.4 | 0.00 |
| -54.1 | 38.6 | 0.00 | | -44.1 | -11.4 | 0.00 |
| -54.1 | 43.6 | 0.00 | | -44.1 | -6.4 | 0.00 |
| -54.1 | 48.6 | 0.00 | | -44.1 | -1.4 | 0.00 |
| -54.1 | 53.6 | 0.00 | | -44.1 | 3.6 | 0.00 |
| -54.1 | 58.6 | 0.00 | | -44.1 | 8.6 | 0.00 |
| -49.1 | -61.4 | 0.00 | | -44.1 | 13.6 | 0.00 |
| -49.1 | -56.4 | 0.00 | | -44.1 | 18.6 | 0.00 |
| -49.1 | -51.4 | 0.00 | | -44.1 | 23.6 | 0.00 |
| -49.1 | -46.4 | 0.00 | | -44.1 | 28.6 | 0.00 |
| -49.1 | -41.4 | 0.00 | | -44.1 | 33.6 | 0.00 |
| -49.1 | -36.4 | 0.00 | | -44.1 | 38.6 | 0.00 |
| -49.1 | -31.4 | 0.00 | | -44.1 | 43.6 | 0.00 |
| -49.1 | -26.4 | 0.00 | | -44.1 | 48.6 | 0.00 |
| -49.1 | -21.4 | 0.00 | | -44.1 | 53.6 | 0.00 |
| -49.1 | -16.4 | 0.00 | | -44.1 | 58.6 | 0.00 |
| -49.1 | -11.4 | 0.00 | | -39.1 | -61.4 | 0.00 |
| -49.1 | -6.4 | 0.00 | | -39.1 | -56.4 | 0.00 |
| -49.1 | -1.4 | 0.00 | | -39.1 | -51.4 | 0.00 |
| -49.1 | 3.6 | 0.00 | | -39.1 | -46.4 | 0.00 |
| -49.1 | 8.6 | 0.00 | | -39.1 | -41.4 | 0.00 |
| -49.1 | 13.6 | 0.00 | | -39.1 | -36.4 | 0.00 |
| -49.1 | 18.6 | 0.00 | | -39.1 | -31.4 | 0.00 |
| -49.1 | 23.6 | 0.00 | | -39.1 | -26.4 | 0.00 |
| -49.1 | 28.6 | 0.00 | | -39.1 | -21.4 | 0.00 |
| -49.1 | 33.6 | 0.00 | | -39.1 | -16.4 | 0.00 |
| -49.1 | 38.6 | 0.00 | | -39.1 | -11.4 | 0.00 |
| -49.1 | 43.6 | 0.00 | | -39.1 | -6.4 | 0.00 |
| -49.1 | 48.6 | 0.00 | | -39.1 | -1.4 | 0.00 |
| -49.1 | 53.6 | 0.00 | | -39.1 | 3.6 | 0.00 |

Table E-2(c) Continued

| Longitudinal position relative to the pier (cm) | Transverse position relative to the pier (cm) | Scour depth (cm) | | Longitudinal position relative to the pier (cm) | Transverse position relative to the pier (cm) | Scour depth (cm) |
|---|---|---|---|---|---|---|
| -39.1 | 8.6 | 0 | | -29.1 | -46.4 | 0 |
| -39.1 | 13.6 | 0 | | -29.1 | -41.4 | 0 |
| -39.1 | 18.6 | 0 | | -29.1 | -36.4 | 0 |
| -39.1 | 23.6 | 0 | | -29.1 | -31.4 | 0 |
| -39.1 | 28.6 | 0 | | -29.1 | -26.4 | 0 |
| -39.1 | 33.6 | 0 | | -29.1 | -21.4 | 0 |
| -39.1 | 38.6 | 0 | | -29.1 | -16.4 | 0 |
| -39.1 | 43.6 | 0 | | -29.1 | -11.4 | 0 |
| -39.1 | 48.6 | 0 | | -29.1 | -6.4 | 0 |
| -39.1 | 53.6 | 0 | | -29.1 | -1.4 | 0 |
| -39.1 | 58.6 | 0 | | -29.1 | 0 | 0 |
| -34.1 | -61.4 | 0 | | -29.1 | 3.6 | 0 |
| -34.1 | -56.4 | 0 | | -29.1 | 8.6 | 0 |
| -34.1 | -51.4 | 0 | | -29.1 | 13.6 | 0 |
| -34.1 | -46.4 | 0 | | -29.1 | 18.6 | 0 |
| -34.1 | -41.4 | 0 | | -29.1 | 23.6 | 0 |
| -34.1 | -36.4 | 0 | | -29.1 | 28.6 | 0 |
| -34.1 | -31.4 | 0 | | -29.1 | 33.6 | 0 |
| -34.1 | -26.4 | 0 | | -29.1 | 38.6 | 0 |
| -34.1 | -21.4 | 0 | | -29.1 | 43.6 | 0 |
| -34.1 | -16.4 | 0 | | -29.1 | 48.6 | 0 |
| -34.1 | -11.4 | 0 | | -29.1 | 53.6 | 0 |
| -34.1 | -6.4 | 0 | | -29.1 | 58.6 | 0 |
| -34.1 | -1.4 | 0 | | -24.1 | -61.4 | 0 |
| -34.1 | 0 | 0 | | -24.1 | -56.4 | 0 |
| -34.1 | 3.6 | 0 | | -24.1 | -51.4 | 0 |
| -34.1 | 8.6 | 0 | | -24.1 | -46.4 | 0 |
| -34.1 | 13.6 | 0 | | -24.1 | -41.4 | 0 |
| -34.1 | 18.6 | 0 | | -24.1 | -36.4 | 0 |
| -34.1 | 23.6 | 0 | | -24.1 | -31.4 | 0 |
| -34.1 | 28.6 | 0 | | -24.1 | -26.4 | 0 |
| -34.1 | 33.6 | 0 | | -24.1 | -21.4 | 0 |
| -34.1 | 38.6 | 0 | | -24.1 | -16.4 | 0 |
| -34.1 | 43.6 | 0 | | -24.1 | -11.4 | 0 |
| -34.1 | 48.6 | 0 | | -24.1 | -6.4 | 0 |
| -34.1 | 53.6 | 0 | | -24.1 | -1.4 | 0 |
| -34.1 | 58.6 | 0 | | -24.1 | 0 | 0 |
| -29.1 | -61.4 | 0 | | -24.1 | 3.6 | 0 |
| -29.1 | -56.4 | 0 | | -24.1 | 8.6 | 0 |
| -29.1 | -51.4 | 0 | | -24.1 | 13.6 | 0 |

Table E-2(c) Continued

| Longitudinal position relative to the pier (cm) | Transverse position relative to the pier (cm) | Scour depth (cm) | | Longitudinal position relative to the pier (cm) | Transverse position relative to the pier (cm) | Scour depth (cm) |
|---|---|---|---|---|---|---|
| -24.1 | 18.6 | 0 | | -22.3 | 48.6 | 0 |
| -24.1 | 23.6 | 0 | | -22.3 | 53.6 | 0 |
| -24.1 | 28.6 | 0 | | -22.3 | 58.6 | 0 |
| -24.1 | 33.6 | 0 | | -19.1 | -61.4 | 0 |
| -24.1 | 38.6 | 0 | | -19.1 | -56.4 | 0 |
| -24.1 | 43.6 | 0 | | -19.1 | -51.4 | 0 |
| -24.1 | 48.6 | 0 | | -19.1 | -46.4 | 0 |
| -24.1 | 53.6 | 0 | | -19.1 | -41.4 | 0 |
| -24.1 | 58.6 | 0 | | -19.1 | -36.4 | 0 |
| -22.3 | -61.4 | 0 | | -19.1 | -31.4 | 0 |
| -22.3 | -56.4 | 0 | | -19.1 | -26.4 | 0 |
| -22.3 | -51.4 | 0 | | -19.1 | -21.4 | 0 |
| -22.3 | -46.4 | 0 | | -19.1 | -16.4 | 0 |
| -22.3 | -41.4 | 0 | | -19.1 | -11.4 | -0.01 |
| -22.3 | -36.4 | 0 | | -19.1 | -6.4 | -1.54 |
| -22.3 | -31.4 | 0 | | -19.1 | -4.4 | -1.88 |
| -22.3 | -26.4 | 0 | | -19.1 | -1.4 | -2.3 |
| -22.3 | -21.4 | 0 | | -19.1 | 0 | -2.44 |
| -22.3 | -16.4 | 0 | | -19.1 | 3.6 | -2.16 |
| -22.3 | -11.4 | 0 | | -19.1 | 8.6 | -1.24 |
| -22.3 | -6.4 | 0 | | -19.1 | 13.6 | -0.02 |
| -22.3 | -4.4 | 0 | | -19.1 | 18.6 | 0 |
| -22.3 | -3.4 | -0.02 | | -19.1 | 23.6 | 0 |
| -22.3 | -2.4 | -0.04 | | -19.1 | 28.6 | 0 |
| -22.3 | -1.4 | -0.09 | | -19.1 | 33.6 | 0 |
| -22.3 | 0 | -0.12 | | -19.1 | 38.6 | 0 |
| -22.3 | 0.6 | -0.14 | | -19.1 | 43.6 | 0 |
| -22.3 | 1.6 | -0.16 | | -19.1 | 48.6 | 0 |
| -22.3 | 2.6 | -0.14 | | -19.1 | 53.6 | 0 |
| -22.3 | 3.6 | -0.14 | | -19.1 | 58.6 | 0 |
| -22.3 | 4.6 | -0.09 | | -14.1 | -61.4 | 0 |
| -22.3 | 5.6 | -0.06 | | -14.1 | -56.4 | 0 |
| -22.3 | 8.6 | -0.02 | | -14.1 | -51.4 | 0 |
| -22.3 | 13.6 | 0 | | -14.1 | -46.4 | 0 |
| -22.3 | 18.6 | 0 | | -14.1 | -41.4 | 0 |
| -22.3 | 23.6 | 0 | | -14.1 | -36.4 | 0 |
| -22.3 | 28.6 | 0 | | -14.1 | -31.4 | 0 |
| -22.3 | 33.6 | 0 | | -14.1 | -26.4 | 0 |
| -22.3 | 38.6 | 0 | | -14.1 | -21.4 | 0 |
| -22.3 | 43.6 | 0 | | -14.1 | -17.9 | 0 |

Table E-2(c) Continued

| Longitudinal position relative to the pier (cm) | Transverse position relative to the pier (cm) | Scour depth (cm) | | Longitudinal position relative to the pier (cm) | Transverse position relative to the pier (cm) | Scour depth (cm) |
|---|---|---|---|---|---|---|
| -14.1 | -16.4 | -0.54 | | -9.1 | 31.6 | -0.02 |
| -14.1 | -11.4 | -2.84 | | -9.1 | 33.6 | 0 |
| -14.1 | -6.4 | -4.04 | | -9.1 | 38.6 | 0 |
| -14.1 | -1.4 | -4.24 | | -9.1 | 43.6 | 0 |
| -14.1 | 0 | -4.3 | | -9.1 | 48.6 | 0 |
| -14.1 | 3.6 | -4.4 | | -9.1 | 53.6 | 0 |
| -14.1 | 8.6 | -3.96 | | -9.1 | 58.6 | 0 |
| -14.1 | 11.6 | -2.94 | | -4.1 | -61.4 | 0 |
| -14.1 | 13.6 | -2.04 | | -4.1 | -56.4 | 0 |
| -14.1 | 18.6 | -0.76 | | -4.1 | -51.4 | 0 |
| -14.1 | 23.6 | -0.06 | | -4.1 | -46.4 | 0 |
| -14.1 | 25.6 | -0.02 | | -4.1 | -41.4 | 0 |
| -14.1 | 28.6 | 0 | | -4.1 | -36.4 | 0 |
| -14.1 | 33.6 | 0 | | -4.1 | -31.4 | 0 |
| -14.1 | 38.6 | 0 | | -4.1 | -26.4 | -0.04 |
| -14.1 | 43.6 | 0 | | -4.1 | -21.4 | -1.94 |
| -14.1 | 48.6 | 0 | | -4.1 | -16.4 | -2.44 |
| -14.1 | 53.6 | 0 | | -4.1 | -14.4 | -1.54 |
| -14.1 | 58.6 | 0 | | -4.1 | -13.4 | -1.14 |
| -9.1 | -61.4 | 0 | | -4.1 | -12.4 | -0.84 |
| -9.1 | -56.4 | 0 | | -4.1 | -11.4 | -0.3 |
| -9.1 | -51.4 | 0 | | -4.1 | -6.4 | 0 |
| -9.1 | -46.4 | 0 | | -4.1 | -4.9 | 0 |
| -9.1 | -41.4 | 0 | | -4.1 | 4.1 | 0 |
| -9.1 | -36.4 | 0 | | -4.1 | 8.6 | 0 |
| -9.1 | -31.4 | 0 | | -4.1 | 10.1 | -0.42 |
| -9.1 | -26.4 | 0 | | -4.1 | 13.6 | -1.04 |
| -9.1 | -23.4 | -0.1 | | -4.1 | 18.6 | -2.04 |
| -9.1 | -21.4 | -1.24 | | -4.1 | 21.1 | -1.16 |
| -9.1 | -16.4 | -2.24 | | -4.1 | 23.6 | -1.98 |
| -9.1 | -11.4 | -2.22 | | -4.1 | 28.6 | -1.54 |
| -9.1 | -6.4 | -1.5 | | -4.1 | 33.6 | -1.04 |
| -9.1 | -1.4 | -1.34 | | -4.1 | 35.1 | -0.04 |
| -9.1 | 0 | -1.44 | | -4.1 | 38.6 | 0 |
| -9.1 | 3.6 | -1.74 | | -4.1 | 43.6 | 0 |
| -9.1 | 8.6 | -2.12 | | -4.1 | 48.6 | 0 |
| -9.1 | 13.6 | -3.1 | | -4.1 | 53.6 | 0 |
| -9.1 | 18.6 | -1.48 | | -4.1 | 58.6 | 0 |
| -9.1 | 23.6 | -2.14 | | 0 | -61.4 | 0 |
| -9.1 | 28.6 | -0.66 | | 0 | -56.4 | 0 |

Table E-2(c) Continued

| Longitudinal position relative to the pier (cm) | Transverse position relative to the pier (cm) | Scour depth (cm) | | Longitudinal position relative to the pier (cm) | Transverse position relative to the pier (cm) | Scour depth (cm) |
|---|---|---|---|---|---|---|
| 0 | -51.4 | 0 | | 0.9 | -14.4 | -2.04 |
| 0 | -46.4 | 0 | | 0.9 | -12.4 | -1.04 |
| 0 | -41.4 | 0 | | 0.9 | -11.4 | -0.2 |
| 0 | -36.4 | 0 | | 0.9 | -6.4 | 0 |
| 0 | -31.4 | 0 | | 0.9 | 6.6 | 0 |
| 0 | -27.9 | -0.1 | | 0.9 | 8.6 | 0 |
| 0 | -26.4 | -0.44 | | 0.9 | 12.1 | -1.74 |
| 0 | -21.4 | -1.24 | | 0.9 | 13.6 | -1.04 |
| 0 | -16.4 | -2.64 | | 0.9 | 15.6 | -0.74 |
| 0 | -16.4 | -1.44 | | 0.9 | 18.6 | -1.64 |
| 0 | -14.4 | -2.04 | | 0.9 | 23.6 | -1.14 |
| 0 | -12.4 | -1.04 | | 0.9 | 28.6 | -3.64 |
| 0 | -11.4 | -0.2 | | 0.9 | 33.6 | -2.46 |
| 0 | -6.4 | 0 | | 0.9 | 38.6 | -0.02 |
| 0 | 6.6 | 0 | | 0.9 | 43.6 | 0 |
| 0 | 8.6 | 0 | | 0.9 | 48.6 | 0 |
| 0 | 12.1 | -1.74 | | 0.9 | 53.6 | 0 |
| 0 | 13.6 | -1.04 | | 0.9 | 58.6 | 0 |
| 0 | 15.6 | -0.74 | | 5.9 | -61.4 | 0 |
| 0 | 18.6 | -1.64 | | 5.9 | -56.4 | 0 |
| 0 | 23.6 | -1.14 | | 5.9 | -51.4 | 0 |
| 0 | 28.6 | -3.64 | | 5.9 | -46.4 | 0 |
| 0 | 33.6 | -2.46 | | 5.9 | -41.4 | 0 |
| 0 | 38.6 | -0.02 | | 5.9 | -36.4 | -1.44 |
| 0 | 43.6 | 0 | | 5.9 | -31.4 | -2.54 |
| 0 | 48.6 | 0 | | 5.9 | -26.4 | -3.04 |
| 0 | 53.6 | 0 | | 5.9 | -21.4 | -2.44 |
| 0 | 58.6 | 0 | | 5.9 | -16.4 | -1.54 |
| 0.9 | -61.4 | 0 | | 5.9 | -11.4 | -1.24 |
| 0.9 | -56.4 | 0 | | 5.9 | -6.4 | 0 |
| 0.9 | -51.4 | 0 | | 5.9 | -2.4 | 0 |
| 0.9 | -46.4 | 0 | | 5.9 | 3.6 | 0 |
| 0.9 | -41.4 | 0 | | 5.9 | 8.6 | 0 |
| 0.9 | -36.4 | 0 | | 5.9 | 13.6 | -1.94 |
| 0.9 | -31.4 | 0 | | 5.9 | 16.6 | -0.9 |
| 0.9 | -27.9 | -0.1 | | 5.9 | 18.6 | -1.74 |
| 0.9 | -26.4 | -0.44 | | 5.9 | 23.6 | -2.74 |
| 0.9 | -21.4 | -1.24 | | 5.9 | 28.6 | -4.28 |
| 0.9 | -16.4 | -2.64 | | 5.9 | 33.6 | -3.44 |
| 0.9 | -16.4 | -1.44 | | 5.9 | 38.6 | -1.44 |

Table E-2(c) Continued

| Longitudinal position relative to the pier (cm) | Transverse position relative to the pier (cm) | Scour depth (cm) | | Longitudinal position relative to the pier (cm) | Transverse position relative to the pier (cm) | Scour depth (cm) |
|---|---|---|---|---|---|---|
| 5.9 | 41.6 | -0.02 | | 15.9 | -31.4 | -5.04 |
| 5.9 | 43.6 | 0 | | 15.9 | -26.4 | -5.84 |
| 5.9 | 48.6 | 0 | | 15.9 | -21.4 | -5.64 |
| 5.9 | 53.6 | 0 | | 15.9 | -16.4 | -4.64 |
| 5.9 | 58.6 | 0 | | 15.9 | -11.4 | -2.64 |
| 10.9 | -61.4 | 0 | | 15.9 | -6.4 | -1.04 |
| 10.9 | -56.4 | 0 | | 15.9 | -1.4 | -0.54 |
| 10.9 | -51.4 | 0 | | 15.9 | 0 | -0.34 |
| 10.9 | -48.4 | -0.05 | | 15.9 | 3.6 | -0.64 |
| 10.9 | -46.4 | -0.84 | | 15.9 | 8.6 | -1.14 |
| 10.9 | -41.4 | -2.44 | | 15.9 | 13.6 | -2.34 |
| 10.9 | -36.4 | -3.44 | | 15.9 | 18.6 | -4.94 |
| 10.9 | -31.4 | -4.14 | | 15.9 | 23.6 | -5.14 |
| 10.9 | -26.4 | -4.44 | | 15.9 | 28.6 | -4.54 |
| 10.9 | -21.4 | -4.58 | | 15.9 | 33.6 | -1.64 |
| 10.9 | -16.4 | -3.44 | | 15.9 | 38.6 | -1.04 |
| 10.9 | -11.4 | -2.1 | | 15.9 | 43.6 | -0.14 |
| 10.9 | -6.4 | 0 | | 15.9 | 48.6 | 0 |
| 10.9 | -1.4 | 0 | | 15.9 | 53.6 | 0 |
| 10.9 | 0 | 0 | | 15.9 | 58.6 | 0 |
| 10.9 | 3.6 | 0 | | 20.9 | -61.4 | 0 |
| 10.9 | 7.6 | 0 | | 20.9 | -56.4 | 0 |
| 10.9 | 8.6 | -0.24 | | 20.9 | -55.4 | -0.16 |
| 10.9 | 13.6 | -1.84 | | 20.9 | -51.4 | -2 |
| 10.9 | 18.6 | -3.74 | | 20.9 | -46.4 | -3.24 |
| 10.9 | 23.6 | -4.04 | | 20.9 | -41.4 | -4.04 |
| 10.9 | 28.6 | -5.34 | | 20.9 | -36.4 | -4.64 |
| 10.9 | 33.6 | -3.24 | | 20.9 | -31.4 | -5.14 |
| 10.9 | 38.6 | -1.54 | | 20.9 | -26.4 | -6.04 |
| 10.9 | 43.6 | -0.02 | | 20.9 | -21.4 | -6.24 |
| 10.9 | 48.6 | 0 | | 20.9 | -16.4 | -5.24 |
| 10.9 | 53.6 | 0 | | 20.9 | -11.4 | -2.54 |
| 10.9 | 58.6 | 0 | | 20.9 | -6.4 | -0.74 |
| 15.9 | -61.4 | 0 | | 20.9 | -1.4 | -0.14 |
| 15.9 | -56.4 | 0 | | 20.9 | 0 | -0.16 |
| 15.9 | -52.9 | -0.2 | | 20.9 | 3.6 | -0.24 |
| 15.9 | -51.4 | -0.94 | | 20.9 | 8.6 | -0.64 |
| 15.9 | -46.4 | -2.74 | | 20.9 | 13.6 | -3.24 |
| 15.9 | -41.4 | -3.64 | | 20.9 | 18.6 | -5.24 |
| 15.9 | -36.4 | -4.34 | | 20.9 | 23.6 | -5.64 |

Table E-2(c) Continued

| Longitudinal position relative to the pier (cm) | Transverse position relative to the pier (cm) | Scour depth (cm) | | Longitudinal position relative to the pier (cm) | Transverse position relative to the pier (cm) | Scour depth (cm) |
|---|---|---|---|---|---|---|
| 20.9 | 28.6 | -2.92 | | 30.9 | -31.4 | -4.84 |
| 20.9 | 33.6 | -2.84 | | 30.9 | -26.4 | -4.44 |
| 20.9 | 38.6 | -1.24 | | 30.9 | -21.4 | -4.64 |
| 20.9 | 43.6 | -1.04 | | 30.9 | -16.4 | -3.94 |
| 20.9 | 47.6 | -0.24 | | 30.9 | -11.4 | -1.84 |
| 20.9 | 48.6 | 0 | | 30.9 | -6.4 | -0.04 |
| 20.9 | 53.6 | 0 | | 30.9 | -1.4 | -0.05 |
| 20.9 | 58.6 | 0 | | 30.9 | 0 | -0.04 |
| 25.9 | -61.4 | 0 | | 30.9 | 3.6 | 0.06 |
| 25.9 | -56.4 | -0.04 | | 30.9 | 8.6 | 0.56 |
| 25.9 | -51.4 | -1.24 | | 30.9 | 13.6 | -2.04 |
| 25.9 | -46.4 | -3.04 | | 30.9 | 18.6 | -3.64 |
| 25.9 | -41.4 | -3.74 | | 30.9 | 23.6 | -3.54 |
| 25.9 | -36.4 | -4.24 | | 30.9 | 28.6 | -3.24 |
| 25.9 | -31.4 | -4.74 | | 30.9 | 33.6 | -3.04 |
| 25.9 | -26.4 | -5.24 | | 30.9 | 38.6 | -2.24 |
| 25.9 | -21.4 | -5.84 | | 30.9 | 43.6 | -1.54 |
| 25.9 | -16.4 | -4.84 | | 30.9 | 48.6 | -0.24 |
| 25.9 | -11.4 | -2.34 | | 30.9 | 53.6 | 0 |
| 25.9 | -6.4 | -0.54 | | 30.9 | 58.6 | 0 |
| 25.9 | -1.4 | -0.16 | | 35.9 | -61.4 | 0 |
| 25.9 | 0 | -0.04 | | 35.9 | -56.4 | -0.02 |
| 25.9 | 3.6 | 0.16 | | 35.9 | -51.4 | -0.34 |
| 25.9 | 8.6 | -0.14 | | 35.9 | -46.4 | -0.14 |
| 25.9 | 13.6 | -2.9 | | 35.9 | -41.4 | -1.64 |
| 25.9 | 18.6 | -4.34 | | 35.9 | -36.4 | -2.94 |
| 25.9 | 23.6 | -5.14 | | 35.9 | -31.4 | -4.64 |
| 25.9 | 28.6 | -4.04 | | 35.9 | -26.4 | -4.84 |
| 25.9 | 33.6 | -3.44 | | 35.9 | -21.4 | -3.44 |
| 25.9 | 38.6 | -2.74 | | 35.9 | -16.4 | -2.94 |
| 25.9 | 43.6 | -1.94 | | 35.9 | -11.4 | -1.34 |
| 25.9 | 48.6 | -0.04 | | 35.9 | -6.4 | -0.04 |
| 25.9 | 53.6 | 0 | | 35.9 | -3.9 | -0.34 |
| 25.9 | 58.6 | 0 | | 35.9 | -1.4 | -0.02 |
| 30.9 | -61.4 | 0 | | 35.9 | 0 | 0.16 |
| 30.9 | -56.4 | 0 | | 35.9 | 3.6 | -0.24 |
| 30.9 | -51.4 | 0.16 | | 35.9 | 8.6 | -0.14 |
| 30.9 | -46.4 | -1.64 | | 35.9 | 13.6 | -1.84 |
| 30.9 | -41.4 | -2.74 | | 35.9 | 18.6 | -2.64 |
| 30.9 | -36.4 | -3.54 | | 35.9 | 23.6 | -3.44 |

Table E-2(c) Continued

| Longitudinal position relative to the pier (cm) | Transverse position relative to the pier (cm) | Scour depth (cm) | | Longitudinal position relative to the pier (cm) | Transverse position relative to the pier (cm) | Scour depth (cm) |
|---|---|---|---|---|---|---|
| 35.9 | 28.6 | -3.84 | | 45.9 | -26.4 | -4.24 |
| 35.9 | 33.6 | -3.54 | | 45.9 | -21.4 | -4.94 |
| 35.9 | 38.6 | -1.64 | | 45.9 | -16.4 | -3.04 |
| 35.9 | 43.6 | -0.24 | | 45.9 | -11.4 | -1.14 |
| 35.9 | 48.6 | -0.02 | | 45.9 | -6.4 | -1.04 |
| 35.9 | 53.6 | 0 | | 45.9 | -1.4 | 0.16 |
| 35.9 | 58.6 | 0 | | 45.9 | 0 | 0.36 |
| 40.9 | -61.4 | 0 | | 45.9 | 2.1 | 1.36 |
| 40.9 | -56.4 | -0.54 | | 45.9 | 3.6 | 0.96 |
| 40.9 | -51.4 | -1.84 | | 45.9 | 8.6 | -1.04 |
| 40.9 | -46.4 | -0.74 | | 45.9 | 13.6 | -1.64 |
| 40.9 | -41.4 | -0.64 | | 45.9 | 18.6 | -1.94 |
| 40.9 | -36.4 | -3.24 | | 45.9 | 23.6 | -2.74 |
| 40.9 | -31.4 | -3.64 | | 45.9 | 28.6 | -1.44 |
| 40.9 | -26.4 | -4.24 | | 45.9 | 33.6 | 0.56 |
| 40.9 | -21.4 | -3.04 | | 45.9 | 38.6 | 0.96 |
| 40.9 | -16.4 | -2.24 | | 45.9 | 43.6 | 0.46 |
| 40.9 | -11.4 | -1.14 | | 45.9 | 48.6 | -0.84 |
| 40.9 | -6.4 | -0.58 | | 45.9 | 53.6 | -1.64 |
| 40.9 | -1.4 | -0.02 | | 45.9 | 58.6 | -0.44 |
| 40.9 | 0 | 0.46 | | 50.9 | -61.4 | -0.14 |
| 40.9 | 3.6 | 0.06 | | 50.9 | -56.4 | -1.44 |
| 40.9 | 8.6 | -1.44 | | 50.9 | -51.4 | -1.84 |
| 40.9 | 13.6 | -1.74 | | 50.9 | -46.4 | -0.84 |
| 40.9 | 18.6 | -1.34 | | 50.9 | -41.4 | -1.94 |
| 40.9 | 23.6 | -2.44 | | 50.9 | -36.4 | -1.64 |
| 40.9 | 28.6 | -3.84 | | 50.9 | -31.4 | -2.84 |
| 40.9 | 33.6 | -1.54 | | 50.9 | -26.4 | -4.34 |
| 40.9 | 38.6 | 0.26 | | 50.9 | -21.4 | -4.14 |
| 40.9 | 43.6 | 0.46 | | 50.9 | -16.4 | -3.74 |
| 40.9 | 48.6 | 0 | | 50.9 | -11.4 | -2.14 |
| 40.9 | 53.6 | 0 | | 50.9 | -6.4 | -0.68 |
| 40.9 | 58.6 | 0 | | 50.9 | -1.4 | 1.06 |
| 45.9 | -61.4 | 0 | | 50.9 | 0 | 0.98 |
| 45.9 | -56.4 | -1.54 | | 50.9 | 3.6 | 0.46 |
| 45.9 | -51.4 | -2.24 | | 50.9 | 8.6 | -0.26 |
| 45.9 | -46.4 | -1.54 | | 50.9 | 13.6 | -2.24 |
| 45.9 | -41.4 | -1.04 | | 50.9 | 18.6 | -1.34 |
| 45.9 | -36.4 | -1.24 | | 50.9 | 23.6 | -1.54 |
| 45.9 | -31.4 | -1.16 | | 50.9 | 28.6 | -0.64 |

Table E-2(c) Continued

| Longitudinal position relative to the pier (cm) | Transverse position relative to the pier (cm) | Scour depth (cm) | | Longitudinal position relative to the pier (cm) | Transverse position relative to the pier (cm) | Scour depth (cm) |
|---|---|---|---|---|---|---|
| 45.9 | -26.4 | -4.24 | | 50.9 | 33.6 | -0.34 |
| 45.9 | -21.4 | -4.94 | | 50.9 | 38.6 | -0.35 |
| 45.9 | -16.4 | -3.04 | | 50.9 | 43.6 | -1.66 |
| 45.9 | -11.4 | -1.14 | | 50.9 | 48.6 | -2.64 |
| 45.9 | -6.4 | -1.04 | | 50.9 | 53.6 | -2.9 |
| 45.9 | -1.4 | 0.16 | | 50.9 | 58.6 | -2.34 |
| 45.9 | 0 | 0.36 | | 55.9 | -61.4 | -0.44 |
| 45.9 | 2.1 | 1.36 | | 55.9 | -56.4 | -2.54 |
| 45.9 | 3.6 | 0.96 | | 55.9 | -51.4 | -2.46 |
| 45.9 | 8.6 | -1.04 | | 55.9 | -46.4 | -2.04 |
| 45.9 | 13.6 | -1.64 | | 55.9 | -41.4 | -0.64 |
| 45.9 | 18.6 | -1.94 | | 55.9 | -36.4 | -0.94 |
| 45.9 | 23.6 | -2.74 | | 55.9 | -31.4 | -2.14 |
| 45.9 | 28.6 | -1.44 | | 55.9 | -26.4 | -1.84 |
| 45.9 | 33.6 | 0.56 | | 55.9 | -21.4 | -1.74 |
| 45.9 | 38.6 | 0.96 | | 55.9 | -16.4 | -2.54 |
| 45.9 | 43.6 | 0.46 | | 55.9 | -11.4 | -1.24 |
| 45.9 | 48.6 | -0.84 | | 55.9 | -6.4 | 0.36 |
| 45.9 | 53.6 | -1.64 | | 55.9 | -1.4 | 2.26 |
| 45.9 | 58.6 | -0.44 | | 55.9 | 0 | 1.98 |
| 50.9 | -61.4 | -0.14 | | 55.9 | 3.6 | 0.86 |
| 50.9 | -56.4 | -1.44 | | 55.9 | 8.6 | -1.24 |
| 50.9 | -51.4 | -1.84 | | 55.9 | 13.6 | -1.02 |
| 50.9 | -46.4 | -0.84 | | 55.9 | 18.6 | -0.04 |
| 50.9 | -41.4 | -1.94 | | 55.9 | 23.6 | -1.94 |
| 50.9 | -36.4 | -1.64 | | 55.9 | 28.6 | -1.04 |
| 50.9 | -31.4 | -2.84 | | 55.9 | 33.6 | -0.74 |
| 50.9 | -26.4 | -4.34 | | 55.9 | 38.6 | -1.34 |
| 50.9 | -21.4 | -4.14 | | 55.9 | 43.6 | -2.94 |
| 50.9 | -16.4 | -3.74 | | 55.9 | 48.6 | -3.54 |
| 50.9 | -11.4 | -2.14 | | 55.9 | 53.6 | -2.74 |
| 50.9 | -6.4 | -0.68 | | 55.9 | 58.6 | -1.14 |
| 50.9 | -1.4 | 1.06 | | 65.9 | -61.4 | -1.84 |
| 50.9 | 0 | 0.98 | | 65.9 | -56.4 | -1.44 |
| 50.9 | 3.6 | 0.46 | | 65.9 | -51.4 | -0.44 |
| 50.9 | 8.6 | -0.26 | | 65.9 | -46.4 | -0.84 |
| 50.9 | 13.6 | -2.24 | | 65.9 | -41.4 | -1.44 |
| 50.9 | 18.6 | -1.34 | | 65.9 | -36.4 | -0.94 |
| 50.9 | 23.6 | -1.54 | | 65.9 | -31.4 | -1.84 |
| 50.9 | 28.6 | -0.64 | | 65.9 | -26.4 | -2.64 |

Table E-2(c) Continued

| Longitudinal position relative to the pier (cm) | Transverse position relative to the pier (cm) | Scour depth (cm) | | Longitudinal position relative to the pier (cm) | Transverse position relative to the pier (cm) | Scour depth (cm) |
|---|---|---|---|---|---|---|
| 65.9 | -26.4 | -2.64 | | 75.9 | 38.6 | -1.4 |
| 65.9 | -21.4 | -3.04 | | 75.9 | 43.6 | -0.94 |
| 65.9 | -16.4 | -2.04 | | 75.9 | 48.6 | -1.64 |
| 65.9 | -11.4 | 0.66 | | 75.9 | 53.6 | -1.94 |
| 65.9 | -6.4 | 2.56 | | 75.9 | 58.6 | -0.24 |
| 65.9 | -1.4 | 2.96 | | 85.9 | -61.4 | -1.34 |
| 65.9 | 0 | 2.76 | | 85.9 | -56.4 | -0.84 |
| 65.9 | 3.6 | 2.06 | | 85.9 | -51.4 | -0.04 |
| 65.9 | 8.6 | 1.96 | | 85.9 | -46.4 | -0.64 |
| 65.9 | 13.6 | 1.76 | | 85.9 | -41.4 | -1.84 |
| 65.9 | 18.6 | -0.44 | | 85.9 | -36.4 | -2.04 |
| 65.9 | 23.6 | -0.74 | | 85.9 | -31.4 | -2.24 |
| 65.9 | 28.6 | -0.84 | | 85.9 | -26.4 | -1.24 |
| 65.9 | 33.6 | -0.34 | | 85.9 | -21.4 | 0.56 |
| 65.9 | 38.6 | -1.74 | | 85.9 | -16.4 | 1.72 |
| 65.9 | 43.6 | -3.04 | | 85.9 | -11.4 | 2.46 |
| 65.9 | 48.6 | -1.92 | | 85.9 | -6.4 | 2.96 |
| 65.9 | 53.6 | -1.84 | | 85.9 | -1.4 | 2.74 |
| 65.9 | 58.6 | -3.14 | | 85.9 | 0 | 2.76 |
| 75.9 | -61.4 | -1.44 | | 85.9 | 3.6 | 3.26 |
| 75.9 | -56.4 | -1.04 | | 85.9 | 8.6 | 2.56 |
| 75.9 | -51.4 | -0.84 | | 85.9 | 13.6 | 2.1 |
| 75.9 | -46.4 | -1.46 | | 85.9 | 18.6 | 1.66 |
| 75.9 | -41.4 | -0.74 | | 85.9 | 23.6 | 0.46 |
| 75.9 | -36.4 | -1.26 | | 85.9 | 28.6 | 0.08 |
| 75.9 | -31.4 | -1.04 | | 85.9 | 33.6 | -1.44 |
| 75.9 | -26.4 | -1.54 | | 85.9 | 38.6 | -1.64 |
| 75.9 | -21.4 | -1.34 | | 85.9 | 43.6 | -1.24 |
| 75.9 | -16.4 | -0.84 | | 85.9 | 48.6 | -2.64 |
| 75.9 | -11.4 | 0.56 | | 85.9 | 53.6 | -2.04 |
| 75.9 | -6.4 | 2.56 | | 85.9 | 58.6 | -1.14 |
| 75.9 | -1.4 | 2.52 | | 95.9 | -61.4 | -0.44 |
| 75.9 | 0 | 3.56 | | 95.9 | -56.4 | -1.94 |
| 75.9 | 3.6 | 3.7 | | 95.9 | -51.4 | -0.14 |
| 75.9 | 8.6 | 3.16 | | 95.9 | -46.4 | 0.06 |
| 75.9 | 13.6 | 2.56 | | 95.9 | -41.4 | -0.94 |
| 75.9 | 18.6 | 1.26 | | 95.9 | -36.4 | -0.78 |
| 75.9 | 23.6 | 0.86 | | 95.9 | -31.4 | -2.14 |
| 75.9 | 28.6 | -1.44 | | 95.9 | -26.4 | -2.04 |
| 75.9 | 33.6 | -0.88 | | 95.9 | -21.4 | -0.04 |

Table E-2(c) Continued

| Longitudinal position relative to the pier (cm) | Transverse position relative to the pier (cm) | Scour depth (cm) | | Longitudinal position relative to the pier (cm) | Transverse position relative to the pier (cm) | Scour depth (cm) |
|---|---|---|---|---|---|---|
| 95.9 | -16.4 | 2.06 | | 105.9 | 48.6 | 0.66 |
| 95.9 | -11.4 | 3.36 | | 105.9 | 53.6 | 2.96 |
| 95.9 | -6.4 | 3.46 | | 105.9 | 58.6 | 2.66 |
| 95.9 | -1.4 | 2.42 | | 115.9 | -61.4 | -0.64 |
| 95.9 | 0 | 2.56 | | 115.9 | -56.4 | -0.94 |
| 95.9 | 3.6 | 2.56 | | 115.9 | -51.4 | 0.56 |
| 95.9 | 8.6 | 2.14 | | 115.9 | -46.4 | -1.14 |
| 95.9 | 13.6 | 2.26 | | 115.9 | -41.4 | -2.24 |
| 95.9 | 18.6 | 1.96 | | 115.9 | -36.4 | -0.84 |
| 95.9 | 23.6 | 1.36 | | 115.9 | -31.4 | -0.24 |
| 95.9 | 28.6 | -1.14 | | 115.9 | -26.4 | 0.56 |
| 95.9 | 33.6 | -1.04 | | 115.9 | -21.4 | 2.66 |
| 95.9 | 38.6 | -0.74 | | 115.9 | -16.4 | 4.06 |
| 95.9 | 43.6 | 0.4 | | 115.9 | -11.4 | 5.56 |
| 95.9 | 48.6 | 0.36 | | 115.9 | -6.4 | 5.76 |
| 95.9 | 53.6 | 1.34 | | 115.9 | -1.4 | 4.66 |
| 95.9 | 58.6 | 0.66 | | 115.9 | 0 | 4.46 |
| 105.9 | -61.4 | -2.14 | | 115.9 | 3.6 | 4.56 |
| 105.9 | -56.4 | -1.14 | | 115.9 | 8.6 | 3.6 |
| 105.9 | -51.4 | -0.78 | | 115.9 | 13.6 | 1.96 |
| 105.9 | -46.4 | -0.94 | | 115.9 | 18.6 | -0.46 |
| 105.9 | -41.4 | -0.74 | | 115.9 | 23.6 | -1.74 |
| 105.9 | -36.4 | -1.64 | | 115.9 | 28.6 | -0.04 |
| 105.9 | -31.4 | -0.54 | | 115.9 | 33.6 | 0.76 |
| 105.9 | -26.4 | 1.16 | | 115.9 | 38.6 | 0.16 |
| 105.9 | -21.4 | 1.66 | | 115.9 | 43.6 | 0.38 |
| 105.9 | -16.4 | 3.16 | | 115.9 | 48.6 | 0.52 |
| 105.9 | -11.4 | 3.76 | | 115.9 | 53.6 | 1.56 |
| 105.9 | -6.4 | 4.76 | | 115.9 | 58.6 | 0 |
| 105.9 | -1.4 | 4.92 | | 125.9 | -61.4 | -0.14 |
| 105.9 | 0 | 4.76 | | 125.9 | -56.4 | 0.06 |
| 105.9 | 3.6 | 4.36 | | 125.9 | -51.4 | -0.54 |
| 105.9 | 8.6 | 2.36 | | 125.9 | -46.4 | -2.24 |
| 105.9 | 13.6 | 1.66 | | 125.9 | -41.4 | -1.04 |
| 105.9 | 18.6 | 0.96 | | 125.9 | -36.4 | -0.14 |
| 105.9 | 23.6 | 0.22 | | 125.9 | -31.4 | 0.02 |
| 105.9 | 28.6 | 1.16 | | 125.9 | -26.4 | 0.22 |
| 105.9 | 33.6 | 0.36 | | 125.9 | -21.4 | 0.96 |
| 105.9 | 38.6 | -1.02 | | 125.9 | -16.4 | 1.46 |
| 105.9 | 43.6 | -1.04 | | 125.9 | -11.4 | 3.36 |

Table E-2(c) Continued

| Longitudinal position relative to the pier (cm) | Transverse position relative to the pier (cm) | Scour depth (cm) |
|---|---|---|
| 125.9 | -6.4 | 3.96 |
| 125.9 | -1.4 | 4.46 |
| 125.9 | 0 | 4.56 |
| 125.9 | 3.6 | 3.86 |
| 125.9 | 8.6 | 2.66 |
| 125.9 | 13.6 | 1.94 |
| 125.9 | 18.6 | 1.36 |
| 125.9 | 23.6 | 0.96 |
| 125.9 | 28.6 | 0.26 |
| 125.9 | 33.6 | 0.56 |
| 125.9 | 38.6 | 0.16 |
| 125.9 | 43.6 | 0.34 |
| 125.9 | 48.6 | -0.24 |
| 125.9 | 53.6 | 0.36 |
| 125.9 | 58.6 | 0.16 |
| 135.9 | -61.4 | -0.04 |
| 135.9 | -56.4 | 0 |
| 135.9 | -51.4 | 0.56 |
| 135.9 | -46.4 | -0.84 |
| 135.9 | -41.4 | -0.24 |
| 135.9 | -36.4 | 0.76 |
| 135.9 | -31.4 | 1.96 |
| 135.9 | -26.4 | 1.98 |
| 135.9 | -21.4 | 3.46 |
| 135.9 | -16.4 | 3.56 |
| 135.9 | -11.4 | 4.66 |
| 135.9 | -6.4 | 5.46 |
| 135.9 | -1.4 | 5.66 |
| 135.9 | 0 | 5.16 |
| 135.9 | 3.6 | 3.86 |
| 135.9 | 8.6 | 3.46 |
| 135.9 | 13.6 | 2.76 |
| 135.9 | 18.6 | 1.66 |
| 135.9 | 28.6 | 0.66 |
| 135.9 | 33.6 | -0.24 |
| 135.9 | 38.6 | -0.14 |
| 135.9 | 43.6 | -0.12 |
| 135.9 | 48.6 | -0.06 |
| 135.9 | 53.6 | -0.64 |
| 135.9 | 58.6 | 0.96 |

## APPENDIX E-2(d)

Table E-2(d) shows the data for the longitudinal profile of the scour hole across the centre of the pier for a Series 3 test for a pier with a 3D collar. The data are plotted and analysed in Section 4.6.2.2.

Table E-2(d). Data for the longitudinal scour profile along the centreline of the pier for Series 3 test: With a 3D collar

| Longitudinal position relative to the pier (cm) | Scour depth (cm) |
|---|---|
| -84.1 | 0 |
| -79.1 | 0 |
| -74.1 | 0 |
| -69.1 | 0 |
| -64.1 | 0 |
| -59.1 | 0 |
| -54.1 | 0 |
| -49.1 | 0 |
| -44.1 | 0 |
| -39.1 | 0 |
| -34.1 | 0 |
| -29.1 | 0 |
| -24.1 | 0 |
| -22.3 | -0.12 |
| -19.1 | -2.44 |
| -14.1 | -4.3 |
| -9.1 | -1.44 |
| -4.1 | 0 |
| 0 | 0 |
| 0.9 | 0 |
| 5.9 | 0 |
| 10.9 | 0 |
| 15.9 | -0.34 |
| 20.9 | -0.16 |
| 25.9 | -0.04 |
| 30.9 | -0.04 |
| 35.9 | 0.16 |
| 40.9 | 0.46 |
| 45.9 | 0.36 |
| 50.9 | 0.98 |
| 55.9 | 1.98 |
| 65.9 | 2.76 |
| 75.9 | 3.56 |
| 85.9 | 2.76 |
| 95.9 | 2.56 |
| 105.9 | 4.76 |
| 115.9 | 4.46 |
| 125.9 | 4.56 |
| 135.9 | 5.16 |

## APPENDIX E-2(e)

The data for the transverse profile of the scour hole across the centre of the pier for the Series 3 test for a pier with a 3D collar are shown in Table E-2(e). The data are plotted and analysed in sSction 4.6.2.3.

Table E-2(e). Data for the transverse scour profile along the centreline of the pier for Series 3 test: With a 3D collar

| Transverse position relative to the pier (cm) | Scour depth (cm) |
|---|---|
| -61.4 | 0 |
| -56.4 | 0 |
| -51.4 | 0 |
| -46.4 | 0 |
| -41.4 | 0 |
| -36.4 | 0 |
| -31.4 | 0 |
| -27.9 | -0.1 |
| -26.4 | -0.44 |
| -21.4 | -1.24 |
| -16.4 | -2.64 |
| -16.4 | -1.44 |
| -14.4 | -2.04 |
| -12.4 | -1.04 |
| -11.4 | -0.2 |
| -6.4 | 0 |
| -5.14 | 0 |
| -0.14 | 0 |
| 2.86 | 0 |
| 4.86 | 0 |
| 6.6 | 0 |
| 8.6 | 0 |
| 12.1 | -1.74 |
| 13.6 | -1.04 |
| 15.6 | -0.74 |
| 18.6 | -1.64 |
| 23.6 | -1.14 |
| 28.6 | -3.64 |
| 33.6 | -2.46 |
| 38.6 | -0.02 |
| 43.6 | 0 |
| 48.6 | 0 |
| 53.6 | 0 |
| 58.6 | 0 |